Tissue-specific variants of translation elongation factor eEF1A and their role in cancer

Justyna Janikiewicz

Thesis submitted for the degree of Doctor of Philosophy

The University of Edinburgh

2010

Declaration

I here declare that this thesis has been composed by me and that all the work presented within is my own, unless clearly indicated otherwise. This work has not been submitted for any other degree or professional qualification.

Justyna Janikiewicz

Acknowledgements

First and foremost, I am extremely appreciative of the support and scientific guidance of my supervisor Professor Cathy Abbott. I could not have imagined a better mentor for my PhD and I am very grateful for an interesting research opportunity and trust I was encountered to complete this project. I am also particularly grateful to Professor David Porteous and Dr Simon Langdon to be on board of my thesis committee as I received a substantial amount of practical tips for future directions within this project. Great assistance from Dr Langdon regarding *in vitro* transformation assays will not be forgotten. Also, Professor David Harrison shared with immunohistology advice and I am very grateful for his help.

Thank you also to all past and present members of the Abbott group, including Dr Julia Boyd for expression plasmids, Dr Helen Newbery for critical reading of this thesis and Jennifer Doig for all the help in the laboratory. I could not forget to mention fellow PhD students-Cheryl, Lowri and Miriam for all the discussions and laughs, trips to cinema and restaurants. A special mention goes to Mariam and Li for all their love, kindness and optimism and whose real friendship gave me a lot of support and was the best remedy for every problem. I wish them further successes with their PhDs and a bright future as scientists.

I could not also forget to thank Dr Shaun Mackie for various technical expertise and Dr Gillian Hamilton for all laughs and support during long hours in tissue culture and finally, for reading of my chapters. Special thanks to Dr Mary O'Connell for helpful advice regarding my experiments with radioactivity, Dr Lynne Marshall for providing me with the positive controls for transformation assays and Professor David Melton and Dr Rob Van't Hof for letting me use some of their laboratory equipment.

A great appreciation goes to the College of Medicine and Veterinary Medicine for my scholarship and opportunity to be a student of the Edinburgh University.

Finally, I would like to thank Kuba whose enormous love, patience, encouragement and support kept me strong and motivated every day to fulfil this scientific mission and for creating a peaceful environment to finish my writing. To all the family and friends back at home who believed in me and showed interest in my work I would like to say a big thank you-“dziękuję”.

Table of contents

List of figures

List of tables

Abbreviations and symbols

aa-tRNA	aminoacyl-tRNA
ABP	actin binding protein
AFB1	aflatoxin B1
ALS	amyotrophic lateral sclerosis
AMPS	ammonium persulfate
APC	adenomatous polyposis coli
ARS	A-rich sequence
ATP	adenosine triphosphate
ATRA	all-*trans*-retinoic acid
B2m	β-2-microglobulin (mouse gene)
BSA	bovine serum albumin
cAMP	cyclic adenosine monophosphate
CARL	calreticulin
CDK4	cyclin-dependent kinase 4
CDKN2A	cyclin-dependent kinase inhibitor 2A
cDNA	complementary DNA
CEA	carcinoembryonic antigen
CGH	comparative genomic hybridization
CIMP	CpG island methylation phenotype
CIN	chromosomal instability
CMM	cutaneous malignant melanoma
CRC	colorectal cancer
Cys	cysteine
DLC1	deleted in liver cancer 1
DMEM	Dulbecco's Modified Eagle Medium
DMSO	dimethyl sulphoxide
DNA	deoxyribonucleic acid
4E-BP1	eukaryotic translation initiation factor 4E-binding protein 1
4E-BP2	eukaryotic translation initiation factor 4E-binding protein 2
4E-BP3	eukaryotic translation initiation factor 4E-binding protein 3
EDTA	ethylenediaminetetraacetic acid
eEF1A	eukaryotic translation elongation factor 1A
EEF1A1	eukaryotic translation elongation factor 1A1 (human gene)

Eef1a1	eukaryotic translation elongation factor 1A1 (mouse gene)
Eef1a1	eukaryotic translation elongation factor 1A1 (mouse protein)
eEF1A1	eukaryotic translation elongation factor 1A1 (protein)
EEF1A2	eukaryotic translation elongation factor 1A2 (human gene)
Eef1a2	eukaryotic translation elongation factor 1A2 (mouse gene)
Eef1a2	eukaryotic translation elongation factor 1A2 (mouse protein)
eEF1A2	eukaryotic translation elongation factor 1A2 (protein)
eEF1B	eukaryotic translation elongation factor 1B
eEF1Bα	eukaryotic translation elongation factor 1B alpha
eEF1Bγ	eukaryotic translation elongation factor 1B gamma
eEF1Bδ	eukaryotic translation elongation factor 1B delta
eEF2	eukaryotic translation elongation factor 2
eIF1	eukaryotic translation initiation factor 1
eIF1A	eukaryotic translation initiation factor 1A
eIF2	eukaryotic translation initiation factor 2
eIF2α	eukaryotic translation initiation factor 2 alpha
eIF2B	eukaryotic translation initiation factor 2B
eIF3	eukaryotic translation initiation factor 3
eIF3a	eukaryotic translation initiation factor 3a
eIF3b	eukaryotic translation initiation factor 3b
eIF3c	eukaryotic translation initiation factor 3c
eIF3e	eukaryotic translation initiation factor 3e
eIF3f	eukaryotic translation initiation factor 3f
eIF3h	eukaryotic translation initiation factor 3h
eIF3i	eukaryotic translation initiation factor 3i
eIF4A	eukaryotic translation initiation factor 4A
eIF4B	eukaryotic translation initiation factor 4B
eIF4E	eukaryotic translation initiation factor 4E
eIF4F	eukaryotic translation initiation factor 4F
eIF4G	eukaryotic translation initiation factor 4G
eIF5	eukaryotic translation initiation factor 5
eRF1	eukaryotic release factor 1
eRF3	eukaryotic release factor 1
Exp5	exportin-5
FACS	fluorescence-activated cell sorting

FBS	foetal bovine serum
FGF2	fibroblast growth factor 2
FISH	fluorescence *in situ* hybridization
G418	geneticin
GAPDH	glyceraldehyde-3-phosphate dehydrogenase
GDP	guanosine diphosphate
GST	glutathione S-transferase
GTP	guanosine triphosphate
H_2O_2	hydrogen peroxide
hBUB	budding uninhibited by benzimidoazoles
HBV	hepatitis B virus
HBx	hepatitis B protein x
HCC	hepatocellular carcinoma
HCl	hydrochloric acid
HCV	hepatitis C virus
Her-2	human epidermal growth factor receptor 2
hMAD	mitotic arrest-deficient
HNPCC	hereditary non-polyposis colorectal cancer
hnRNP A1	heterogeneous nuclear ribonucleoprotein A1
H-Ras	Harvey rat sarcoma
HSE	heat shock elements
HSF-1	heat shock transcription factor-1
HSP	heat shock protein
Hsp70	heat shock protein 70
HSR-1	heat shock RNA-1
ICC	immunocytochemistry
INFα	interferon α
INFγ	interferon γ
IHC	immunohistochemistry
IL1β	interleukin-1 beta
IL6	interleukin-6
IP	immunoprecipitation
IRES	internal ribosome entry site
kb	kilobase pairs
KCIP-1	14-3-3 protein zeta/delta (protein kinase C inhibitor protein-1)

kDa	kilodaltons
MAPK1	mitogen activated protein kinase 1
MDM2	murine double minute 2 protein
Met	methionine
Met-tRNA$_i$	initiating methionine-tRNA
MGMT	O^6-methylguanine-DNA methyltransferase
MGUS	monoclonal gammopathy of undetermined significance
microRNA	micro ribonucleic acid
MM	multiple myeloma
MMR	mismatch repair
mRNA	messenger ribonucleic acid
mRNP	messenger ribonucleoprotein particle
MSI	microsatellite instability
MTX	methotrexate
NAFLD	non-alcoholic fatty liver disorder
NBCS	newborn calf serum
nt	nucleotide
ODC	ornithine decarboxylase
OPN	osteopontin
PABP	Poly (A) binding protein
PASKIN	PAS domain serine/threonine kinase
PBS	phosphate buffered saline
PCR	polymerase chain reaction
PCT	plasmacytoma
PDGFR	plateled-derived growth factor receptor
Pi	phosphate
PI(3,4)P$_2$	phosphatidylinositol (3,4)-biphosphate
PI(3,4,5)P$_3$	phosphatidylinositol (3,4,5)-triphosphate
PI(4,5)P$_2$	phosphatidylinositol (4,5)-biphosphate
PI3K	phosphatidylinositol-3 kinase
PI4KIIIβ	phosphatidylinositol 4-kinase beta
PI4P	phosphatidylinositol 4-phosphate
PIK3CA	PI3K, catalytic alpha polypeptide
PKC	protein kinase C
PKR	protein kinase R

Prdx1	peroxiredoxin-1
PTEN	phosphatase and tensin homolog deleted on chromosome 10
RanBPM	Ran-binding protein in the microtubule-organizing center
Rhox5	reproductive homeobox on the X chromosome 5 (mouse gene)
RNA	ribonucleic acid
RP	ribosomal protein
rpm	revolutions per minute
rpS16	40S ribosomal protein S16
RT	reverse transcriptase
SAGE	serial analysis of gene expression
SAM	sterile alpha motif
SCL	stable cell line
SD	standard deviation
SDS	sodium dodecyl sulphate
SEM	standard error of the mean
Ser	serine
SOD-1	superoxide dismutase 1
Srpx2	Sushi repeat containing protein, X-linked 2 (mouse gene)
18S rRNA	18S ribosomal RNA (mouse gene)
STAT1	signal transducer and activator of transcription 2
Tbp	TATA box binding protein (mouse gene)
TβR-I	transforming growth factor β type I receptor
TCA	trichloroacetic acid
TCTP	translationally controlled tumour protein
TD-NEM	transcription dependent nuclear export mechanism
TERT	telomerase reverse transcriptase
TGFβ	transforming growth factor beta
Thr	threonine
TMA	tumour microarray
TNFα	tumor necrosis factor-alpha
5'TOP	5'terminal oligopyrimidine tract
Tpd52	tumour protein D52 (mouse gene)
tRNA	transfer ribonucleic acid
TSPY	testis-specific protein Y-encoded
TxnlI	thioredoxin-like protein I

Tyr	tyrosine
uORF	upstream reading frame
UTR	untranslated region
VEGF	vascular endothelial growth factor
VHL	von Hippel-Lindau tumour suppressor
wst	wasted

NAMES OF CONSTRUCTS:

A1	coding sequence of human eEF1**A1**
1.1	5'UTR from human eEF1**A1** linked to its own coding sequence
2.1	5'UTR from human eEF1**A2** linked to coding sequence of human eEF1**A1**
A2	coding sequence of human eEF1**A2**
2.2	5'UTR from human eEF1**A2** linked to its own coding sequence
1.2	5'UTR from human eEF1**A1** linked to coding sequence of human eEF1**A2**

Abstract

Eukaryotic translation elongation factor eEF1A exists in two closely related variant forms, eEF1A1 and eEF1A2, that are encoded by separate loci. The former is the second most abundant protein in the cell and is almost ubiquitously expressed but eEF1A2 expression is more limited and its presence was defined predominantly in neurons and muscle cells. Both perform equally well in translation elongation and are responsible for delivering aminoacylated tRNA to the A site of the ribosome in a GTP-dependent manner.

Translation factor eEF1A2 was identified as an oncogene due to inappropriate expression being observed in the high proportion of ovarian, breast, lung, colon and pancreatic tumours. Additionally, its forced expression in rodent fibroblasts resulted in soft agar colony formation along with tumours when overexpressing cells were injected into nude mice. The mechanism by which eEF1A2 contributes to oncogenesis remains unclear. Gene amplification is not solely responsible for eEF1A2 upregulation and neither activating mutations nor methylation status changes are seen in tumours. Interestingly, no connection of eEF1A1 with any malignancy has been made. It is proposed that the oncogenic properties of eEF1A2 might be associated with its conventional role in translation or perhaps with non-canonical functions that differ from those of the eEF1A1 variant.

The main objectives of this PhD project were to elucidate the differential functions of both variants of eEF1A in cancer and to investigate other possible mechanism of eEF1A2 upregulation.

In order to compare the contribution of overexpressed eEF1A variants to cellular transformation, stable cell lines were generated in NIH-3T3 mouse fibroblasts and tested in a panel of *in vitro* transformation assays. Mammalian expression plasmids used for transfection contained each eEF1A variant coding sequence with or without its own 5'UTR and each variant with the 5'UTR from the other eEF1A form.

Transient transfections with the same mammalian expression plasmids were performed to observe that incorporation of exogenous eEF1A1 and eEF1A2 resulted in a decrease of the endogenous eEF1A1 expression at the mRNA and protein level. The dynamic interplay between exogenous and endogenous variants occurred within the first 48 hours post transfection but Eef1a1 returned to the levels seen in controls as soon as the expression of any of the exogenous eEF1A forms started to decline. In contrast, in almost all tested stable cell lines, the levels of endogenous eEF1A1 remained unchanged, at both the mRNA and protein level.

NIH-3T3 lines constitutively expressing eEF1A forms were subsequently subjected to various *in vitro* transformation assays. Stable cell lines of eEF1A1 coding sequence origin formed colonies and foci but with lower efficiency when compared to the eEF1A2 coding sequence variant. It was also shown that anchorage independent growth and foci formation were affected by incorporating either the eEF1A1 or eEF1A2 5'UTR in front of either eEF1A1 or eEF1A2 coding sequence. There was no apparent increase in migration and invasion of the cell lines stably expressing eEF1A. No significant association between protein synthesis rate or increased overall eEF1A level and transformed phenotype in all tested stable cell lines was observed.

Expression of eEF1A1 or eEF1A2 was also determined immunohistologically in panels of different tumour arrays. Moderate to high expression of eEF1A2 protein was observed in 43% of colorectal cancers analysed. The level of eEF1A2 expression appeared to be inversely correlated ($P = 0.024$) with metastasis in lymph nodes in one of the tested colorectal tumour arrays. Moreover, no substantial upregulation of eEF1A2 at the protein level was confirmed in hepatocellular carcinoma and malignant melanoma arrays. In contrast, eEF1A1 protein expression was mostly weak or absent in these malignancies.

Chapter 1: Introduction

1.1 Protein synthesis

The central dogma of molecular biology determines the flow of biological information where the instructions from DNA are transcribed into mRNA - a template which will be used to produce a particular protein (Crick, 1970). Each cellular protein needs to be available in the correct structure, at the appropriate level and at the particular time and location to permit proper physiological functioning of the cells. Protein synthesis, known also as translation, requires a high amount of energy to proceed and many additional components are involved through the whole process. Three essential stages of protein synthesis exist: initiation, elongation and termination, which are mediated by particular stage-specific translation factors (Livingstone et al., 2010).

Initiation

During translation initiation, the start codon is base-paired with the anticodon of the initiating methionine-tRNA (Met-$tRNA_i$) at the peptidyl-site (P-site) of the 80S ribosome. Early events of mammalian translation initiation require the formation of a 'ternary complex' which consists of the GTP-coupled eukaryotic initiation factor 2 (eIF2) and Met-$tRNA_i$. Subsequently, the complex is placed on the 40S ribosomal subunit, already attached to eIF3, eIF1 and eIF1A, and the novel 43S pre-initiation complex is formed. Another factor, eIF4E, is recruited to the 5' end cap structure of the mRNA selected for translation and then bridged with eIF4G. A set of inhibitory proteins (4E-BP1, 4E-BP2 and 4E-BP3) competes with eIF4G to prevent its association with eIF4E but this effect can be suppressed by phosphorylation of the inhibitory proteins. eIF4G is a scaffolding protein and possesses additional binding sites for the ATP-dependent RNA helicase eIF4A and eIF3. Three bridged initiation factors - eIF4A, eIF4G and eIF4E form a mulitimer known as eIF4F, which finally brings the 43S pre-initiation complex and mRNA together.

After the ribosome subunit is positioned on the mRNA, it starts to scan downstream of the cap, until the initiation codon in the optimum context is identified. The scanning process is assisted by eIF4A and its cofactor eIF4B, both of which promote RNA unwinding. Following AUG recognition, eIF5 mediates hydrolysis of eIF2-associated GTP, joining of a 60S ribosomal unit and release of the initiation factors in order to begin elongation of the polypeptides. eIF2B promotes GDP-GTP exchange and recycling of eIF2 for the next initiation cycle (Jackson et al., 2010).

If cap-dependent translation is compromised due to cellular stress conditions, for instance during hypoxia, heat shock or nutrient withdrawal, translation is activated through internal ribosome entry sites (IRES) and ribosomes are positioned at or near the AUG codon, without scanning. This mechanism was first identified in picornaviruses but it was also found in a set of mammalian transcripts (Le Quesne et al., 2009).

Elongation

Throughout the elongation phase, amino acids are conjugated to the appropriate tRNA and the polypeptide chain is assembled according to the open reading frame sequence of the mRNA. One of the crucial players in this stage is eukaryotic translation elongation factor 1A (eEF1A), existing, at least in mammals, in two variants: eEF1A1 and eEF1A2.

The GTP-associated eEF1A delivers the correct aminoacyl-tRNA (aa-tRNA) to the aminoacyl-site (A-site) of the ribosome. Subsequently, the nascent polypeptide (bound to the tRNA at the P-site) is connected with the new amino acid at the A-site what results in elongation of the peptide chain. To complete the cycle, the deacylated tRNA and the peptidyl-tRNA are transferred to the ribosomal exit-site (E-site) and P-site, respectively. Simultaneously, the mRNA is moved forward by exactly one codon with respect to the ribosome. These translocations are mediated by another elongation factor-eEF2 which utilizes energy from GTP hydrolysis to catalyze the process. Due to the shift, the A-site becomes available for the new aa-tRNA and the next round

of the elongation can begin (reviewed in Rodnina and Wintermeyer, 2009). A schematic illustration of the elongation cycle is displayed in Figure 1.1.

The eukaryotic translation elongation factor 1B (eEF1B) serves as a GTP-GDP exchange complex (consisting of eEF1Bα, eEF1Bδ and eEF1Bγ subunits) for eEF1A and promotes its recycling for the new aa-tRNA binding. Both eEF1A forms appear to function equally well during in an *in vitro* translation elongation reaction but they show distinct GDP dissociation rates, seven-fold higher for eEF1A1 than for eEF1A2. eEF1A2 binds GDP more strongly than GTP and the opposite is true for eEF1A1 (Kahns et al., 1998). It would suggest that eEF1A2 is more dependent on a GTP-exchange factor but Mansilla and co-workers reported that eEF1A2 showed absent or very weak affinity for the molecules of the eEF1B complex in the yeast two-hybrid system, in contrast to a strong eEF1A1:eEF1B partnership. Perhaps an alternative guanine nucleotide exchange factor cooperates with eEF1A2 (Mansilla et al., 2002).

Translationally controlled tumour protein (TCTP) was shown to interact with eEF1A and eEF1B in a yeast two-hybrid screen. TCTP preferentially stabilized the GDP-bound eEF1A form and impaired the guanine nucleotide exchange reaction governed by eEF1B (Cans et al., 2003). Since an antibody recognising both eEF1A variants was used in the Cans analysis, it remains unknown whether this interaction was specific for eEF1A1 or eEF1A2, or both forms.

Termination

Termination is mediated by the release factors eRF1 and eRF3. The elongation stage of translation is continued until the ‘stop’ nucleotide triplet enters the ribosomal A-site and eRF1 can be positioned instead of the aa-tRNA. eRF1 and eRF3 assemble into a heterodimer complex to promote hydrolysis of the last peptidyl-tRNA bond in a GTP-dependent manner, hence facilitating release of the completed polypeptide and recycling of the ribosome subunits for the next round of translation (reviewed in Rodnina and Wintermeyer, 2009).

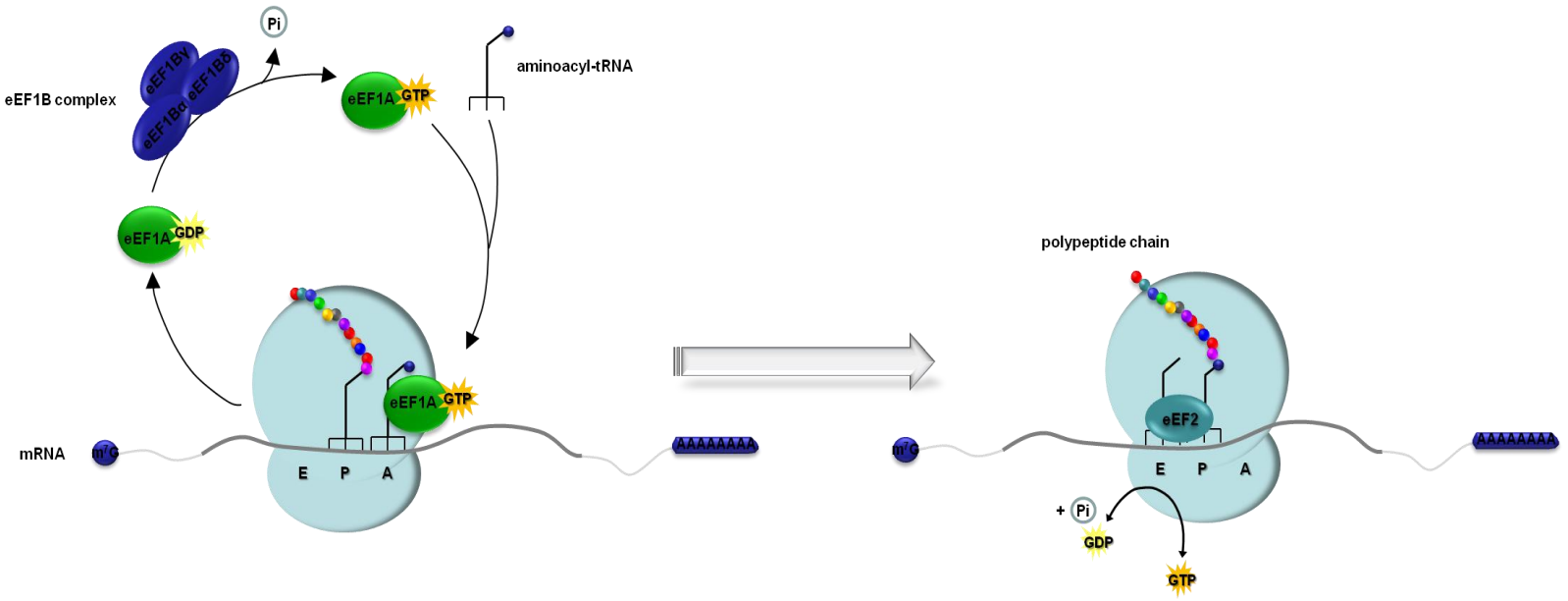

Figure 1.1 A schematic diagram illustrating translation elongation stage in mammals. Translocation of tRNAs between A-E-P-sites on ribosome is dependent on energy of GTP-GDP exchange.

1.2 Eukaryotic translation elongation factor 1A

1.2.1 Genes

The translation elongation factor 1A is encoded by a multigene family that has been conserved among prokaryotes and eukaryotes. In many species there is more than one copy present per haploid genome, and some of these genes are expressed in a tissue specific or developmental stage manner. For example, in plants, 10-15 *EEF1A* genes were reported in maize (Carneiro et al., 1999) and 9 genes in cotton (Xu et al., 2007). There are two equivalents of the *EEF1A* gene (*EF-Tu*) in *Escherichia coli* (Jaskunas et al., 1975). There are two *EEF1A* genes (*TEF1* and *TEF2)* in the yeasts *Saccharomyces cerevisiae* and *Candida albicans*, whereas in *Schizosaccharomyces pombe* three homologs were discovered (Schirmaier and Philippsen, 1984, Sundstromet al.,1990, Mita et al., 1997). In *Drosophila melanogaster* two *EEF1A* genes were found and they are expressed depending on the developmental phase (Hovemann et al., 1988). There are three *EEF1A* genes in *Xenopus laevis* (Dje et al., 1990) and five in *Solea senegalensis* (Infante et al., 2008) which are also expressed differently throughout the development of these organisms.

The mammalian genome contains several *EEF1A* sequences but only *EEF1A1* and *EEF1A2* are actively transcribed. The remaining genes are considered to be retropseudogenes, arising from *EEF1A1* (Madsen et al., 1990, Lee et al., 1993b, Lund et al., 1996). The *EEF1A2* gene was first isolated in rat on the grounds of its antigenic similarity to statin and shares 78% homology with the human *EEF1A1* (Ann et al., 1991).

The genomic regions to which human *EEF1A1* and *EEF1A2* map are 6q14 and 20q13.3, respectively (Lund et al., 1996). A low level of similarity was observed in the introns, promoter regions, 5'UTRs and 3'UTRs between *EEF1A1* and *EEF1A2*, however there is a 75% similarity in the coding regions. In addition, the structure of the two genes is conserved (Knudsen et al., 1993, Bischoff et al., 2000). *EEF1A1* spans 3.5 kb and consist of 8 exons and 7 introns (Uetsuki et al., 1989) whereas *EEF1A2* is

approximately 12 kb (including a 2 kb upstream promoter region), although it is similarly composed of 8 exons and 7 introns. The introns of *EEF1A1* are substantially smaller than those of *EEF1A2* (Bischoff et al., 2000).

The promoter of *EEF1A1* stimulated *in vitro* transcription at least 2 times more efficiently than the adenovirus major late promoter, indicating its high strength. A typical TATA box has been found in the promoter region of *EEF1A1* as well as a few Sp1 binding sites. Sequences similar to the AP1 binding site were identified within the 5' flanking region and the first intron (Uetsuki et al., 1989). Several *cis*-regulatory elements, including E-boxes, binding sites for the EGR family of proteins and a MEF2 binding site have been predicted based on a sequence analysis within promoter region of the *EEF1A2*. Additionally, there is an Inr element which mediates transcriptional activity. No TATA element was found within a 2kb 5'flanking promoter region of *EEF1A2* (Bischoff et al., 2000).

The transcription of *EEF1A1* starts from a cytosine residue which is followed by a stretch of 5 uninterrupted thymidines (Ts) (Uetsuki et al., 1989, Slobin and Rao, 1993). This structural motif is known as the 5'-terminal oligopyrimidine tract (5'TOP), hence eEF1A1 belongs to the family of the TOP mRNAs, which encode many proteins involved in the translational machinery, for example ribosomal proteins or most translation initiation and elongation factors (Meyuhas, 2000, Yoshihama et al., 2002, Iadevaia et al., 2008, Avni et al., 1997). The TOP sequence is a *cis*-acting element which is necessary for translational regulation of these mRNAs in conditions of growth restraint as they are distributed between active polysomes and inactive subpolysomal mRNPs (messenger ribonucleoprotein particles) (Levy et al., 1991, Avni et al., 1994, Hornstein et al., 2001). Variation in the number of Ts has been found in eEF1A1 mRNA and at least three Ts were required at its 5'TOP for the high transcriptional activity of the *EEF1A1* promoter (Shibui-Nihei et al., 2003). The TOP sequence was not found in the eEF1A2 mRNA (Bischoff et al., 2000).

1.2.2 Proteins

Translation elongation factor 1A is the second most abundant protein in the cell (Slobin, 1980, Condeelis, 1995). Mammalian eEF1A exists in two tissue-specific forms, eEF1A1 (formerly known as eEF1α) and eEF1A2. The latter has been confirmed in all mammals investigated to date, as well as in *Xenopus* and *Gallus gallus* (Newbery et al., 2007, Boardman et al., 2002). Since there is no experimental evidence of the existence of an eEF1A2 orthologue, for instance in fruit fly or in other lower organisms, its presence might be limited to vertebrates.

Human forms of eEF1A share 92% identity and 98% similarity with respect to their amino acid sequence (Tomlinson et al., 2005, Soares et al., 2009). The ClustalW (Thompson et al., 1994) protein line up is shown in Figure 1.2. A similar level of correspondence was seen between eEF1A1 and eEF1A2 proteins among other mammalian species (Knudsen et al., 1993, Kahns et al., 1998). Alignment of the eEF1A2 amino acid sequence from different mammals shows a high degree of similarity. For example, the rabbit and human proteins are identical and they differ by only one amino acid from their mouse and rat counterparts (Kahns et al., 1998, Lee et al., 1994). The amino acids that distinguish eEF1A2 from the eEF1A1 variant are conserved between different species, indicating distinct functions or properties of both eEF1A forms that could have arisen through evolutionary selection (Lee et al., 1994, Soares et al., 2009). Two variants within the same animal were less identical than independent eEF1A forms compared among different mammalian species (Knudsen et al., 1993, Kahns et al., 1998, Ann et al., 1992).

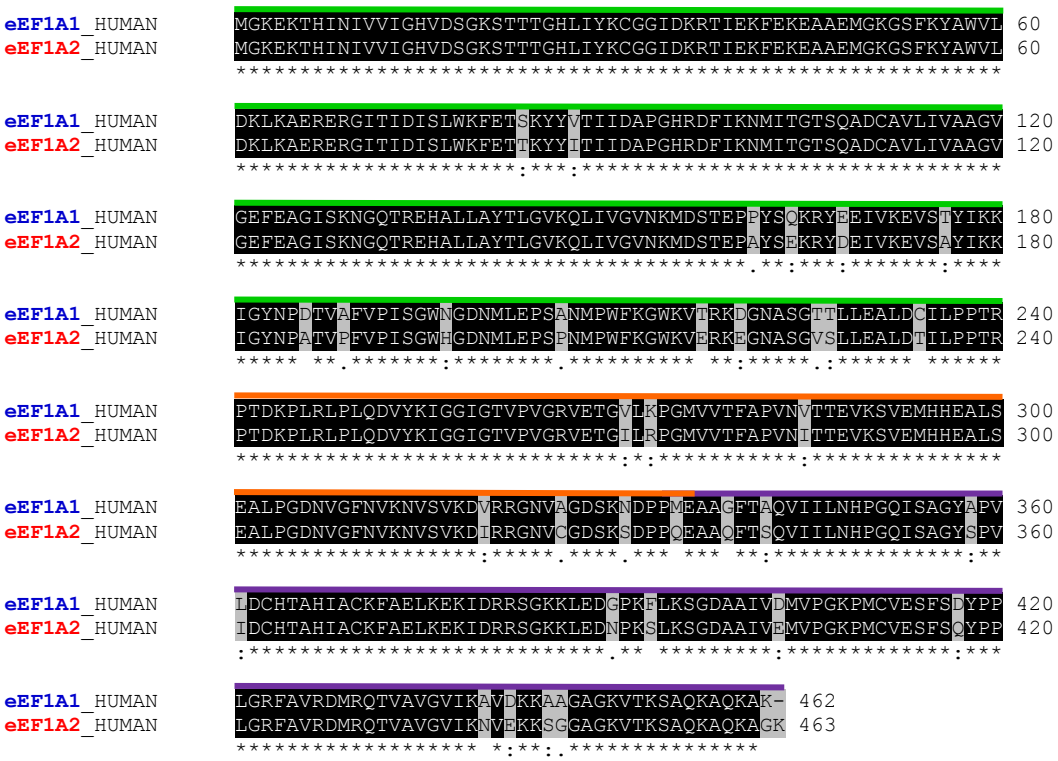

Figure 1.2 Amino acid sequence alignment between human eEF1A1 and eEF1A2. Identical residues have black background whereas variant differences are shown in grey. One dot denotes semi-conservative amino acid residues and two dots mean conserved substitutions. Domain boundaries: green (domain I), orange (domain II), purple (domain III) (adapted and modified from Soares et al., 2009).

1.2.2.1 Post-translational modifications and structural domains

As eEF1A1 and eEF1A2 proteins share 92% identity, small differences in modifications of amino acids between the two eEF1A variants will be important to understand any differences in functioning and activity of the two forms.

eEF1A1 from rabbit reticulocytes was chemically sequenced and seven post-translational modifications were revealed. These included dimethylation of lysines at positions 55 and 165, trimethyllysine residues at 36, 79 and 318, and the incorporation of ethanolamine to glutamic acids at positions 301 and 374 (Dever et al., 1989).

The last modifications were also reported at the same residues for human eEF1A1 in the K562-48 erythroleukemia cell line (Rosenberry et al., 1989) and in eEF1A2 from rabbit skeletal muscle (Kahns et al., 1998). In contrast to eEF1A1, lysines at positions 55 and 165 were not dimethylated but trimethylated in rabbit eEF1A2 (Kahns et al., 1998).

Eckhardt *et al.* used mass spectrometry and site-directed mutagenesis to confirm phosphorylation of human eEF1A1 at Thr432 by PASKIN (PAS Domain serine/threonine) kinase (Eckhardt et al., 2007). Analysis of phosphopeptides from human embryonic kidney 293T cells demonstrated phosphorylation of eEF1A1 at Tyr29 and Ser163 (Molina et al., 2007). Phosphorylated tyrosine was also detected for both eEF1A forms by Panasyuk et al., but specific localisation of the modification within the amino acid sequence was not determined. eEF1A2 was shown to be characterized by a greater phosphorylation level than eEF1A1 (Panasyuk et al., 2008). Lamberti and colleagues showed INFα-mediated phosphorylation of the eEF1A protein at serine and threonine residues by C-Raf in H1355 cells. Serines 18, 157, 316, 383 and threonines 242, 432 were extrapolated as the most probable phosphorylation sites for C-Raf in the 3D model of human eEF1A, hypothesizing that this increases cell survival activity and cellular stability of translation factor (Lamberti et al., 2007). These residues are conserved between the two variants. A vast repertoire of modifications by phosphorylation at serine, threonine and tyrosine amino acids was shown for eEF1A. However, it should be stressed that the majority of these studies identified peptides that fit within completely conserved regions of both variants, making it impossible to resolve whether changes are specific to eEF1A1 or eEF1A2.

A high resolution crystal structure of *Saccharomyces cerevisiae* eEF1A revealed various functionally important sequences spread across three structural domains of the protein (Andersen et al., 2000, Andersen et al., 2001). Three consensus GTP-binding motifs were found in domain I (Dever et al., 1987), whereas domain II is implicated in the interaction with aminoacylated-tRNA (Andersen et al., 2000). Both domains interact

with eEF1Bα during the exchange of GDP for GTP (Andersen et al., 2000). It was shown that domain II and domain III carry residues important for the interaction of eEF1A with the actin cytoskeleton in *S.cerevisiae*, rat or *Dictyostelium* (Gross and Kinzy, 2005, Gross and Kinzy, 2007, Liu et al., 2002). Various GFP-fusions of carrot eEF1A were introduced into fava bean leaf epidermal cells and it was determined that domain III was involved in the unconditional binding of eEF1A with microtubules (Moore and Cyr, 2000). Three-dimensional models of human eEF1A1 and eEF1A2 variants were bioinformatically assessed on the platform of the yeast counterpart, showing high conservativeness of the residues linked to the translation-related functions of eEF1A (Soares et al., 2009).

1.2.2.2 Expression pattern

The two variants of the mammalian translation elongation factor 1A exhibit distinct expression patterns. While eEF1A1 is almost ubiquitously expressed, eEF1A2 abundance is definitely more limited. Its expression was confirmed in the brain, heart and skeletal muscle of mice, rats, rabbits and humans (Chambers et al., 1998, Lee et al., 1992, Kahns et al., 1998, Knudsen et al., 1993). However, the above analyses were confirmed exclusively by Northern blotting. Lee and co-workers shed some light on the presence of eEF1A2 in the rat brain by *in situ* hybridization studies and they observed this variant in neurons of the cerebral cortex, motor neurons of the medulla and in cerebellar Purkinje cells (Lee et al., 1993a).

Analysis of the expression of eEF1A variants in different tissues was later expanded by studies at the protein level as different groups started to generate specific antibodies. These were in overall agreement with the specific expression patterns seen at the mRNA levels. Therefore, the eEF1A2 protein is strictly expressed in heart, skeletal muscle and brain whereas the eEF1A1 variant is highly abundant (except in adult muscle), as confirmed in mice, rats and humans (Khalyfa et al., 2001). Both variants of eEF1A present reciprocal expression patterns in mice brains and spinal

cords. Whereas eEF1A2 is solely confined to neurons, eEF1A1 is mostly seen in white matter and glial cells (Khalyfa et al., 2001, Pan et al., 2004). However eEF1A1 was also seen trapped in the nucleus of spinal cord motor neurons (Newbery et al., 2007).

Apart from the established expression of eEF1A2 in muscle and brain tissues, there is evidence of its abundance in other cell specific locations. Detection of eEF1A2 was confirmed by immunohistochemistry in sporadic pancreatic islets (predominantly glucagon-producing), neuroendocrine cells in stomach and in up to two enteroendocrine cells within a single colon crypt. Expression of the eEF1A variant in the novel cell types was conserved in human and mouse, indicating a possible functional relevance of the presence of eEF1A2 at these locations (Newbery et al., 2007).

It appears that expression of the eEF1A1 and eEF1A2 in heart, skeletal muscle and brain is tightly regulated in development. The former variant is present in mice and rats muscles throughout embryonic stages but is gradually downregulated within the first two postnatal weeks. Thereafter, eEF1A1 is completely abolished and replaced by eEF1A2 which becomes the major translation elongation factor 1A in muscles (Chambers et al., 1998, Khalyfa et al., 2001, Lee et al., 1993b, Lee et al., 1995).

In the brain of mouse embryos (E16), eEF1A1 was reported to be located in the perikaryon of the developing neurons (Pan et al., 2004). Although eEF1A1 is postnatally expressed in glial cells and eEF1A2 presence is limited to neurons, the status of the developmental transition between eEF1A forms at the level of whole brain tissue remains less clear (Khalyfa et al., 2001, Pan et al., 2004).

The direct mechanism and the reason for the developmental switch between two eEF1A forms remains an open question. It has been implied that the transition of eEF1A1 into eEF1A2 is associated with terminal differentiation of the neurons, myocytes and cardiomyocytes (Lee et al., 1995). However there are other cell types, for instance keratinocytes, which are also terminally differentiated but do not express eEF1A2 (Newbery et al., 2007). Since the two eEF1A variants have equivalent functioning at the translation elongation stage (Kahns et al., 1998), a plausible hypothesis is that certain cells substitute eEF1A1 with eEF1A2 to modify

or avoid non-canonical properties assigned to the former variant. On the other hand, it may be the lack of eEF1A1 rather than presence of eEF1A2 which is the key issue (Newbery et al., 2007).

1.3 The wasted mouse

Information about the effects of compromised expression of the eEF1A2 variant was obtained from studies in the wasted mouse. Wasted (*wst*) is a spontaneous autosomal recessive mutation that occurred in the HRS/J mice stock at the Jackson Laboratory in 1972. Mice homozygous for this mutation grow normally until around three weeks after birth but later, they develop body weight loss, tremors, gait abnormalities as well as progressive atrophy of the spleen and thymus, and die by postnatal day 28 (Shultz et al., 1982).

The genetic lesion in wasted mice is a 15.6 kb deletion that removes all promoter elements and the first noncoding exon of the *Eef1a2* gene, leading to its complete inactivation (Chambers et al., 1998). Expression of the eEF1A1 in wild-type mouse muscle gradually declines until almost undetectable levels by around 21 days when it is subsequently replaced by eEF1A2. In wasted animals both eEF1A variants are absent in muscles, since after eEF1A1 is shut down, there is no eEF1A2 to compensate in translation elongation (Chambers et al., 1998, Khalyfa et al., 2001). Therefore, the abnormal muscular phenotype coincides perfectly with the loss of the eEF1A2 activity in muscle and the dramatic loss of the muscle bulk appears to be a major cause of the body weight decline (Chambers et al., 1998, Newbery et al., 2005).

The site of the major pathological changes in wasted mice is in the spinal cord, which displays vacuolar degeneration of motor neurons (Newbery et al., 2005, Lutsep and Rodriguez, 1989). In the spinal cords of *wst/wst* mutants eEF1A1 was present in white matter and glial cells (as in wild-type counterparts), but eEF1A2 was not detectable in the cytoplasm of motor neurons, therefore one would predict no translation elongation activity (Newbery et al., 2007). Signs of ataxia and Purkinje cells loss were

also reported for wasted mice (Shultz et al.,1982). This corresponds with the observation that eEF1A2, but not eEF1A1, is expressed in the Purkinje cells of wild-type animals (Newbery et al., 2007).

It has been clarified that the neuromuscular abnormalities in wasted mice coincides with a developmental switch between eEF1A forms at 21 days after birth and that the loss of the eEF1A2 function is fully responsible for the wasted phenotype. Constructs carrying a human PAC or a mouse BAC with a functionally active eEF1A2 were sufficient to rescue wasted phenotype in transgenic lines, and no other genes appear to be affected by the presence of the deletion in the wasted animals (Newbery et al., 2007).

1.4 The non-canonical functions of eEF1A

Translation elongation factor 1A1 has been called a moonlighting protein. In addition to its well established role in translation, it has been also implicated in a wide repertoire of non-canonical functions (reviewed in Ejiri, 2002, Mateyak and Kinzy, 2010). This implicates eEF1A1 in the coordination of multiple biological processes which correlates with the high abundance of this protein within cells. On the other hand, biochemical studies of eEF1A2 are incomplete and even though the two variants exhibit high similarity at the amino acid level, it has not yet been established whether these unconventional roles are shared between eEF1A1 and eEF1A2 or whether the two variants have different properties. Knowledge about the functional differences in performing noncanonical roles could be beneficial for explaining the developmental switch between eEF1A forms, as well as the potential association of eEF1A1 and eEF1A2 with oncogenic transformation.

1.4.1 Protein degradation

Evidence from several studies demonstrates that eEF1A1 might be a common factor in coordinating two opposite pathways: protein synthesis and protein degradation. However, the precise mechanism of this quality control remains elusive.

Eukaryotic translation elongation factor 1A in *S.cerevisiae* was proposed to participate in the binding of nascent and misfolded proteins that were ubiquitinated after translational damage, thus facilitating their delivery onto the proteasome (Chuang et al., 2005).

Gonen and co-workers reported that eEF1A1 promoted degradation of certain N^{α}-acetylated proteins *in vitro*, namely the core nucleosomal histone H2A, actin and α-crystallin in the presence of the 26S protease complex. It is suggested that eEF1A1 might function as an enzyme or as a chaperone which changes the conformation of ubiquitin-conjugated proteins and makes them more susceptible to degradation by the 26S proteasome (Gonen et al., 1994).

Recent findings from Andersen and colleagues have shown that eEF1A1 is targeted *in vivo* in HEK293 cells by thioredoxin-like protein I (TxnlI), the novel redox component of the proteasome's 19S regulatory complex. The authors suggest that under oxidative stress, TxnlI prevents eEF1A1 from oxidative inactivation in order to ensure efficient degradation of the damaged proteins (Andersen et al., 2009).

1.4.2 Cytoskeleton interactions and remodelling

A wealth of data supports the concept of a physical link between cytoskeletal and translational components, and its benefit for global and local protein synthesis (reviewed by Kim and Coulombe, 2010). Substantial evidence from many laboratories supports a functional relationship between eukaryotic translation elongation factor 1A and the cytoskeleton.

Originally, a 50kDa protein designated as ABP-50 was isolated from *Dictyostelium discoideum* and was found to display actin binding and bundling properties (Demma et al., 1990). ABP-50 was soon confirmed as the functional eEF1A of *Dictyostelium* amoebae (Yang et al., 1990). Resting cells in this organism exhibit a diffuse distribution of eEF1A in the cytosol, whereas upon the addition of cAMP eEF1A was localized in the filopodia. About 10% of total eEF1A was associated with the cytoskeleton in nonstimulated cells (Dharmawardhane et al., 1991). Immunoprecipitated eEF1A was bound to nonfilamentous actin or G-actin, but this interaction was inhibited by GTP. In contrast, bundling of F-actin by eEF1A was unaffected by guanine nucleotides (Dharmawardhane et al., 1991), but was dependent on pH changes (Edmonds et al., 1995). Liu *et al.* demonstrated that binding of F-actin or aa-tRNA to the eEF1A of *D. discoideum* was mutually exclusive and the interaction between eEF1A and aa-tRNA was not dictated by pH ranges (Liu et al., 1996). Additionally, in actin bundles associated with eEF1A, a unique type of filament crosslinking was seen (Owen et al., 1992, Munshi et al., 2001). Here, filaments were rotated by 90 degrees in relation to each other and remaining actin bundling proteins were excluded from these special square packed actin arrangements (Owen et al., 1992).

Association of eEF1A with the actin cytoskeleton is not solely restricted to the slime mold but has been also established across species, from yeast to mammals. Interaction between eEF1A and actin was confirmed *in vivo* in *Schizosaccharomyces pombe*. When eEF1A was overexpressed, abnormal localization of F-actin, disturbed branching and growth polarity were observed (Suda et al., 1999). Growth defects, abnormal morphology and similarly altered actin distribution were reported for *Saccharomyces cerevisiae* overexpressing eEF1A. Disruption of the actin cytoskeleton by upregulation of eEF1A did not affect protein synthesis (Munshi et al., 2001). eEF1A mutants of *S. cerevisiae* with impaired ability to bind and bundle actin shared a phenotype matching the one with the eEF1A overexpression; however no substantial changes in overall protein synthesis or in the rate of elongation were present in these

mutants, suggesting the two roles of eEF1A are distinct (Gross and Kinzy, 2005). On the other hand, the same group showed that different classes of mutation displayed more severe actin phenotypes which were correlated with slow growth and a block in translation initiation (Gross and Kinzy, 2007).

Bassell and co-workers postulated that in human fibroblasts eEF1A colocalized with polysomes and poly(A) mRNA at actin filament intersections (Bassell et al., 1994). Ultimately, eEF1A has been also implicated in indirect simulation of the actin cytoskeleton arrangements due to its involvement in phosphatidylinositol 3- and 4-kinases signalling (Yang et al., 1993, Yang and Boss, 1994, Amiri et al., 2006, Jeganathan and Lee, 2007, Jeganathan et al., 2008). This aspect will be described more extensively in another section of this chapter.

Since eEF1A and actin are two of the most abundant proteins in eukaryotic cells, the possibility of their cooperation is not surprising, especially since in contrast to yeast, an intact cellular actin filament network is required for efficient mammalian protein synthesis (Stapulionis et al., 1997).

Several studies have also suggested an association between eEF1A and microtubule dynamics. Durso and Cyr isolated a 50kDa polypeptide that bound and bundled microtubules of carrot cells *in vitro* which was identified as eEF1A. Binding and bundling between eEF1A and microtubules in *Daucus carota* was coordinated in a Ca^{2+}/calmodulin-dependent manner. According to the authors, eEF1A was implicated in the modulation of the assembly, dynamics and stability of the microtubules (Durso and Cyr, 1994, Moore et al., 1998). Moore and Cyr also reported the *in vivo* association of eEF1A and microtubules in the epidermal cells of fava bean leaves (Moore and Cyr, 2000). The key regulatory component of the centrosome and the mitotic apparatus of the sea urchin eggs was structurally and functionally related to eEF1A (Kuriyama et al., 1990, Ohta et al., 1990). Overexpression of eEF1A in fission yeast *Schizosaccharomyces pombe* led to a disturbance in the normal organization of the microtubule cytoskeleton and a curled phenotype around the ends of the cells was observed (Suda et al., 1999). eEF1A1 from rabbit liver and EF1A isolated from

Xenopus laevis egg extracts modulated the severing of taxol-stabilized microtubules *in vitro*. Moreover, human recombinant eEF1A also displayed microtubule binding and fragmentation activity *in vitro* and when microinjected into rat 3Y1 fibroblasts (Shiina et al., 1994).

The ability of eEF1A to influence the assembly and stability of the cytoskeleton might influence cellular motility and also it would place this elongation factor as a common denominator in the coordination of transport, anchorage and efficient translation of most cytoplasmic mRNAs (Condeelis, 1995). Alternatively, this role might not be associated with its canonical functioning in translation. A clear and in-depth delineation of how/if both forms are precisely interconnected with cytoskeleton is highly important.

1.4.3 Apoptosis

Several lines of evidence suggest that eEF1A1 might be involved in apoptosis. In BALB/c fibroblasts subjected to serum deprivation, cell death and protein synthesis rate were reduced when the cells had stably downregulated expression of the eEF1A1 protein. In contrast, fibroblasts with constant overexpression of eEF1A1 exhibited increased apoptosis upon serum restraint in culture although the rate of protein synthesis remained unchanged, suggesting these two processes are independent (Duttaroy et al., 1998).

Substantial upregulation of eEF1A1 in cardiac myocytes was also implicated in conditions of oxidative stress induced apoptosis. On the other hand, transient transfections with antisense eEF1A1 cDNA were sufficient to rescue this embryonic rat heart cell line from H_2O_2-mediated cell death. Chen and colleagues suggested that increased abundance of eEF1A1 is necessary to execute apoptosis during oxidative stress and the high availability of the actively translatable eEF1A1 mRNA is dependent on its 5'TOP sequence (Chen et al., 2000).

In a further set of experiments, an erythroleukemic cell line carrying the temperature-sensitive p53 mutant was susceptible to apoptosis at 32^{o}C, but not at 37^{o}C. This model was used to screen for genes associated with cell death. *EEF1A1* was identified as the predominant candidate and the gene was found to contain three conserved p53-response elements within its sequence. The authors propose that cell death was mediated by the microtubule-severing abilities of the p53-upregulated eEF1A1 (Kato et al., 1997).

Kobayashi *et al*. showed that Chinese hamster ovary cells (CHO) induced to drive impaired chromosomal condensation and tetraploidy were eliminated by a caspase-independent apoptosis, which was associated with the downregulation of eEF1A1 (Kobayashi and Yonehara, 2008). Accumulation of the translationally inactive eEF1A1 mRNA was confirmed in processing bodies and the 5'TOP sequence was suggested as the driving force behind this transition. Interestingly, induction of short hairpin RNA specific for eEF1A1 led to similar caspase-independent cell death but the restored expression of eEF1A1 significantly inhibited apoptosis in tetraploid cells. In the model proposed by the authors, downregulation of eEF1A1 contributes to the elimination of tetraploidy and inhibition of tumourgenesis by provoking apoptosis. The effect of eEF1A2 overexpression in this system was less clear as the corresponding data were not shown directly. However, Kobayashi and co-workers reported that in spite of addition of exogenous eEF1A2 (the endogenous counterpart was not present in CHO cells), withdrawal of endogenous eEF1A1 was still observed on schedule but inhibition of the cell death response was observed instead (Kobayashi and Yonehara, 2008). This would fit with the notion of the prosurvival character of the eEF1A2 and thus could explain the involvement of eEF1A2 in oncogenesis.

For instance, Ruest and colleagues suggested opposing functions of eEF1A forms during caspase 3-dependent apoptosis. Upon differentiation of C2C12 and L6 myoblast cells, eEF1A1 decreased but eEF1A2 increased. In myotubes subjected to serum deprivation-induced apoptosis, the effect was completely reciprocal to that seen during the differentiation process. In overexpression experiments, eEF1A2 or antisense

eEF1A1 cDNA transfected cultures were rescued from cell death whereas upregulation of eEF1A1 did not have a prosurvival effect (Ruest et al., 2002).

Additionally, mouse eEF1A2 was used as bait in a yeast two-hybrid screen of mouse brain cDNA library and peroxiredoxin-1 (Prdx1) was identified as the interactor with the highest number of hits. Despite high homology between the two eEF1A forms, eEF1A1 from cultured cell extracts and mouse tissues did not co-precipitate in a complex with Prdx1. NIH-3T3 cells stably co-expressing eEF1A2 and Prdx1 were subjected to H_2O_2 treatment which was sufficient to protect cultures from oxidative stress–induced apoptosis. Single transfectants were characterised by partial resistance to cell death. Moreover, the complex of eEF1A2 and Prdx1 blocked apoptosis signalling through a rise in Akt abundance and a concomitant decrease in the levels of caspase 3 and 8 activation (Chang and Wang, 2007).

1.4.4 Nuclear transport

The potential involvement of eEF1A in nuclear transport (of eEF1A itself or when it is mediating transport of other proteins) is very inconclusive and it remains a speculative matter as to whether this ability is truly a noncanonical function or if it is linked to the conventional role of eEF1A, for instance in the tRNA channelling process during protein synthesis (Mateyak and Kinzy, 2010).

Two independent groups observed that eEF1A was actively exported from the nucleus upon its aa-tRNA dependent recruitment to the exportin-5 (Exp5)/RanGTP complex. Exactly how eEF1A could be trapped in the nucleus is not yet understood. Under normal conditions, no obvious eEF1A shuttle system was confirmed by these studies, indeed eEF1A was completely excluded from the cell nucleus (Bohnsack et al., 2002, Calado et al., 2002). The nuclear presence of aa-tRNA could be the prerequisite for eEF1A export. Such export seems rather to be a consequence of the interaction between aa-tRNA and Exp5 as they can bind without the assistance of eEF1A. Therefore, removal of eEF1A from the nucleus by Exp5 could be considered as

a correction mechanism if eEF1A is trapped in nucleus (for instance after cell division) (Calado et al., 2002). Nonetheless, some studies suggest that eEF1A can access the nucleus as shown in *msn5*Δ mutants of *S.cerevisiae* (msn5 is a yeast counterpart of Exp5) or in HeLa cells depleted of Exp5 (Murthi et al., 2010, Lund et al., 2004).

More recently, eEF1A was reported by Khacho and colleagues to be a novel component of the transcription dependent nuclear export mechanism (TD-NEM) in mammalian cells (Khacho et al., 2008). eEF1A specifically interacted with the TD-NEM sequence found in certain proteins, for instance in PABP (Poly (A) binding protein) or in the von Hippel-Lindau (VHL) tumour suppressor. Nuclear export activity of eEF1A was clearly uncoupled from its canonical role in translation and was also independent of the Exp5 pathway. As eEF1A was not observed in the nuclear compartment, it was proposed that eEF1A executed its role in the nuclear export mechanism from the cytoplasmic side by receiving proteins after they pass through the nuclear pore complexes (Khacho et al., 2008). A similar assumption was made in yeast where cytoplasmic eEF1A was shown to facilitate transport of the aa-tRNA from the nucleus and nuclear accumulation of mature tRNAs was observed upon downregulation or mutations of eEF1A (Grosshans et al., 2000).

1.4.5 Heat shock

In vertebrates, the heat shock transcription factor 1 (HSF-1) binds to heat shock elements (HSE) on the *HSP* promoters upon environmental or physiological stress stimuli to induce expression of the specific heat shock proteins (as reviewed in Shamowsky and Nudler, 2008).

Translation elongation factor 1A from whole cell lysates of HeLa and BHK-21 cells was retained on Sepharose-immobilized HSF-1. Full HSF1 activation requires two elements, trimerization and the gain of specific DNA-binding activity, both of which were induced by the eluted eEF1A-containing fraction as shown by an electromobility shift assay and protein-protein crosslinking. Purified eEF1A from rat liver was shown to

activate recombinant mouse HSF-1 *in vitro,* exclusively in tandem with a novel non-coding RNA, approximately 600 nucleotides long, named by the authors heat shock RNA-1 (HSR-1). Shamovsky and co-workers suggested that upon heat shock-induced collapse of the cytoskeleton and the general shut down of proteins synthesis, substantial amounts of eEF1A are released and concomitantly become more available for HSF-1 activation (Shamovsky et al., 2006). Unfortunately, apart from the *in vitro* reconstitution experiment where it was clearly stated that eEF1A was purified from rat liver (which is known to express only eEF1A1), the description of techniques used in the referenced studies does not allow a conclusion to be formed about whether heat-shock response is specific to eEF1A1 or eEF1A2, or both.

Batulan and colleagues showed that cultured motor neurons, motor neurons of spinal cords from SOD-1 transgenic mice and ALS patients failed to express Hsp70 after different heat shock conditions stimulation. This suggests that these cells exhibit a high threshold for induction of the temperature-induced stress response. The authors implicated the compromised ability of motor neurons to activate HSF-1 as the origin of their failure to mount a heat shock response (Batulan et al., 2003). Additionally, motor neurons express eEF1A2 in cytoplasm but not eEF1A1 (some expression of which was seen in nucleus) (Newbery et al., 2007) and if the latter is involved in HSF-1 activation, then this would fit with the notion of motor neurons having an impaired heat shock response. Consequently, possible differential behaviour of both eEF1A variants in terms of the stress response could relate back to diseases, for example to ALS where motor neurons are predominantly vulnerable, or to cancer.

In many tumours HSP are expressed in increased amounts which correlates with patients being more resistant to therapeutic treatment and poor survival prognosis (Ciocca and Calderwood, 2005). Overexpression of Hsp70 was implicated in the inhibition of programmed cell death and the enhanced activity of oncogenes such as *MYC* or *RAS.* Cancer cells exhibiting higher expression of HSF-1 and Hsp70 were characterised by increased invasion and metastasis (as reviewed in Calderwood et al., 2006).

1.5 Translation and cancer connection

Deregulation or misexpression of several translational machinery components is commonly seen in many cancers where translational control is seriously compromised. As the intracellular availability of these components is increased, preferential expression of specific cell proliferation- or survival-related proteins is consequently upregulated (Ruggero and Pandolfi, 2003, Le Quesne et al., 2009, Silvera et al., 2010). Perhaps the best characterized translation factor that has been linked to tumour development is the cap-binding protein eIF4E. This protein was shown to transform NIH-3T3 and Rat2 fibroblasts when overexpressed and the resulting cells were highly tumourigenic in nude mice (Lazaris-Karatzas et al., 1990). This initiation factor transcript was overexpressed in many malignant cell lines (Miyagi et al., 1995) and elevated protein levels were demonstrated for solid tumours, including colorectal, breast, bladder, lung and head and neck, to name but a few (Rosenwald et al., 1999, Li et al., 1997, Crew et al., 2000, Rosenwald et al., 2001, Nathan et al., 1999). It was postulated that overexpressed eIF4E executes transformation by increasing the translation of a subset of particular mRNAs which contain a highly structured 5'UTR. These particular mRNAs encode proteins involved in cell cycle progression, angiogenesis, growth or survival such as ODC (ornithine decarboxylase), VEGF (vascular endothelial growth factor), FGF2 (fibroblast growth factor 2), cyclin D1, c-Myc (reviewed in Mamane et al., 2004).

1.5.1 eEF1A1 and cancer

Regardless of the high degree of structural and functional relatedness of both eEF1A variants, eEF1A1 has not been directly implicated in a transformed phenotype. Although *EEF1A1* maps to the 6q14 region which has been amplified in some childhood brain tumours (Shlomit et al., 2000), it is more frequently a loss of this region that is associated with cancer (Verhagen et al., 2002, Kobayashi et al., 2008).

It has therefore been suggested that 6q14 might contain a tumour suppressor gene (Thornton et al., 2003) and that perhaps the *U50* snoRNA gene could be one of the candidates (Dong et al., 2008).

However, Tatsuka and co-workers reported a mouse fibroblast cell line variant BALB/c A31-I-13, constitutively expressing eEF1A1 that was highly susceptible to chemically or physically induced neoplastic transformation. In order to explain this oncogenic effect, it was proposed that the overexpression of eEF1A1 forces the cells to be competitive for growth rather than hypersensitive to carcinogens or ultraviolet light. Alternatively, it could lead to rearrangements of actin filaments or enhanced translation of growth related proteins (Tatsuka et al., 1992). In addition, overexpression of eEF1A1 was observed in the MTLn3 metastatic line compared to the weakly metastatic MTC cells in rat mammary adenocarcinoma (Edmonds et al., 1996). The main concern is that the vast majority of studies published so far have been explored with antibodies or DNA probes that do not distinguish between the two eEF1A forms. Indeed, in some cases, mass spectrometry analysis picked up peptides whose sequence is conserved between eEF1A1 and eEF1A2.

Inappropriate expression of eEF1A1 at the RNA level was seen in different tumours and cancer cell lines, namely primary glioblastoma, oral tongue squamous cell carcinoma, prostate cancer, pancreatic adenocarcinoma, hepatocellular carcinoma or colon cancer (Scrideli et al., 2008, Zhou et al., 2006, Mohler et al., 2002, Grant et al., 1992, Grassi et al., 2007, Alon et al., 1999). A few cancer related interactors of eEF1A1 were also indentified, for example osteopontin (OPN) which is overexpressed in many human tumours and is the main phosphoprotein secreted during advanced metastasis (Zhang et al., 2009). Authors investigated the possibility that eEF1A1 was an actin dependent regulator of the OPN mRNA stability and expression. A higher abundance of OPN was seen in invasive HepG2 cells upon low levels of F-actin and lack of eEF1A1 binding to OPN 5'UTR. Association of OPN mRNA with F-actin via binding of eEF1A1 led to decreased expression of OPN and a less invasive phenotype of the Hep3B cell line (Zhang et al., 2009). Kido and Lau identified testis-specific protein

Y-encoded (TSPY) as a novel interactor of eEF1A1 in yeast two-hybrid screen of a mouse foetal gonadal cDNA library (Kido and Lau, 2008). TSPY is frequently overexpressed in gonadoblastoma and testicular germ cell tumours. Either eEF1A1 or eEF1A2 co-localized in cytoplasm with TSPY in COS7 co-transfected cells and interact with TSPY in GST-pull down assay. TSPY was co-expressed with eEF1A in both human normal testicular germ cells and germ cells tumours (but an antibody cross-reacting with both eEF1A variants was used). The authors suggest that by interacting with eEF1A, TSPY could modulate protein synthesis and upregulate the genes involved in cellular proliferation and tumour development (Kido and Lau, 2008).

The *EEF1A1* gene was differentially expressed in several cancer cell lines subjected to treatment with pharmacological compounds suggesting that it might be a potential therapeutic target. Overexpression of *EEF1A1* by at least a 2-fold change was seen in MIA PaCa-2 (pancreatic cancer), K562 (erythroblastic leukaemia) and Saos-2 (osteosarcoma) cell lines resistant to methotrexate (MTX) in comparison to the sensitive line counterparts (Selga et al., 2009). Harris and colleagues reported a list of proteins modulated in NB4 acute promyelocytic leukaemia line that was exposed to treatment with all-*trans*-retinoic acid (ATRA) and downregulation of eEF1A1 protein but unchanged mRNA levels were observed (Harris et al., 2004). Overexpression of eEF1A1 at the mRNA level was reported in UMSCC 10b/Pt-S15 head and neck carcinoma cell line which acquired resistance to cisplatin (Johnsson et al., 2000). Differential modulation of eEF1A1 expression observed in cell lines subjected to MTX, cisplatin or ATRA treatment might be attributed to the proapoptotic abilities displayed by eEF1A1.

1.5.2 eEF1A2 as an oncogene

While the tumourigenicity status of the eEF1A1 is less clear, eEF1A2 has been clearly implicated as an oncogene (Anand et al., 2002). A wealth of data supports this concept (reviewed in Lee and Surgh, 2009). The majority of generally accepted

oncogenes are characterised by the hyperactivation or expression at abnormally high levels in primary human cancers, and by capacity to induce a transformed phenotype in rodent cell lines cultured *in vitro* (usually NIH-3T3 or Rat1) (Lee, 2003).

Amplification of the 20q13 genomic region (*EEF1A2* maps to 20q13.3) is a frequent chromosomal alteration and number of putative oncogenes has been identified within this region. Increased copy number at this locus was documented in breast, ovarian, colorectal and lung cancers by CGH or FISH (Kallioniemi et al., 1994, Tanner et al., 1994, Suehiro et al., 2000, Aust et al., 2004, Zhu et al., 2007). Indeed, these tumours were associated with a worse survival prognosis and faster cancer progression (Isola et al., 1995, Tanner et al., 2000, Aust et al., 2004).

It seems that high eEF1A2 expression at the RNA and protein level is a common property in a large proportion of transformed cell lines, regardless of their tumour origin (Joseph et al., 2004, Tomlinson et al., 2005, Tomlinson et al., 2007, Cao et al., 2009). Joseph and colleagues performed studies of the eEF1A2 cDNA hybridization on a cancer profiling array which contained 241 paired samples of several tumours and normal tissues. It was revealed that the *EEF1A2* transcript was overexpressed by at least two-fold in 35% of colon, 24% of lung, 22% of rectum, 20% of kidney and 21% of ovary cancer cases when compared to the corresponding controls (Joseph et al., 2004).

Anand *et al*. demonstrated that 25% of primary ovarian tumours exhibited *EEF1A2* amplification and high eEF1A2 expression at the RNA level was seen in around 30% of ovarian tumours and ovarian cancer cell lines. No detectable *EEF1A2* transcript was reported in normal ovarian epithelium. Moreover, forced expression of eEF1A2 in NIH-3T3 and Rat1 fibroblasts resulted in colony formation in soft agar, accelerated growth rate and foci formation, respectively. NIH-3T3 and ES-2 clear cell carcinoma lines generated to express eEF1A2 were reported to form tumours when the cells were injected into nude mice (Anand et al., 2002). In addition, microarray analysis of gene expression from 113 ovarian epithelial tumours showed *EEF1A2* to be upregulated in clear cell carcinoma by an average 4-fold over other major histological types of ovarian cancer (Schwartz et al., 2002). In another study, 33% of all ovarian

tumours tested overexpressed *EEF1A2* at the mRNA level. Expression of eEF1A2 was associated with the clear cell tumour subtype and eEF1A2 upregulation at both, RNA and protein level was present in up to 75% of ovarian clear cell carcinomas (Tomlinson et al., 2007). Furthermore, Pinke and colleagues reported that the eEF1A2 protein was highly expressed in 32% of the 500 primary ovarian tumours tested in a tissue microarray but respectively 50% and 30% of these were of serous and endometrioid type. Ectopic expression of eEF1A2 in SK-OV-3 clear cell carcinoma line led to enhanced proliferation *in vitro* and allowed tumour-like spheroids to develop in hanging drop culture (Pinke et al., 2008).

Kulkarni *et al*. determined that high protein and mRNA expression of eEF1A2 occurs in up to 60% of primary breast tumours. They suggest that high eEF1A2 expression may coincide with an increased probability of 20-year survival, therefore this could serve as a prognostic outcome marker of breast cancer (Kulkarni et al., 2007). In studies of Tomlinson *et al*., eEF1A2 was shown to be barely detected at the mRNA level in normal human breast tissue or benign breast tumours whereas it was expressed up to 30-fold higher in malignant breast tumours. About 63% of breast tumours that were subjected to immunohistochemistry analysis displayed a significant overexpression of eEF1A2 protein (Tomlinson et al., 2005).

Strong upregulation of eEF1A2 at the protein level was also found in 83% of pancreatic cancer tissues whereas there was little expression in normal pancreas or chronic pancreatitis tissues. Moreover, the SW1990 pancreatic adenocarcinoma cell line with ectopic expression of eEF1A2 showed accelerated growth and proliferation, increased invasion and migration *in vitro* and development of tumours when the line was xenografted in nude mice (Cao et al., 2009).

In a gene profiling study of four newly established lung adenocarcinoma cell lines (HKULC1-4), *EEF1A2* was shown to be significantly overexpressed when compared to normal bronchial epithelial cells (Lam et al., 2006). Moreover, quantitative RT-PCR analysis performed on normal lung tissue and 27 primary lung adenocarcinomas revealed a substantial increase in *EEF1A2* expression by 127.9-fold

in tumours (Zhu et al., 2007). Using simultaneous CGH, transcript microarray and mass spectrometry analysis of six lung adenocarcinoma cell lines, Li *et al*. identified four genes (*PRDX1, EEF1A2, CALR* and *KCIP-1*) in which increased protein expression was in agreement with elevated DNA copy number and mRNA transcripts. In addition, specific inhibition of eEF1A2 in four of these cell lines reduced their proliferation rate and led to increased apoptosis. When immunohistochemical analyses of eEF1A2 expression were performed on a tissue microarray with samples from pathologic stage I non-small-cell lung cancer patients, its presence was confirmed in 28% cases (but note that antibody that detects both eEF1A forms was used). Expression of eEF1A2 was associated with a shorter survival time (Li et al., 2006). As *PRDX1* amplification and expression are both elevated in this study alongside *EEF1A2* and also, the corresponding proteins were found to act synergistically against the peroxide-induced death of NIH-3T3 cells through Akt modulation (Chang and Wang, 2007), it is possible they block apoptosis in a similar manner in lung cancer. It is noteworthy that overexpression of eEF1A2 was seen in a large proportion of primary lung tumours (Julia Boyd, unpublished observations).

Increased expression of *Eef1a2* transcript was also reported among unique primary B cell lineage neoplasms of mice-plasmacytomas (PCT) (Li et al., 2010). Moreover, elevated levels of *EEF1A2* were found in human multiple myeloma (MM, human plasma cell neoplasm) but very high levels of the eEF1A2 protein were seen only in 15% of primary MM samples. They were tested alongside normal bone marrow plasma cells and non-transformed precursors to MM, known as the monoclonal gammopathy of undetermined significance (MGUS). It was shown that expression of the *EEF1A2* transcript gradually increased during the progression of normal plasma cells to MGUS and then to MM. Elevated levels of eEF1A2 were also a hallmark of a subset of the mouse PCT and human MM origin cell lines. In addition, silencing of the *Eef1a2* transcript and protein in PCT cell lines was associated with reduced growth, probably due to a delayed cell cycle entry from G1/G0 to S and these cells were sensitive to apoptosis only upon serum withdrawal (Li et al., 2010).

1.5.3 Oncogenicity mechanism of eEF1A2

The mechanism by which eEF1A2 contributes to oncogenesis remains elusive. For other genes, overexpression seems to be result of gene amplification but this cannot be considered as a general cause behind tumourigenicity of the eEF1A2. In Anand *et al*. studies of primary ovarian tumours overexpressing eEF1A2, one of three samples displayed elevated *EEF1A2* expression but had no increase in gene copy number (Anand et al., 2002). In the Tomlinson study there was no correlation between gene expression and copy number at the *EEF1A2* locus, suggesting the existence of an alternative mechanism that mediated upregulation (Tomlinson et al., 2007). Also, increased amplification of the *EEF1A2* gene was seen in ovarian tumours that did not express eEF1A2. In fact, sequencing of the gene from low copy number tumours has shown no activating mutations or mutations leading to eEF1A2 upregulation. In addition, no correlation between expression and methylation status of the gene was observed (Tomlinson et al., 2007). Similarly, in the few cases of mouse plasmacytomas, overexpression of *Eef1a2* was not due to increased copy number or mutation of the *Eef1a2* coding sequence (Li et al., 2010).

It is yet not clear why eEF1A2 drives oncogenesis in tissues where eEF1A1 is so highly abundant. It was shown in eEF1A2-overexpressing ovarian and pancreatic tumours that levels of the *EEF1A1* transcript remained unaffected (Anand et al., 2002, Cao et al., 2009) but there is no information available about protein expression status in these samples. In general, at least two possible explanations have been suggested to solve the role of eEF1A2 in tumourgenesis.

Firstly, the mechanism of oncogenicity might be associated with the canonical function of eEF1A2 in translational elongation. Thornton suggested that eEF1A2 might lead to a straightforward increase in overall protein synthesis, resulting in elevated proliferation (Thornton et al., 2003). It is not clear whether tumours with upregulated eEF1A2 would have a greater protein synthesis capacity since eEF1A is already in excess over the other translation elongation machinery components (Slobin, 1980)

and it is rather initiation that is a limiting step of translation (Hershey, 1991). In fact, increased elongation rate in *S. cerevisiae* was linked to an elevated level of translational errors (Song et al., 1989, Carr-Schmid et al., 1999). Alternatively, upregulated eEF1A2 could specifically promote the expression of proteins associated with growth activation or apoptosis inhibition (like c-Myc or Bcl-2) thus following the oncogenicity-driving mechanism of eIF4E (Thornton et al., 2003).

Secondly, regardless of the 92% identity at the amino acid level between eEF1A variants (Soares et al., 2009), it has been suggested that both forms might perform only subtly or completely distinct noncanonical roles, therefore eEF1A2 could enhance oncogenesis independently of the translation network (Anand et al., 2002, Kulkarni et al., 2007). For instance, this notion would fit with the opposite role of eEF1A variants in apoptosis where eEF1A2 was anti-apoptotic and the opposite was true for eEF1A1 (Ruest et al., 2002, Chang and Wang, 2007).

Alternatively, the cytoskeletal modifying properties of eEF1A could be the next possibility to explore. Amiri *et al.* reported that eEF1A2 expression increased the formation of spike shaped structures called filopodia in rodent and human cells (Amiri et al., 2006). These cell membrane protrusions consist of parallel actin bundles and are critical for cell migration or invasion (Chodniewicz and Klemke, 2004, Yamaguchi et al., 2005). This increase in eEF1A2 expression caused elevated motility and invasion of the BT-549 breast cancer cell line *in vitro* (Amiri et al., 2006). Moreover, they found that the capacity of eEF1A2 to promote filopodia formation is phosphatidylinositol-3 kinase (PI3K) and Akt kinase dependent, although no direct physical interaction between them and eEF1A2 was confirmed (Amiri et al., 2006, Jeganathan et al., 2008). On the other hand, eEF1A1 was confirmed as a binding partner for Akt2 (Lau et al., 2006) and eEF1A was identified in the phosphorylated Akt kinase interactome of breast cancer cells (Pecorari et al., 2009). Several lines of evidence led to the conclusion that PI3K/Akt signalling is linked to tumourigenesis due to its role in cell proliferation stimulation, actin filaments remodelling abilities and apoptosis suppression (Martelli et al., 2006, Vivanco and Sawyers, 2002, Bunney and Katan, 2010).

Amiri *et al.* suggest that the ability of eEF1A2 to regulate actin rearrangement and to activate Akt may occur through phosphoinositide-dependent signalling (Amiri et al., 2006).

Furthermore, eEF1A2 was also shown to directly bind to PI4KIIIβ in rodent and human cells and to increase its lipid kinase activity *in vitro*. An increase in intracellular phosphatidylinositol 4-phosphate (PI4P) abundance was also reported upon overexpression of eEF1A2 in Rat2 and BT-549 cells (Jeganathan and Lee, 2007). PI4P is a regulatory precursor for $PI(3,4)P_2$, $PI(4,5)P_2$ and $PI(3,4,5)P_3$ which are well known products of PI3K and PI4K-driven phosphorylation and also the second messengers that regulate actin cytoskeleton organization, proliferation and apoptosis (Pendaries et al., 2003, Bunney and Katan, 2010, Martelli et al., 2006). Jeganathan and co-workers hypothesize that high levels of eEF1A2 in tumours might lead to activation of PI3K or PI4KIIIβ, followed by the accumulation of the cellular pool of phosphoinositides and stimulation of filopodia formation, sufficient to execute the neoplastic phenotype of the cells (Jeganathan and Lee, 2007, Jeganathan et al., 2008).

There is also some evidence that eEF1A2 might be dependent on microRNA (miRNA) expression alterations. Over the last decade, these 20-24 nucleotide long noncoding RNAs have emerged as significant regulators of many biological processes, including cellular proliferation, apoptosis or differentiation timing. miRNAs target sites in the 3'UTR and posttranscriptionally regulate gene expression by either repressing/activating translation or promoting mRNA degradation (Chekulaeva and Filipowicz, 2009). Malfunction of the expression pattern of miRNAs is associated with most malignancies and, depending whether they are down- or upregulated, miRNAs can act as tumour suppressors or as oncogenes (Esquela-Kerscher and Slack, 2006). Dahiya and colleagues identified eEF1A2 as a plausible candidate for let-7f regulation because when this miRNA was overexpressed in BG-1 ovarian cancer cell line, there was an over 500 fold increase in *EEF1A2* transcript expression (Dahiya et al., 2008).

1.6 Hepatocellular carcinoma

A recent epidemiological study has shown that liver cancer was the sixth common malignancy around the world but ranked as third as a cause of death. An estimated 748 000 new cases and approximately 695 000 deaths appeared in 2008 (Ferlay et al., 2010b). Estimates of liver cancer incidence and mortality in 2008 for Europe were 60 200 and 60 100, respectively (Ferlay et al., 2010a). Approximately 24 120 new cases of liver cancer are expected to occur in the USA during 2010, accompanied by an estimated 18 910 deaths. More than 80 % of the primary liver cancer cases in adults are qualified as hepatocellular carcinoma (HCC) (American Cancer Society, 2010). Incidence and mortality rates are more common among men than women (Ferlay et al., 2010b). The occurrence of HCC varies distinguishably between geographical areas due to differences in risk factors. Approximately 80% of new HCC incidents are identified in developing countries, especially in sub-Saharan Africa, and East and Southeast Asia. There is a lower incidence in areas of Northern and Western Europe as well as North America, however the numbers of HCC new cases in Europe and the USA are increasing, partially due to elevated levels of hepatitis C virus (HCV) infections (Wong and Ng, 2008).

The most prominent risk factors linked to the development of HCC are chronic hepatitis B virus (HBV) and HCV infections, alcohol abuse or consumption of aflatoxin B1-contaminated food. Other etiological causes are also implicated in HCC, including tobacco smoking, obesity and some diseases like diabetes, hereditary haemochromatosis or non-alcoholic fatty liver disorder (NAFLD) (Farazi and DePinho, 2006).

Hepatocarcinogenesis is considered as a multistep and long process (Figure 1.3). Liver injury is followed by inflammation, accompanied by continuous rounds of destruction and proliferation of hepatocytes, resulting in chronic liver disease. Such cycles of necrosis and regeneration increase the risk of spontaneous mutations due to an insufficient time to repair altered DNA and ultimately, accumulation of these changes leads to uncontrolled growth of hepatocytes and activation of stellate cells. Eventually, stellate cells produce extracellular matrix as a scaffold for development of

liver fibrosis – a prerequisite step before cirrhosis. In cirrhosis, abnormal nodules gradually progress to dysplastic nodules and finally to HCC (Michielsen et al., 2005, Farazi and DePinho, 2006).

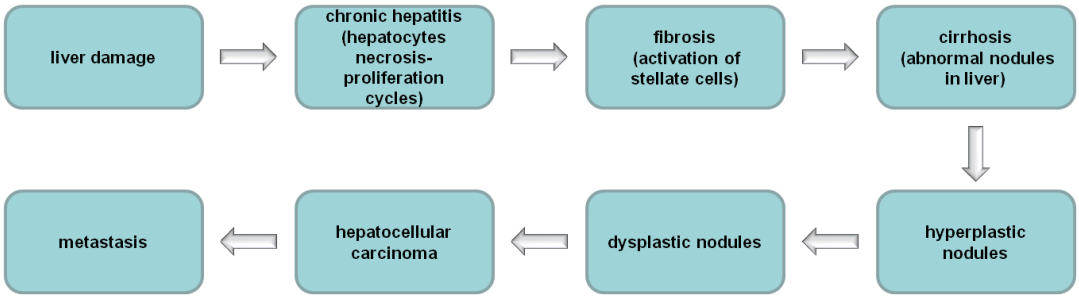

Figure 1.3 Diagram of hepatocellular carcinoma progression. Model was adapted and modified from Farazi and DePinho, 2006.

Progressive changes during hepatocellular malignancy develop not only as a result of cellular transitions, but also due to genetic alterations, chromosomal aberrations or changes in signalling pathways. The Wnt/β-catenin network is frequently deregulated in HCC which developed due to HBV/HCV infections and alcohol abuse mediated cirrhosis. In such cases, mutations in β-catenin prevent its phosphorylation, ubiqitination and proteasome degradation, regardless of the activation status of the Wnt pathway. Here, β-catenin accumulates in the nucleus and induces transcription of cell differentiation- and proliferation-related genes like *MYC* or *CJUN* (Aravalli et al., 2008, Whittaker et al., 2010). In many HCC cases, CGH studies have shown DNA copy number losses at 1p, 4q, 6q, 8p, 13q and 17p and gains on 1q, 6p, 8q, 17q or 20q chromosomal arms (Farazi and DePinho, 2006).

A large proportion of HCC cases usually develops on a background of chronic hepatitis or cirrhosis but there are also incidents of aflatoxin-induced liver malignancy (Thorgeirsson and Grisham, 2002). Aflatoxin B1 (AFB1) is a secondary metabolite of *Aspergillus flavus* and its ingestion elevates the risk of HCC development. Approximately 28.2 % of HCC cases worldwide are cases associated with toxin

consumption. The risk of AFB1-mediated HCC increases upon concomitant exposure to HBV infection, especially in regions of rural Africa and Far East (Liu and Wu, 2010, Farazi and DePinho, 2006). AFB1 induces a specific mutation in the p53 tumour suppressor gene (one nucleotide substitution in codon 249). This particular mutation is characteristic for early events in HCC, and it is seen also in malignancy-free areas of liver chronically exposed to toxin. Mutations of *TP53* in non-AFB1-induced cases are associated with late progression of hepatocarcinogenesis and were identified in dysplastic nodules (Liu and Wu, 2010, Zender et al., 2010).

The most potent causes of liver cirrhosis worldwide are the chronic intake of high dosages of alcohol and viral HBV/HCV infections. Frequent consumption of ethanol is thought to drive liver damage by the induction of inflammation or by oxidative stress. In the former situation, circulating metabolic toxins activate the release of chemokines and cytokines (TNFα, IL1β, IL6, prostaglandin E_2) by Küpffer cells and this promotes higher sensitivity of hepatocytes to the cytotoxic effect of TNFα. This exposes them to chronic necrosis-regeneration cycles, induction of stellate cells and finally cirrhosis. Oxidative stress contributes to HCC not only by lipid peroxidation-induced damage of hepatocytes, culminating in liver fibrosis, but also by compromising the IFNγ-mediated activation of STAT1 and protection of hepatocytes (signal transducer and activator of transcription 1) (Farazi and DePinho, 2006).

The risk of HCC incidence is elevated up to 15- and 17-fold in chronic HBV and HCV-infected patients, respectively. About 20-30% of chronic carriers will develop hepatic cirrhosis in a 20-30 year period (Tsai and Chung, 2010). HBV and HCV are indirectly linked to HCC initiation by propagation of liver inflammation and frequent necrosis-regeneration cycles, or directly by viral-host protein interactions and integration into the hepatocyte genome (Michielsen et al., 2005).

HCV, as an RNA virus, does not integrate into the host genome. Proteins of the viral core induce the overexpression of TGFβ which in turns leads to elevated fibrosis and the risk of cirrhosis (Farazi and DePinho, 2006). Incorporation of HBV DNA into host genomes accounts for up to 90% of HBV-mediated HCC cases and it is commonly

associated with microdeletions. Such integration occurs at sites linked to cell signalling regulation, proliferation or viability. Telomerase reverse transcriptase (*TERT*), plateled-derived growth factor receptor (*PDGFR*), mitogen activated protein kinase 1 (*MAPK1*), 60S ribosomal protein genes or cyclin A2 are common genetic targets of HBV integration. Additionally, HBV incorporates its own gene sequence - *HBx* (hepatitis B protein x) whose product interacts with p53 or propagates *TP53* transcriptional repression. As a result, viral infection leads to a decrease in apoptosis, compromised cell cycle regulation and faulty DNA damage repair. HBx is also responsible for the transactivation of several signalling networks, including PI3K, JAK/STAT, Wnt or JNK (Tsai and Chung, 2010).

1.7 Malignant melanoma

Abnormal proliferation of epidermal melanocytes gives rise to melanocytic naevi, malignant lesions and finally to cutaneous malignant melanoma (CMM). Melanocytes reside within the basal layer of the epithelial surfaces and arise from a population of migratory embryonic cells called neural crest cells. Melanocytes specialise in production, storage and transfer of melanin pigments to the surrounding epithelium (Uong and Zon, 2010). Most melanomas present on the skin but tumours can also occur in other tissues, including the inner ear, uveal tract of the eye or oral and sinus mucosa (Houghton and Polsky, 2002). CMM occurrence continues to increase worldwide, however the highest numbers are reported for Australia, New Zealand, North America and Northern Europe (Parkin et al., 2005). According to the most recent GLOBOCAN estimates, approximately 197 000 new cases were diagnosed with CMM and an estimated 46 000 deaths occurred due to this malignancy in 2008 (Ferlay et al., 2010b). In 2008, incidents and mortality for Europe were 84 000 and 20 100, respectively (Ferlay et al., 2010a). In the USA, approximately 68 000 people are expected to be diagnosed and about 8700 will die from malignant melanoma of the skin in 2010 (American Cancer Society, 2010). Even though CMM accounts for 3% of skin

cancers, it is associated with the highest mortality among all skin-related malignancies (Cummins et al., 2006a). It occurs more frequently in females than males and women have better survival prognosis (Parkin et al., 2005).

Development of CMM is predominantly associated with prolonged exposure to the sun and other sources of ultraviolet radiation. Also, people with high sun sensitivity, a history of sunburns and extensive skin damage, compromised immune system and family history of CMM are in a higher risk group. Specific ethnic background determines predisposition to CMM, frequently among populations with light pigmentation of eyes, hair and skin, for instance in patients of the Central or Northern European ancestry. Approximately 30% of CMM develop from acquired or congenital melanocytic naevi and the risk increases with the number of observed skin lesions or alterations in their appearance (Cummins et al., 2006a).

The 'ABCDE' clinical system states for **a**symmetry, **b**orders (and surface) irregularities, **c**olour, **d**iameter (>6mm), **e**volving and facilitates screen for abnormal moles. Subsequent evaluation of the biopsy from suspicious lesions is necessary for the correct diagnosis and eventual treatment. Detection of melanoma as early as possible is crucial for cure and survival (Goldstein and Goldstein, 2001). There are four major groups of CMM: superficial spreading melanoma (the most common type with prolonged horizontal growth phase), lentigo maligna melanoma (a less aggressive type which occurs on highly sun-damaged areas of skin), nodular melanoma (the second most common and the most aggressive type with extremely short radial growth) and acral lentiginous melanoma (characteristic in populations with dark skin pigmentation) (Cummins et al., 2006a, Goldstein and Goldstein, 2001).

The generally accepted model of the melanoma progression (Figure 1.4) states that abnormal proliferation of melanocytic clones could promote the assembly of benign or dysplastic naevus (atypical mole). Overcoming cell senescence would subsequently lead to an *in situ* melanoma which is defined by radial growth. The radial growth phase is characterised by horizontal spreading of transformed melanocytes within the epidermis along with small clusters of invasive cells present in the upper part of the

dermis. If left untreated, this can promote the vertical growth phase, defined by deeper invasion through the dermis and subcutaneous tissue. Reaching metastasis in distant sites is a culminating point where, for example, suppression of apoptosis is highly required (Houghton and Polsky, 2002, Zabierowski and Herlyn, 2010).

Figure 1.4 Schematic model of linear melanoma progression. RGP-radial growth phase, VGP-vertical growth phase. The cartoon was adapted and modified from Zabierowski and Herlyn, 2008.

The cumulative sequence of genetic and molecular changes is suggested to complement the pathologic mechanism underlying melanocytic transformation. Alterations in the mitogen-activated protein kinase signalling maintain increased proliferation across the linear progression phase of melanoma. Mutagenic activation of the MAPK network is seen in up to 90% of melanomas, mostly due to mutations in *NRAS* or *BRAF*, which occur in a mutually exclusive manner. Activating *NRAS* mutations are common in about 26% of sporadic melanoma cases. Somatic *BRAF* missense mutations account for 60-70% of all melanoma cases and in about 90% of these, a single substitution of valine for glutamic acid at position 600 is the most common. The V600E mutation keeps BRAF constitutively activated, which in turn promotes continuous MEK/ERK signalling in cells without assistance of extracellular stimuli. The *BRAF* and *NRAS* mutations are as common in benign naevi as in melanoma, suggesting that they promote melanocytic proliferation and growth arrest but are not sufficient to fully activate malignant transformation, see review (Palmieri et al., 2009, Meyle and Guldberg 2009, Fecher et al., 2007).

The overcoming of the cellular senescence is the next step to facilitate neoplastic transition. The *CDKN2A* (cyclin-dependent kinase inhibitor 2A) gene encodes two proteins via alternative splicing: $p16^{INK4a}$ and $p14^{ARF}$ which function as tumour

suppressors in two separate pathways. Deletions, mutations or hypermethylation of the *CDKN2A* promoter are responsible for the gene inactivation in the vast majority of the melanoma cases. Hence, loss of the CDKN2A function leads to serious alterations in the Rb and p53 networking. The $p16^{INK4a}$ blocks CDK4 (cyclin-dependent kinase 4) complex-mediated phosphorylation of the retinoblastoma protein. As a result, activated Rb binds and represses the E2F transcription factor, and cell cycle transition from phase G1 to S is held. Alternatively, $p14^{ARF}$ complements the $p16^{INK4a}$ –mediated senescence barrier by interacting with the murine double minute 2 protein (MDM2), hence stabilizing p53. MDM is an ubiquitin ligase which targets p53 for proteasome degradation. C*DKN2A* is also recognised as a melanoma susceptibility gene and mutations of the gene are frequently reported in patients with a strong family history of melanoma (~10% of familial cases). The pentrance of the *CDKN2A* mutations depends on UV exposure and geographical location. *CDK4* is implicated as a second melanoma susceptibility gene. Germline mutations of *CDK4* (R24C, R24H) are very rare and are carried only by a small number of melanoma-predisposed families across the world. These substitutions are most commonly seen among somatic mutations of *CDK4* and they affect binding of CDK4 protein to $p16^{INK4}$ (Palmieri et al., 2009, Meyle and Guldberg 2009, Fecher et al., 2007).

When pre-melanoma cells overcome the senescence barrier, suppression of apoptosis is the next level in facilitating the vertical growth and metastasis phases. Phosphatase and tensin homolog deleted on chromosome 10 (PTEN) is a negative regulator of the PI3K/Akt signalling pathway. PTEN promotes dephosphorylation of PIP_3 through the lipase phosphatase activity. Loss of this tumour suppressor gene was reported in 5-20% of uncultured melanomas and in 30-50% of melanoma cell lines. Somatic mutations of *PTEN* were found in 10-20% of primary melanomas and 40-60% of melanoma cell lines. Inactivating mutations of *PTEN* and activating mutations in *NRAS* were reported be rare within the same tumour, thus it is likely they function mutually exclusively. The inactivation of PTEN by deletions or mutations leads to constant activation of the PI3K network and mediates malignancy. In a study of 548

melanoma cases and 548 benign neavi samples, PI3K expression was shown to be higher in CMM and metastatic cases than in naevis, indicating an association of PI3K with late tumour progression. Activating mutations in the p110 alpha subunit of *PI3K* occurred in 1% of primary melanomas and 3% of melanoma metastases, but amplifications of PI3K subunits have not been confirmed by array CGH so far. IHC studies showed overexpression of phospho-Akt in about 54% of naevi and in 71% of primary and metastatic melanomas. Increased expression of phospho-Akt was associated with tumour progression and lower survival rate. Akt3 is the predominantly overexpressed Akt variant found in CMM. The complete overview of genetic alterations and pathways linked to melanoma can be found in reviews above.

Interestingly, about 26-50% of CMM was reported to originate from naevi, indicating that melanoma can arise from skin of normal appearance, regardless of the linear model of progression and corresponding genetic alterations. An alternative hypothesis states that transformed melanocytic stem cells or melanocyte progenitors are precursors of melanoma. Interaction of precursors with the tumour microenvironment might promote their transition directly into normal, benign or transformed and metastatic melanocytic cells, without occurrence of intermediates (Zabierowski and Herlyn, 2010).

1.8 Colorectal cancer

According to the 2008 worldwide cancer statistics, tumours of the colon and rectum were ranked third in terms of incidence (1 233 000 new cases) and were the fourth most common cancer-related mortality in 2008 (608 000 deaths). The highest incidence rates were observed in regions of Australia/New Zealand and Western Europe. Colorectal cancer occurs more frequently in men than in women (Ferlay et al., 2010b). In 2008, estimates for Europe predicted 435 000 new cases and 212 000 deaths (Ferlay et al., 2010a). The American Cancer Society expects approximately 142 000 new cases and 51 000 deaths associated with colorectal cancer in the USA in 2010 (American Cancer Society, 2010).

The risk of colorectal cancer (CRC) development increases with age and more than 90% of cases are diagnosed in patients of at least 50 years old. Increased risk is associated with obesity, type 2 diabetes, a family history of CRC or polyps, inherited genetic mutations, physical inactivity, alcohol abuse, smoking and a diet high in red meat. A large proportion of CRC cases (~95%) are classified as adenocarcinomas (American Cancer Society, 2010). In the vast majority of cases primary CRC is sporadic but inherited factors accounts for about 15% of cases (Kinzler and Vogelstein, 1996). Germline mutations are the genetic basis for either familial adenomatous polyposis coli (APC) syndrome or hereditary non-polyposis colorectal cancer (HNPCC) (Markowitz et al., 2002).

Colorectal cancers evolve over several years through a series of chronological events known as the 'adenoma-carcinoma' sequence (Figure 1.5). It starts from the transformation of epithelial cells lining the lumen of the colon or rectum, followed by the formation of aberrant crypt foci, then larger adenomatous lesions and finally, the progression to invasive cancer. Importantly, this sequence of phenotypic alterations throughout tumour development is complemented by a repertoire of genetic changes (Markowitz et al., 2002).

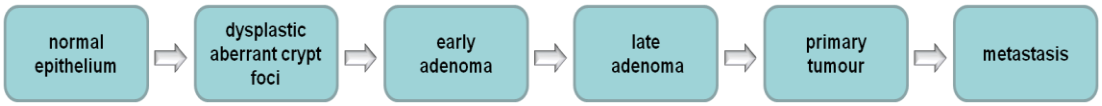

Figure 1.5 Colorectal cancer progression. Diagram of adenoma-carcinoma series was taken and modified from Markowtiz et al., 2002.

At least two genetic characteristics have been identified: chromosomal instability (CIN) and microsatellite instability (MSI), which can be also supplemented by CpG island methylation phenotype (CIMP). Colorectal tumours might display a combination of these features, however CIN and MSI correlate inversely (Pino and Chung, 2010).

CIN is reported in about 75% of CRC sporadic cases and refers to losses/gains of the whole or just fragments of the chromosome. CIN can be associated with defects

in the spindle checkpoint genes like *hMAD* (mitotic arrest-deficient) or *hBUB* (budding uninhibited by benzimidoazoles) and subsequent mis-segregation of chromosomes. Apart from karyotypic aberrations, accumulation of mutations in tumour suppressor genes and oncogenes is characteristic for CIN and crucial for pathology of CRC (Pino and Chung, 2010). APC is a tumour suppressor of Wnt signalling-mediated transcription as it catalyzes the ubiquitin-dependent degradation of β-catenin. Germline inactivating mutations in *APC* are responsible for APC syndrome and carriers have almost a 100% risk of developing CRC by 40 years of age. Importantly, somatic mutations and deletions occur in about 70 % of non-familiar CRCs. On this occasion, APC mutations are frequently carried in aberrant crypt foci and adenomas which indicate that functional loss of the gene is associated with early events of CRC development. In addition, hypermethylation of the *APC* promoter was reported in 18% of adenomas and primary CRCs (Pino and Chung, 2010, Markowitz et al., 2002). The second key genetic event in CRC is mutational inactivation of *TP53* and loss of its function was seen in up to 26% of early adenomas, 50% of late adenomas and 75% of CRCs, suggesting that such dysfunction is coupled to adenoma-invasive carcinoma transition (Pino and Chung, 2010).

Many colorectal tumours with MSI have unaffected APC expression. Instead, they exhibit mutations in β-catenin, which prevents its interaction with APC and subsequent degradation of β-catenin by proteasome (Boland and Goel, 2010). It is commonly accepted that aberrations in DNA mismatch repair genes are associated with the MSI phenomenon. Inability to repair errors within repetitive elements of the DNA sequence drives changes in the size of microsatellites stretches. MSI-mediated CRCs is observed in the majority of patients with HNPCC syndrome where mutations in the MMR (mismatch repair genes *MLH1*, *MSH2*, *MSH6* and *PMS2*) are germline transmitted or their second alleles are somatically inactivated (Balmana et al., 2010, Boland and Goel, 2010, Markowitz et al., 2002). Moreover, somatic inactivation of MMR genes was seen in approximately 15% of non-familial colorectal tumours.

Sporadic CRCs associated with MSI are frequently characterised by biallelic silencing of the *MLH1* promoter or absence of MLH1 and PMS2 proteins (Boland and Goel, 2010).

1.9 Field cancerization

Based on the studies of oral cancers, Slaughter introduced a new concept called 'field cancerization' (Slaughter et al., 1953). The term was proposed to explain the development of multiple primary tumours and occurrence of the second primary tumour sites following surgery of the initial carcinoma. Field cancerization has been described in a large proportion of tumour studies of the head and neck, lung, skin, breast, ovary, colon or bladder. It underlines the importance of an expanding preneoplastic field in epithelial carcinogenesis. Epithelial cells frequently undergo renewal and are commonly exposed to environmental factors or carcinogens. Consequently, they are predisposed to aberrant proliferation and initiation of genetically altered cancer fields, hyperplasia and finally tumours. The concept of field cancerization fits with the linear model of cancer progression where an accumulation of genetic alterations accompany transition from a normal cell to neoplasm.

The theory of field cancerization proposes that in the initial phase, a stem cell acquires genetic changes and forms a patch of daughter cells sharing a common genotype. The new genetic events facilitate conversion of patches into cells with a growth advantage which in turn develops into an expanding field. As the field grows, additional genetic hits propagate the formation of various subclones within the lesion. Following clonal divergence and selection, a subclone will eventually evolve into invasive cancer. Regardless of a cancer-negative outcome from biopsy evaluation, there is still a risk for growth of another malignancy if the field remains after surgical tumour resection. Field effect in skin neoplasms is associated with *TP53* mutations whereas a gradient of CEA expression (carcinoembryonic antigen) or epigenetic silencing of *MGMT* (O^6-methylguanine-DNA methyltransferase) are linked to field

effect in colorectal cancer. The concept of field cancerization is reviewed elsewhere (Braakhuis et al., 2003, Dakubo et al., 2007).

1.10 Project aims

The majority of studies on the involvement of the eEF1A in cancer have focused upon eEF1A2, but very little is known specifically about eEF1A1 and its eventual role in tumourigenicity. One of the main aims of this PhD project was to investigate whether eEF1A1 is capable of driving neoplastic transformation in a similar manner to eEF1A2 using rodent fibroblasts stably expressing eEF1A variants followed by a variety of different *in vitro* oncogenicity assays. The relationship between increased expression of two eEF1A forms and global protein synthesis rate was also determined in the stable cell lines in order to investigate possible mechanisms of oncogenicity. The final aim was to establish the distribution and expression pattern of eEF1A1 and eEF1A2 in liver, skin and colorectal cancers using commercial tumour arrays. The data obtained could be used to screen for possible associations with clinicopathological features and provide some insight into the role of eEF1A in these malignancies and its significance for diagnosis or therapy.

Chapter 2: Materials and methods

2.1 Materials

2.1.1 Buffers and solutions

A list of buffers and solutions that were used throughout this study, along with their corresponding recipes is presented in Table 2.1.

Table 2.1 *Review of solutions and buffers required for performing experiments within the project.*

NAME	COMPOSITION
10 x Laemmli running buffer	250 mM Tris-HCl pH 8.3 1.9 M glycine 10% (v/v) SDS
2 x Laemmli Sample Buffer	50 µl β-mercaptoethanol 950 µl Laemmli Sample Buffer (Bio-Rad)
3,3'-diaminobenzidine (DAB) solution (Vector Laboratories)	5 ml dH_2O 2 drops of buffer Stock Solution 4 drops of DAB Stock Solution 2 drops of the Hydrogen Peroxide Solution
Transfer buffer	25 mM Tris 192 mM glycine dH_2O up to 1 liter
Blocking buffer for Western blots	5% (w/v) Marvel dried skimmed milk 0.2 % (v/v) Tween 20, PBS
Citric acid solution for antigen retrieval in immunohistochemistry	0.1 M citric acid pH 6.0 dH_2O up to 1 liter
Clarke's fixative	Glacial acetic acid and methanol at the 1:3 ratio
Crystal violet solution	0.4 g of crystal violet 100 ml methanol
ECL solution (GE Healthcare)	Detection reagent 1and detection reagent 2 at the 1:1ratio

Freezing medium for liquid nitrogen stocks	10% (v/v) newborn calf serum 90% (v/v) DMSO
Labeling/Cell Detachment Mixture (Calbiochem)	3.25 µl Calcein-AM solution per 1 ml Cell Detachment Buffer
Lithium carbonate solution	67.7 mM lithium carbonate dH_2O up to 1 litre
Orange G loading buffer	30% (v/v) glycerol 100 mg Orange G dH_2O up to 50ml
Peroxidase blocking solution	2 ml of 30% (v/v) hydrogen peroxide solution 2.5 ml of 10 % sodium azide dH_2O up to 400 ml
Phosphate Buffered Saline (PBS)	1 PBS tablet (Sigma) 100 ml dH_2O Autoclaved, stored at 4^oC
Radioimmuno- precipitation assay (RIPA) buffer	50 mM Tris-HCl pH 7.5 150 mM sodium chloride 1% (v/v) NP-40 0.5 % (w/v) sodium deoxycholate 0.1% (v/v) SDS 1 tablet of Protease Inhibitor Cocktail (Roche) dH_2O up to 10 ml Stored at -20^oC after tablets were added
Membranes stripping buffer	10% (v/v) SDS 0.5 M Tris-HCl pH 6.8 0.8 % (v/v) β-mercaptoethanol dH_2O up to 100 ml
TBE (Tris-Borate-EDTA)	90 mM Tris-Borate, 2 mM EDTA pH 8.0
TE buffer	10mM Tris-HCl pH 8.0 1mM EDTA

2.1.2 Antibodies

In order to carry out this project, a wide range of different antibodies was used in various applications. A review of the antibodies used along with their working solutions for each type of assay can be found in Table 2.2.

Table 2.2 *List of antibodies together with conditions for performing Western Blotting (WB) and immunohistochemistry (IHC).*

NAME/TARGET	COMPANY	SOURCE	APPLICATION AND DILUTION
Anti-goat biotynylated	Dako	Rabbit	IHC 1:500
Anti-goat HRP	Dako	Rabbit	WB 1:1000-4000
Anti-mouse HRP	Dako	Rabbit	WB 1:1000
Anti-rabbit HRP	Dako	Goat	WB 1:1000
EF1A1-1	Custom (Helen Newbery[1])	Sheep	WB 1:400 IHC 1:10
EF1A1-3	Custom (Helen Newbery)	Sheep	WB 1:400 IHC 1:40
EF1A2-1	Custom (Helen Newbery)	Sheep	WB 1:200 IHC 1:25
EF1A2-3	Custom (Helen Newbery)	Rabbit	IHC 1:10
GAPDH	Chemicon (Millipore)	Mouse	WB 1:30000
V5	Invitrogen	Mouse	WB 1:5000

1. Dr Helen Newbery is a Postdoctoral researcher working in Prof Cathy Abbott's group. A detailed procedure of obtaining of the anti-eEF1A1 and anti-eEF1A2 peptide antibodies is described in Newbery et al., 2007.

2.1.3 Primers

A list of the primers used throughout this project is shown in Table 2.3. Primers were designed with the Primer3 programme (Rozen and Skaletsky, 2000) or retrieved from RTPrimerDB (Lefever et al., 2009) and ordered from Invitrogen or Sigma. Upon arrival, all the primers were dissolved in dH_2O to a final concentration of 100 µM and stored at -20^{o}C until later use. Before amplification reactions, fresh working solutions (usually 5 µM unless specified otherwise) were prepared each time.

Table 2.3 *Primer sequences used for different PCR applications.*

NAME	TARGET	SPECIES	SEQUENCE 5' TO 3'
mTBP F	TATA-binding protein	Mouse	CCCCACAACTCTTCCATTCT
mTBP R	TATA-binding protein	Mouse	GCAGGAGTGATAGGGGTCAT
mB2MG F	β-2-microglobulin	Mouse	CATGGCTCGCTCGGTGACC
mB2MG R	β-2-microglobulin	Mouse	AATGTGAGGCGGGTGGAACTG
m18S F	18S ribosomal RNA	Mouse	CGGACAGGATTGACAGATTG
m18S R	18S ribosomal RNA	Mouse	CAAATCGCTCCACCAACTAA
mA1/3U F2	Eef1a1	Mouse	CGTGACATGAGGCAGACAGT
mA1/3U R2	Eef1a1	Mouse	GTGGCAGGTGTTAGGGGTAA
hA1/V5 F1	EEF1A1	Human	AAGTCTGCCCAGAAAGCTCA
hA1/V5 R	EEF1A1	Human	AGACCGAGGAGAGGGTTAGG
mhE2/3 1A1 F	eEF1A1	Mouse Human	GCCCCAGGACACAGAGACTT
mhE2/3 1A1 R	eEF1A1	Mouse Human	CCAGCTTCAAATTCACCAAC
Q m1A2 F	Eef1a2	Mouse	GCTCCAGGACACCGAGACTT
Q m1A2 R	Eef1a2	Mouse	GAGTGCGTGTTCCCGGGTT
Q h 1A2 R	EEF1A2	Human	AAGTCGCGGTGGCCGGGGGC
F3A2 (Qh1A2F)	EEF1A2	Human	GCGGAGGTATTGACAAAAGG
Q h1A2/V5 F	EEF1A2	Human	TAGGCGTCATCAAGAACGTG
QEF1A F2B	eEF1A	Human Mouse	CACATTGCCTGCAAGTTTGC
QEF1A R2	eEF1A	Human Mouse	GAGAAGCTCACAACACACATGGG
R1V5	V5 tag	-	AGACCGAGGAGAGGGTTAGG
A1 attB1	EEF1A1	Human	GGGGACAAGTTTGTACAAAAAAGCA GGCTTCACCATGGGAAAGGAAAAGA CTCATATC
A1 attB2	EEF1A1	Human	GGGGACCACTTTGTACAAGAAAGCT GGGTGTTTAGCCTTCTGAGCTTTCTG GGC

GAPDH F	GAPDH	Human Mouse	CATCACCATCTTCCAGGAGC
GAPDH R	GAPDH	Human Mouse	ATGACCTTGCCCACAGCCTT
M13 F	plasmids	M13	GTAAAACGACGGCCAG
M13 R	plasmids	M13	CAGGAAACAGCTATGAC

2.1.4 Plasmids

Plasmids that were used for cloning purposes are reviewed in Table 2.4.

Table 2.4 *Plasmids used for cloning and expression applications*

NAME	INSERT/NOTE	VECTOR	ANTIBIOTIC	SOURCE
pDONR221	-	pDONR221	kanamycin	Invitrogen
pDEST40	C-terminal V5/His tag	pDEST40	ampicillin, geneticin	Invitrogen
pcDNA3.1 GS	C-terminal V5/His tag	pcDNA3.1GS	ampicillin, zeocin	Invitrogen
4107346	*EEF1A1* complete coding sequence (IMAGE clone)	pDNR	chloramphenicol	GeneService
RG001792 (A2-V5)	*EEF1A2* complete coding sequence (GeneStorm Expression Ready Clone)	pcDNA3.1/GS	zeocin	Invitrogen
1.1-V5	5'UTR sequence from *EEF1A*1 in front of the *EEF1A1* complete coding sequence	pDEST40	geneticin	Julia Boyd[1]
2.1-V5	5'UTR sequence from *EEF1A2* in front of the *EEF1A1* complete coding sequence	pDEST40	geneticin	Julia Boyd
2.2-V5	5'UTR sequence from *EEF1A2* in front of the *EEF1A2* complete coding sequence	pDEST40	geneticin	Julia Boyd
1.2-V5	5'UTR sequence from *EEF1A1* in front of the *EEF1A2* complete coding sequence	pDEST40	geneticin	Julia Boyd
A1-V5	*EEF1A1* complete coding sequence	pDEST40	geneticin	Justyna Janikiewicz

1. Former Postdoctoral researcher in Professor Cathy Abbott's group

2.1.5 Cell lines

The cell lines used in this study are listed in Table 2.5.

Table 2.5 *Panel of cell lines used in different tissue culture applications*

CELL LINE NAME	SPECIES	CELL TYPE	MAINTENANCE MEDIUM	SOURCE
NIH-3T3	Mouse	Embryo fibroblast	DMEM+10% NBCS	ATCC
HeLa	Human	Cervical cancer epithelial	DMEM+10%FBS	ATCC
Rat 2	Rat	Embryo fibroblast	DMEM +10% FBS	ATCC
A2 7.2 **A2 9.6** **A2 10.2**	Mouse	Fibroblast; Stable cell line overexpressing EEF1A2 coding sequence	DMEM+10%NBCS+ 450 µg/ml zeocin	Justyna Janikiewicz
A1 3.2 **A1 8.6** **A1 10.2**	Mouse	Fibroblast; Stable cell line overexpressing EEF1A1 coding sequence	DMEM+10%NBCS+ 600 µg/ml geneticin	Justyna Janikiewicz
1.1-9 **1.1-23**	Mouse	Fibroblast; Stable cell line expressing 5'UTR of EEF1A1 and EEF1A1 coding sequence	DMEM+10%NBCS+ 600 µg/ml geneticin	Justyna Janikiewicz
2.1-1 **2.1-15** **2.1-18**	Mouse	Fibroblast; Stable cell line expressing 5'UTR of EEF1A2 and EEF1A1 coding sequence	DMEM+10%NBCS+ 600 µg/ml geneticin	Justyna Janikiewicz

2.2-1 **2.2-33** **2.2-52**	Mouse	Fibroblast; Stable cell line expressing 5'UTR of EEF1A2 and EEF1A2 coding sequence	DMEM+10%NBCS+ 600 µg/ml geneticin	Justyna Janikiewicz
1.2-2 **1.2-39** **1.2-59**	Mouse	Fibroblast; Stable cell line expressing 5'UTR of EEF1A1 and EEF1A2 coding sequence	DMEM+10%NBCS+ 600 µg/ml geneticin	Justyna Janikiewicz
pcDNA3.1GS control SCL	Mouse	Fibroblast; Control stable cell line expressing empty vector (pcDNA 3.1 GS)	DMEM+10%NBCS+ 450 µg/ml zeocin	Justyna Janikiewicz
pDEST40 control SCL	Mouse	Fibroblast; Control stable cell line expressing empty vector (pDEST 40)	DMEM+10%NBCS+ 600 µg/ml geneticin	Justyna Janikiewicz
EJTF2	Mouse	Fibroblast; Control stable cell line expressing H-Ras oncogene	DMEM+10% FBS	Lynne Marshall[1]
HT-1080	Human	Fibrosarcoma	DMEM+10% FBS	Abigail Wilson[2]

1. Lynne Marshall; Beatson Institute for Cancer Research, Garscube Estate, Switchback Road, Bearsden, Glasgow G61 1BD, UK

2. Abigail Wilson; University of Edinburgh, Molecular Medicine Centre, Western General Hospital, Crewe Road, Edinburgh EH4 2XU, UK

2.1.6 Tumour microarrays (TMAs)

A selection of commercially available TMAs used to investigate the expression of eEF1A forms is displayed in Table 2.6.

Table 2.6 *Commercial TMAs used in immunohistochemical assays*

COMPANY	TYPE OF TISSUE	NUMBER OF CORES/SLIDE
BioChain	Colon cancer	64
Folio BioScience	Liver cancer + normal liver tissue	41 + 37
Folio BioScience	Melanoma + normal skin	32 in duplicate + 8
Biomax	Melanoma + normal skin	40 + 8
Zymed	Colon cancer	20+20 cancer adjacent mucosa+20 remote mucosa from a normal colon epithelium
Accumax	Normal tissues: liver, lung, stomach, colon, brain, heart, kidney, breast, Fallopian tube, pancreas, spleen, skin	12

2.2 Methods

2.2.1 Cell culture

2.2.1.1 Maintenance of the cell cultures

For experiments and maintaining cultures, all the cell lines were grown in DMEM (Gibco) supplemented with 10% (v/v) of an appropriate serum (Gibco) and a suitable antibiotic unless stated otherwise in the text of this thesis. Usually, two types of serum were used, either New Born Calf Serum (NBCS) or Fetal Bovine Serum (FBS). Growing cells were kept at 37^{o}C in a 5% CO_2 incubator until they reached 90% confluence. After that, used media were aspirated; cells were washed once with prewarmed DBPS (Gibco) and incubated in 5 ml of trypsin (Gibco) for 5 minutes. Next, an equal volume of warm DMEM was added to the detached cells and the suspension was subjected to centrifugation at 1200 rpm for 5 minutes. The supernatant was discarded and the cell pellet was resuspended in 5 ml of fresh DMEM. Cells were split either 1 in 5 or 1 in 10 depending on the further assay or cell volumes required. Cells were grown in Cell Start T25, T75 or T175 flasks (Greiner Bio-One) in 10 ml, 25 ml or 50 ml of culture media, respectively. In a standard maintenance, cells were split every 3-5 days and kept growing until they reached passage number 20 when they were utilized.

2.2.1.2 Cell counting

Monolayers of growing cells were washed with DPBS and trypsinized. Subsequently, amounts of DMEM equal to amounts of trypsin were added to the flask and cells were collected in falcons for centrifugation (1200 rpm, 5 min). Next, cells were suspended in 5 ml of DMEM and 100 µl of the cell suspension were transferred to 9.9 ml of isoton (Beckman Coulter). Finally, cells were subjected to automatic counting by Coulter Counter Z2 series (Beckman Coulter).

2.2.1.3 Cryopreservation of the cell lines

In order to obtain liquid nitrogen stocks of the cultured cell lines, cells were maintained in T75 flasks and subjected to trypsinization as stated in 2.2.1.1. Next, cell pellets were suspended in 10 ml of 90% NBCS/10% DMSO mixture and transferred into 1ml screw cap CryoTube vials (Nunc). The tubes were wrapped in a paper towel, put into a polystyrene box and placed in the -70^{o}C freezer for 24 hours. Next day, the vials were moved to the liquid nitrogen tank for a longer storage.

2.2.1.4 Transfection by nucleofection

The Lonza Nucleofector system was used to incorporate DNA into the cells. Cells were grown at 37^{o}C in a 5% CO_2 incubator in DMEM supplemented with 10% of appropriate serum (Gibco) until 80-90% confluence was reached. Next day, cells were trypsinized and counted as described before (2.2.1.2).

Subsequently, 1x10^{6} cells were centrifuged at 900 rpm for 5 minutes and the pellet was suspended in one hundred microlitres of the appropriate Nucleofector Solution (as listed in Table 2.7). Next, the Nucleofector Solution/cell pellet mixture was added to approximately 5µl of plasmid DNA (1-5 µg) and then moved to the cuvette provided by Lonza. The cuvette was placed inside the Nucleofector machine and cells were electroporated using the appropriate programme.

After transfection, 500µl of prewarmed DMEM was added to the cuvette and cells were immediately transferred into a well of the 6 well-plate that already contained 1.5 ml of DMEM. Following transfection, cells were put back into the humidified 37^{o}C/5% CO_2 incubator until further usage.

Storing the cell suspension longer than 15 minutes in Nucleofector Solution was avoided due to possible reduction of cell viability and gene transfer efficiency. Cells with the addition of DNA and Nucleofector Solution but not subjected to electroporation or cells with electroporation but no DNA inclusion were used as controls.

Table 2.7 *List of the cell lines transfected by nucleofection and corresponding solutions required for efficient DNA delivery*

CELL LINE TYPE	NUCLEOFECTOR SOLUTION	NUCLEOFECTOR PROGRAMME
NIH-3T3	R	U-030
HeLa	R	I-013
Rat2	R	T-030

2.2.2 Methods for protein analysis

2.2.2.1 Protein extraction

To obtain whole cell lysates, cells were grown until reaching 80-90% confluence. Culture dishes were placed on ice. Next, cell culture maintaining medium was removed, cells were washed twice with ice-cold DPBS and depending on the cell volumes, 200-500 µl of the radioimmune precipitation buffer (supplemented with Complete Protease Inhibitor Cocktail, Roche) was added to the dish. Subsequently, cells were scraped from a dish surface and the cell suspension was transferred to the pre-cooled micro-centrifuge tubes. Tubes were then placed on a rotating wheel for 30 minutes at 4^{o}C for cell membranes disruption. After that, prospective extracts were centrifuged at 13000 rpm for 30 minutes. The pellet was discarded and the supernatant (proper cell lysate) was taken to -20^{o}C for storage until needed in further experiments.

2.2.2.2 Quantification of the protein concentration in cell lysates

Total protein concentration in cell lysates obtained as in 2.2.2.1 was determined by the Lowry method, using the Bio-Rad DC quantification system and compared with BSA standard curve.

To establish standard curve, a series of BSA dilutions in lysis buffer (range from 0-4 mg/ml) was prepared in triplicate. A mixture of 20 µl of reagent S per each milliliter of reagent A was combined in advance to produce reagent A1. Next, 10 µl of each standard dilution was added to dry tubes, followed by 50 µl of reagent A1 and 400 µl of reagent B and mixed immediately. Tubes were left aside for fifteen minutes at room temperature and absorbance was read at 750 nm. In order to produce the standard curve, the absorbance value for each BSA standard was plotted against the standard concentration.

To quantify protein concentration in the whole cell lysates, exactly the same procedure was followed with all reagents. The value of absorbance from the cell extract was then plotted on the standard curve and its protein concentration was obtained.

2.2.2.3 Immunoblot analysis

2.2.2.3.1 Preparing samples

Fifty microlitres of β-mercaptoethanol were mixed with 950 µl of loading buffer (Bio-Rad) in advance. Usually, ten to fifteen micrograms of a total protein extract of known concentration (Section 2.2.2.2) was combined with loading buffer to obtain 20 µl final volume. In order to disrupt the protein complexes and denature proteins, samples were kept in a heat block for 5 minutes at 98^{o}C before being subjected to electrophoretic separation on a gel.

Control samples of wild type and wasted mouse tissues (brain, muscle, liver) were kindly provided by Yuan Cao, fellow PhD student.

2.2.2.3.2 SDS-PAGE electrophoresis

This assay was performed to separate proteins by molecular weight. Separating gel (10%) was prepared as follows (enough for 3 gels):

30% acrylamide	5.2 ml
1.5 M Tris-HCl pH 8.8	4.0 ml
dH_2O	6.68 ml
20% SDS	80 µl
25% AMPS	40 µl
TEMED	10 µl

The gel mixture was poured between two glass plates (Bio-Rad) up to 1 cm from the top edge and the remaining gap was filled with 100 µl of water. Next, gels were put aside at room temperature for at least 30 minutes to set. After that, water was aspirated off and replaced with 4.3 % stacking gel solution prepared as below (enough for 4 gels):

30% acrylamide	1.45 ml
0.5M Tris-HCl pH 6.8	2.5 ml
dH_2O	5.95 ml
20% SDS	50 µl
25% AMPS	50 µl
TEMED	5 µl

Subsequently, depending on the needs of the experiment, a comb of 10 or 15 slots was put on the top and the gels were put aside at room temperature for 25 minutes to set. After the gels were ready, the gel apparatus was assembled (Mini Protean 3, Bio-Rad) and filled with about 500 ml of 1x Laemmli running buffer.

The combs were removed and samples prepared as stated in Section 2.2.2.3.1 were loaded onto individual wells. The first well was always filled with 5-7 µl of the protein size marker (Full-Range Rainbow, Amersham, GE Healthcare). Next, separation was performed at 100V through stacking gel (15 minutes) and at 120V through separating gel until the blue dye front reached the bottom edges of the glass plates.

2.2.2.3.3 Western blot transfer

When the electrophoretic separation was finished, glass plates were disassembled and gels were placed in a tray with a transfer buffer. Six Whitman filter papers (7cm x 9 cm each) as well as two sponges per gel were prepared in advance and soaked in a transfer buffer. For each gel, a piece of Hybond-P PVDF transfer membrane

(Amersham, GE Healthcare) of 6 cm by 8 cm was cut and transferred to a dish containing methanol.

Next, a blot package was assembled on a plastic blotter as follows: first sponge, 3 sheets of the Whitman filter paper, gel, the membrane, 3 sheets of the Whitman filter paper, second sponge. The whole package was closed and placed into a transfer apparatus, filled with a transfer buffer; the apparatus also contained a magnetic stirrer and a pre-frozen ice pack. Transfer was then carried out at 100V/400A in a cold room for 70 minutes. Subsequently, the blotting package was disassembled, the membrane recovered and blocked either overnight or 1 hour at 4^{o}C in 5% (w/v) powdered milk/ 0.2% (v/v) Tween 20 in PBS.

2.2.2.3.4 Immunostaining

After blocking, the membrane was probed with a primary antibody, diluted to an appropriate concentration in 5% (w/v) powdered milk/ 0.2% (v/v) Tween 20 in PBS as listed in Table 2.2. The membrane was incubated for a minimum of 1 hour with gentle agitation before washing (5 minutes x 4) with cold PBS.

Next, the membrane was probed with a species-specific anti-immunoglobulin conjugated to horseradish peroxidase (DAKO) diluted in blocking buffer (Table 2.1), at room temperature for 1 hour. After washing in cold PBS (5 minutes x 4), immunoreactive bands on the membrane were visualized by the ECL Western blotting detection system (Amersham, GE Healthcare) according to the manufacturer's instructions.

2.2.2.3.5 Densitometric analysis

Selected pictures of the Western blot results were scanned into a computer and quantification of the signal intensity of the immunoreactive bands was measured using ImageJ software (Abramoff et al., 2004).

2.2.2.3.6 Re-probing the membranes

If membrane re-probing with a different antibody was necessary, it was washed in a cold PBS (10 minutes x 2) to get rid of the remaining ECL and transferred to a closed dish with stripping buffer (Table 2.1), prewarmed at 50^{o}C. This process was performed at 50^{o}C for up to 50 minutes with gentle agitation. Next, stripping solution was disposed of; the membrane was rinsed with cold PBS (10 minutes x 4) and blocked in 5% milk-PBS-0.2 % Tween20 solution before re-probing with a new antibody as described in Section 2.2.2.3.4.

2.2.2.4 Immunohistochemistry

To compare expression of both eEF1A variants at the cellular level in colon, skin and liver cancer, immunohistochemistry was performed on commercially available tumour microarrays (TMA). The slides used for this assay were paraffin-embedded and sometimes formalin-fixed as summarized in Table 2.6.

Sections were first deparaffinised twice with xylene for 5 minutes each time. Next, slides were rehydrated in a series of solutions for 5 minutes as follows: absolute ethanol x 2, 70% ethanol x 2 and washed in distilled water. In case of formalin-fixed slides, an additional step of incubation in picric acid was performed for 15 minutes, followed by washing in distilled water. Subsequently, slides were subjected to antigen retrieval by microwaving sections in citric acid at pH 6, cooling, and then washing in running tap water and loaded onto Shandon ® Sequenzas (Thermo Scientific).

For immunohistochemistry with primary antibodies raised in rabbit, slides were washed with PBS for 5 minutes, treated with peroxidase blocking solution (Table 2.1) for 5 minutes and washed again with PBS for 5 minutes. Next, sections were incubated with 100 µl of goat serum (diluted 1:5 in PBS) for 10 minutes and then 100 µl of

primary antibody at an appropriate concentration (in PBS) were applied for 30 minutes (or overnight). Sections were washed in PBS and three drops of Dako REAL EnVision Detection System solution (Dako Cytomation) were added onto each slide. Slides were incubated for 30 minutes at room temperature and then washed with PBS for 5 minutes.

Alternatively (when primary antibodies were raised in sheep), after the antigen retrieval step, sections were treated with 3% hydrogen peroxide for 10 minutes on a rocker in order to remove endogenous hydrogen peroxidase activity and then washed in a running water for 5 minutes. Next, slides were incubated for 10 minutes in 100 µl of blocking serum. Serum was diluted 1 in 5 in PBS and came from the same animal species as the secondary antibody was raised in. Then sections were incubated with an appropriate concentration of the primary antibody for 30 minutes (or overnight), followed by washing with PBS and then incubation with 100 µl of biotynylated secondary antibody (Dako Cytomation). After washing slides with PBS for 5 minutes, three drops of Vectastatin R.T.U. *Elite*® ABC Reagent (Vector Laboratories) were added per slide and treated at a room temperature for another 30 minutes. Sections were then again washed in PBS for 5 minutes.

Next, no matter which of the above methods was performed, slides were unloaded from Sequenzas, put on a tray and treated with diaminobenzidine solution (Table 2.1) for 2 minutes that was applied to cover the whole section. The slides were washed with water, counterstained in haematoxylin and lithium carbonate solution. Sections were later dehydrated in series of the solutions (70% ethanol, absolute ethanol x 2), cleared in xylene twice and mounted in pertex.

The slides were viewed by light microscopy on Olympus BX51 and pictures were captured using DP software (Olympus) or on Olympus BX60 with capturing pictures by Cell* Imaging Software (Olympus).

All antibody dilutions were prepared in PBS and the required concentrations are listed in Table 2.2. Slides treated with no primary antibody but just with biotinylated secondary antibody or Dako REAL EnVision Detection System solution were used as negative controls.

Immunohistological scoring was performed by two independent researchers. For each core on the TMA, the score based on the staining strength was established as 3 when staining was strong, as 2 when staining was moderate, as 1 when staining was low and 0 when staining was negative. The percentage of a tumour tissue (excluding stroma) was then evaluated for each score type. Results were obtained by multiplying the percentage of a tumour tissue in each of the staining categories by the score they were assigned to (1, 2 or 3) and then these values were summarized to give a maximum score of 300.

2.2.3 Molecular biology

2.2.3.1 RNA extraction

Cell pellets were collected from cultured cells straight after centrifugation (Section 2.2.1.1) and either kept on ice for immediate use or stored at -70^{o}C until needed. Total RNA from cell line pellets was extracted with the help of the RNeasy Mini Kit (Qiagen) as recommended by the manufacturer. During extraction, RNA was treated for 15 minutes with DNase I (Qiagen) to exclude any DNA contamination.

RNA concentration (ng/µl) in samples was assessed using a NanoDrop® 1000 device (Fisher Scientific) and the absorbance was measured at 230 nm (the blank was the buffer that RNA was dissolved in).

2.2.3.2 Synthesis of cDNA

In order to synthesize cDNA, First Strand cDNA Synthesis Kit for RT-PCR (Roche) and 1 µg of RNA were used. The reaction mixture was prepared as follows:

10 x Reaction Buffer	2.0 µl
25 nM Magnesium chloride	4.0 µl
Deoxynucleotide Mix	2.0 µl
Random primers	2.0 µl
RNase Inhibitor	1.0 µl
MV Reverse Transcriptase	0.8 µl
RNA sample	depending on concentration
dH_2O	up to 20 µl

Next, the following set of incubation steps was performed:

Step 1	25^{o}C	10 minutes
Step 2	42^{o}C	60 minutes
Step 3	99^{o}C	5 minutes
Step 4	4^{o}C	5 minutes

Samples that contained reaction mixture but no RNA, or one that included RNA but no AMV reverse transcriptase were used as negative controls and were subjected to the same procedure as other samples. When reactions were finished, samples were stored at -20^{o}C until later use.

2.2.3.3 Polymerase chain reaction and associated methods

Depending on experimental requirements and assay purposes, different PCR systems were set.

2. 2. 3. 3. 1 PCR with Phusion polymerase

Most of the cloning reactions were performed with proof-reading Phusion High-Fidelity DNA Polymerase (Finnzymes) in order to obtain a high accuracy of the resulting templates for further analysis. All steps of setting up the reactions were performed on ice. A reaction mixture was prepared as listed below:

dH_2O	up to 20 µl
2 x Phusion™ Master Mix	10 µl
Primer 1 (0.25 µM)	1.0 µl
Primer 2 (0.25 µM)	1.0 µl
Template cDNA or plasmid	1.0 µl
DMSO (optional)	0.6 µl

The reactions were then processed on a thermal cycler with the following conditions:

Step 1	x 1	98^{o}C	2 minutes	Initial denaturation
Step 2	x 25-28	98^{o}C	10 seconds	Denaturation
		X^{o}C	30 seconds	Annealing
		72^{o}C	**X**	Extension
Step 3	x 1	72^{o}C	1 minute	Final extension
Step 4	x 1	4^{o}C	5 minutes	

The temperature of annealing depended on the primers' melting temperature (Tm). Usually the range was between 55-63^{o}C and for primers > 20 nucleotides annealing was performed at a Tm +3^{o}C of the lower Tm primer. For primers ≤ 20 nucleotides, an annealing temperature equal to the Tm of the lower Tm primer was used. As for extension time, this depended on the amplicon length and complexity. As a basic rule for this polymerase, it was determined that a time of 15 seconds was efficient for extension of a 1 kb DNA fragment. Resulting products were kept at -20^{o}C until further use or loaded onto agarose gels to confirm presence of the specific bands of a desired size.

2. 2. 3. 3. 2 PCR with *Taq* Polymerase

In a routine PCR amplification, each reaction was prepared as follows:

10x PCR buffer	2.5 µl
10 mM dNTPs mixture (0.2 mM each)	1.0 µl
50 mM $MgCl_2$	1.5 µl
Primer 1 (0.25 µM)	1.0 µl
Primer 2 (0.25 µM)	1.0 µl
Template DNA	1.0 µl
Taq DNA polymerase	0.4 µl
dH_2O	up to 25 µl

Every component of the mixture was purchased from Invitrogen. Subsequently, the tubes were processed on a thermal cycler with the programme established as listed below:

Step 1	x 1	94^{o}C	3 minutes
Step 2	x 30	94^{o}C	45 seconds
		55-60^{o}C	30 seconds
		72^{o}C	90 seconds
Step 3	x 1	72^{o}C	10 minutes
Step 4	x 1	4^{o}C	5 minutes

2. 2. 3. 3. 3 Real-time PCR

The accumulation of PCR product was detected by a fluorescent SYBR Green dye (Finnzymes). Primers were designed to amplify a template region of 100-180 bp and to be free of any secondary structures or complementarity presence (primer-dimer formation). Primers were also designed to possess a GC content of 50-60% and a melting temperature between 50 and 65^{o}C. Whenever possible, PCR primers were created at splice junctions to avoid producing a product from genomic DNA.

Reaction mixture was made up as follows:

2 x DyNAmo Flash Master mix	10 µl
Primer 1	final concentration of 0.1; 0.125; 0.25 or 0.5 µM
Primer 2	final concentration of 0.1; 0.125; 0.25 or 0.5 µM
cDNA	2.0 µl
dH_2O	up to 20 µl

No template sample (containing water and reaction mix), no Reverse Transcriptase sample and just dH_2O were used as negative controls.

Next, reactions were transferred to MyiQ Thermal Cycler (Bio-Rad) and the programme was run as follows:

Step 1	x 1	95^{o}C	6 minutes
Step 2	x 40	95^{o}C	10 seconds
		60^{o}C	20 seconds
		72^{o}C	20 seconds – data collection
Step 3	x 1	95^{o}C	1 minute
Step 4	x 1	60^{o}C	1 minute
Step 5	x 80	60^{o}C	10 seconds – data collection
		(Setpoint temperature was increased by 0.5^{o}C per each cycle for melt curve data collection and analysis)	

A standard curve was conducted as a series of control cDNA dilutions (1:10; 1:100; 1:1000; 1:10000 and 1:100000) for each pair of primers. In order to construct a standard curve, the logarithms of the particular RNA amounts were plotted along the x-axis and their respective C_t values for each dilution were plotted along the y-axis. Reaction efficiencies between 90-110% and $R^2 > 0.99$ were considered as acceptable for further analysis. The results of the reaction for each amplicon of interest were normalised against three reference genes: 18S rRNA, TBP and β-2-microglobulin. Real-time PCR results analyses were determined by a standard curve method to evaluate relative mRNA levels. All reactions were conducted in three technical repeats, in triplicate unless stated otherwise. The melting curve was performed at the end of each reaction to confirm specificity of the PCR products where a single sharp peak indicated a single amplicon.

2. 2. 3. 3. 4 Sequencing

2. 2. 3. 3. 4. 1 Pre-sequencing PCR

When PCR product rather than plasmid DNA was used as a template for further sequencing, it was subjected to a reaction with ExoSAP-IT (USB). Two microlitres of ExoSAP-IT were added per 5 µl of PCR product and incubation conditions were established at 37°C for 15 minutes, followed by 15 minutes at 80°C. Next, BigDye (Applied Biosystems) pre-sequencing PCR was performed as follows:

Reaction mixture

5x BigDye sequencing buffer	1.5 µl
2.5 x BigDye mastermix	1.0 µl
Primer (only one, forward or reverse)	1.5 µl
Template (PCR product, plasmid DNA)	3.0 µl
dH_2O	3.0 µl

Conditions of reaction in thermal cycler

Step 1	x 1	96°C	1 minute
Step 2	x 24	96°C	30 seconds
		50°C	15 seconds
		64°C	4 minutes
Step 3	x1	hold at 4°C until needed	

2. 2. 3. 3. 4. 2 Cleaning of pre-sequencing reaction products

When the reaction was finished, 2.5 µl of 125 mM EDTA was added strictly to the bottom of the each well, followed by 30 µl of absolute ethanol. Next, the plate was sealed and inverted 4 times to mix and then left for 15 minutes at a room temperature. Samples were centrifuged at 3000 rpm for 30 minutes; plates were put upside down

on a paper towel and then briefly spun down at 1000 rpm in order to remove most of the ethanol. After that, 30 µl of 70% ethanol was added to each well and centrifuged at 3000 rpm at 8^{o}C for additional 15 minutes. Plates were again inverted over the paper towel and centrifuged for the few seconds at 1000 rpm to remove the remains of the ethanol. Wells were left to air dry at room temperature before storing at -20^{o}C. The sequencing reactions were performed by Agnes Gallagher in the MRC HGU Unit.

2. 2. 3. 3. 5 Colony screening by PCR

In order to confirm the presence of a cloned insert in bacterial colonies, a set of PCR tubes was pre-filled with 5 µl of dH_2O. A single colony was touched with a fresh toothpick, which was then dipped into individual PCR tube. Usually, at least 15-20 colonies were randomly chosen for screening each time. Next, each PCR tube with individual clone was filled with 15 µl of PCR master mix and the amplification reaction was established as stated in Section 2.2.3.3.2.

Following screening, independent Falcon tubes filled with 5 ml of LB Broth (with suitable antibiotics) were inoculated with positively PCR-verified clones and left overnight at 37^{o}C incubator with the constant shaking. Mini-preps were prepared next day from 4.5 ml of broth cultures using QIAprep Spin Miniprep kit (Qiagen) as recommended by the manufacturer. The remaining 0.5 ml of the each culture was mixed with 0.5 ml of glycerol and stored at -70^{o}C as stock.

If necessary, the presence of the correct insert was additionally confirmed by sequencing mini-prep DNA as described in Section 2.2.3.3.4.

2. 2. 3. 3. 6 PCR product purification

Amplification reaction products were subjected to a direct purification process on the QIAquick columns with the help of the QIAquick PCR Purification Kit (Qiagen) according to the manufacturer's recommendations. Purified DNA was analyzed on an agarose gel.

2. 2. 3. 3. 7 Agarose gels

In order to confirm the presence of specific DNA bands and their correct size after PCR or to isolate a particular DNA fragment, agarose gels were prepared in advance. The concentration of agarose in 0.5 x TBE buffer (Table 2.1) varied from 0.9%-2% (w/v), depending on the expected size of the bands. Usually, when large DNA fragments were analyzed (3-10 kb), 0.9%-1.5% gels were prepared. In case of the small bands (0.2-1 kb), 2 % agarose gels were conducted. Agarose was weighted, mixed with 0.5 x TBE buffer and microwaved for at least 2 minutes to let agarose dissolve. Next, the solution was cooled and 5 µl of SYBR Safe (Invitrogen) were added per 100 ml of the mixture. It was then poured into a plastic tray with combs and left to set at room temperature. Subsequently, Orange G loading buffer (Table 2.1) was added to the samples to constitute 10% of the total sample volume and reactions were loaded onto a gel. Separated bands were compared to the 1kb or 50 bp molecular ladders (Invitrogen) loaded into the first well. The agarose gel was then run at 100V in a tank pre-filled with 0.5 x TBE running buffer until the frontal orange line was approximately 0.5 cm from the gel's edge. Bands on the gel were visualized under ultraviolet light using the UVIdoc Gel Documentation System (UVItec).

2. 2. 3. 3. 8 Purification of DNA from agarose gel

In order to extract and purify DNA after enzymatic reactions, samples were run on an agarose gel and then bands of the required size were excised. Subsequently, agarose fragments were dissolved and DNA was recovered with QIAquick Gel Extraction kit following the manufacturer's instructions (Qiagen).

2.2.3.4 Cloning techniques and associated methods

2. 2. 3. 4. 1 Generating of the C-terminally V5-tagged human eEF1A1 construct

To produce full-length eEF1A1 with the C-terminal V5 tag, cDNA was cloned into the pDEST40 vector using the Gateway Cloning System (Invitrogen). Full-length cDNA of human eEF1A1 was recovered by PCR (Section 2.2.3.3.1) from a corresponding Image clone (Table 2.4). Both primers were designed to include *attB* sites to facilitate recombination, followed by the Kozak sequence in forward primer and with reverse primer not containing a stop codon. The sequences of primers used, along with their names, are listed in Table 2.3. After amplification of the cDNA, PCR products were run on a 1% agarose gel (Section 2.2.3.3.7) to confirm expected size and purified with QIAquick PCR purification kit (Qiagen) as described in Section 2.2.3.3.8.

2. 2. 3. 4. 1. 1 BP recombination reaction

Purified PCR product was combined with pDONR221 donor vector and the BP reaction was conducted according to the manufacturer's instructions. In general, BP Clonase II enzyme mix would catalyze recombination between *attB* sites of the PCR product and *attP*-containing donor vector to produce an entry clone. One microlitre of each BP reaction was used to transform competent cells as described below. Clones were isolated from the plate and screened as listed in Section 2.2.3.3.5 to confirm the presence of the insert.

2. 2. 3. 4. 1. 2 Transformation of bacteria

One microlitre of recombination BP reaction mix was gently combined with TOP10 competent cells and left on ice for 30 minutes. After incubation, cells were heat-shocked for 20 seconds in a 42^{o}C waterbath and then cooled on ice for 2 minutes. After adding 250 µl of S.O.C. medium (Invitrogen) to the cells, they were next incubated for 2 hours at 37^{o}C in an Innova 4300 Incubator (New Brunswick Scientific)

with constant shaking at 180 rpm. Approximately 50 µl of bacteria were spread on the LB plate containing ampicillin (100µg/ml) and a dish was then left overnight at 37^{o}C incubator (Plus II, Gallencamp). The pUC19 DNA plasmid (Invitrogen) was used in the transformation protocol as above as a positive control.

2. 2. 3. 4. 1. 3 LR recombination reaction

Once the presence of a positive clone of eEF1A1 in pDONR221 was confirmed, LR Clonase II Enzyme mix was used according to the Invitrogen instructions in order to create an expression clone in pDEST40 destination vector. In a LR reaction, plasmid DNA from the mini-prep of the positive clone was combined with DNA of the vector and then used to transform competent bacterial cells as described above. Next, well developed colonies were isolated and screened as described in Section 2.2.3.3.5.

2. 2. 3. 4. 2 Plasmid preparation

In order to purify plasmid for applications like cloning, PCR or sequencing, mini-preps were prepared as described in Section 2.2.3.3.5.

If high yields of ultrapure DNA were needed (for example for mammalian cell transfections), 200 ml LB cultures of bacteria were centrifuged at 6000 rpm for fifteen minutes at 4^{o}C and the cell pellet was subjected to plasmid purification with the HiSpeed® Plasmid Maxi Kit (Qiagen) according to the manufacturer's instructions.

Eluted DNA was dissolved in TE buffer provided with each kit and retrieved samples were analyzed by agarose gel electrophoresis (Section 2.2.3.3.7). DNA concentration (ng/µl) in samples was assessed using the NanoDrop® 1000 device (Fisher Scientific) and absorbance was measured at 260 nm after blanking with TE buffer.

2.2.4 Cell culture assays

2.2.4.1 Generation of stable cell lines

2. 2. 4. 1. 1 Killing curve

In order to generate a stable cell line that will express the protein of interest from a mammalian expression construct, the minimum concentration of selection antibiotic required to kill untransfected host cell line (NIH-3T3) was determined. Cells were plated at 5 $x10^5$ cells per Ø 10 cm dish in 9 repeats and were grown for 24 hours. The medium was removed and DMEM containing varying concentrations of Zeocin™ or Geneticin® (G418) was added to each plate. Concentrations used in this assay were as follows: 0, 100, 200, 300, 400, 500, 600, 800 and 1000 µg/ml. Next, the selective medium was replenished every 3-4 days and the percentage of surviving cells was observed on each occasion. A concentration of 450 µg/ml for Zeocin™ or 600 µg/ml for G418 was established as the minimal one that kills majority of the cells within 2 weeks of culturing.

2. 2. 4. 1. 2 Selection of the stable transfectants

Cells were harvested and counted as described in section 2.2.1.2. One million cells were subjected to nucleofection with the gene of interest (Section 2.2.1.4). Two Falcon tubes containing 50 ml of pre-warmed DMEM+10%NBCS were prepared and a nucleofection reaction of total 600 µl was divided into those Falcons, 300 µl each. Next, 10 ml of the cell suspension were transferred to Ø 10 cm dish such that each of the ten plates contained $1x10^5$ cells in total. Cells were left to grow for 24 hours and the following day, medium was replaced with fresh DMEM+10% NBCS containing the determined concentration of a selective antibiotic. Cells were fed with selective medium every 3-4 days until distinct cell colonies started to appear after 2-4 weeks.

2. 2. 4. 1. 3 Isolation of the drug resistant clones

After clearly visible colonies developed, dishes were washed with DPBS and ten random, well separated clones on each plate were marked in a circle. Next, cloning discs (Sigma) were soaked in trypsin (Gibco) and each disc was put on the top of the marked colony. These were then left for 5 minutes at a room temperature in order to stick the cells to the discs. Discs containing colonies were transferred to the individual wells of the 96-well plate filled with selective medium in advance. Cells were grown in selective DMEM to near confluence before being shifted to the larger format dishes. The abundance of insert in every colony was confirmed by conventional Reverse Transcription PCR (Sections 2.2.3.2 and 2.2.3.3.1) as well as by Western blotting (Section 2.2.2.3).

2.2.4.2 In vitro tumourigenesis assays

2. 2. 4. 2. 1 Focus formation assay

Selected NIH-3T3 stable cell lines were harvested and counted as described previously (Section 2.2.1.2). $3x10^5$ cells were plated per Ø 10 cm dish and 10 ml of DMEM + 10% NBCS with the correct antibiotic concentration was added. Cells were fed every 3-4 days and kept growing for 3 weeks after reaching 100% confluence. After 3 weeks media were aspirated off, cells were washed with DPBS and incubated for 10 minutes with 4 ml of Clarke's fixative (Table 2.1). Next, the solution was removed and 4 ml of 0.4% (w/v) crystal violet solution was poured on the top of the cells for additional 10 minutes. Subsequently, dishes were washed several times with dH_2O and dried. Photographs of the stained cell surfaces and foci were documented on the Olympus BX60 microscope using the corresponding Cell* Imaging Software.

2. 2. 4. 2. 2 Colony formation assay

Assays of colony formation in soft agar were performed to assess the anchorage-independent growth ability of cells. Autoclaved select agar (1.2%; Sigma) was mixed with an equal volume of DMEM + 20% NBCS and poured into individual wells of a six-well plate resulting in a 0.6% base agar layer. Cells at a concentration of $1x10^5$ per well were suspended in 0.3% agar containing DMEM + 20% NBCS + the appropriate concentration of antibiotic (Zeocin™ or G418) and the mixture was immediately overlaid on the base layer of agar. Plates were left to grow for at least 3 weeks in the 37°C/5% CO_2 incubator and then subjected to counting of colonies. Colonies were documented on Axiovert200 (Zeiss) microscope with the QCapture software.

2. 2. 4. 2. 3 Cell migration assay

In order to study cell motility in response to a chemical attractant, the InnoCyte™ Cell Migration assay (Calbiochem) was performed following the manufacturer's recommendations.

Briefly, cells were harvested and counted as described in Section 2.2.1.2. A cell suspension of 3 x 10^5cells/ml was prepared in serum-free DMEM and 150 µl of DMEM + 10% NBCS were added to each well of the lower chamber. After the cell culture insert was assembled, 150 µl of the cell suspension was transferred to designated wells. The lid was replaced and the chamber was incubated overnight in a CO_2 incubator at 37°C.

The following day, 200 µl of the Labelling/Cell Detachment solution were transferred to the corresponding wells into an additional 96-well tray, provided by the manufacturer. The media were discarded from the upper compartment; the chamber was assembled with the additional tray and then incubated for 30 minutes in the 37°C/5% CO_2 incubator.

Next, the upper part of the migration chamber was tilted several times in order to facilitate dislodgement of the cells. The tray containing detached cells was covered with a lid and subjected to further incubation for 45 minutes.

After incubation, 150 µl from each well containing dislodged and labelled cells were transferred to corresponding wells of the black 96-well plate (Thermo Scientific) and the fluorescence values were retrieved at 485 nm excitation and 520 nm emission by fluorescent microplate reader (BioTek Synergy HT).

2. 2. 4. 2. 4 Cell invasion assay

In order to investigate the invasive capacity of the cells, InnoCyte™ Laminin-based 96-well cell invasion assay (Calbiochem) was conducted according to the manufacturer's instructions.

Briefly, 100 µl of serum-free DMEM was added to each compartment of the pre-warmed upper chamber in order to re-hydrate the laminin protein layer. After 30 minutes of incubation, media were aspirated off, the upper chamber was lifted and 150 µl of DMEM + 10% NBCS were added to each well of the lower chamber. When the chambers were assembled again, 150 µl of the cell suspension (3×10^5 cells/ml) were added to appropriate wells of the cell culture insert and the whole compartment was incubated overnight in the $37^oC/5\%$ CO_2 incubator.

The following day, 200 µl of the Labelling/Cell Detachment Mixture were transferred to the additional tray provided by the manufacturer, combined with upper chamber of the cell culture insert and incubated for 30 minutes in the $37^oC/5\%$ CO_2 incubator. Next, the upper chamber was tilted several times in order to facilitate dislodgement of the cells; the tray with cells was covered with a lid and subjected to further incubation for thirty minutes.

After incubation, 150 µl from each well containing detached and labelled cells were transferred to corresponding wells of a black 96-well plate (Thermo Scientific) and the fluorescence measurements were taken at 485 nm excitation and 520 nm emission using a fluorescent microplate reader (BioTek Synergy HT).

2.2.4.3 Proliferation assay with AlamarBlue®

AlamarBlue® (AbD Serotec) staining responds to the chemical reduction of medium by growing cells due to its oxidation-reduction indicator. Either fluorimetric excitation or emission contributes to the cell proliferation readout (Voytik-Harbin et al., 1998).

The assay was performed in a 96-well plate format during three independent experiments, within 5 small wells on the plate per cell line on every occasion. Readings were collected for 8 days.

Briefly, cells in the logarithmic phase of the growth were harvested and counted as described before (Section 2.2.1.2). The cell count was adjusted to obtain 2 x 10^3 cells in 150 µl of DMEM + 10% NBCS per well. Cells were then plated and on particular days exposed for 5 hours to the test agent in an amount equal to 10% of the volume in the well. Cell proliferation was measured using a fluorescent microplate reader (BioTek Synergy HT) with excitation at 530 nm and emission at 590 nm.

2.2.4.4 Protein synthesis assay

To measure the rate of protein synthesis (Welsh and Proud, 1992), cells of interest were counted (Section 2.2.1.2) and plated at 2x10^3 cells per well of a 24-well plate. Cells were left to grow overnight in a humidified 37^{o}C/5% CO_2 incubator. The following day, medium was discarded and replaced with 0.5 ml of the fresh DMEM without methionine and cysteine (Sigma). After 20 minutes of incubation, media was aspirated off and replaced with 0.5 ml of fresh DMEM (methionine and cysteine free) with Expre^{35}S^{35}S labelling mix (Perkin Elmer) in each well. Five microcuries of ^{35}S-Met and ^{35}S-Cys were added per 1 ml of medium. After 1 hour, the radioactive medium was discarded; cells were washed once with ice-cold DPBS and lysed in 0.5 ml of 0.2 % (v/v) SDS. Next, ice-cold trichloroacetic acid (TCA) was added to 20% (v/v), cells were scraped carefully and precipitated proteins were collected onto GF/C glass-fibre filters (Whatman). Each well was washed four times

with 1 ml of 10% (w/v) ice-cold TCA and then four times with 1 ml of 95% (v/v) ethanol. Subsequently, filters were air dried and subjected to liquid scintillation counting in 3 ml of Ecoscint 0 (National Diagnostics) using a LS6500 Multi-Purpose Scintillation Counter (Beckman Counter) in the MRC HGU unit.

Chapter 3: Characterization of eEF1A variants interactions at the mRNA and protein levels

3.1 Introduction

Eukaryotic translation elongation factor 1A plays a crucial role in protein synthesis as it catalyzes the first step of the elongation cycle. In its active GTP-bound state, eEF1A delivers aminoacylated tRNA to the A site of the ribosome. Two highly similar eEF1A variants, eEF1A1 and eEF1A2, act equally well in that process, however the latter one has more affinity for GDP than for GTP. Additionally, they also have been implicated in non-canonical functions like apoptosis and cytoskeletal remodelling. While the eEF1A1 form is almost ubiquitously expressed, the presence of the eEF1A2 variant is more limited. It is found in certain types of cells like neurons and muscle cells where eEF1A1 is down-regulated. Expression of both variants is observed only in tumours and cultured cell lines. Cell lines that only express eEF1A2 but not eEF1A1, do not exist to our knowledge.

In order to determine the effects of overexpression of eEF1A1 or eEF1A2 in cells, different constructs were designed for transfections. These include constructs with the full coding sequence of each variant or constructs with the coding sequence preceded by the 5'UTR from its own or the other variant. A structural hallmark of the eEF1A1 5'UTR is the 5' terminal oligopyrimidine tract (5'TOP sequence) which acts as a *cis*-regulatory element and which is not seen in the eEF1A2 5'UTR, therefore it was crucial to determine whether the lack of eEF1A2 translational repression via this mechanism has any link to cancer. Studies were performed on transiently and stably transfected NIH-3T3 mouse fibroblasts that do not express eEF1A2. Expression of exogenous constructs and their effects on endogenous forms of eEF1A were determined at the RNA and protein level.

3.2 Results

3.2.1 Generation and validation of expression constructs with eEF1A variants

In order to address the contribution of different eEF1A variants to cellular transformation, a panel of constructs was engineered in mammalian expression vectors (pcDNA3.1 or pDEST40). Constructs were designed to contain the full coding sequence of each human eEF1A variant preceded with its own or the reciprocal 5'UTR. Alternatively, plasmids that exclusively expressed the coding sequence of human eEF1A1 or eEF1A2 were also generated. Expression was driven by the CMV promoter of the vector and additionally, each construct was tagged with a COOH-terminal V5 epitope downstream of the cloned sequence. A schematic map of the constructs is shown in Figure 3.1.

Constructs of 1.1, 2.1, 2.2 and 1.2 were generated and sequenced by Dr Julia Boyd, a former member of Professor Cathy Abbott research group. Variants of A1, 1.1, 2.1, 2.2 and 1.2 were cloned into the pDEST40 vector. The A2 construct was purchased from Invitrogen as pcDNA3.1-EEF1A2 GeneStorm ready-to-express clone.

To determine whether the constructs could be expressed (before stable cell line generation experiments were conducted), NIH-3T3 mouse fibroblast cells were transfected independently by nucleofection either with the experimental construct or with an empty vector control (pcDNA3.1 or pDEST40). Samples for Reverse Transcription PCR along with Western blot detection were prepared from cells collected the day after nucleofection was performed.

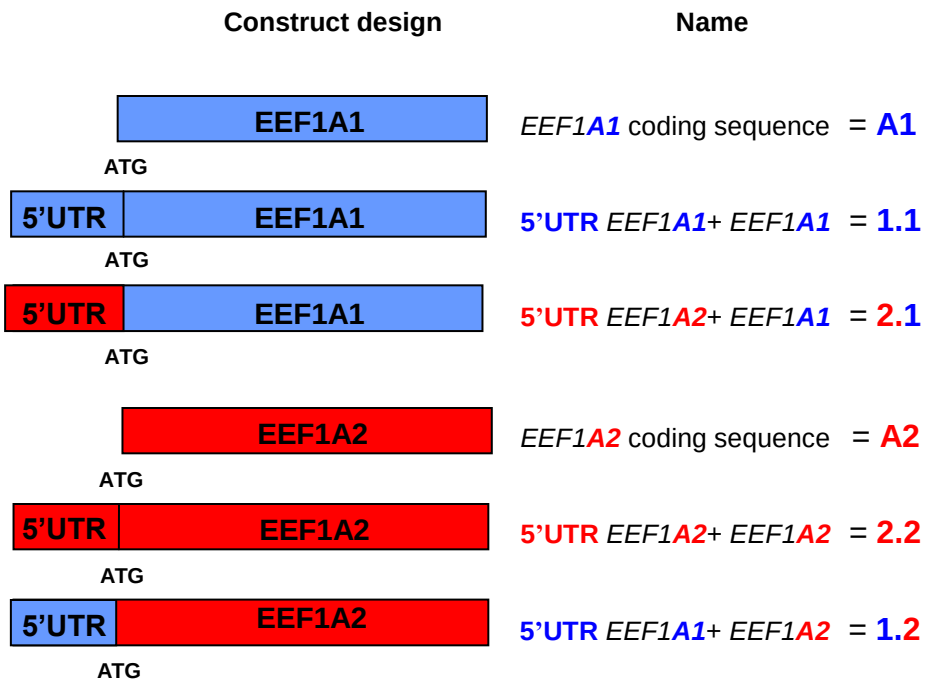

Figure 3.1 Diagram of eEF1A variant constructs. Specific regions of each expression construct are colour coded in **blue** for ***EEF1A1* origin** or in **red** for ***EEF1A2* origin**. Plasmids were designated A1 (*EEF1A1* coding sequence construct), 1.1 (*EEF1A1* coding sequence preceded by its own 5'UTR), 2.1 (*EEF1A1* coding sequence preceded by *EEF1A2* 5'UTR), A2 (*EEF1A2* coding sequence construct), 2.2 (*EEF1A2* coding sequence preceded by its own 5'UTR) and 1.2 (*EEF1A2* coding sequence preceded by the *EEF1A1* 5'UTR), respectively.

Reverse Transcription PCR was carried out using primers specifically designed to amplify regions within the coding sequence of *EEF1A1* or *EEF1A2* and the V5 tag. As shown in Figure 3.2, PCR results were the correct molecular size for A1 (125 base pairs), A2 (150 base pairs), 1.1/2.1 (800 base pairs) and 2.2/1.2 (410 base pairs). The empty vector transfected cells and untransfected NIH-3T3 cells, acting as negative controls, showed no amplification. Samples which were Reverse Transcriptase negative (RT-) or did not contain any cDNA were run to confirm lack of genomic DNA or reaction reagents contamination, respectively.

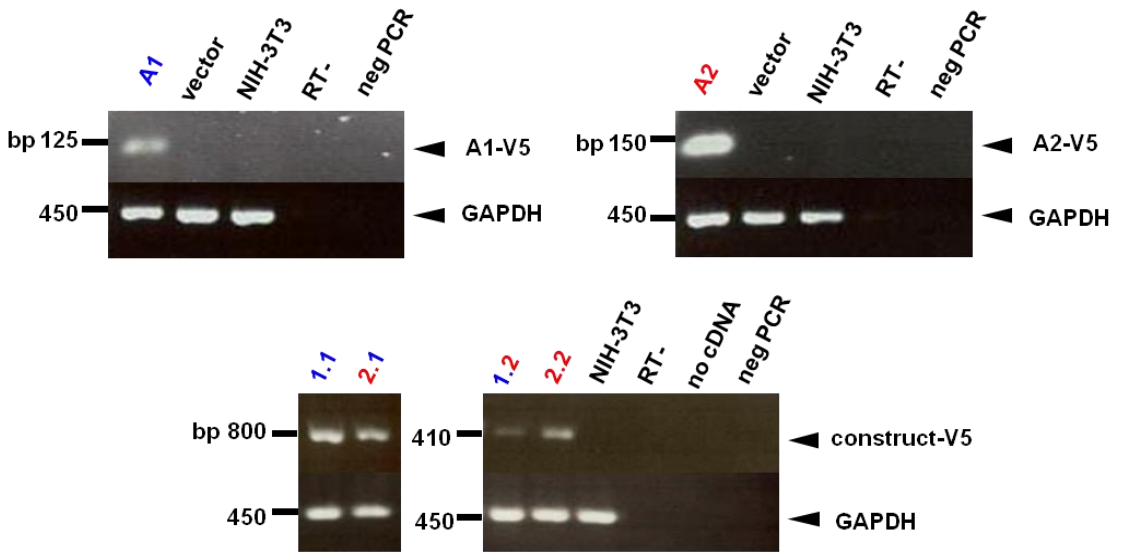

Figure 3.2 RT-PCR analysis of eEF1A variants expression in NIH-3T3 fibroblasts. Mouse fibroblasts were transfected with **A1**, **1.1**, **2.1**, **A2**, **2.2**, **1.2** and empty vectors (pcDNA3.1, pDEST40). Total RNA was extracted from cell pellets 24 hours after nucleofection in order to synthesize cDNA. Negative controls: RT- (no Reverse Transcriptase added for cDNA synthesis), no cDNA (no RNA added for cDNA synthesis) and neg PCR (negative PCR; only mastermix used in reaction). GAPDH was used as an internal control.

Immunoblot analysis of transfectants from different eEF1A1 plasmids was performed using anti-V5 tag or anti-eEF1A1 antibodies (Figure 3.3, panel A). Expression obtained with eEF1A2 construct variants was analysed by probing membranes with anti-V5 or anti-eEF1A2 antibodies as presented in Figure 3.3, panel B. Ectopic expression of proteins from mammalian plasmids was verified successfully for all constructs on membranes subjected to probing with anti-V5 antibody. As expected, a single major band was detected for tagged proteins of 52kDa molecular weight, whereas no bands were observed for parental cells or cells transfected with empty vector. This preliminary result suggests that incorporation of the 5'UTR from eEF1A2 in front of the eEF1A1 coding sequence results in increased expression when compared to the 5'UTR from eEF1A1, but not as robust as with eEF1A1 coding

sequence only. In contrast, eEF1A2 with its own 5'UTR was expressed more effectively than 1.2-V5 but not at as high a level as A2-V5 (without any 5'UTR).

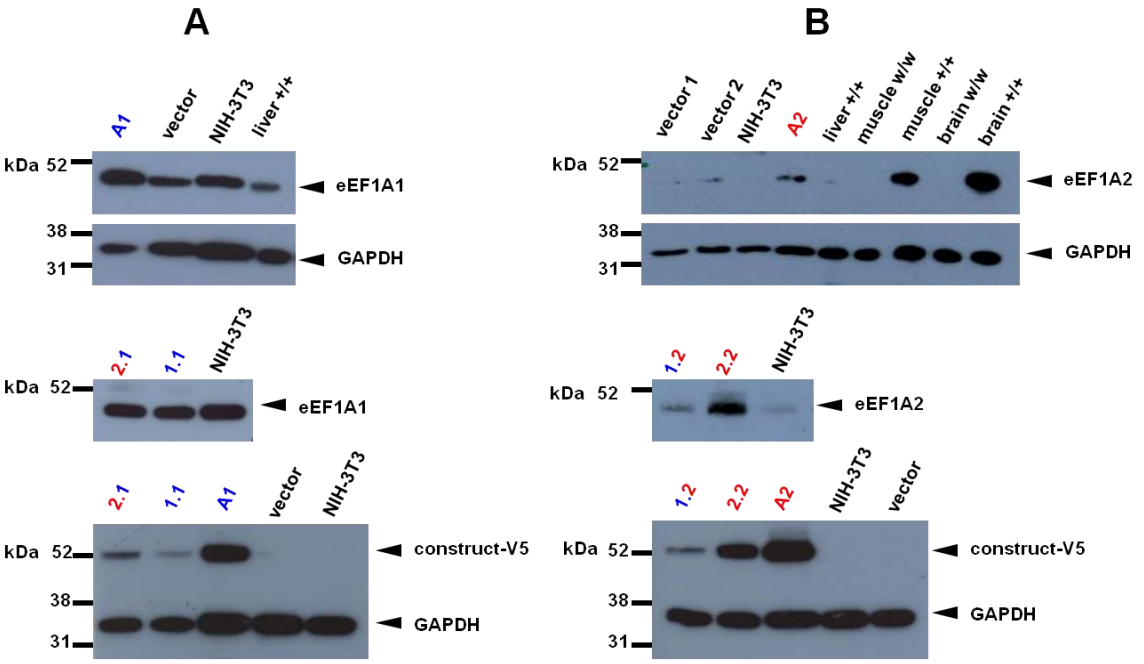

Figure 3.3 Overexpression of A1, 1.1, 2.1, A2, 2.2 and 1.2 variants in NIH-3T3 mouse fibroblasts. The lysates from the NIH-3T3 transfectants were subjected to Western blot. Detection of expression for eEF1A1 origin constructs is shown in the panel A, while the presence of eEF1A2 variants is exhibited in the panel B. Samples from untransfected parental cells along with NIH-3T3 cells transfected with empty vector were used as negative controls for V5 tagged constructs. Tissue extracts from wild-type mouse (27 day old) were used as indicators for positive expression of eEF1A1 (liver +/+) or eEF1A2 protein (muscle+/+, brain +/+). In contrast, tissue extracts from 25 day old wasted mouse (muscle w/w, brain w/w) and wild-type liver (liver +/+) were used as a negative control for eEF1A2 expression. GAPDH was used as a loading control.

Predicted protein products were also obtained with the anti-eEF1A1 and anti-eEF1A2 antibodies. These antibodies work equally well for proteins of human and mouse origin (Newbery et al., 2007). Whereas eEF1A1 levels were similar, eEF1A2 levels significantly increased when compared to almost undetectable endogenous expression in NIH-3T3 cells transfected with empty vector or parental cells.

Extracts from selected mouse tissues were used to demonstrate antibodies specificity, as described in Figure 3.3.

3.2.2 Generation of stable cell lines in NIH-3T3 mouse fibroblasts

Once it was demonstrated that the expression constructs produced the predicted protein products, NIH-3T3 mouse fibroblast cells were transfected by nucleofection with either one of expression plasmids (A1, A2, 1.1, 2.1, 2.2, 1.2) or the empty control vector (pcDNA3.1, pDEST40). Cells transfected with A2 and pcDNA3.1 vector were subjected to selection with Zeocin™ while cells transfected with the remaining plasmids were selected with G418® (geneticin).

Individual clones that appeared to be resistant to antibiotic selection were randomly isolated for each construct and grown further in order to obtain sufficient material for subsequent analysis. Cell lysates were then prepared and a total of 306 colonies were screened for positive expression of exogenous proteins by Western blotting against the V5-tag antibody. Only clones that exhibited a single band of 52kDa were considered as positive (data not shown). A comparison of the yield of stable cell lines for different eEF1A plasmids is presented in Table 3.1. While a few clones were positive for A1 (6/34, 18%), 1.1 (4/56, 7%) or 2.1 (10/48, 21%) expression, the majority of clones for A2 (38/52, 73%), 2.2 (47/56, 84%) or 1.2 (28/60, 47%) demonstrated expression.

Table 3.1 *Summary of stable cell lines generation efficiency in NIH-3T3 mouse fibroblasts*

Type of stable cell line		Number of clones analyzed	Number of eEF1A-V5 variant positive clones
eEF1A1	(A1)	34	6
eEF1A2	(A2)	52	38
5'UTR eEF1A1+eEF1A1	(1.1)	56	4
5'UTR eEF1A2+eEF1A1	(2.1)	48	10
5'UTR eEF1A2+eEF1A2	(2.2)	56	47
5'UTR eEF1A1+eEF1A2	(1.2)	60	28

For further analysis, a few clones that exhibited V5-specific bands were chosen and re-screened by RT-PCR and Western blot for confirmation before further experiments.

The results of screening for several representative clones of the three **eEF1A1** origin constructs (A1, 1.1 or 2.1) are shown in Figure 3.4. As expected, proteins of 52kDa were detected for **A1 clones** number 3.2 and 8.6 but to a lesser extent in clones number 10.2, 8.3, 6.4 and 4.6 (panel A). No expression was noticeable for clone designated as 1.3. A protein lysate sample collected from NIH-3T3 cells 24 hours post transfection with the A1 construct was used as a positive control. No detection was observed for NIH-3T3 or pcDNA3.1 vector transfected cell lines.

The majority of A1 clones exhibit mRNA of the expected molecular size (850 bp) while clones number 3.3, 3.4, 4.5 or 7.2 were negative for predicted transcripts (panel A). An artefact in gel running suggests uneven amounts of GAPDH PCR products for clones 1.1-3.4. It is noteworthy that even when mRNA levels are high, for example in clone 1.3, 6.4 or 8.3, the protein levels for these clones remain from very low to undetectable.

Analysis of representative **1.1 clones** is shown in Figure 3.4, panel B. A fifty two kilodalton protein was detected in all four clones (panel B), with the lowest expression level for clone number 1.1-54. The presence of exogenous transcripts was also confirmed at the mRNA level by detecting a 740 bp product.

Results from the investigation of representative **2.1 clones** are presented in Figure 3.4, panel C. Four (2.1-9, 2.1-15, 2.1-18 and 2.1-27) out of five clones were positive for 52kDa exogenous protein expression while clone 2.1-21 was negative (but note that GAPDH results suggest uneven loading). The same four clones gave a 740 bp fragment at the mRNA level. RT-PCR products for clone 2.1-21 and RT- sample were run on a separate gel.

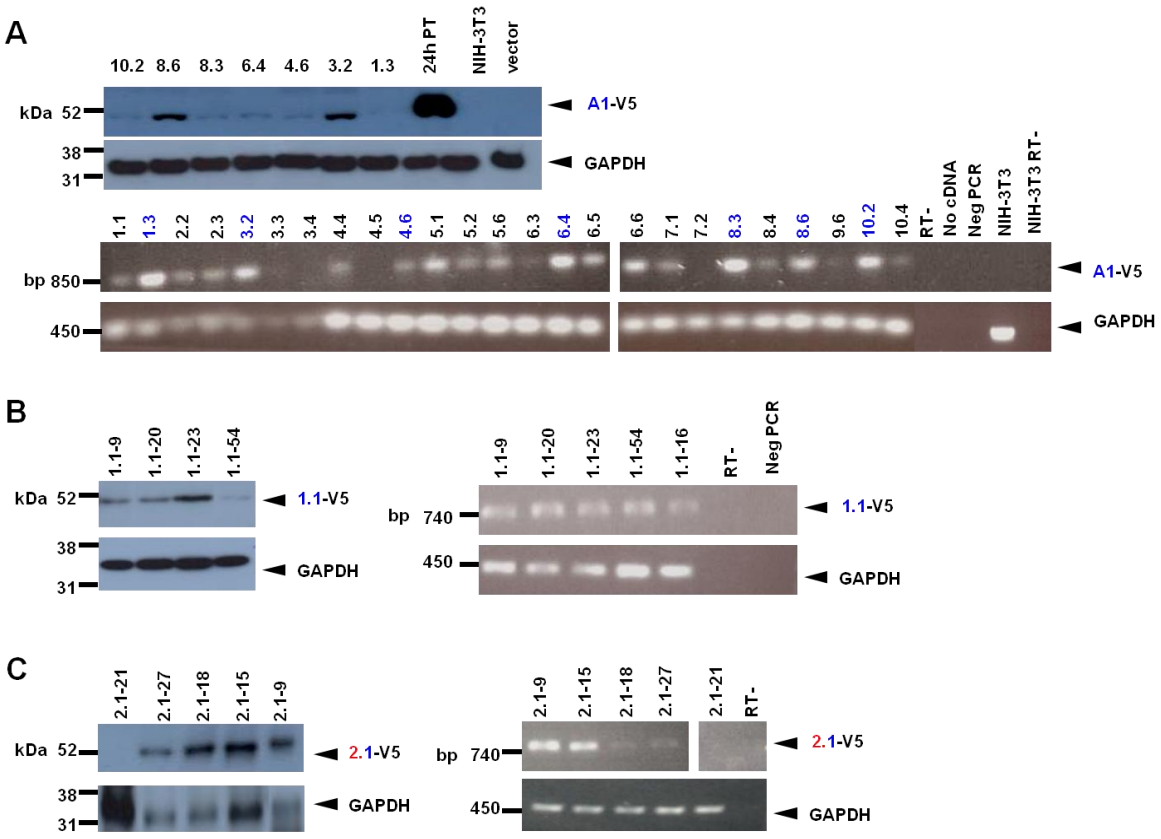

Figure 3.4 Verification of stable cell lines generated with eEF1A1 expression plasmids in NIH-3T3 mouse fibroblasts. Pictures reflect several representative clones for each construct. Detection of **A1** (panel A), **1.1** (panel B) and **2.1** (panel C) plasmids was assessed by immunoblotting with anti-V5 tag antibody and Reverse Transcriptase PCR. Parental NIH-3T3 cells and vector transfected cells were used as negative controls in Western blots. Negative controls in RT-PCR were: minus Reverse Transcriptase (RT-), no template samples (no cDNA), PCR mastermix sample (Neg PCR) and parental cells. GAPDH was used as an internal control. The first digit in the names of the A1 construct clones represent the plate from which clone was isolated while the second digit reflects clone number on that plate. Numbers after the 1.1 or 2.1 clone names represent the order in which they were collected.

The results of several representative clones for three **eEF1A2** origin constructs (A2, 2.2 or 1.2) are shown in Figure 3.5. As shown in panel A, proteins of the predicted 52kDa molecular weight were detected at modest levels for all representative **A2 clones**. It is obvious that less protein lysate was loaded for clones designated as 4.3, 4.6, 5.2, 6.8 and 7.1.

Ten clones that were tested for the presence of the *A2* transcript by RT-PCR showed a 940 bp PCR product. The unequal intensity of GAPDH-derived bands suggests the possibility of higher V5-transcript amounts for clones 6.1, 6.8 and 7.2. Additionally, low *GAPDH* mRNA levels were detected for parental cells. The difference in size of the mRNA bands for clones number 6.8 and 7.2 is a gel running artefact.

Detection of exogenous 52kDa V5-tagged protein was confirmed for **1.2 clones** designated as 2, 9, 27, 39, 42 and 56 while clones 11 and 16 were negative as shown in Figure 3.5, panel B. GAPDH protein loading was not equal. RT-PCR amplification mirrored the protein detection. RT-PCR reactions of for clone 1.2-11 and minus reverse transcriptase were run on the next gel so this picture is separate from the picture of the remaining clones.

Analysis of eleven **2.2 construct clones** (Figure 3.5, panel C) confirmed expression of the expected exogenous protein (52kDa) for clones number 2, 6, 9, 18, 33, 46, 52 and 55 while clones 4 and 25 were negative (but note uneven GAPDH protein loading). The results from protein analysis are reflected by the presence of 940 bp long V5 tagged-transcripts.

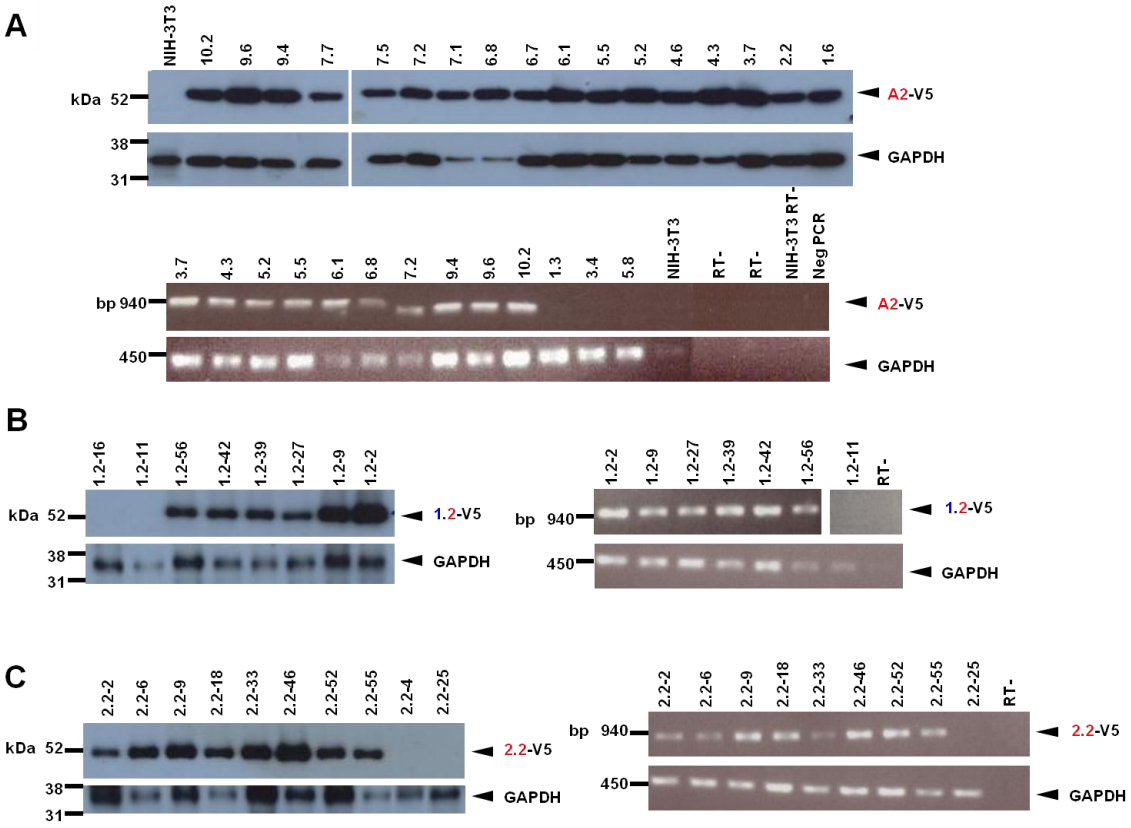

Figure 3.5 Verification of stable cell line generation with expression plasmids of eEF1A2 origin in NIH-3T3 mouse fibroblasts. Pictures reflect several representative clones for each construct. Detection of **A2** (panel A), **2.2** (panel B) and **1.2** (panel C) plasmids was assessed by immunoblotting with anti-V5 tag antibody and Reverse Transcriptase PCR. NIH-3T3 cells were used as negative controls for Western blots. Negative controls for RT-PCR were: minus Reverse Transcriptase (RT-), PCR mastermix sample (Neg PCR) and parental NIH-3T3 cells. GAPDH was used as an internal control. The first digit in the names of A2 construct clones represents the plate from which the clone was isolated while the second digit reflects the clone number on that plate. Numbers standing after 2.2 or 1.2 clone names represent order in which they were collected.

3.2.3 Evaluation of eEF1A variants at the mRNA and protein level in selected stable cell lines

3.2.3.1 Levels of total eEF1A1 protein remain unchanged in representative NIH-3T3 stable cell lines

After establishing which colonies were positive, representative stable cell lines of each construct had to be chosen for experimental assays. A list of cell lines that were used in experiments is given in Table 3.2.

Table 3.2 *Names of different eEF1A stable cell lines selected for experiments.*
The lack of a third clone for 1.1 stable cell lines is marked with minus.

Stable cell line type	Clone number		
A1	3.2	8.6	10.2
A2	7.2	9.6	10.2
1.1	9	23	-
2.1	1	15	18
2.2	1	33	52
1.2	2	39	59

When possible, three clones representing mild, moderate and robust protein expression of each construct were selected. The cell lines were double-checked by RT-PCR (Figure 3.6, panel A) along with Western blot (Figure 3.6, panel B and Figure 3.7) to monitor if the expression of the transgenes remained at the same level with increasing passage numbers. Finally, the selected clones were re-cultured in order to obtain more biological material for subsequent experiments and to collect sufficient amount of the cells for liquid nitrogen storage.

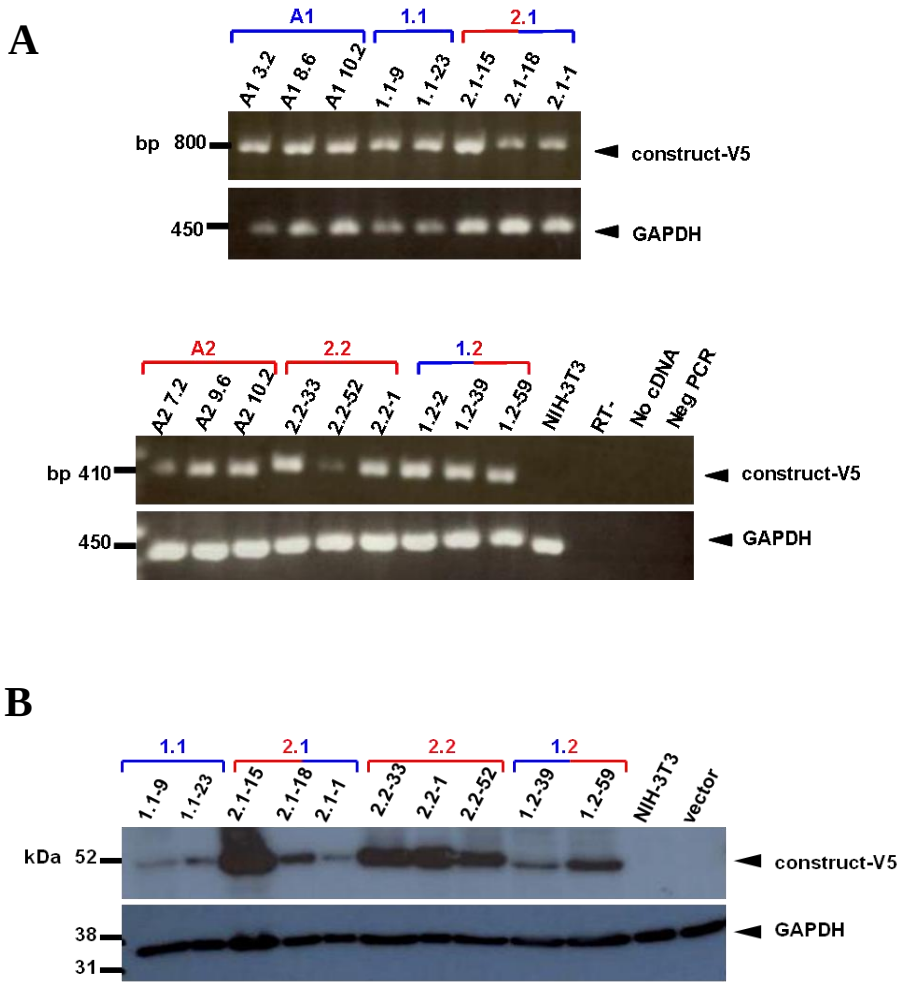

Figure 3.6 Analysis of mRNA and protein levels in different eEF1A transgene stable cell lines. Panel A depicts confirmation of exogenous transcripts presence in selected clones. Primers were designed to amplify within coding sequence of *EEF1A1* or *EEF1A2* and V5 tag. GAPDH represents amplification control. No transcript detection was observed in negative controls (parental cells, RT-, no template samples). Panel B represents Western blot detection of exogenous protein with the anti-V5-tag antibody. GAPDH was used as a loading control.

Expression of eEF1A1 or eEF1A2 proteins in selected lines was also confirmed with the anti-eEF1A1 or anti-eEF1A2 antibodies. Unexpectedly, preliminary Western blot assays for A1 clones indicated unchanged levels of eEF1A1 when compared to the untransfected NIH-3T3 or vector transfected cells (Figure 3.7, panel A). For eEF1A2 stable cell lines (Figure 3.7, panel B), in contrast, parental cells or vector transfected cells showed minimal eEF1A2 presence while A2 7.2, A2 9.6 or A2 10.2 lines showed clear overexpression at the protein level.

Samples for each line were analysed in triplicate to exclude the possibility of artefacts and to increase experimental accuracy. Since the centre of the membrane shown in panel A was not fully accessible to the GAPDH antibody, immunostaining resulted in a very poor signal for clone A1 8.6 and to some extent for A1 10.2. As a consequence, the column representing the relative amount of eEF1A1 for line A1 8.6 on the graph is in excess when compared to the other lines.

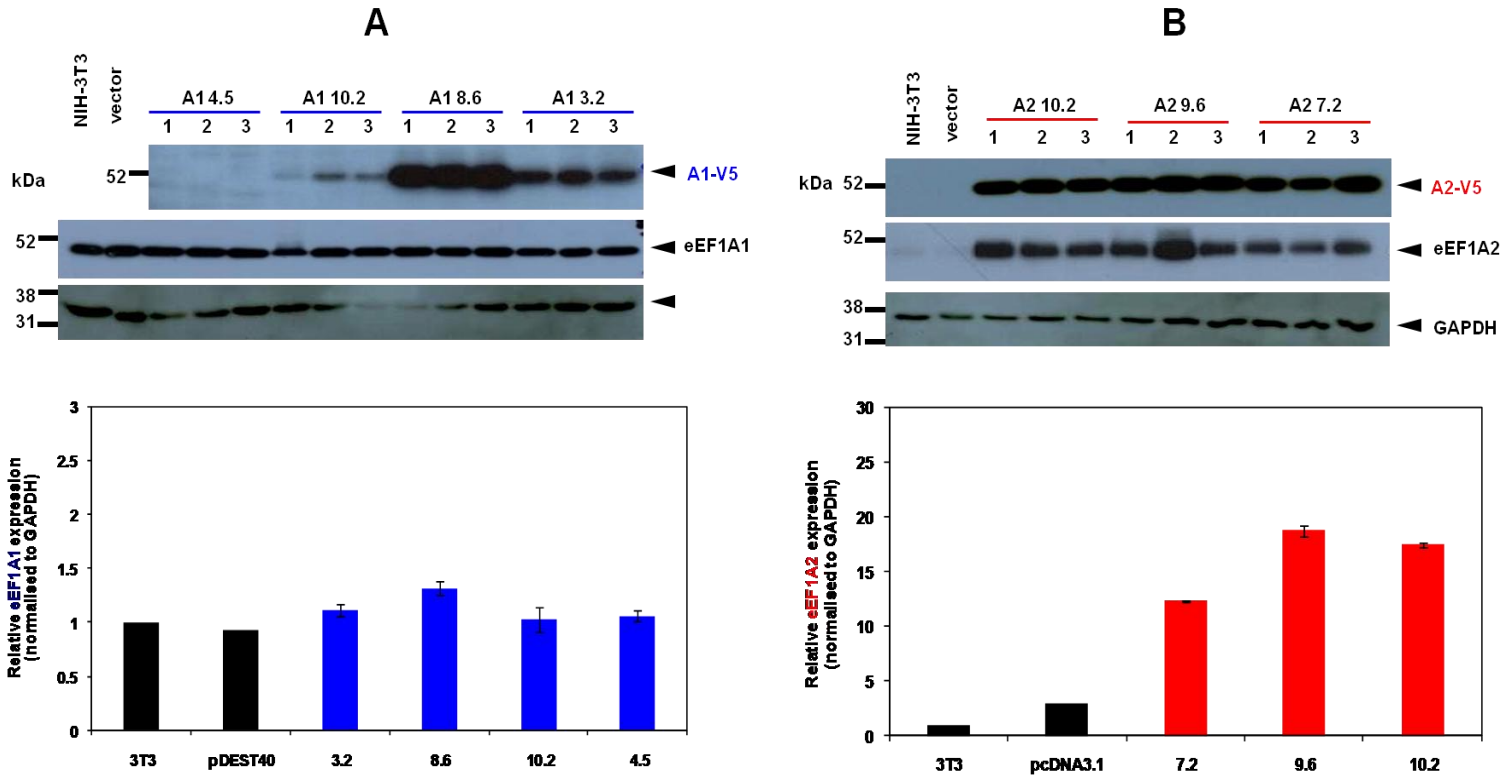

Figure 3.7 Ectopic and endogenous expression of eEF1A transgenes in stable clones derived from NIH-3T3 mouse fibroblasts. Panel A shows expression in cell lysates from parental cells, vector derived NIH-3T3 and 3 independent **A1** clones whereas panel B from **A2** construct lines. Clone A1 4.5 is negative for exogenous insert and was used as an indicator of missing V5-tagged product. Quantification of eEF1A1 or eEF1A2 bands by ImageJ is shown below each immunoblot. The amounts of eEF1A1 or eEF1A2 were first normalised to GAPDH and then expressed relatively to the expression level in NIH-3T3 cells (=1). Results for clones are ± SEM of triplicate.

Levels of eEF1A1 and eEF1A2 were also assessed in the remaining cell lines by Western blotting (Figure 3.8).

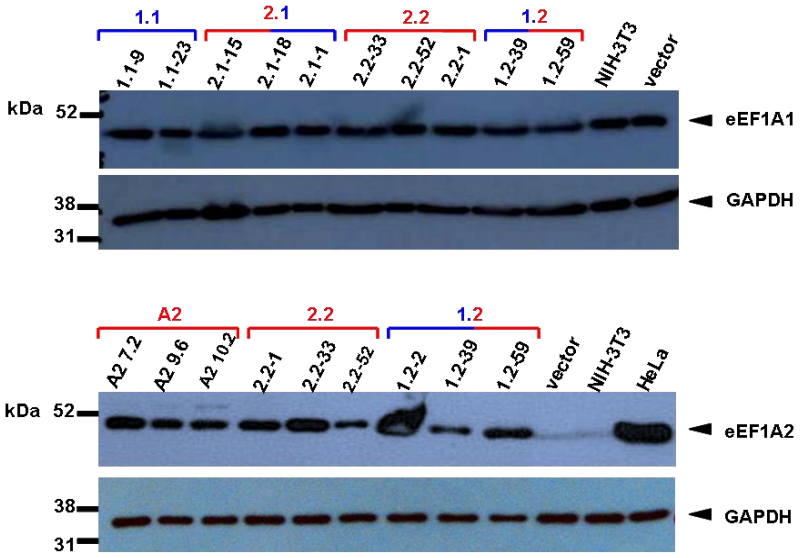

Figure 3.8 Expression of eEF1A1 or eEF1A2 protein in NIH-3T3 stable cell lines.
Ten representative eEF1A variants stable cell lines were screened for eEF1A1 presence and three lines of each A2, 2.2 or 1.2 clone were subjected to detection of eEF1A2 expression. A HeLa cell lysate was used as a positive control for eEF1A2 expression.

The findings from the above preliminary Western blots indicated that even when modest expression of the tagged construct was observed, the level of eEF1A1 in the stable cell lines was not changed when compared to the NIH-3T3 cells. Two possible explanations for this result immediately come to mind.

Firstly, could there be some negative feedback that blocks expression of eEF1A1 at a certain threshold? Secondly, is it possible that the level of transfected human eEF1A1 is so low that an overall level of eEF1A1 appears not to change? Either way, answering these questions could potentially clarify whether eEF1A1 could be involved in oncogenesis. It is tempting to suggest that the cell might have some way of tightly controlling total eEF1A1, which again would relate to any role it could have in

oncogenesis, as this regulation would have to be overcome by the tumour. In order to shed some light on these problems and distinguish between endogenous and exogenous eEF1A1 levels, quantitative real-time PCR was performed on selected stable cell lines, as this made it possible to quantify accurately the expression of the endogenous gene compared with the transgene.

3.2.3.2 Optimization of real-time PCR

In order to quantify expression of different eEF1A variants at the mRNA level, sets of primers were designed to recognise exclusively endogenous *Eef1a1* or *Eef1a2* (mouse), exogenous *EEF1A1* or *EEF1A2* (human), total *EEF1A1/Eef1a1* (residues conserved in both species) and finally total *EEF1A* (residues common for both forms and conserved in both species). Mouse TATA box binding protein (*Tbp*), *18S rRNA* and β-2-microglobulin (*B2m*) were used as reference genes. To ensure that primers were amplifying desired fragments, conventional PCR was performed successfully on control cDNA, followed by agarose gel electrophoresis (data not shown). Subsequently, RNA was extracted from all stable cell lines, followed by cDNA synthesis. Minus RT samples along with no cDNA samples were always used as negative controls. Next, standard curves were conducted in order to obtain reaction efficiencies, optimize primer concentration and temperature of annealing along with optimal cDNA concentrations. At the end of each standard curve, a melting curve was assessed to confirm single transcript amplification. The review of standard curves for all pairs of primers is presented in Figure 3.9 and 3.10 while melting curves are shown in Figure 3.11.

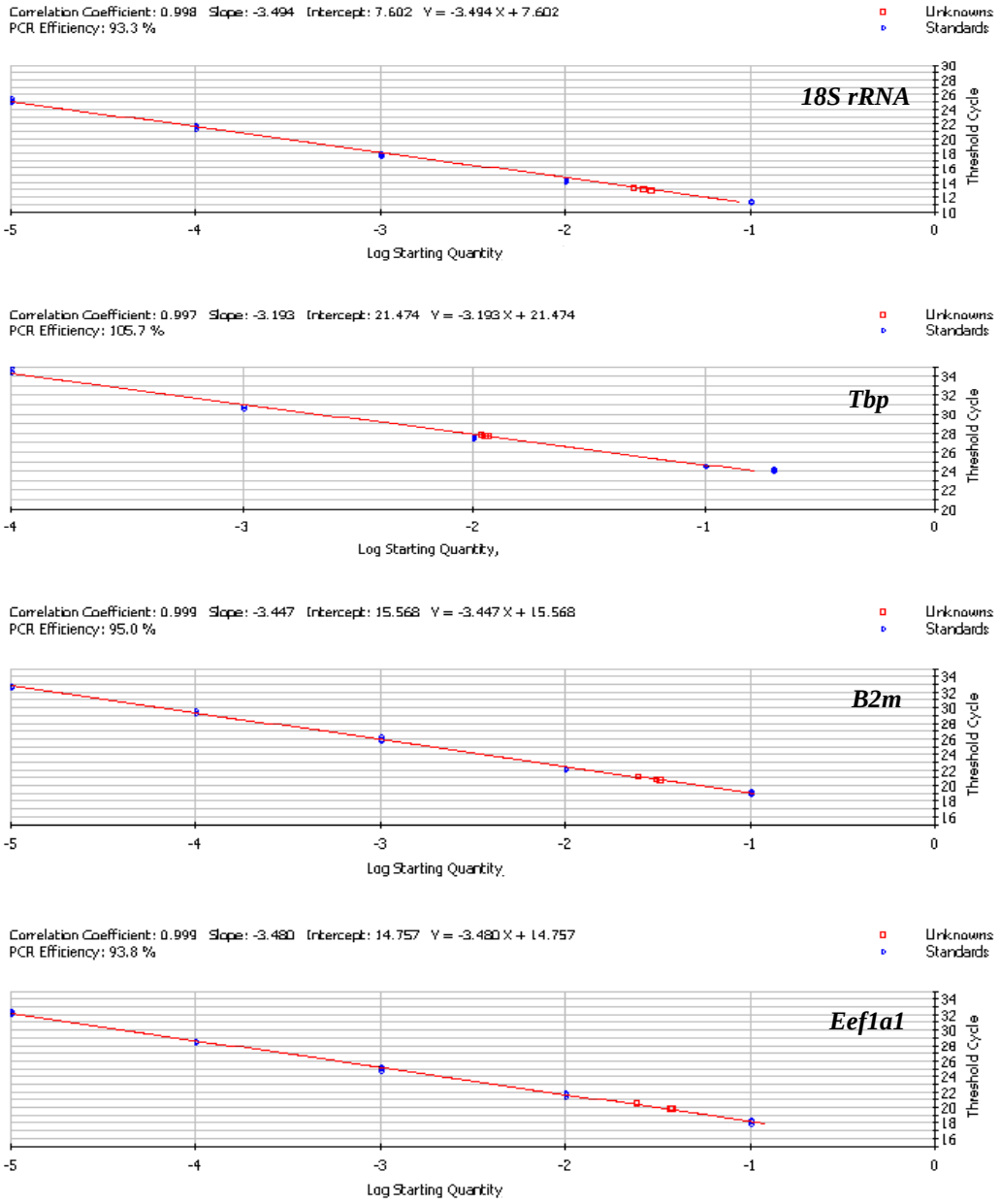

Figure 3.9 Standard curve calibration performed for quantitative real-time PCR (Part 1). Graphs represent standard curves generated for primer sets amplifying *18S rRNA, Tbp, B2m* and *Eef1a1* mRNA fragments, respectively. Log starting quantity on the x-axis of each curve represents a log10 dilution series of the particular cDNA (in triplicate) used for calibration. Only PCR efficiencies between 90-110 % and correlation coefficient R^2 >0.99 were considered acceptable for further analysis.

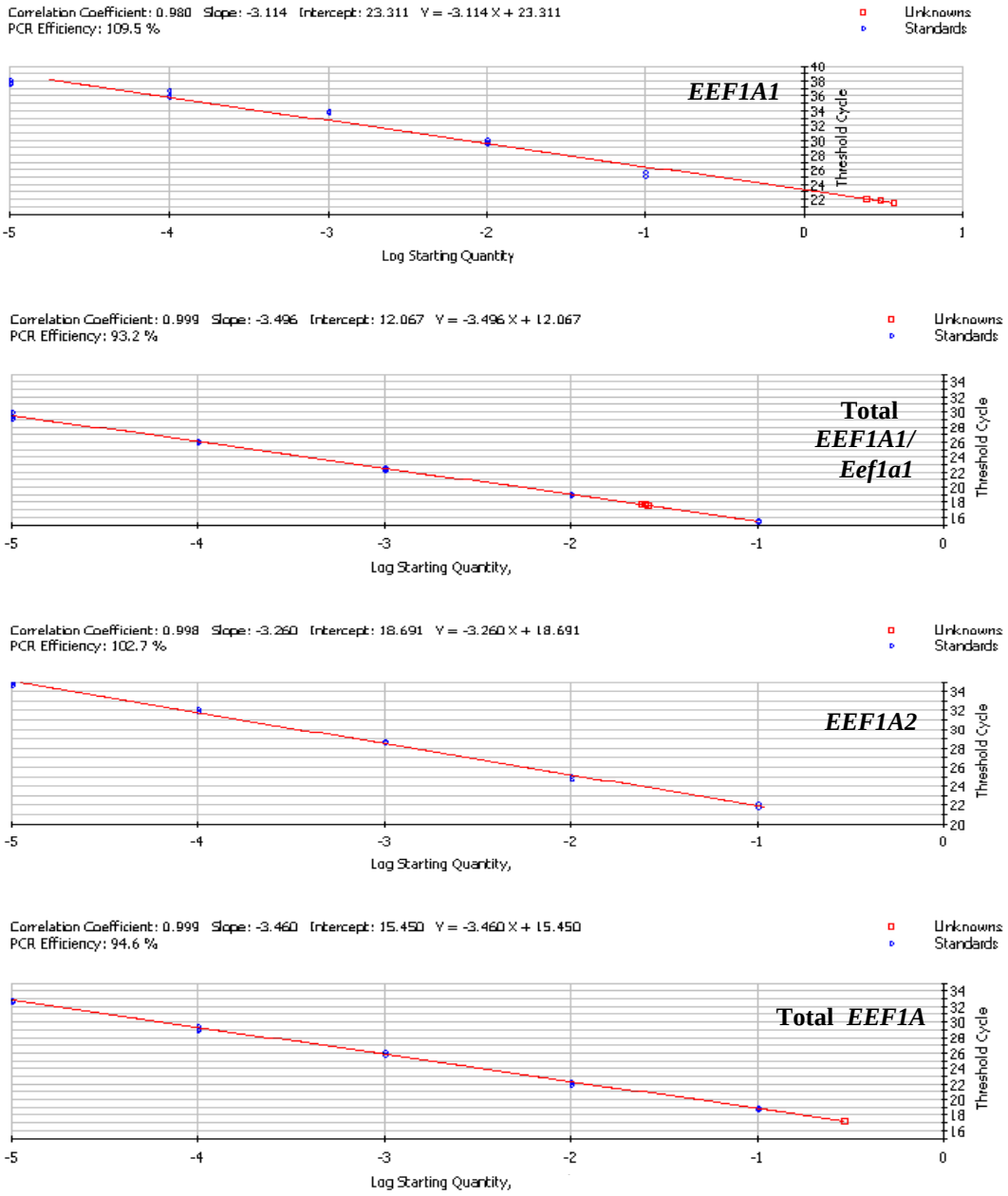

Figure 3.10 Standard curve calibration performed for quantitative real-time PCR (Part 2). Graphs represent standard curves generated for primer sets amplifying *EEF1A1*, *total EEF1A1/Eef1a1*, *EEF1A2* and overall *EEF1A* mRNA fragments, respectively. Log starting quantity on the x-axis of each curve represents a log10 dilution series of the particular cDNA (in triplicate) used for calibration. Amplification of PCR products with efficiency between 90-110 % and correlation coefficient $R^2 > 0.99$ for standard curves were obtained successfully.

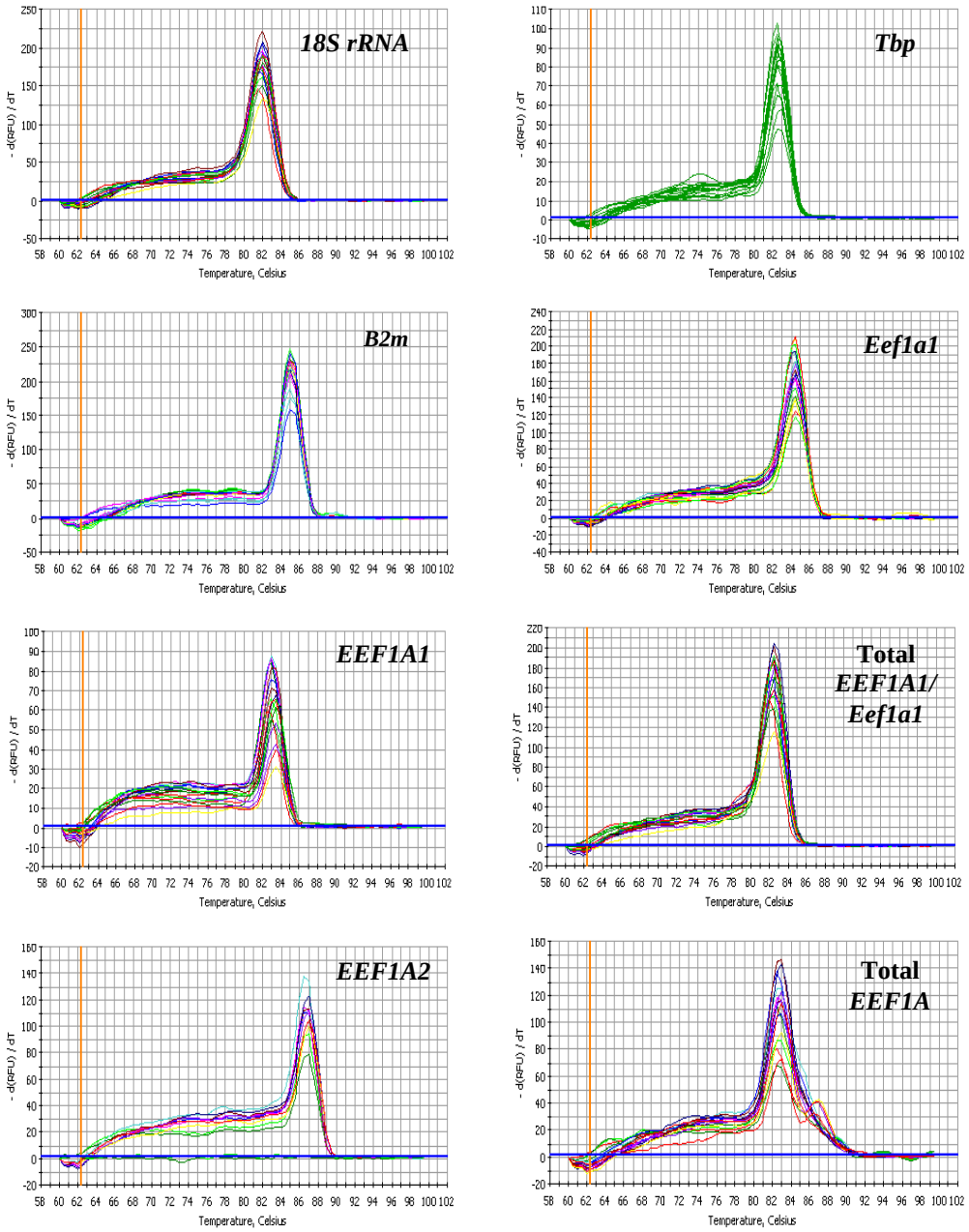

Figure 3.11 Illustration of melting curves analysis. Melt curves for *18S rRNA*, *Tbp*, *B2m*, *Eef1a1*, *EEF1A1*, overall *EEF1A1/Eef1a1*, *EEF1A2* and overall *EEF1A* mRNA primer couples were performed in order to confirm their specificity. The presence of a single prominent peak corresponds to single amplicon detection exclusively.

Analyses of real-time PCR results were determined by a standard curve method to evaluate relative mRNA levels. The results of the reaction for each amplicon of interest were normalised against three reference genes and then exhibited in relation to the empty vector transfected NIH-3T3 cells, valued as 1 relative unit. Every reaction was run in triplicate, and RT- along with no cDNA samples were always used as negative controls.

3.2.3.3 Assessment of eEF1A variants at the mRNA and protein level in different eEF1A1 stable cell lines

NIH-3T3 stable cell lines A1 3.2, A1 8.6, A1 10.2, 1.1-9, 1.1-23, 2.1-1, 2.1-15 and 2.1-18 were subjected to real-time PCR (Figure 3.12) and Western blot analysis (Figure 3.13) in order to characterize the relationship between exogenous eEF1A1, endogenous eEF1A1, total eEF1A1 or total eEF1A at the mRNA and protein level.

The ratios of exogenous *EEF1A1* mRNA did not exceed 1 unit except in clone 2.1-15 suggesting a tight regulation of excessive eEF1A1 amounts in the cell. At the same time, levels of endogenous *Eef1a1* mRNA were not drastically altered when compared to the vector and parental NIH-3T3 cells, except in all three 2.1 clones where an increase was observed. This suggests that constitutive expression of the construct containing the 5'UTR from *EEF1A2* might in some way induce *Eef1a1* transcription.

Surprisingly, the levels of total *EEF1A1/Eef1a1* mRNA were unchanged in all cell lines, even in clone 2.1-15 where overexpression of the 2.1 construct was the highest. Perhaps the human *EEF1A1* transcript competes with mouse *Eef1a1* transcript in order to keep levels of total *EEF1A1/Eef1a1* mRNA unchanged, or the level of the 2.1 constructs constitute just a small percentage of the total amount of eEF1A1.

The levels of total *EEF1A* mRNA in A1, 1.1 or 2.1 cell lines suggest that cells corrected the amount of endogenous *Eef1a1* according to the level of *EEF1A1,* again with the highest increase within 2.1 clones when compared to the vector or parental cells.

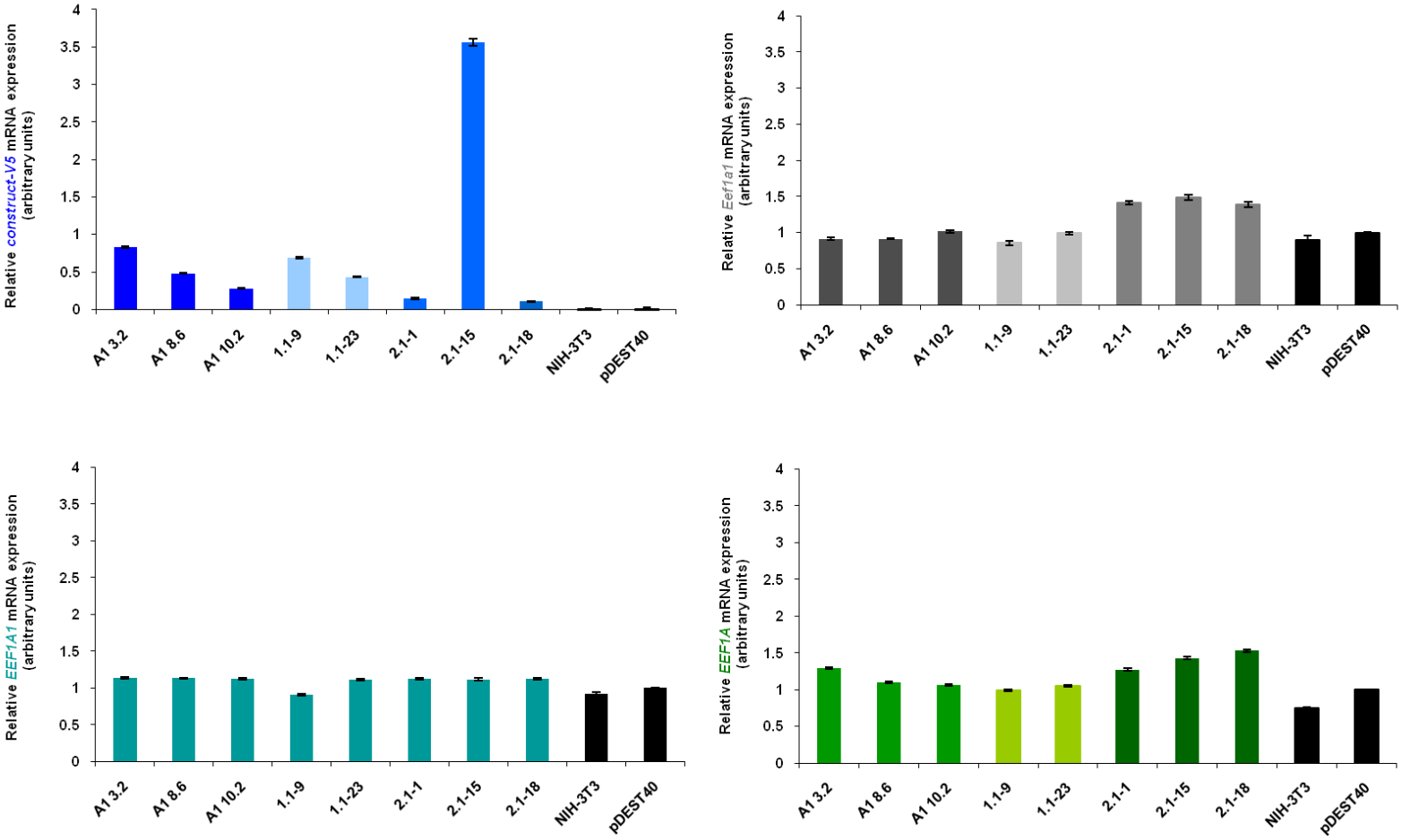

Figure 3.12 Real-time RT-PCR analysis of RNA from selected eEF1A1 origin stable cell lines. **Blue** columns represent **exogenous** transcript, **grey** columns **endogenous** ***Eef1a1*** transcript, **turquoise** columns **total** ***EEF1A1/Eef1a1*** transcript and **green** columns overall ***EEF1A*** detection, respectively. Values are the means ± SD of three independent experiments conducted in three technical repeats for each cell line sample.

Western blot analysis using an anti-V5 antibody showed a band of the expected 52kDa size in every cell line (Figure 3.13). Bands for clones 1.1-9 and 2.1-1 were visible only after longer exposure. A close correspondence between mRNA and protein level was observed only for A1 10.2 and 2.1-15 clones. The construct carrying only eEEF1A1 coding sequence was expressed in excess over the 1.1 and 2.1 plasmids.

To determine the effect of A1, 1.1 and 2.1 constructs on endogenous Eef1a1 protein expression, a Western blot with an anti-eEF1A1 antibody was executed. Western blotting was conducted on the set of the same stable cell lines samples and showed approximately unchanged levels of eEF1A1 expression (50kDa) when compared to the vector transfected or parental NIH-3T3 cells. Only clone 1.1-9 revealed a lower level of eEF1A1 protein but the GAPDH loading control was decreased as well.

A similar trend was observed with a commercial anti-eEF1α antibody. This antibody is not specific to any eEF1A variant and so it recognises both eEF1A1 and eEF1A2, and gives information on total eEF1A protein level. Mouse tissue expression controls (liver +/+, brain +/+, brain w/w, muscle +/+, muscle w/w) were used for this antibody throughout the thesis to show immunodetection of both variants. Almost all stable cell lines along with parental or vector transfected cells showed uniformly equal levels of eEF1A (51kDa), except clone 2.1-1, 2.1-18 and slightly clone 2.1-15.

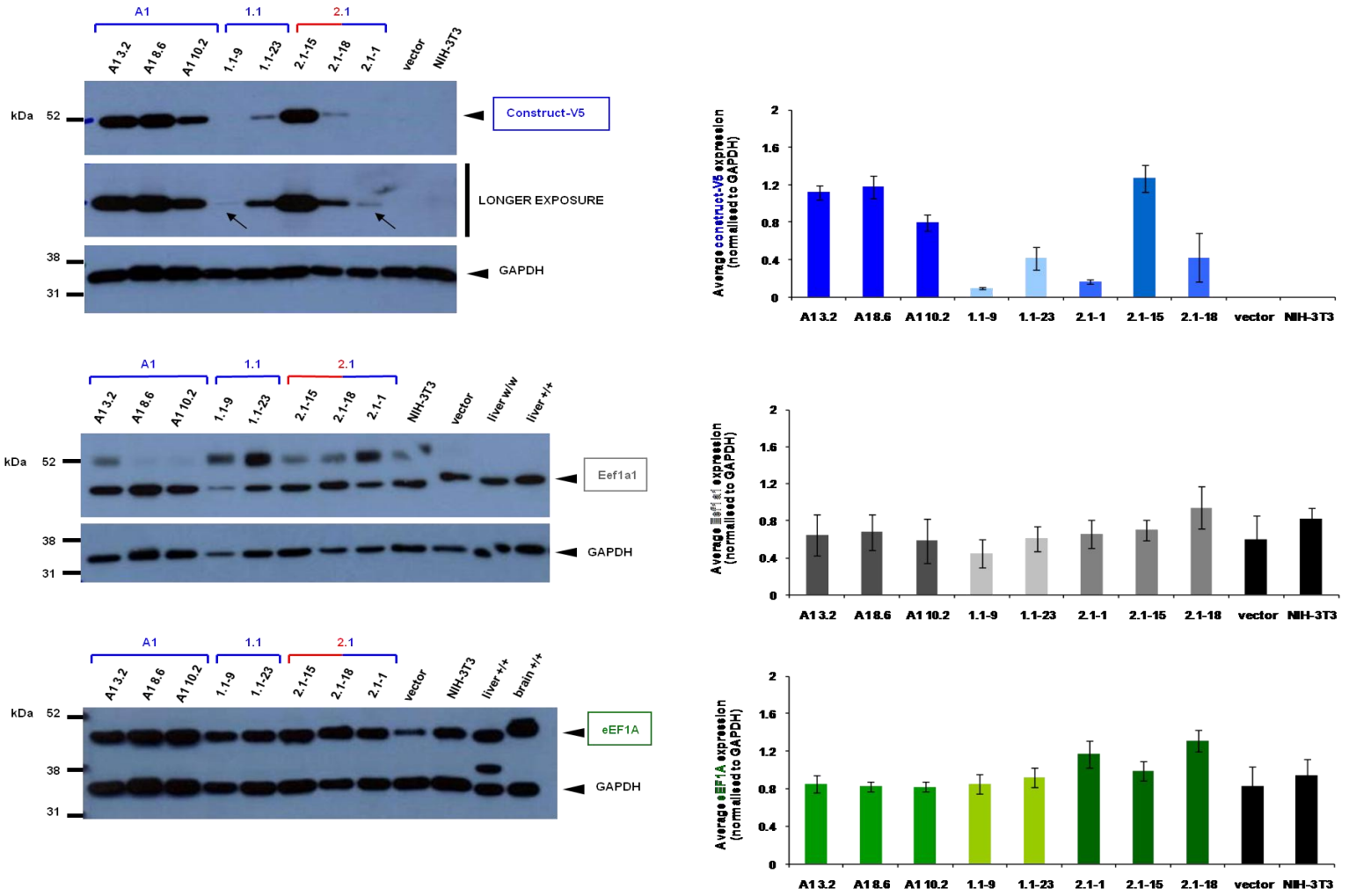

Figure 3.13 Analysis of different eEF1A1 origin plasmids overexpression in stable NIH-3T3 lines. The representative immunoblots present detection of **V5-tagged constructs**, **Eef1a1** and **total eEF1A** proteins. GAPDH was used as a loading control. Graphs represent average densitometric measurements of the bands for each sample (±SEM).

3.2.3.4 Assessment of eEF1A variants at the mRNA and protein level in different eEF1A2 stable cell lines

All selected eEF1A2 stable cell lines (A2 7.2, A2 9.6, A2 10.2, 2.2-1, 2.2-33, 2.2-52, 1.2-2, 1.2-39, 1.2-59) were subjected to real-time PCR and Western blot analysis to determine any influence of the expression of exogenous eEF1A2 on total eEF1A or Eef1a1 at both- mRNA and protein level.

Exogenous eEF1A2 constructs expression was confirmed at the mRNA level in all selected stable cell lines but the lowest transcript levels were detected for 2.2 clones (Figure 3.14).

Next, the ratios of endogenous *Eef1a1* mRNA were determined. The *Eef1a1* levels varied between clones but its expression was roughly comparable to that of controls. The levels of *Eef1a1* transcript did not correspond to exogenous *EEF1A2* mRNA levels.

Investigation of total *EEF1A* transcript amount found it elevated in all stable cell lines when compared to the vector or NIH-3T3 controls. The biggest increase of total translation elongation factor 1A transcript was observed for A2 clones, slightly lower for 1.2 cell lines and the lowest for the three 2.2 clones (but still higher than in untreated control cells).

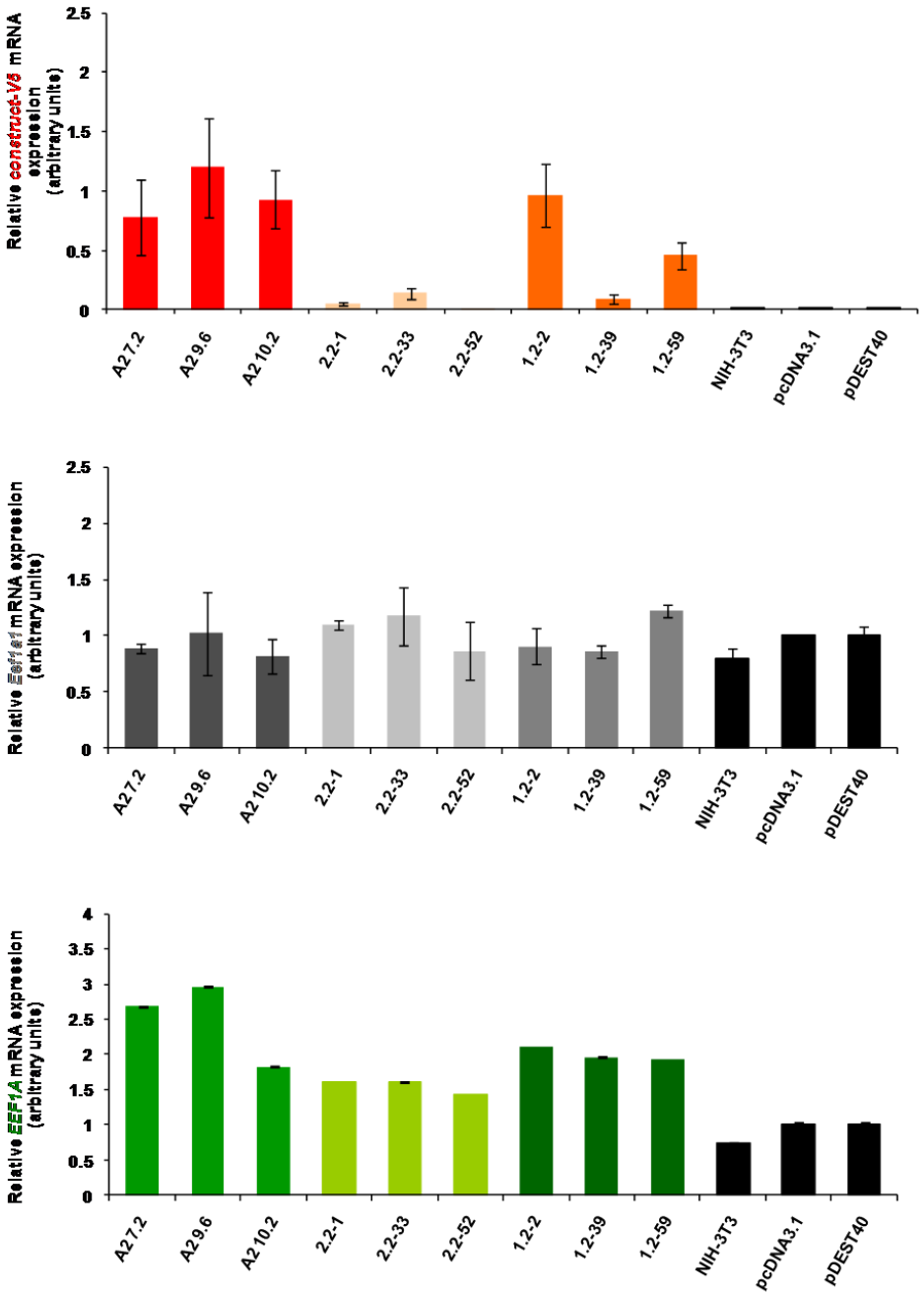

Figure 3.14 Real-time RT-PCR analysis of RNA from selected eEF1A2 origin stable cell lines. **Red** columns represent **exogenous transcript**, **grey** columns **endogenous *Eef1a1*** transcript and **green** columns **overall *EEF1A*** mRNA. Values are the means ± SD of three independent experiments conducted in three technical repeats for each cell line sample.

Western blot analysis of eEF1A2 stable cell lines with the anti-V5 antibody revealed expression of exogenous V5-tagged proteins (52kDa) in all samples apart from negative controls (parental cells and vector transfected NIH-3T3) as showed in Figure 3.15. The expression of constructs without a 5'UTR was higher in comparison to the remaining tagged proteins, consistent with data obtained from the pilot studies. Amounts of eEF1A2 at the mRNA level corresponded to those at the protein level.

The anti-eEF1A2 antibody showed overexpression of the predicted protein at 51kDa. To ensure that this was not a protein of mouse origin, samples were checked at the RNA level for mouse *Eef1a2* and relative expression ratios were confirmed as negative (data not shown). The magnitude of eEF1A2 expression was not consistent with that seen with the anti-V5 antibody. Unexpectedly, an eEF1A2-specific band was detected in vector controls and parental cells, probably due to the over-confluence of the cells when samples were collected.

Western blotting with an anti-eEF1α antibody determined the effect of constitutive expression of different eEF1A2 constructs on total eEF1A protein level. Lines A2, 2.2 and 1.2 showed a modest increase in total eEF1A protein expression (51kDa) when compared to the vector controls or the parental cell line. Expression of endogenous Eef1a1 protein in 2.2 and 1.2 cell lines remained unchanged (Figure 3.8).

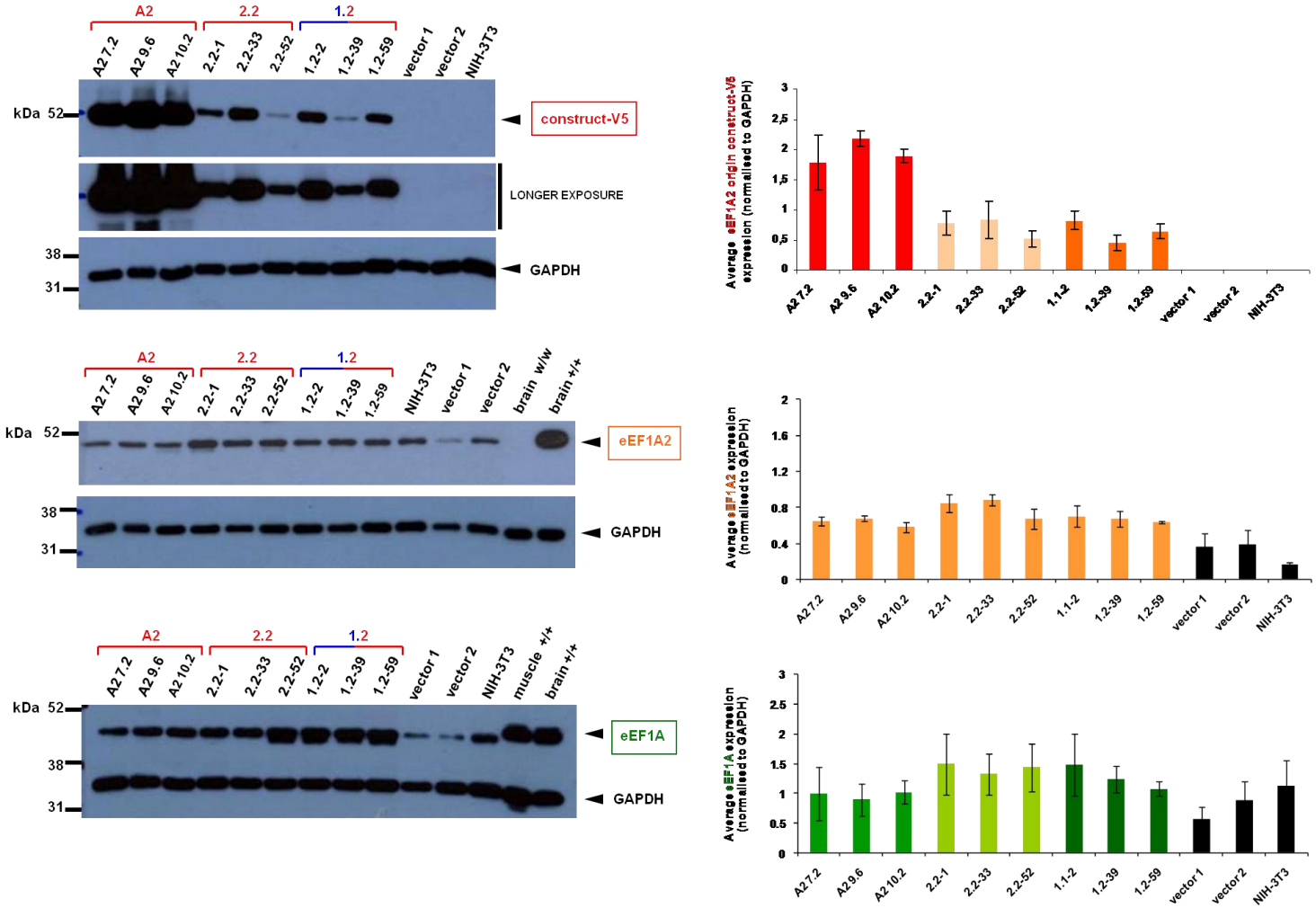

Figure 3.15 Overexpression of eEF1A2 origin plasmids in NIH-3T3 stable cell lines. The representative Western blots exhibit detection of **V5-tagged constructs**, **eEF1A2** and **eEF1A** proteins. GAPDH was used as a loading control. Graphs correspond to an average densitometric reading of the band intensities for each sample (± SEM).

3.2.4 Evaluation of the transiently expressed eEF1A variants at the mRNA and protein level

3.2.4.1 Pilot studies in NIH-3T3, Rat2 and HeLa cell lines

The initial experiment with stable cell lines demonstrated unchanged levels of eEF1A1 in A1 clones and clear overexpression of eEF1A2 in A2 clones. With regard to the above observation, a pilot experiment was carried out on two rodent fibroblast cell lines (NIH-3T3 and Rat2) which were subjected to nucleofection with the A1-V5 construct to see whether any effect is observed in a transient experiment. Exogenous eEF1A1 was detected with the anti-V5 antibody while eEF1A1 was confirmed using an anti-eEF1A1 antibody (Figure 3.16). Untransfected, vector or mock transfected cells were used as negative controls.

Expression of exogenous eEF1A1 consistently decreased up to 4 or 6 days post transfection in NIH3T3 and Rat2 cells, respectively. The level of eEF1A1 slightly decreased in samples from day 1 but then remained unchanged on subsequent days when compared to controls.

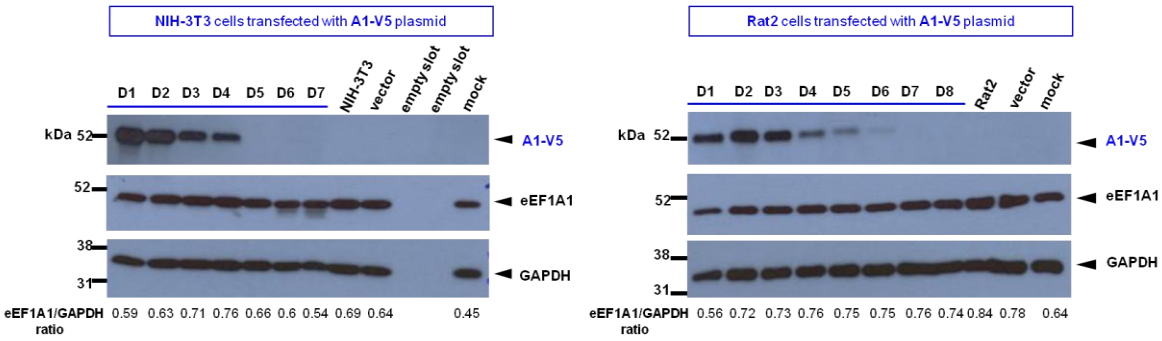

Figure 3.16 Overexpression of eEF1A1 alters expression levels of endogenous Eef1a1 on the first day after transfection. NIH-3T3 and Rat2 cells were nucleofected with A1-V5 plasmid. Expression of human eEF1A1 and overall eEF1A1 was monitored for 7/8 consecutive days. GAPDH was used as a loading control. Band intensities measured for eEF1A1 were normalised against GAPDH expression and calculated ratios are indicated below the blots.

While NIH-3T3 and Rat2 cells do not express eEF1A2, one more cell line was tested to monitor possible interaction between eEF1A1 and eEF1A2, as HeLa cells express both eEF1A forms. Cells were nucleofected either with A1-V5 construct or empty vector as control. Expression of the exogenous construct was observed up to 5 days (with some trace amounts on day 6 and 7) for the A1-V5 plasmid (Figure 3.17).

Interestingly, when the A1-V5 plasmid was incorporated into HeLa cells, there was a noticeable decrease in eEF1A2 expression on day 1 and 2 after transfection. The level of eEF1A1 in sample on day 1 is lower but this is likely to be a loading artefact as GAPDH was also lower.

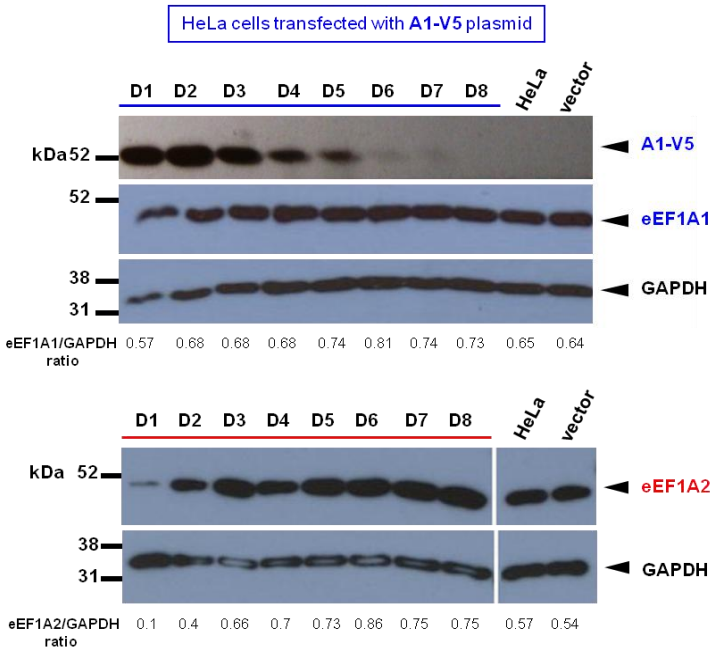

Figure 3.17 Overexpression of eEF1A1 or eEF1A2 indicates dynamic interplay between exogenous and endogenous variants of eEF1A on the first day after transfection. HeLa cells were transiently transfected with A1-V5 plasmids and expression of V5-tagged, eEF1A1 and eEF1A2 proteins was monitored up to 8 days. Relative ratios of eEF1A1 or eEF1A2 to GAPDH were calculated from band intensity measurements using ImageJ and put below appropriate blots.

3.2.4.2 Transient transfections in NIH-3T3 cell line

Firstly, the mRNA and protein levels of different eEF1A variants were herein investigated in NIH-3T3 cell lines, after constitutive expression of different constructs had occurred. Next, dynamic interplay between two eEF1A variant forms existed when one of them exhibited overexpression, according to the above data obtained in initial experiments with three different cell lines. To understand the observations from these pilot experiments, NIH-3T3 cells were transfected with the plasmids used for stable cell line generation. Cell pellets were collected on 5 consecutive days or on 7 days after nucleofection and then subjected to analysis using real-time PCR or Western blotting, respectively. On this occasion, protein and mRNA of different eEF1A constructs were assessed in transiently transfected NIH-3T3 cells to determine possible relationships between exogenous and endogenous eEF1A variants immediately after the former are incorporated into cells.

After real-time PCR assessment, each transcript's level was normalised to three mouse reference genes (*Tbp*, *B2m*, and *18S rRNA*). Then relative units of expression were calculated as a fold change, in a relation to the specific mRNA level in the control pcDNA3.1 or pDEST40 vector transfected cells (1 unit). Moreover, control real-time PCR for mouse *Eef1a2* mRNA detection was performed and did not exhibit any of this transcript induction, as expected (data not shown).

Cell lysates of nucleofected NIH-3T3 cells were subjected to Western blotting using anti-V5, anti-eEF1α and anti-eEF1A1 antibodies. GAPDH was always used as a loading control.

3. 2. 4. 2. 1 Effects of transient A1, 1.1 and 2.1 overexpression in NIH-3T3 cells

The assessment of expression of the representative exogenous transcripts (***A1*** and ***1.1***), ***Eef1a1*** and overall ***EEF1A*** mRNA was shown in Figure 3.18. Similar information was obtained in 1.1 and 2.1 transfectants.

Forced expression of the A1-V5 construct was confirmed up to fourth day post transfection whereas some remaining traces on day 5 were still seen for the 1.1 and 2.1 constructs. The highest relative expression at 9 hours was observed for *1.1* (around 98 units) and *2.1* mRNA (42 units, data not shown) but for *A1* transcript it was only 4 units.

To determine what is happening with mouse *Eef1a1* when the human counterpart was incorporated into the cells, real-time PCR was performed to amplify a 101 bp fragment of the endogenous transcript. Surprisingly, samples from 9 hours and day 1 showed a small decrease in *Eef1a1* mRNA expression among A1 transfectants while more a distinguishable decline was seen at these time points within 1.1 and 2.1 transfections. Apparently, the endogenous transcript was diminished when the *EEF1A1* transcript level was at its highest, indicating a strict regulation of the overall eEF1A1 levels in the cell. As the exogenous transcript decrease was proceeding on the following days, endogenous *Eef1a1* transcript amounts were increasing and reached a level comparable to that of controls.

As expected, total *EEF1A* mRNA level in 1.1 and 2.1 transfectants was elevated for samples at 9 hours post nucleofection, in agreement with the highest levels of exogenous 1.1 and 2.1 at this particular time point, but then decreased on subsequent days as the exogenous transcript declined. Investigation of the total *EEF1A* transcript in A1-V5 transfected cells revealed that its level remained almost the same for up to three days, by which time exogenous *EEF1A1* mRNA was barely present and then it slightly increased on fourth day as the eventual repression became relieved. Alternatively, the human *EEF1A1* mRNA might represent only a small percentage of the overall *EEF1A1/Eef1a1* amount in the A1-V5 transfected cells.

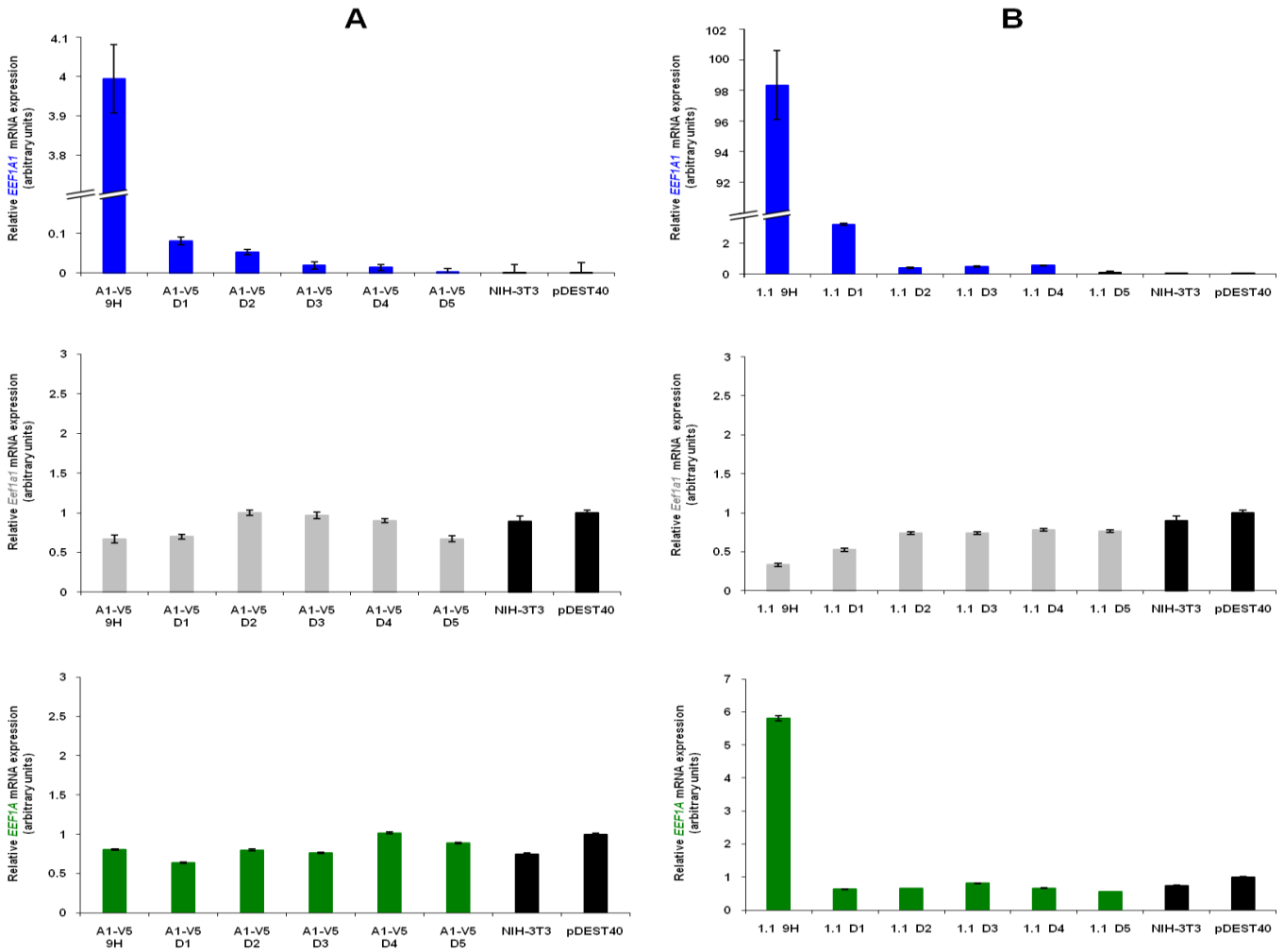

Figure 3.18 Real-time PCR analysis of mRNA from NIH-3T3 cells collected at 9 hours (9H) and on 5 consecutive days (D) after transfection with A1 (panel A) and 1.1 (panel B) construct. Blue columns represent **exogenous *EEF1A1***, **grey** columns **endogenous *Eef1a1*** and **green** columns **overall *EEF1A*** mRNA expression. Values are the means ± SD of three independent experiments conducted in triplicate for each sample.

Western blot analyses were performed on the same collection of samples and are shown in Figure 3.19 for A1-V5 transfectants and in Figure 3.20 for NIH-3T3 cells after nucleofection with 2.1 construct. Similar information was obtained for A1-V5 and 1.1 samples. GAPDH showed equal amounts of the protein in every line.

Membranes probed with anti-V5 antibody detected expression of exogenous **A1** and 1.1 protein of the expected size (52kDa) for four consecutive days after transfection, in agreement with their mRNA levels. Furthermore, ectopic expression of the **2.1** construct was recorded for five consecutive days post transfection, also in close correspondence to its mRNA expression timing, but the highest protein amount was seen at day one. There were no bands in negative controls of parental cells or empty vector nucleofected NIH-3T3 cells.

Endogenous **Eef1A1** protein expression (50kDa) was confirmed with a specific anti-eEF1A1 antibody. A small decrease at 9 hours and then on the first day post transfection for A1-transfected cells or just at 9 hours for 1.1 was seen. At the remaining time points its levels were around the same level of expression exhibited for vector controls and parental cells. In contrast, levels of endogenous Eef1a1 protein in 2.1 transfectants were slightly higher than controls at 9 hours, day 1 and day 2 lysates but then dropped to the control levels.

The anti-eEF1A1 antibody should also recognize the human plasmid. The bands of 52kDa were missing or were present in random A1, 1.1 and 2.1 lysates from 9 hours to day 6 or 7 but the intensity of these bands did not correspond to the decreasing amounts of the exogenous proteins after nucleofection. Even though bands were not seen in controls, perhaps the addition of the V5 tag changed the conformation of the protein and made the epitopes unrecognizable by antipeptide antibody. The possibility of nonspecific immunostaining or the presence of additional nucleofection stress-induced protein also cannot be excluded.

The **overall eEF1A** protein detection (51kDa) was performed with the anti-eEF1α antibody and its increased expression was observed mostly at 9 hours in A1, 1.1 and 2.1 transfected cells. In the remaining time point samples, the eEF1A expression

remained almost unchanged and was sustained at levels similar to that seen in parental or vector control cells.

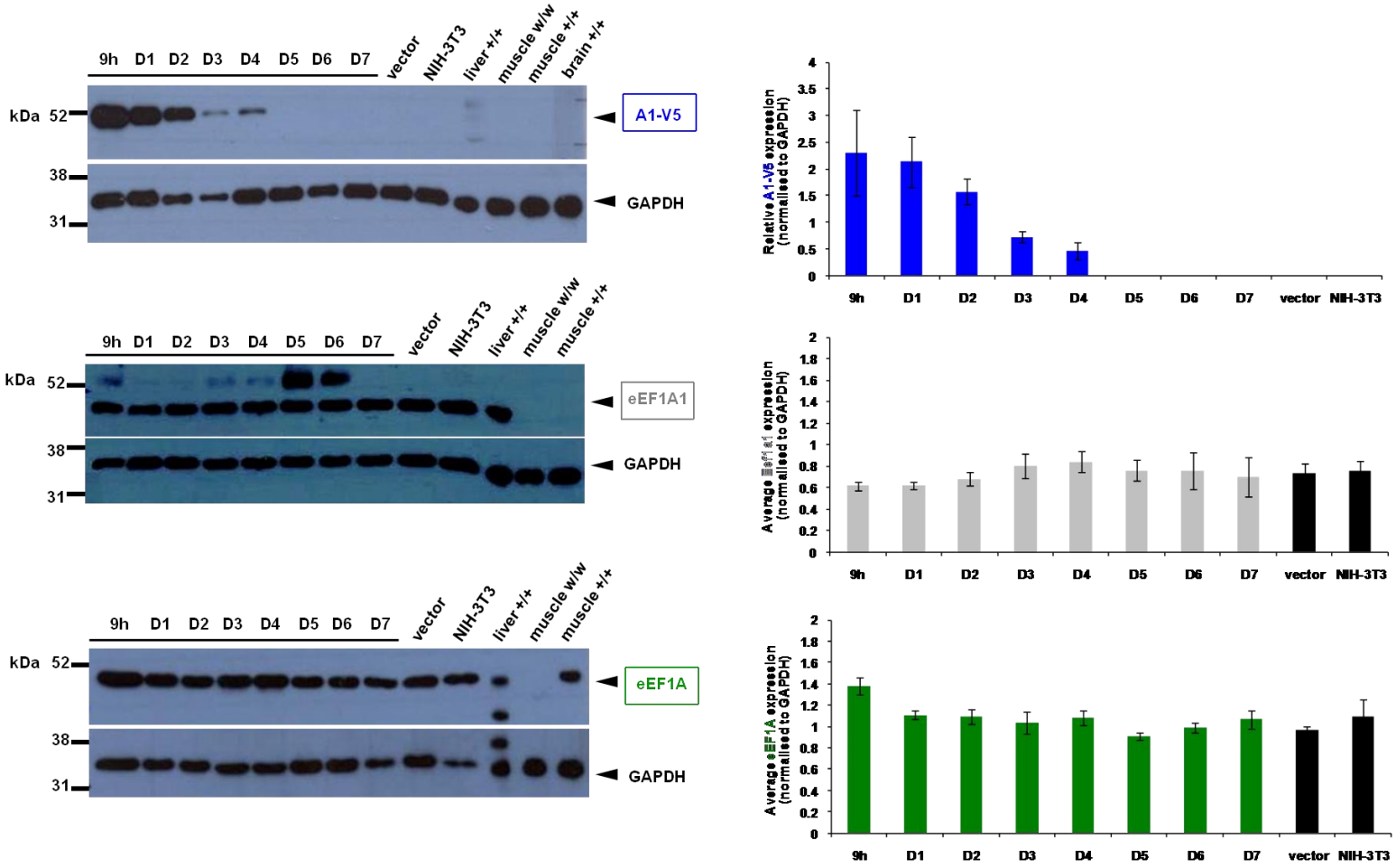

Figure 3.19 Overexpression of A1-V5 in NIH-3T3 mouse fibroblasts. After transfection, cell lysates collected from NIH-3T3 cells were subjected to Western blot. Expression of **V5-tagged construct**, **endogenous Eef1a1** or **total level of eEF1A** was monitored at 9 hours (9h) and 7 consecutive days (D). Corresponding quantification of the band intensities was determined by ImageJ (±SEM).

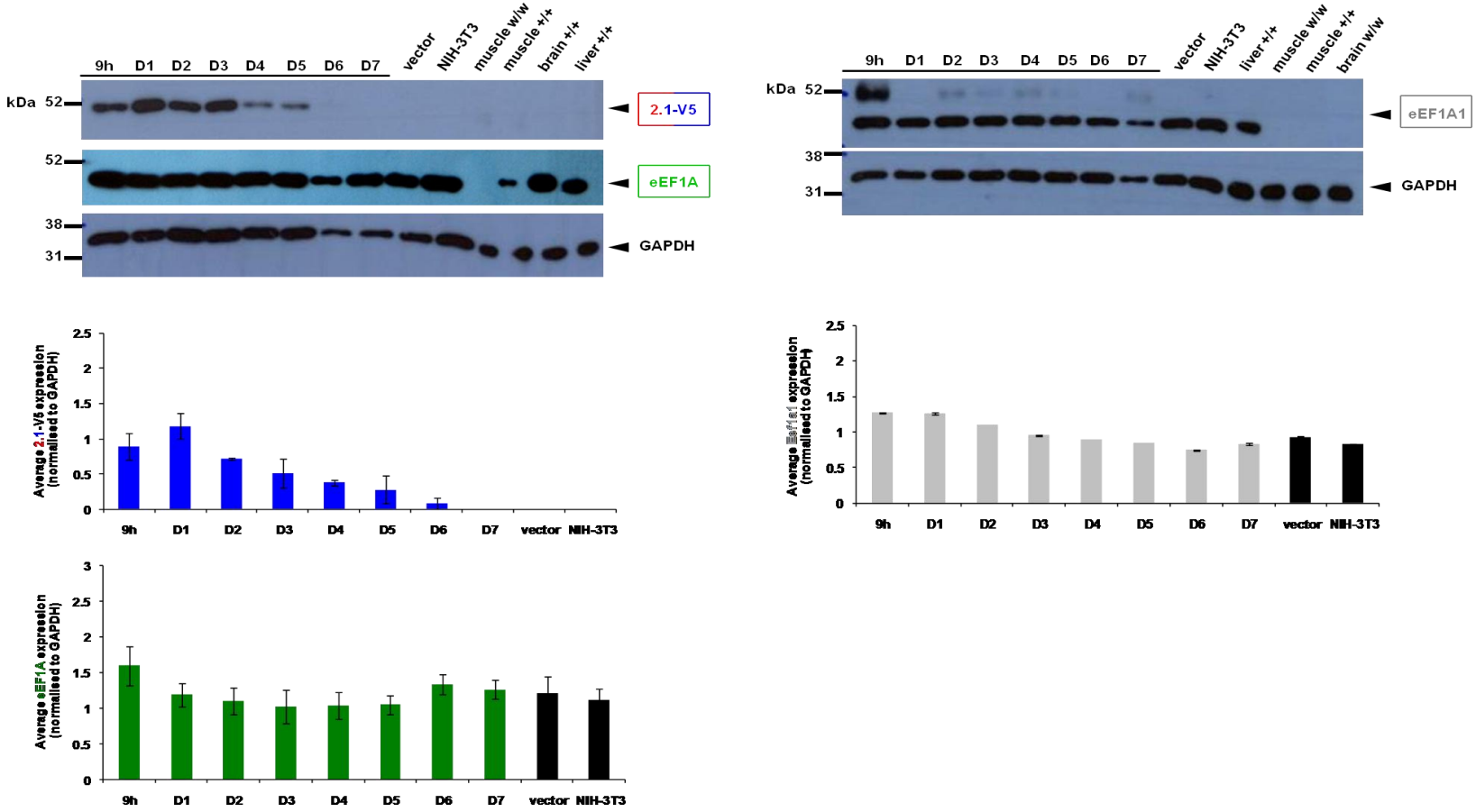

Figure 3.20 Analysis of expression of 2.1-V5, endogenous Eef1A1 and overall eEF1A proteins in transiently transfected NIH-3T3 cells. Expression was monitored at 9 hours and then on every day for a week after nucleofection. The average band intensities quantified for corresponding proteins are shown in graphs below representative Western blots (±SEM).

3. 2. 4. 2. 2 Effects of transient A2, 2.2 and 1.2 overexpression in NIH-3T3 cells

The relationship between exogenous ***A2*** or ***2.2*** transcripts and endogenous ***Eef1a1*** or **total *EEF1A*** mRNA is shown in Figure 3.21. Similar information was obtained for 2.2 and 1.2 transfectants.

The presence of *A2* transcript was seen at all experimental time points while expression of *2.2* and *1.2* mRNA was confirmed up to 3 days post transfection (with almost undetectable amounts at day 4 and 5). As expected, the relative levels of *A2* (around 67.5 units), *2.2* or *1.2* (24.5 units) mRNA were significantly high at 9 hours after nucleofection and decreased thereafter.

Interestingly, overexpression of eEF1A2 had also an effect on the levels of endogenous *Eef1a1* mRNA in NIH-3T3 cells; its decrease was observed at 9 hours and 1 day, at the times when the *A2* transcript was in the highest excess. The *Eef1a1* transcript levels were diminished up to day 2 even more when the 2.2 construct was overexpressed or up to day 3, coinciding with the highest *1.2* mRNA levels (data not shown). Levels of endogenous *Eef1a1* mRNA increased as soon as expression of the exogenous transcripts began to fall. This again suggests dynamic interaction at the RNA level between two eEF1A variants.

The highest increase of overall *EEF1A* mRNA was observed for A2 transfectants, in agreement with the presence of exogenous transcripts at specific time points. Relative ratios of overall *EEF1A* transcript were decreasing as the A*2* transcript decreased in the cells. It is possible that total *EEF1A* mRNA would acquire values comparable with NIH-3T3 or vector transfected cells after day 5 post nucleofection, but these samples were not tested.

As expected, the total *EEF1A* mRNA expression among 2.2 and 1.2 transfected cells was highest at 9 hours time point. The relative overall *EEF1A* transcript expression on day 1 is suggested to be a combination of exogenous transcripts and endogenous *Eef1a1* mRNA. In contrast, the amounts seen at subsequent days possibly reflect only endogenous *Eef1a1* transcript, or alternatively, the exogenous transcripts constitute only a small percentage of the overall *EEF1A* mRNA.

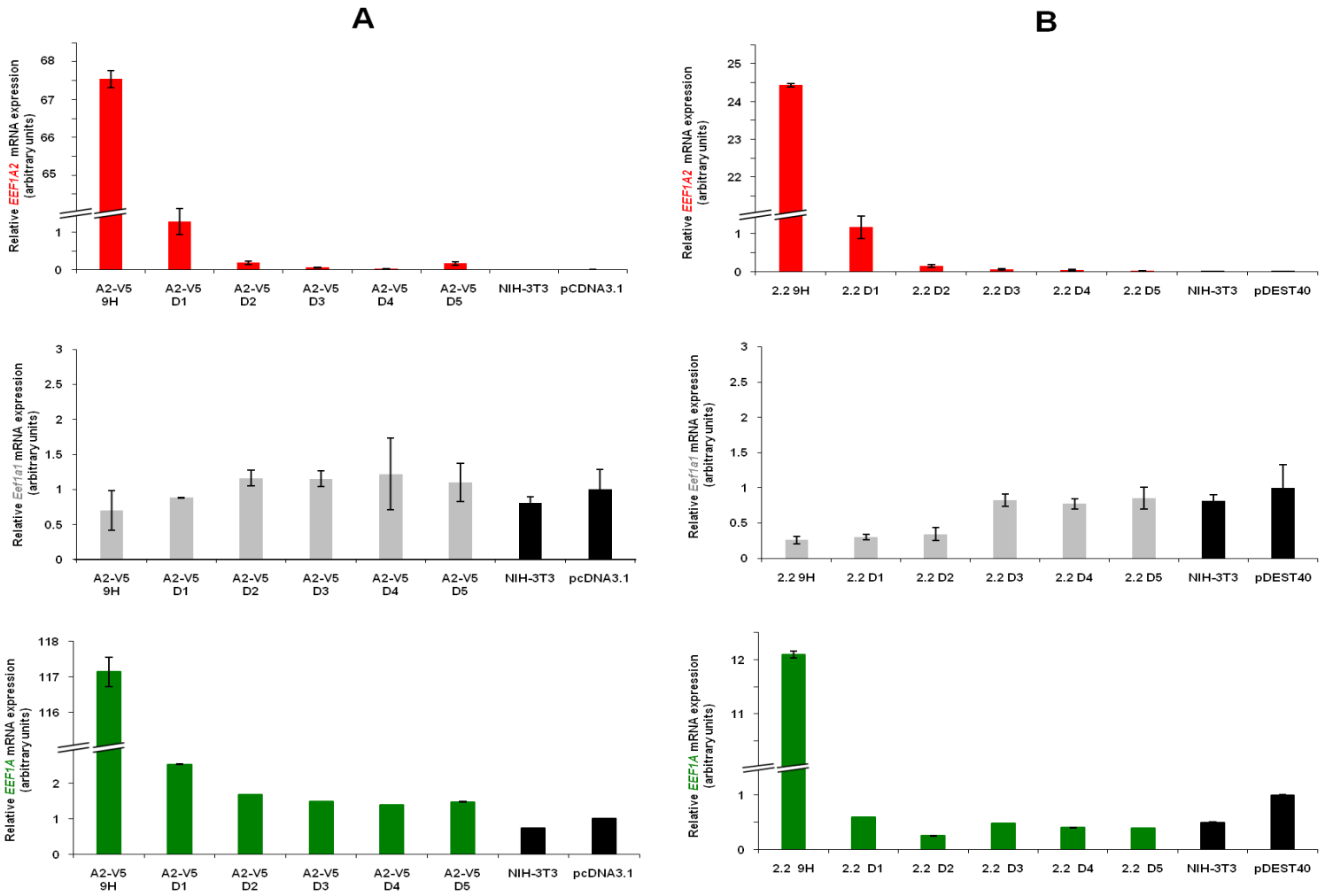

Figure 3.21 Real-time PCR analysis of mRNA from NIH-3T3 cells collected at 9 hours (9H) and on 5 consecutive days (D) after transfection with A2 (panel A) and 2.2 (panel B) construct. Red columns represent **exogenous *EEF1A2***, **grey** columns **endogenous *Eef1a1*** and **green** columns **overall *EEF1A*** mRNA expression. Values are the means ± SD of three independent experiments conducted in triplicate for each sample.

The relationship between eEF1A forms at the protein level was subsequently investigated by Western blotting and representative immunoblot analysis for A2 or 2.2 transfectants are shown in Figures 3.22 and 3.23, respectively. Similar data were received for 2.2 and 1.2 samples. GAPDH showed approximately equal amounts of the proteins loading.

The presence of **A2-V5** protein was confirmed with the anti-V5 antibody and detection of 52kDa band was seen at all tested time points. Investigation of the NIH-3T3 cells transfected with the chimeric 5'UTR constructs shown that 2.2 expression was sustained until the fifth day after nucleofection whereas bands of the expected 52kDa size among 1.2 transfectants were confirmed up to the third day (data not shown). It is worth noting that the highest expression for 2.2 and 1.2 constructs was seen on day 1.

In order to test whether eEF1A2 overexpression can affect the levels of endogenous **Eef1a1** at the protein level, membranes were probed with a specific anti-eEF1A1 antibody. Interestingly, Eef1A1 expression (50kDa) remained almost unchanged in A2-V5 transfected cells but it was slightly increased in comparison to parental or vector controls (but note decrease in GAPDH loading).

In contrast, a noticeable decrease of endogenous Eef1a1 protein was observed on the first day post transfection at the point where the exogenous 2.2 and 1.2 constructs show the highest level of expression. Similarly, a small decrease of Eef1a1 protein was seen in vector control but not at as low a level as in these samples. It cannot be excluded that this is a nucleofection-induced result, as both sample types were collected 24 hours post transfection. These results were not in agreement with *Eef1a1* transcript expression since a decrease in mRNA was mostly observed between the 9 hours and day 2 time points. Samples from subsequent days maintained almost unchanged levels of Eef1a1 protein, at approximately the same levels as seen in parental controls.

The **overall** levels of **eEF1A** protein were assessed by immunoblotting with the anti-eEF1α antibody. As expected, the highest levels of total eEF1A (51kDa) were observed at 9 hours for A2, 2.2 and 1.2 transfectants. On the following days, the expression level of eEF1A stayed almost unchanged, with slight variations between samples without showing any distinct trend.

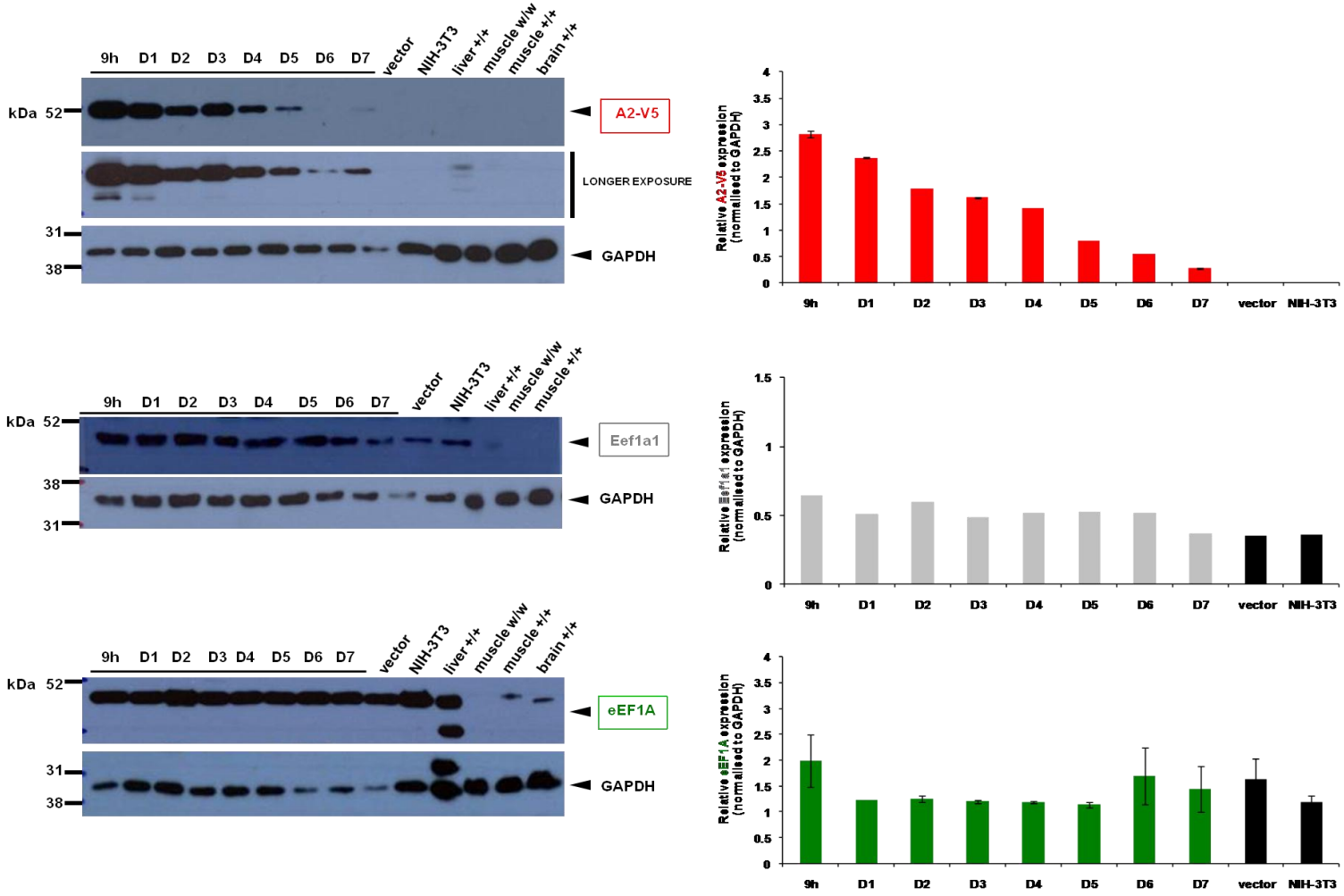

Figure 3.22 Western blot analysis of NIH-3T3 cells transfected with A2-V5 expression plasmid. Samples were subjected to immunoblotting with **anti-V5 tag**, **anti-eEF1α** or **anti-eEF1A1** antibodies. Average densitometric measurements of the band intensities (± SEM) were incorporated into the graphs next to the representative Western blots.

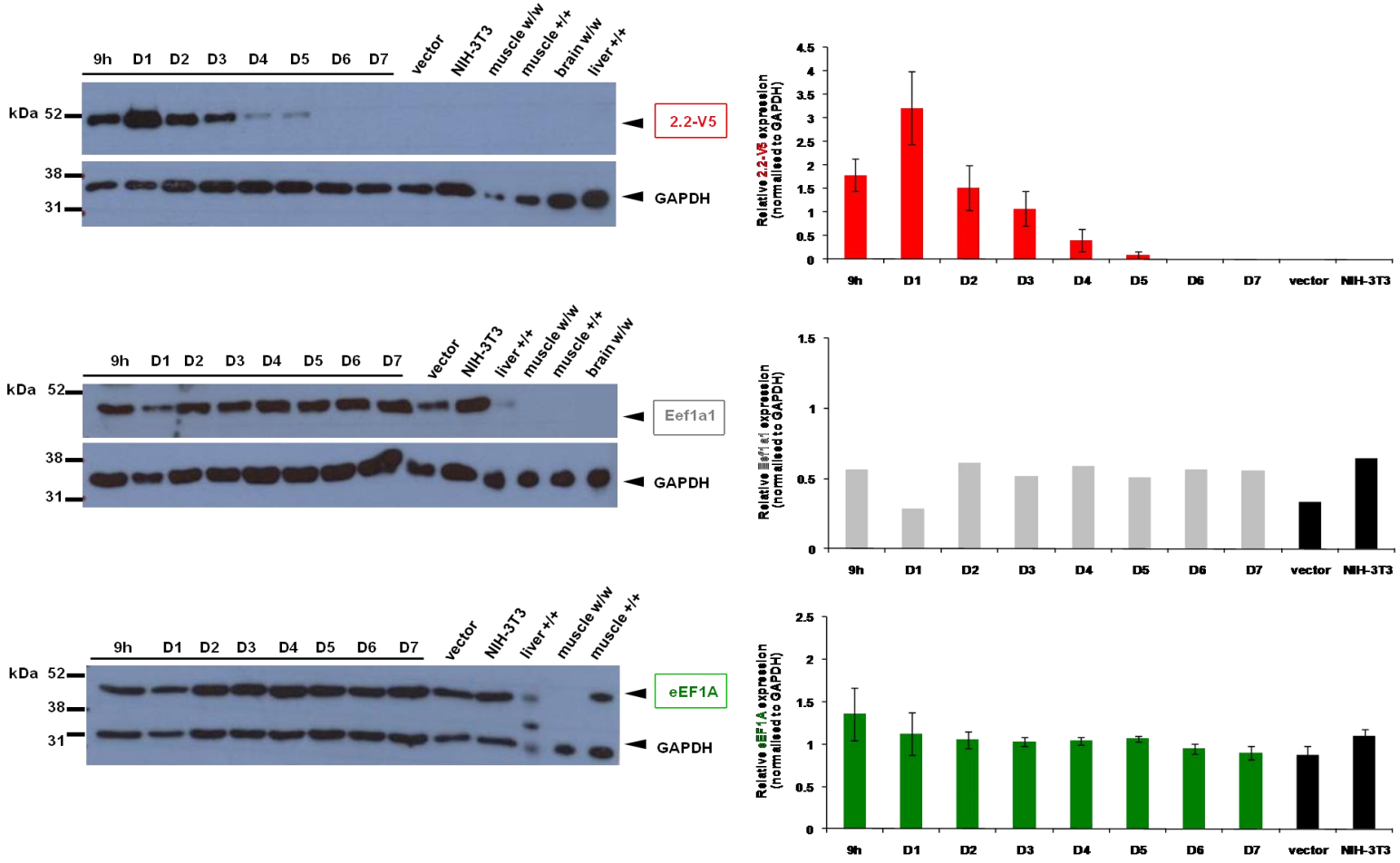

Figure 3.23 Immunoblotting of NIH-3T3 cells transfected with 2. 2-V5 expression plasmid. Expression of **V5-tagged** construct, endogenous **Eef1a1** and **total eEF1A** proteins was monitored up to 7 days post nucleofection. Average densitometric measurements of the band intensities (±SEM) were incorporated into graphs next to the representative Western blots.

3.3 Discussion

In order to elucidate any possible relationship between overexpression of eEF1A forms and the biological significance of their coexistence within cells, a set of different constructs was designed and introduced into NIH-3T3 mouse fibroblasts that do not normally express eEF1A2. Characterization of expression of exogenous versus endogenous eEF1A forms was assessed by transient transfections to examine immediate effects and by stable transfections for potential long-term distance consequences.

It was shown herein that the first 24 hours after nucleofection were crucial in terms of the relationship between endogenous and exogenous eEF1A forms expression. In this study, overexpression of all eEF1A1 origin constructs resulted in significant repression of the endogenous *Eef1a1* mRNA (mostly during 9 hours and the first day post transfection), however a bigger decline was seen if any of the 5'UTRs was present. This was reflected by the small decrease in endogenous protein expression at a 9 hour time point, except for 2.1 transfectants where it was increased. When eEF1A2 origin constructs were overexpressed, a more substantial and longer decrease in *Eef1a1* mRNA was observed in 2.2 and 1.2 transfected NIH-3T3 cells than for A2 counterparts. In contrast, the most significant decrease of Eef1a1 protein levels in 2.2 and 1.2 samples coincided with the highest expression of exogenous proteins at first day post transfection but in A2 transfectants it stayed unchanged.

Changes in endogenous transcripts levels when exogenous counterparts are introduced into the cells are not unprecedented among translation-involved proteins. Wu and Bag showed that overexpression of HeLa cells with exogenous PABP mRNA with a compromised 5'UTR caused repression of endogenous PABP mRNA. In contrast, ectopic expression of PABP mRNA with the proper regulatory element in its 5'UTR did not produce similar effect on endogenous transcript, strongly suggesting involvement of a negative feedback mechanism in controlling expression of PABP mRNA (Wu and Bag, 1998).

Data obtained from transient transfections suggested that incorporation of human eEF1A1 or eEF1A2 into cells significantly altered the expression of endogenous Eef1a1 and that dynamic interplay between different eEF1A variants occurred within the first hours after nucleofection. Translation of both eEF1A forms' messages changed depending on the presence or lack of the chimeric 5'UTRs. It was consistent with primary observations where transfections of constructs carrying chimeric 5'UTRs linked to eEF1A1 or eEF1A2 coding sequences resulted in less efficient expression in comparison to the plasmids containing coding sequences alone. Moreover, introduction of the 5'UTR sequence originating from eEF1A2 in front of either eEF1A1 or eEF1A2 coding sequence caused less repression of exogenous proteins levels than from constructs with the eEF1A1 5'UTR. A significant motif within the 5'UTR sequence of eEF1A1 has already been suggested to participate in modulation of its mRNA translation.

The sequence of the 5'UTR from eEF1A1 contains a cytidine residue followed by an uninterrupted sequence of 5 thymidines (Uetsuki *et al.*, 1989, Slobin and Rao, 1993). This unique structural hallmark is called a 5' terminal oligopyrimidine tract (5'TOP) and therefore, eEF1A1 has been assigned to the family of TOP mRNAs which encode not only ribosomal proteins (RP), most translation initiation and elongation factors but also other proteins associated with translational apparatus (Iadevaia et al., 2008, Avni et al., 1997, Meyuhas, 2000, Yoshihama et al., 2002). Exchange of the single residues within the 5'TOP sequence in rpS16 (40S ribosomal protein S16) or hnRNP A1 (heterogeneous nuclear ribonucleoprotein A1) chimeric constructs indicates that the correct composition of this motif is extremely important for their translational control (Levy et al., 1991, Zhu et al., 2003). The TOP motif is a *cis*-acting regulatory element and is required for translational control of these mRNAs in conditions resulting from cellular stress or poor nutrient status (Caldarola *et al.*, 2004, Hornstein *et al.*, 2001, Avni *et al.*, 1994, Levy *et al.*, 1991). For instance, translational repression of eEF1A1 mRNA was detected upon growth arrest in P1798 mouse lymphosarcoma, human skin

fibroblasts, murine erythroleukemia or NIH-3T3 cells (Avni et al., 1994, Avni et al., 1997, Jefferies et al., 1994, Slobin and Rao, 1993, Thomas and Thomas, 1986). Interestingly, the 5'terminal oligopyrimidine tract is not found within the mRNA sequence of eEF1A2 (Bischoff et al., 2000).

In conjunction with transient transfections, a comparison of the relative expression levels of different eEF1A variants was carried out in stable cell lines. During the long process of their generation, it was discovered that the yield of positive lines with inserts of different eEF1A1 origin was far less successful than with eEF1A2. Even though levels of exogenous eEF1A1 full coding sequence construct were observed in the highest excess within the first 24 hours post transfection, it was almost impossible to achieve this expression magnitude in the stable cell lines. Such a problem was not encountered with the eEF1A2 coding sequence expression plasmid since the yield of the stable cell lines was the highest, whereas numbers of positive clones were gradually lower for 2.2 or 1.2 transfectants. These observations suggest that incorporation of 5'UTR from any of the eEF1A variants could have an influence on effective selection output.

There is some evidence to consider that this observation was not only restricted to NIH-3T3 cells. An attempt to produce stable cell lines with modest eEF1A1 overexpression in Rat2 embryo fibroblasts as well as in HeLa cells was made (note that HeLa express high levels of both eEF1A forms but Rat2 cells lack eEF1A2 protein expression). Only four lines out of 34 Rat2 clones tested for exogenous eEF1A1 were positive whereas HeLa cells did not even survive a selection process (personal observations, data not shown). Selective antibiotic resistance is not likely to be the cause since its concentration was successfully established in advance of the main experiments by performing killing curve assays on the parental cell lines. Furthermore, other researchers encountered similar difficulties (Amiri et al., 2007). On the other hand, a few groups successfully performed experiments in HEK293 cells or similar BALB/c 3T3 mouse fibroblasts stably expressing exogenous eEF1A1 (Duttaroy et al., 1998, Panasyuk et al., 2008). These observations are very puzzling and one can only speculate

whether high levels of eEF1A1 are toxic to the cells or whether cellular feedback exists that blocks expression of eEF1A1 at a certain threshold, or perhaps whether it is a matter of the experimental cell system specificity.

In all A1 or 1.1 NIH-3T3 stable cell lines, the average amounts of endogenous Eef1a1, at both- mRNA and protein level, were roughly the same as in the control line but slightly higher in 2.1 clones (similarly to the observation of 2.1 construct transient transfection). In the majority of eEF1A2 origin stable cell lines *Eef1a1* transcript levels were marginally lower or equal to the controls, but the levels of endogenous protein remained unchanged again. The combined cellular expression of eEF1A was increased in 2.1 lines and all eEF1A2 origin clones at mRNA and protein level.

The attempts to overexpress human eEF1A1 or eEF1A2 in NIH-3T3 cells resulted in preservation of endogenous Eef1a1 at a roughly constant level, suggesting that eEF1A1 expression might be subjected to the strict autoregulation. There may be at least three explanations for this mechanism to consider.

First, it should be kept in mind that in circumstances of any eEF1A variant upregulation, eEF1A1 could shift some of its mRNA into a translationally inactive state due to the regulatory 5'TOP sequence within its 5'UTR (Uetsuki *et al.*, 1989, Slobin and Rao, 1993) .

Alternatively, the possibility of other regulatory sites within eEF1A1 5'UTR cannot be ruled out. These would allow mRNA of eEF1A1 to maintain a balance between translational repression or enhancement, depending on the cell's requirements or external/internal stimuli. The PABP is an excellent example of mRNA that has two well characterized *cis*-acting elements in its 5'UTR, that is a 5'terminal oligopyrimidine tract followed by A-rich sequence (ARS) (Hornstein *et al*., 1999, Wu and Bag, 1998). It is believed that these two elements regulate translation of the PABP mRNA in a distinct manner. While 5'TOP seems to enhance translation due to increased growth requirements, ARS is more predisposed to monitor overall levels of cellular PABP and suppresses its mRNA translation via a feedback mechanism (Wu and Bag, 1998, Bag, 2001).

In addition, Ørom and co-workers confirmed that the 5'TOP sequence of RP mRNAs and microRNA miR-10a are functionally interconnected. Moreover, miR-10a binds immediately downstream of the 5'TOP motif of RP mRNAs and favours their translational enhancement over repression. Therefore, overexpression of miR-10a enhanced RPs synthesis whereas inhibition of endogenous miR-10a resulted in decreased production of RPs. They suggest a mechanism whereby miR-10a competes with a negative acting factor of unknown identity for direct binding downstream of the 5'TOP motif. Interestingly, the supplementary data of this paper contain a table of the top 100 mRNAs from miR-10a pull-out experiments in which eEF1A1 was assigned to position 26 (Ørom et al., 2008). The theoretical strength of interaction between eEF1A1 and miR-10a was calculated using RNAhybrid 2.1 and this prediction was illustrated in Figure 3.34 (Ørom et al., 2008, Rehmsmeier et al., 2004). These data require further experimental validation.

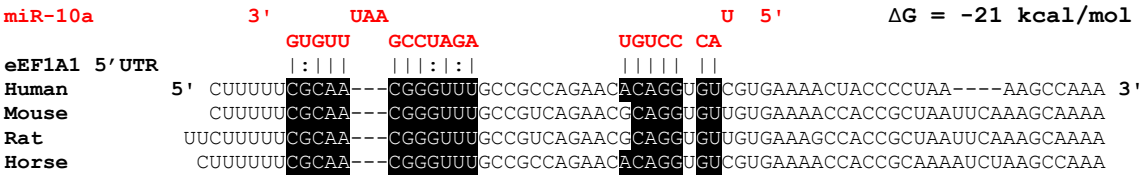

Figure 3.34 Predicted interaction between hsa-miR-10a and eEF1A1 5'UTR sequence. Thermodynamic calculation of ΔG was performed by RNAhybrid 2.1. Sequences of 5'untranslated regions from mouse, rat and horse were shown additionally to indicate evolutionary conserved residues within potential interaction sites.

Finally, a more complex translational regulation mechanism could be involved that requires the assistance of the eEF1A1 3'UTR. Mechanisms of translational control are commonly defined by interactions of different *cis*- or *trans*-regulatory factors within 5'- or 3'- untranslated regions of mRNAs (Pickering and Willis, 2005, Mazumder et al., 2003, de Moor et al., 2005, Wilkie et al., 2003). For instance cross-talk between the 5' uORF and a translational derepression element in the 3'UTR had a profound

effect on translational efficiency of Her-2 (Mehta et al., 2006). On the other hand Kobayashi and Yonehara reported that the 5'UTR was more important for the downregulation of eEF1A1 seen in tetraploid cells than its 3'UTR (Kobayashi and Yonehara, 2008). Nevertheless, the generation of constructs (and possibly stable cell lines) with both eEF1A forms coding sequences linked to their own or reciprocal 3'UTRs would be undoubtedly of great assistance to address this enquiry.

Therefore, the cellular level of eEF1A1 mRNA may dictate how big a pool of the cytoplasmic transcripts will be subjected further to translation. As a consequence, eEF1A1 could be a crucial regulator and/or sensor of total eEF1A amounts in the cells, determining its expression level under normal growth circumstances or during extreme conditions.

On the other hand, since a close correspondence was seen between *Eef1a1* mRNA and protein levels it cannot be excluded that exogenous overexpression of human counterparts did not induce any changes in translational efficiency of the endogenous form. Therefore, even though the combined cellular level of eEF1A was enhanced by the addition of the human eEF1A variants, the cells could be still able to accept that increase without disruption to the performance of their biological functions.

The precise mechanism of eEF1A1-mediated regulation is not fully understood and needs to be further elucidated. More accurate information about the relationships between both eEF1A variants and their exogenous counterparts in stably or transiently transfected NIH-3T3 (or even in a different cell system) could be provided by polysome profile analysis. It would be advantageous to subject cell lysates from these cells to centrifugation in 10-50% sucrose gradients in order to capture the precise mRNA and protein distribution signatures of exogenous versus endogenous eEF1A forms in different fractions.

It is also noteworthy that eEF1A1 comprises up to 3% of the total protein content within the cell, hence it is already in a high excess over the other translational machinery proteins (Hershey, 1991). Most likely, these high optimal amounts

of eEF1A1 are necessary to maintain its various cellular functions as it is a moonlighting protein (Ejiri, 2002). Even though small excess amounts over this threshold might be still tolerated by the cells and allow for normal growth, significant upregulation over a certain limit and an eventual increase in total eEF1A could be deleterious.

As eEF1A1 overexpression and downregulation have been implicated in triggering apoptosis (Ruest et al., 2002), expression of both eEF1A forms is only seen in cultured cells and tumours, and unchanged levels of *EEF1A1* transcript were already observed in certain malignancies and cancer cell lines (Anand et al., 2002, Cao et al., 2009), maintaining eEF1A1 levels unchanged would be undoubtedly beneficial from the eEF1A2-driven oncogenesis point of view.

Although the biological meaning of overall eEF1A overexpression is unknown, inappropriate expression of other translation factors, for instance eEF1Bδ and eEF1Bγ as well as eIF3e, eIF3f or eIF3h subunits of the eIF3 factor, have been linked to cancer. Moreover, these factors also belong to the 5'TOP family (Lei et al., 2002, Zhang et al., 2007, Zhang et al., 2008, Iadevaia et al., 2008, Mimori et al., 1995, Frazier et al., 1998, Mathur et al., 1998). Therefore, it was interesting to know whether incorporation of 5'UTRs from both eEF1A forms independently in front of the eEF1A2 coding sequence, could promote any changes is transformed phenotype of eEF1A2-overexpressing cells or whether a similar effect would be seen for cell lines stably expressing eEF1A1.

Chapter 4: *In vitro* systems for investigation of eEF1A1 and eEF1A2 oncogenic potential

4.1 Introduction

Increased motility, loss of contact inhibition and gain of anchorage independent growth are significant hallmarks of neoplastic cells and characterize the general phenotypes of an oncogene.

In order to investigate the potential role or differences between eEF1A1 and eEF1A2 in oncogenesis, a variety of eEF1A plasmids was constitutively overexpressed in NIH-3T3 mouse fibroblasts as described in Chapter 3. Selected stable cell lines were then subjected to different transformation assays, including foci formation, anchorage independent growth in soft agar and proliferation. In some of these lines, transformed properties were observed that led further to an analysis of their *in vitro* migration and invasion abilities.

As the mechanism underlying induction of eEF1A2-driven oncogenesis has not been completely elucidated, it was hypothesized that its oncogenic potential might be associated with its conventional role in translation or alternatively with its non-canonical functions like, for example, modifications of the cytoskeleton. The rate of global translation was determined in the stable cell lines of different eEF1A1 or eEF1A2 origin in order to establish whether increased expression of either variant caused an overall increase in protein synthesis and transformation.

4.2 Results

4.2.1 *In vitro* transformation assays

4.2.1.1 Focus formation indicates a transforming phenotype

To investigate and compare the oncogenic potential of both eEF1A forms, focus formation assays were performed on selected NIH-3T3 stable cell lines. A transformed phenotype should be observed as a multilayered, crisscrossed growth of spindle-shaped cells (Pastan and Willingham, 1978). Equal numbers of mouse fibroblasts stably expressing A1, A2, 1.1, 2.1, 2.2 or 1.2 were seeded in 10-cm dishes and cultured under standard conditions for 3 weeks. Next, NIH-3T3 cells were fixed in methanol and stained with crystal violet in order to evaluate the morphology of the cells on every plate. If a transformed phenotype was observed, the foci on a dish were counted and photographed.

4.2.1.1.1 Foci formation in A1, 1.1 or 2.1 expressing NIH-3T3 mouse fibroblast cells

As reviewed in Table 3.2, three A1 stable cell lines, two 1.1 lines and three 2.1 clones were subjected to a focus formation assay. NIH-3T3 fibroblasts stably expressing empty vector pDEST40 (vector 2) were used as a negative control whereas EJTF2 cells that stably express the H-Ras^{G12V} oncogene were used as a positive control.

Three weeks after plating, there were no foci in the vector control dishes (Figure 4.2) whereas distinct foci were observed on the experimental plates as shown in Figures 4.1, 4.2 and 4.3. NIH-3T3 cells from the negative control dishes grew in an organized monolayer with contact inhibition while examination of transformed foci revealed cells that had changed shape into spindles and disorganized, multilayered structures, with similar morphology to the positive control of EJTF2 cells. Transforming efficiencies of the H-Ras^{G12V} control in this study were comparable to those reported by Kanda and co-workers (Kanda et al., 2005).

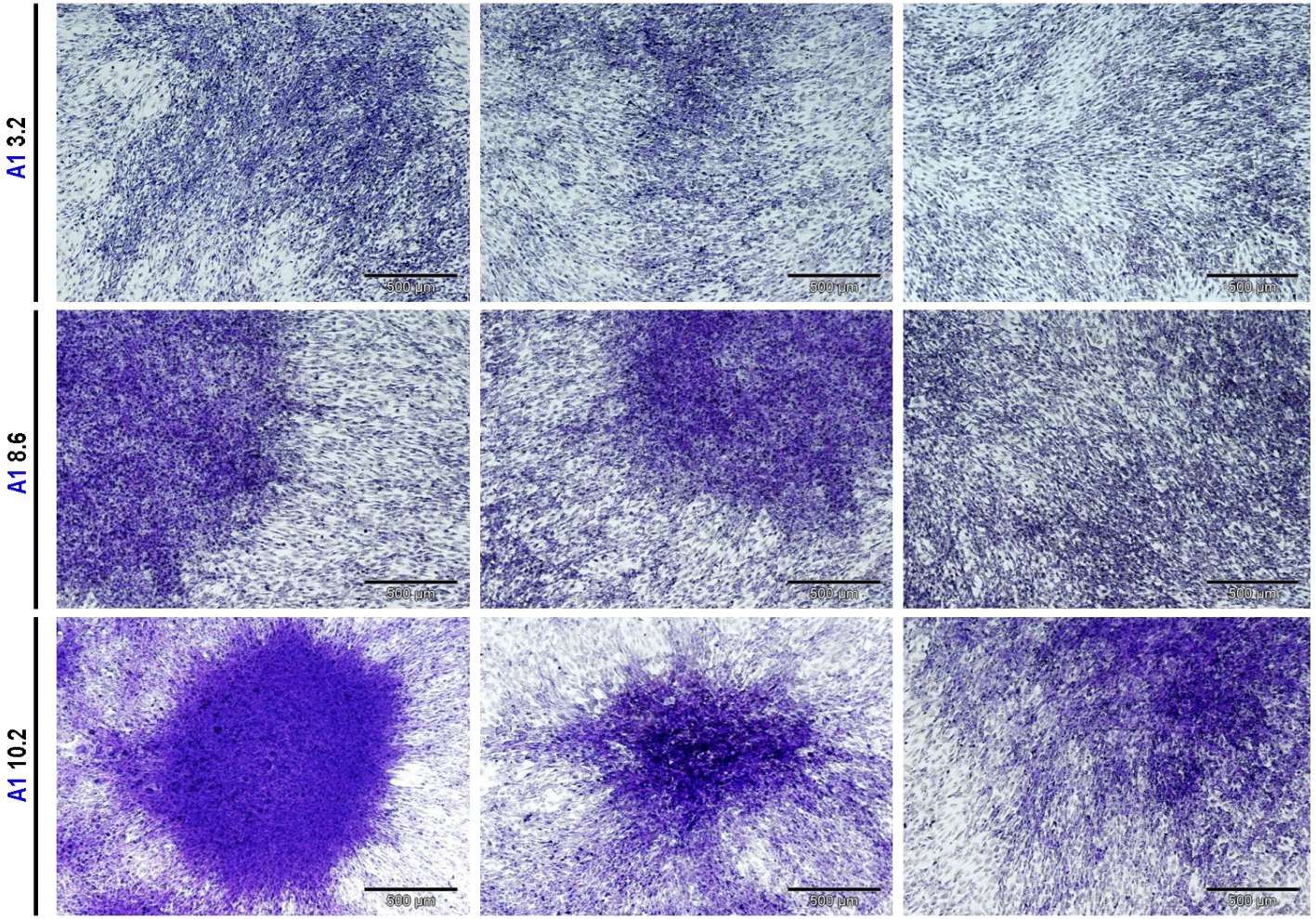

Figure 4.1 Effects of eEF1A1 overexpression on cellular morphology within A1 stable cell lines. NIH-3T3 cells stably transfected with A1 construct were cultured in geneticin-supplemented DMEM for determination of their capacity to produce foci. Three weeks later cells were fixed, stained with crystal violet and their morphology was photographed. Size bars are equal to 500 µm.

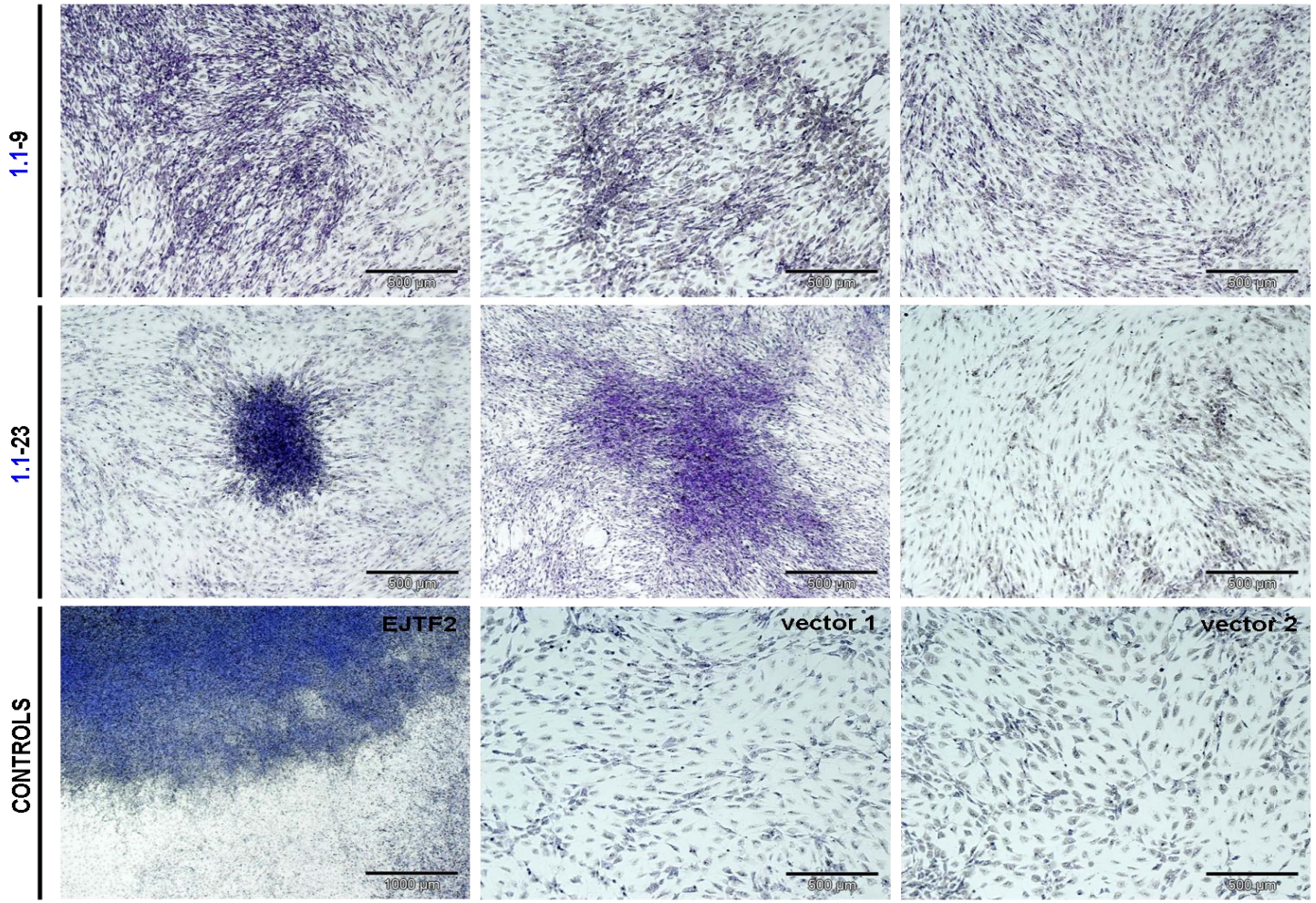

Figure 4.2 Effects of 1.1 overexpression on cellular morphology within 1.1 stable cell lines. NIH-3T3 cells stably transfected with 1.1 construct were cultured in geneticin-supplemented DMEM for determination of their capacity to produce foci. The third row shows positive control (EJTF2 cells) and negative controls (vector transfected cells). Size bars are equal to 500 µm and 1000 µm.

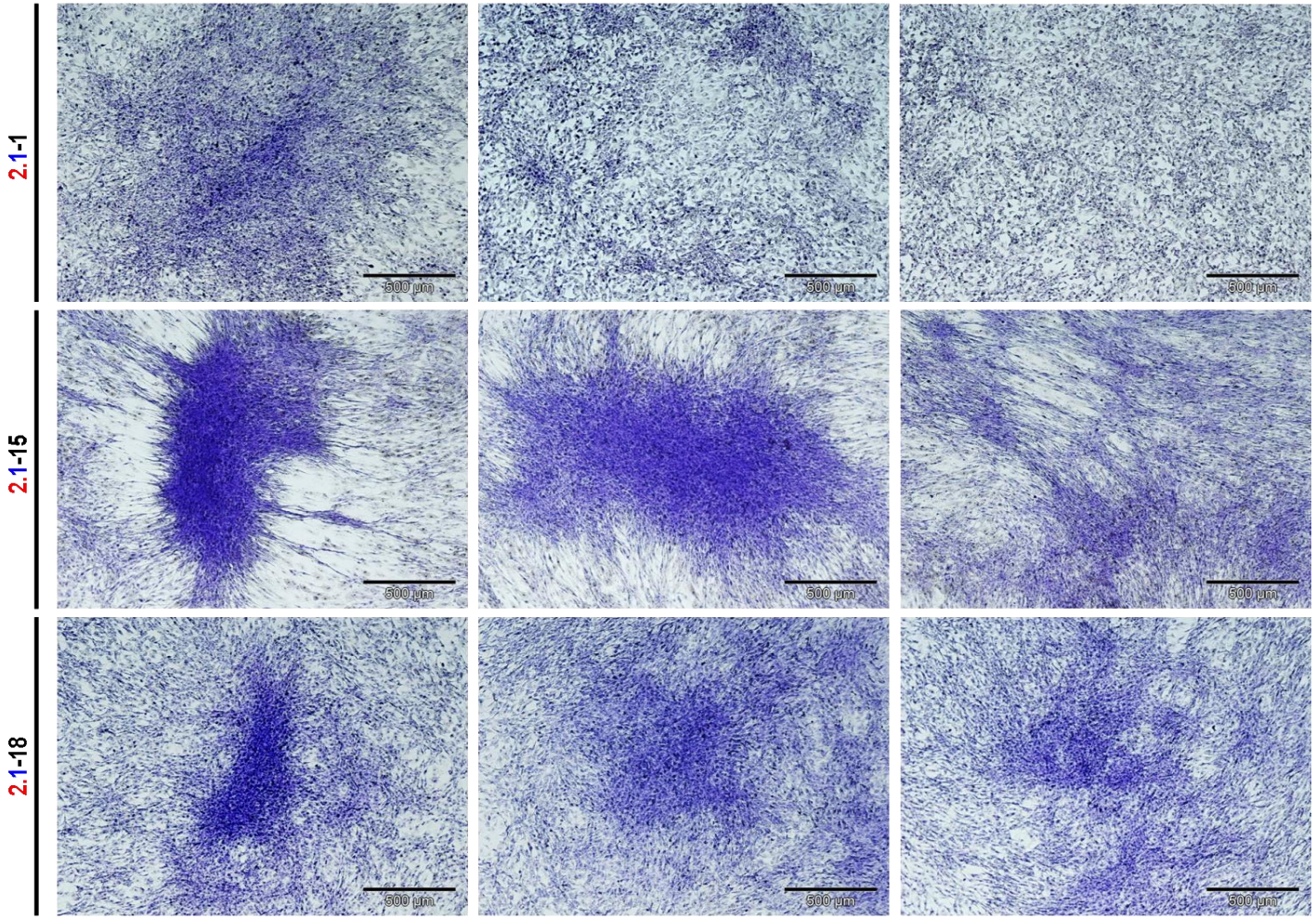

Figure 4.3 Effects of 2.1 overexpression on cellular morphology within 2.1 stable cell lines. NIH-3T3 cells stably transfected with 2.1 construct were cultured in geneticin-supplemented DMEM for determination of their capacity to produce foci. Size bars are equal to 500 µm.

Figure 4.4 shows that overexpression of A1 in NIH-3T3 cells resulted in the acquisition of a transformed phenotype by clones 8.6 and 10.2 but to a lesser extent by clone 3.2 where foci formation was only about 8% of the positive control. It is difficult to explain why this particular line behaved differently; especially it exhibited a moderate level of A1 expression.

In contrast, overexpression of 1.1 or 2.1 caused less efficient foci formation as seen in the 1.1-9, 1.1-23, 2.1-1, 2.1-15 and 2.1-18 clones where transformation was around 12, 31, 8, 39 and 37 % of the positive control of EJTF2 cells. The A1 3.2, 1.1-9, 2.1-1 and 2.1-18 transformants exhibited disorganized orientation, piling up of the cells and very subtle or light-small foci, which were clearly more refractile than the pronounced, sharp-edged foci in A1 8.6, A1 10.2 or 2.1-15 clones.

A summary of the average foci per cell line relative to positive and negative controls is displayed in Table 4.1

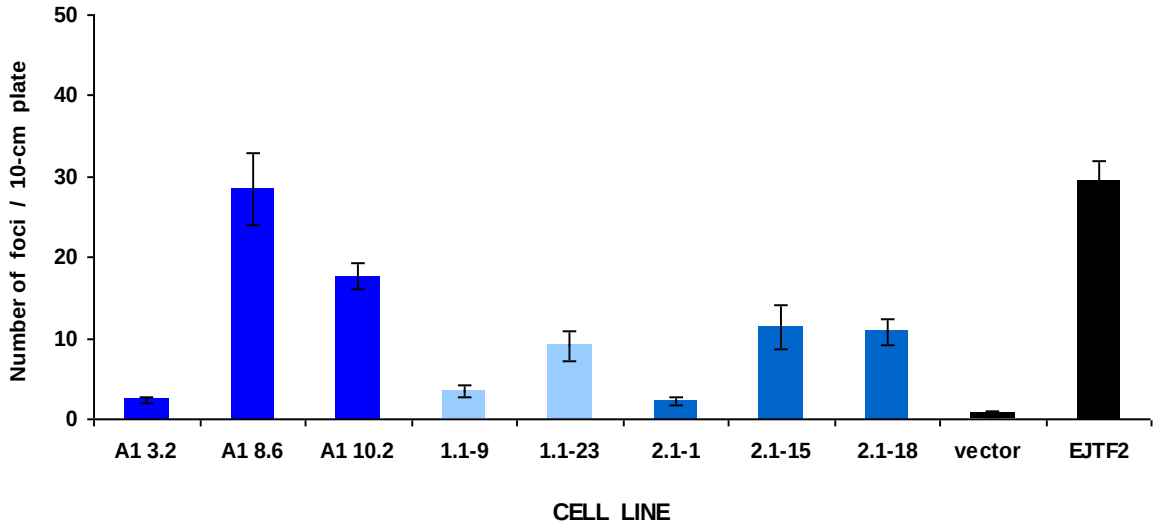

Figure 4.4 Foci formation assay in stable cell lines of eEF1A1 origin. NIH-3T3 cells stably expressing **A1**, 1.1 or **2.1** variants were monitored for loss of contact inhibition. Formed foci were fixed, stained and counted 3 weeks after plating. Results are shown as a mean of three independent experiments performed in triplicates (± SEM).

Table 4.1 *Summary of the focus formation assay results for different stable cell lines of eEF1A1 origin*

CELL LINE	NUMBER OF FOCI PER 10-cm PLATE (±SEM)	% OF CONTROL (EJTF2)	*P* value[a] (versus EJTF2)	*P* value[a] (versus vector)
A1 3.2	2.4 ± 0.34	8.3	<0.001	0.0018
A1 8.6	28.5 ± 4.43	97.0	0.8638	0.0002
A1 10.2	17.6 ± 1.61	60.0	0.0014	<0.001
1.1-9	3.4 ± 0.67	11.7	<0.001	0.0031
1.1-23	9.1 ± 1.81	30.9	<0.001	0.0015
2.1-1	2.2 ± 0.52	7.5	<0.001	0.0230
2.1-15	11.4 ± 2.68	38.9	0.0002	0.0037
2.1-18	10.7 ± 1.67	36.6	<0.001	0.0003
vector	0.6 ± 0.33	2.3	<0.001	
EJTF2	29.4 ± 2.48	**100.0**		<0.001

[a] Student's *t*- test, two-tailed

These results suggest that presence of expression of A1, 1.1 and 2.1 constructs in normal NIH-3T3 mouse fibroblasts leads to loss of contact inhibition and neoplastic phenotype resulting as foci formation. Overexpression of 1.1 or 2.1 does not correspond to complete loss of *in vitro* clonogenicity and is still sufficient to alter morphology of the cells but these lines exhibit less potential to produce foci than fibroblasts stably expressing A1.

4.2.1.1.2 Effect of A2, 2.2 or 1.2 variant overexpression on NIH-3T3 cell foci formation

Three representative A2, 2.2 or 1.2 NIH-3T3 stable cell lines (as presented in Table 3.2) were monitored in terms of contact inhibition loss for 21 days. Mouse fibroblasts harboring a constitutively active H-Ras^{G12V} oncogene were used as a positive control. NIH-3T3 mouse fibroblasts stably expressing pcDNA3.1 (vector 1) or pDEST40 (vector 2) were used as negative controls.

After three weeks of culture it was found that cells overexpressing A2, 2.2 or 1.2 gave rise to foci while cells stably transfected with vectors did not exhibit a transformed phenotype. These cells grew in a monolayer and had a normal fibroblast shape as shown in Figure 4.2. In contrast, the cells on the dishes with noticeable foci revealed highly disoriented crisscrossed morphology and multilayered growth, similar to EJTF2 cells. Microphotographs of the foci are documented in Figures 4.5, 4.6 and 4.7.

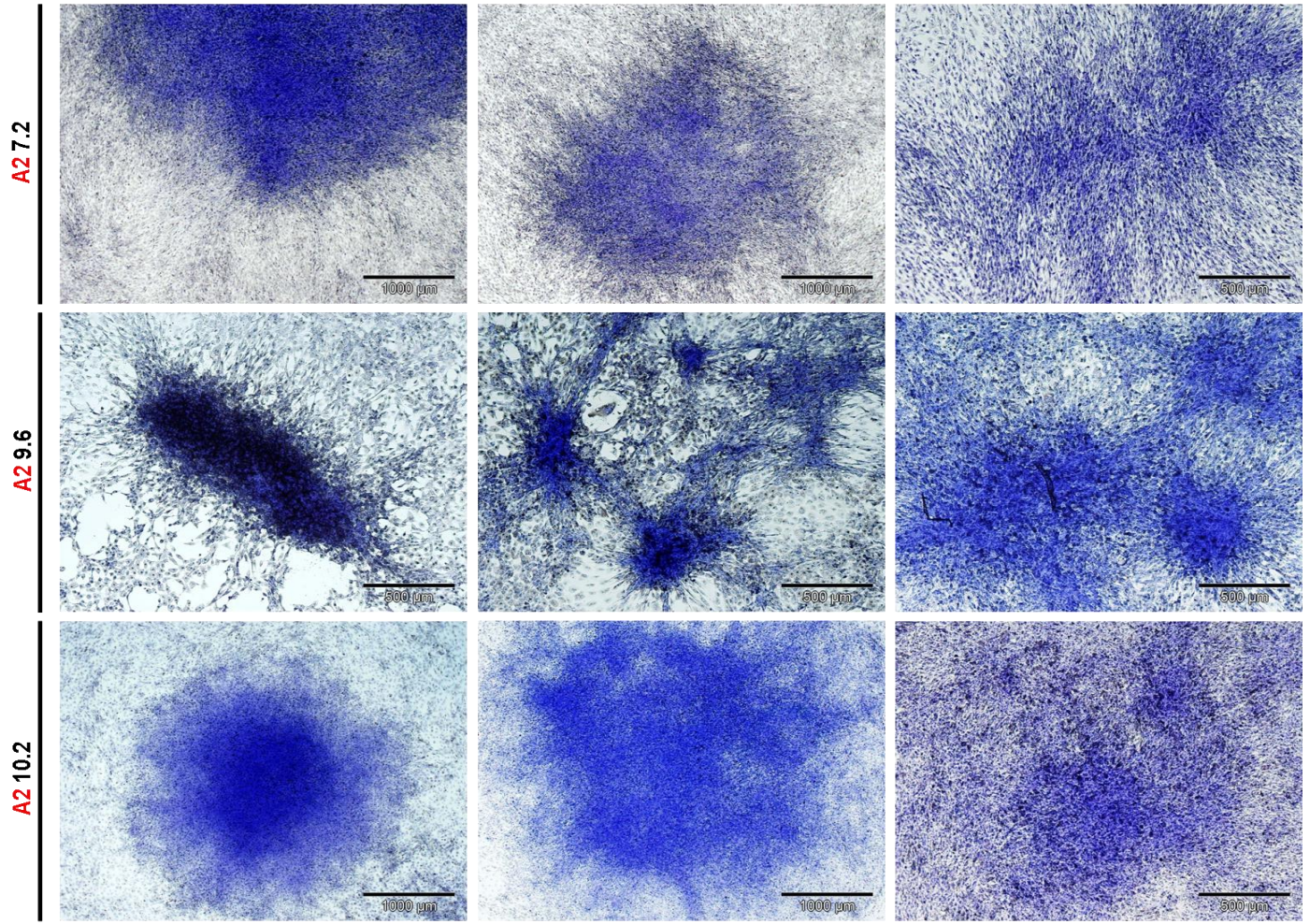

Figure 4.5 Effects of eEF1A2 overexpression on cellular morphology within A2 stable cell lines. NIH-3T3 cells stably transfected with A2 construct were cultured in zeocin-supplemented DMEM for determination of their capacity to produce foci. Three weeks later cells were fixed, stained with crystal violet and their morphology was photographed. Size bars are equal to 500 µm and 1000 µm.

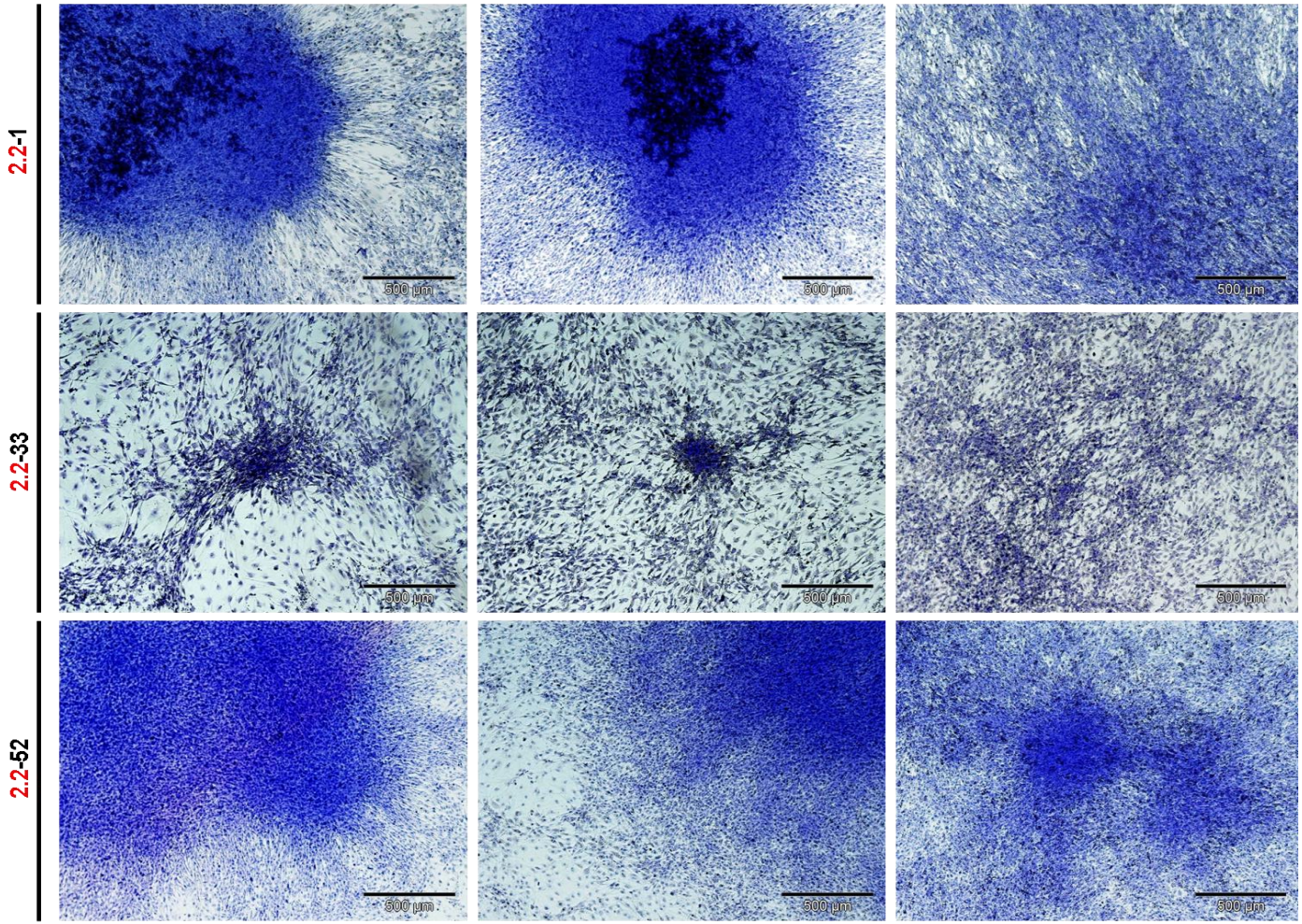

Figure 4.6 Effects of 2.2 overexpression on cellular morphology within 2.2 stable cell lines. NIH-3T3 cells stably transfected with 2.2 construct were cultured in geneticin-supplemented DMEM for determination of their capacity to produce foci. Size bars are equal to 500 µm.

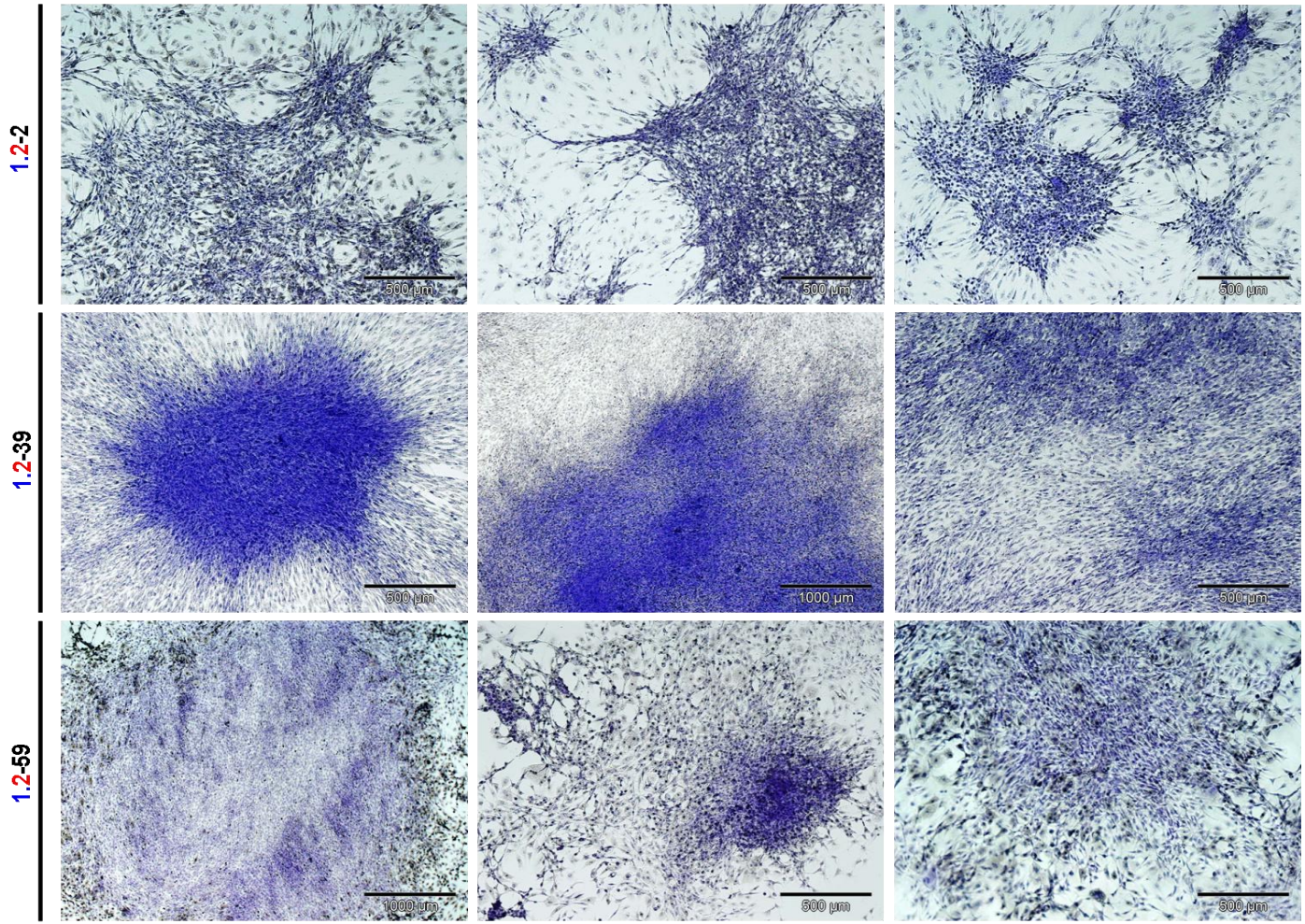

Figure 4.7 Effects of 1.2 overexpression on cellular morphology within 1.2 stable cell lines. NIH-3T3 cells stably transfected with 1.2 construct were cultured in geneticin-supplemented DMEM for determination of their capacity to produce foci. Size bars are equal to 500 µm and 1000 µm.

The morphologies of all three A2 clones, 2.2-1, 2.2-52 or 1.2-39 lines were observed as highly condensed and piled up groups of crisscrossed cells with enormous foci. Foci of the 2.2-33, 1.2-2 and 1.2-59 lines were also spindle-shaped with sharp edges but they displayed smaller dimensions.

Enhanced expression of A2 in NIH-3T3 cells resulted in an increased level of focus forming ability when compared to the EJTF2 control. As showed in Figure 4.8, the number of foci in the 7.2, 9.6 and 10.2 lines was elevated by 23, 25 and 32 %, respectively over the positive control. In contrast, overexpression of 2.2 was less transforming, and focus production in lines 2.2-1 and 2.2-33 was approximately 51 and 30 % of the EJTF2 cells control. Unexpectedly, clone 2.2-52 showed a dramatic increase in foci production by 204% of the positive control level. Additionally, elevated expression of 1.2 in lines 1.2-2, 1.2-39 and 1.2-59 appeared to cause a reduction of transformation and foci formation in these lines consisted about 48, 25 and 27 % of the H-Ras^{G12V} harboring cells, respectively. A summary of the results from the focus formation assay carried out on A2, 2.2 and 1.2 stable cell lines is displayed in Table 4.2.

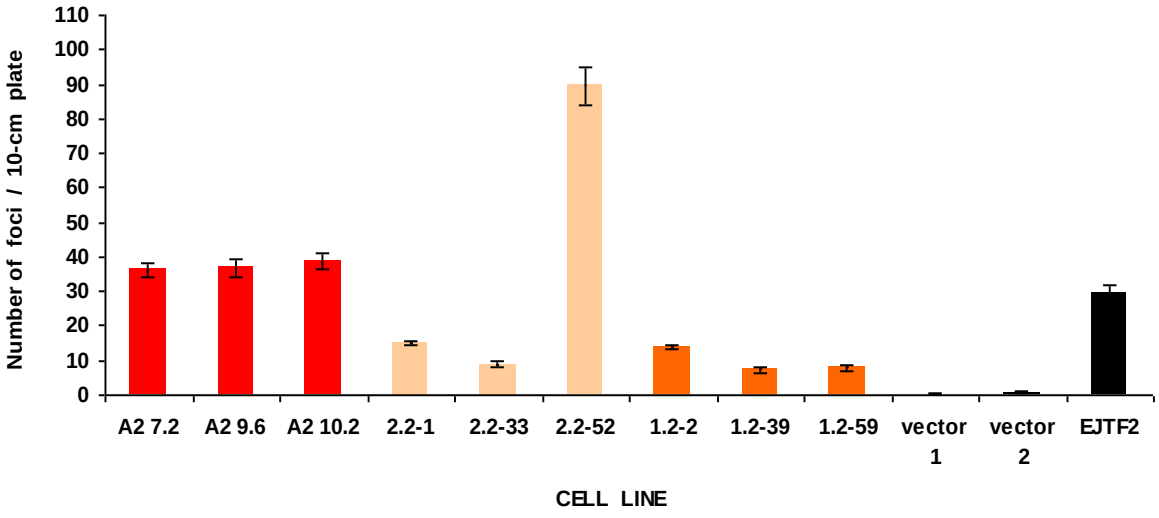

Figure 4.8 Assessment of foci formation ability within stable cell lines of eEF1A2 origin. Normal mouse fibroblasts stably overexpressing **A2**, **2.2** or **1.2** variants were subjected to analysis of transformed phenotype induction. After 21 days of culture, NIH-3T3 cells were fixed and stained and foci were counted. Graph represents mean number of foci originating from three individual experiments that were determined in triplicates (± SEM).

Table 4.2 *Review of focus formation assay for NIH-3T3 stable cell lines of different eEF1A2 origin*

CELL LINE	NUMBER OF FOCI PER 10-cm PLATE (±SEM)	% OF CONTROL (EJTF2)	*P* value[a] (versus EJTF2)	*P* value[a] (versus vector)
A2 7.2	36.3 ± 1.96	123.4	0.0453	<0.001
A2 9.6	36.8 ± 2.36	124.9	0.0479	<0.001
A2 10.2	38.8 ± 2.06	131.7	0.0108	<0.001
2.2-1	15.0 ± 0.78	50.9	0.0003	<0.001
2.2-33	8.9 ± 0.72	30.2	<0.001	<0.001
2.2-52	89.6 ± 5.63	304.2	<0.001	<0.001
1.2-2	14.0 ± 0.6	47.5	<0.001	<0.001
1.2-39	7.4 ± 0.9	25.3	<0.001	<0.001
1.2-59	8.0 ± 0.78	27.2	<0.001	<0.001
vector 1	0.2 ± 0.15	0.7	<0.001	
vector 2	0.7 ± 0.33	2.3	<0.001	
EJTF2	29.4 ± 2.48	**100**		<0.001

[a] Student's *t*-test, two-tailed

The above data indicate that overexpression of the A2 variant resulted in the acquisition of a transformed phenotype *in vitro* by NIH-3T3 cells. Also cells overexpressing 2.2 constructs lost contact inhibition and produced foci but with a lower capacity than A2 coding sequence lines, except clone 2.2-52. The stable induction of 1.2 into mouse fibroblasts was sufficient to form marked foci although level of transformation was decreased in comparison to lines of the 2.2 variant.

4.2.1.2 Anchorage independent growth in soft agar is a hallmark of neoplastic transformation

Following selection in G418 (Geneticin®) or Zeocin™ and isolation of the cell lines overexpressing different eEF1A variants, some clones gained a specific cell morphology and lost contact inhibition as described in Section 4.2.1.1. Consistent with these findings, it was determined whether other neoplastic phenotypes could occur in selected transfectants. The capacity of the cells to proliferate in the absence of attachment to a solid surface and to form colonies in soft agar are well-known characteristics of the transformed phenotype (Shin et al., 1975). In order to evaluate the oncogenicity of eEF1A variants *in vitro*, cells were suspended in a layer of medium-enriched agar and cultured for 3 weeks. Subsequently, colonies were counted in individual wells and representative cell aggregates were photographed.

4.2.1.2.1 Overexpression of eEF1A1 causes transformation of NIH-3T3 fibroblast cells

Three A1 stable cell lines, three 2.1 clones and two 1.1 lines (Table 3.2) were tested in the anchorage independent growth assay to check whether eEF1A1 can act as an oncogene. The EJTF2 cell line stably expressing H-ras^{G12V} was used as a positive control while empty vector transfected NIH-3T3 fibroblasts served as a negative control, as before.

Following 21 days of culture, cells expressing empty vector did not form colonies in soft agar but occasionally 1 or 2 colonies were observed among single cells in a few wells. These were considered as a background level and no increase of their size was seen when dishes were left in culture longer than three weeks.

Interestingly, all three A1 clones evidently provoked colony formation in soft agar whereas cell lines originating from constructs with incorporated 5'UTRs exhibited very poor activity in terms of neoplastic phenotype in comparison to the positive control (Figure 4.9). Again, 1.1 or 2.1 colonies did not change their size over the expanded culturing period.

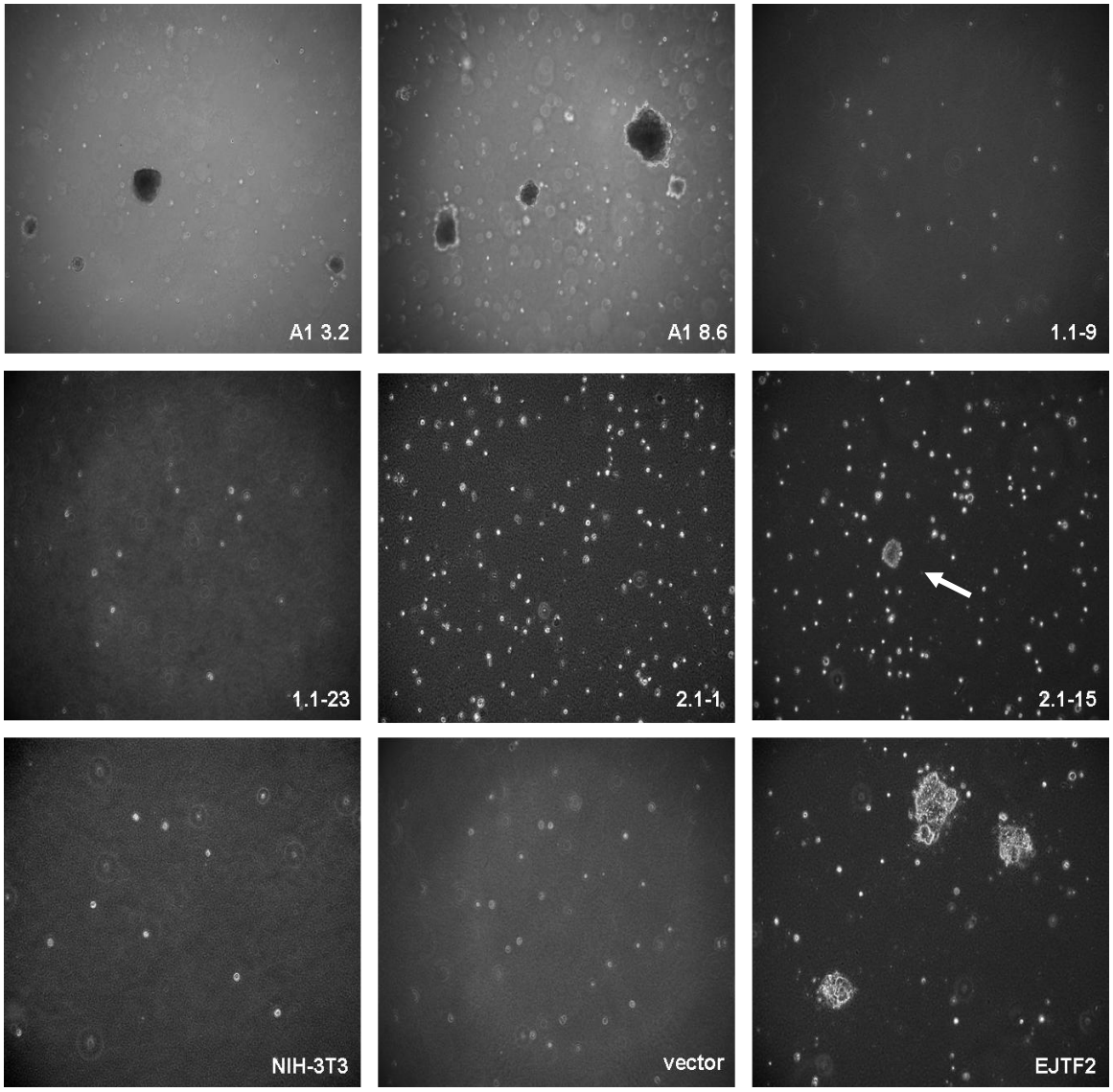

Figure 4.9 Overexpression of eEF1A1 induces oncogenic transformation in NIH-3T3 mouse fibroblasts. Stable cell lines of eEF1A1 origin were used in an anchorage independent growth assay by culturing cells in a semisolid layer of 0.3% agar over 3 weeks. The parental cells or clones stably expressing empty vector were negative controls whereas EJTF2 cells stably expressing H-Ras were used as a positive control. Colony pictures were taken 21 days after plating (magnification 10x). eEF1A1 transfectants and EJTF2 cells displayed a clear transformed phenotype while only single cells were observed for 1.1, 2.1 or vector transfected lines. Names of the photographed lines are documented in the corner of every representative picture, in white.

The average number of colonies for A1 3.2, A1 8.6 and A1 10.2 clones were 73, 106 and 79, respectively. As shown in Figure 4.10, only 3 colonies were produced by either by 1.1-9 or 1.1-23 clones whilst 4, 8 and 1 colonies were produced by 2.1-1, 2.1-15 and 2.1-18 lines respectively. It cannot be excluded that this corresponds simply to background. In contrast, the positive control of EJTF2 cells gave rise to around 150 colonies per well. The number of colonies per cell line expressed as a percentage of the positive control is represented in Table 4.3.

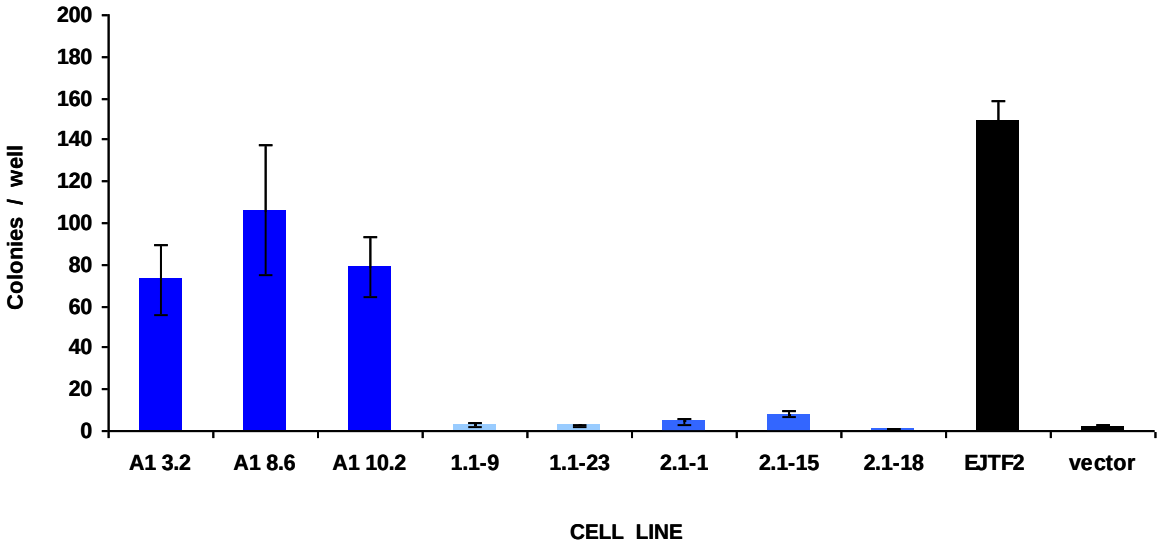

Figure 4.10 Assessment of transformation abilities of eEF1A1 origin stable cell lines. Colonies formed by indicated cell lines were counted after 21 days of culture. At least three independent experiments were performed per cell line and each technical repeat was prepared in triplicate. The results are shown as a mean number of colonies per one well of the dish (± SEM).

Table 4.3 *Anchorage independent growth assay in vector alone, A1, 1.1 and 2.1 stably transfected NIH-3T3 cell lines*

CELL LINE	NUMBER OF COLONIES/WELL (± SEM)	% OF CONTROL (EJTF2)	*P* value[a] (versus EJTF2)	*P* value[a] (versus vector)
A1 3.2	73 ± 17.00	48.7	0.0007	0.0010
A1 8.6	106 ± 31.50	71.0	0.2044	0.0052
A1 10.2	79 ± 14.50	52.7	0.0004	0.0001
1.1-9	3 ± 0.60	2.0	<0.001	0.3860
1.1-23	3 ± 0.50	2.0	<0.001	0.4375
2.1-1	4 ± 1.00	2.9	<0.001	0.0544
2.1-15	8 ± 1.30	5.3	<0.001	0.0012
2.1-18	1 ± 0.30	0.7	<0.001	0.1809
vector	2 ± 9.50	1.3	<0.001	
EJTF2	150 ± 0.60	**100.0**		<0.001

[a] Student's *t*-test, two-tailed

Unfortunately, a high variation in colony numbers counted within A1 clones was observed between all experimental repeats, even though the same protocol was used every time. There were six separate experiments of the soft agar assay performed on A1 cell lines and each was carried out in triplicate. Figure 4.11 shows colony counts after each independent assay. It is hard to determine why colony numbers were so high after the first round of experiment whereas counts of colonies decreased over subsequent repeats. This phenomenon was not observed for other cell assays.

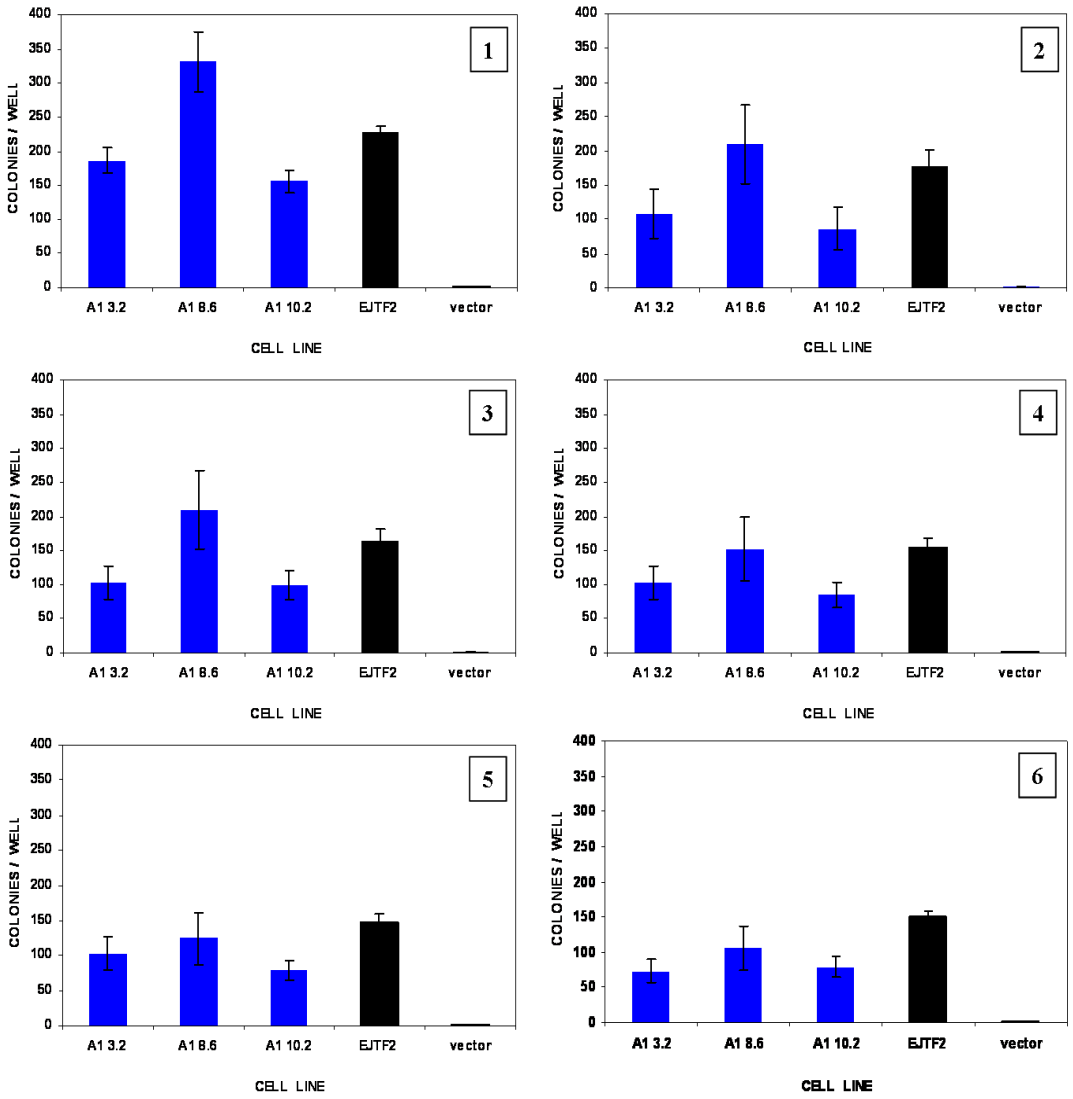

Figure 4.11 Soft agar assay performed on three A1 stable cell lines demonstrating variability in anchorage independent colony formation over six experimental repeats. Graphs represent the mean counts of colonies per well (± SEM) from six consecutive assays performed in triplicate. The number in the corner of every chart indicates the experimental repeat.

From different eEF1A1 origin clones and related controls it was observed that A1 clones formed markedly more colonies in agar than 1.1 or 2.1 clones but not as many as the positive control. It may suggest that the incorporation of a 5'UTR into the construct, regardless its eEF1A variant origin, was sufficient to cause almost complete abolition of the ability of the lines to produce soft agar colonies, such as were observed in A1 overexpressing lines.

4.2.1.2.2 Overexpression of all eEF1A2 origin constructs promotes colony formation in soft agar

Three of each A2, 2.2 or 1.2 cell lines (as reviewed in Table 3.2) were subjected to the anchorage independent growth assay in order to monitor any oncogenic potential, when different eEF1A2 variants were overexpressed in the cells. Control cell lines were as before. The main question addressed in this study was whether lack of translational repression of eEF1A2 might contribute to its role in tumourigenesis. Does the incorporation of a 5'UTR (regardless its eEF1A variant origin) in front of the eEF1A2 coding sequence alter the extent of transformation of the cells?

As expected, after 3 weeks of culture, all eEF1A2 overexpressing transfectants developed colonies in soft agar and no colonies were detected within vector controls as shown in Figure 4.12. Again, an occasional colony was noticed in the wells with vector stable cell lines but these did not change size when cultured for more than three weeks. These are likely to represent the background level of the assay or perhaps an artefact of randomly assembled cells when they were poured over the layer of agar. In contrast, 2.2 and 1.2 cell lines provoked substantially fewer colonies than EJTF2 control or A2 clones over the same period of time. Interestingly, 2.2 clones exhibited also a weaker activity to form colonies in agar than 1.2 clones.

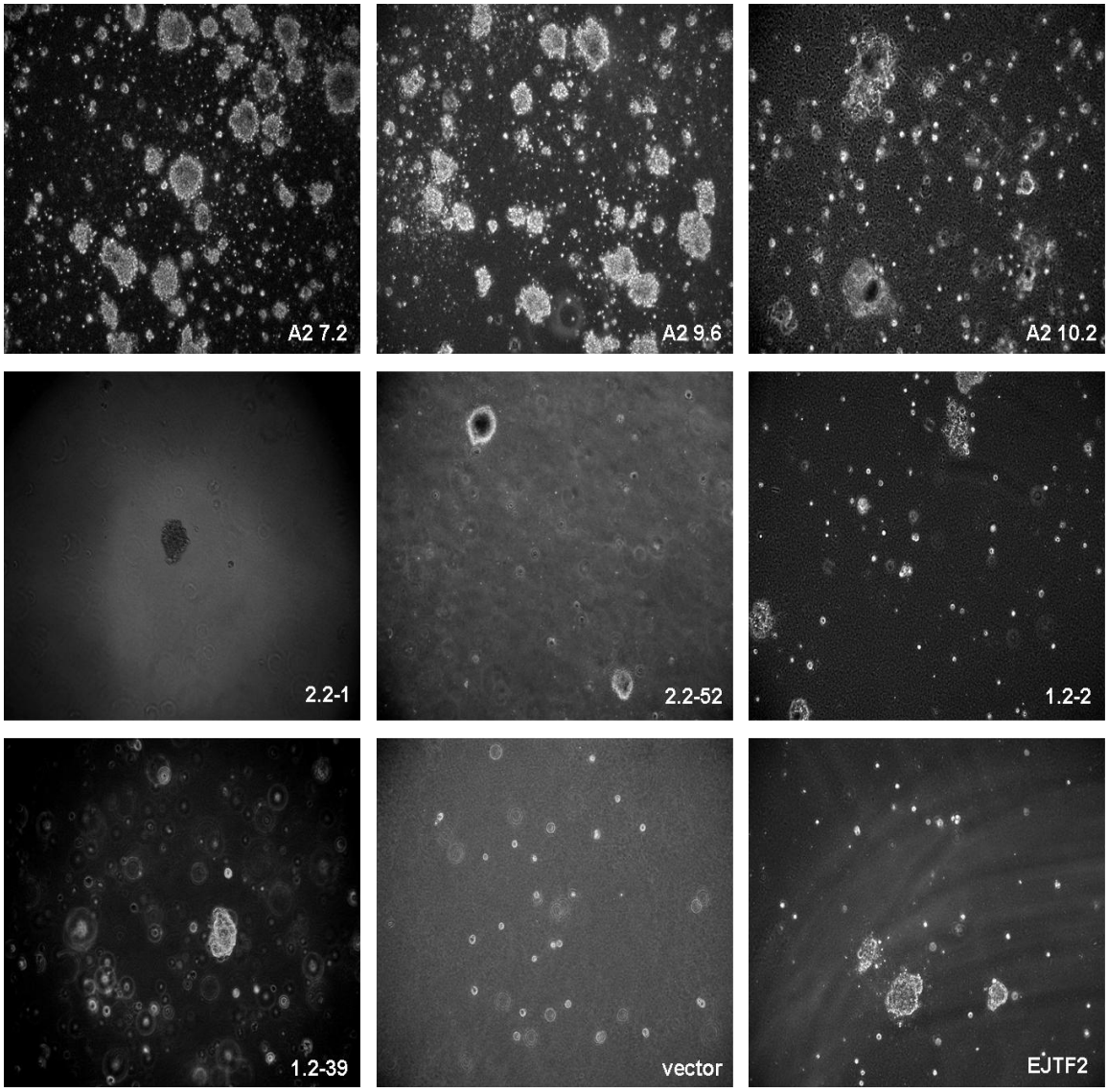

Figure 4.12 Ectopic expression of all eEF1A2 variants in NIH-3T3 cells induces anchorage independent growth. Following 21 days of culture in 0.3% layer of agar, colonies were counted and photographed (magnification 10x). NIH-3T3 cells stably transfected with empty vector were used as a negative control and 3 weeks after plating, single cells were observed within these wells.

As shown in Figure 4.13, the average number of colonies produced by clones A2 7.2, A2 9.6 and A2 10.2 were 119, 131 and 207, respectively, or 79%, 88% and 138% the number of colonies formed by control EJTF2 cells (Table 4.4). In the presence of the eEF1A2 5'UTR (2.2) these numbers decreased to only 26, 17 and 22 colonies for the three tested cell lines. In contrast, in the presence of the eEF1A1 5'UTR, the numbers of colonies in soft agar were 43, 56 and 21, respectively.

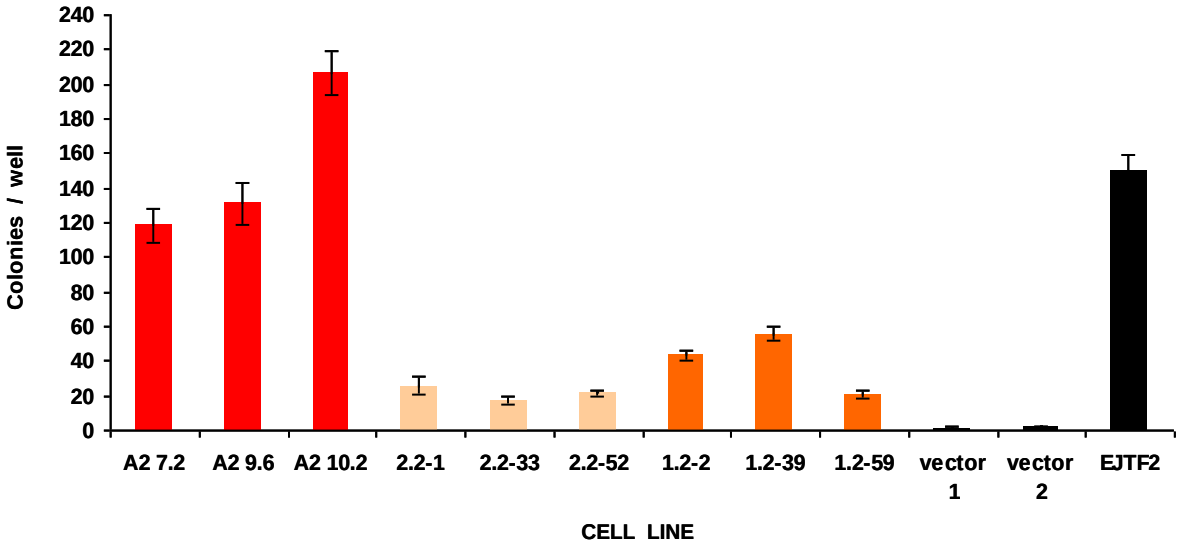

Figure 4.13 Stable overexpression of 2.2 and 1.2 variants gives rise to a neoplastic phenotype as measured by the anchorage independent growth assay. Colony formation in representative **A2**, 2.2 and **1.2** stable cell lines was assessed after 3 weeks by counting viable colonies in individual wells. The results are shown as a mean number of colonies per well (± SEM) from at least three separate experiments performed in triplicate.

Table 4.4 *Anchorage independent growth assay in vector alone, A2, 2.2 and 1.2 stably transfected NIH-3T3 cell lines*

CELL LINE	NUMBER OF COLONIES/WELL (± SEM)	% OF CONTROL (EJTF2)	*P* value[a] (versus EJTF2)	*P* value[a] (versus vector)
A2 7.2	119 ± 10.09	79.3	0.0317	<0.001
A2 9.6	131 ± 12.15	87.9	0.2793	<0.001
A2 10.2	207 ± 12.85	138.3	0.0010	<0.001
2.2-1	26 ± 5.23	17.3	<0.001	0.0003
2.2-33	17 ± 2.45	11.6	<0.001	<0.001
2.2-52	22 ± 1.47	14.4	<0.001	<0.001
1.2-2	43 ± 2.97	29.0	<0.001	<0.001
1.2-39	56 ± 4.34	37.3	<0.001	<0.001
1.2-59	21 ± 1.93	13.9	<0.001	<0.001
vector 1	1 ± 0.47	0.9	<0.001	
vector 2	2 ± 0.58	1.3	<0.001	
EJTF2	150 ± 0.60	**100.0**		<0.001

[a] Student's *t*-test, two-tailed

The above results suggest that after 21 days, NIH-3T3 mouse fibroblasts lost contact inhibition and acquired anchorage independence to grow as colonies in soft agar when either A2, 2.2 or 1.2 variants were overexpressed. The three A2 cell lines produced a substantial number of colonies whereas incorporation of a 5'UTR altered reduced the number of colonies in 2.2 or 1.2 lines.

4.2.2 Effect of overexpressed eEF1A variants on proliferation rate of NIH-3T3 cells

After several lines acquired a transformed phenotype *in vitro* (see section 4.2.1 for details), it was necessary to assess the effect of any eEF1A variant overexpression on cells growth rate. The AlamarBlue® assay was used to determine proliferation of selected stable cell lines over 8 consecutive days. This non-toxic assay is based on the ability of growing cells to induce a chemical reduction of the dye's indicator, observed as a shift of culture media colour from blue to pink. AlamarBlue® dye was applied to the growing cells at indicated time points and fluorescence intensity was measured. The fluorescent signal reflects the magnitude of the reduced environment when a viable cell's growth is still maintained. AlamarBlue® dye was added to the medium without cultured cells as a blank control for the assay.

4.2.2.1 Growth kinetics of eEF1A1 origin clones

Cellular proliferation rates were compared for three A1 stable cell lines, pDEST40 empty-vector control and EJTF2 cells that stably express H-Ras^{G12V}, as shown in Figure 4.14. It was observed that the proliferation magnitude of A1 3.2, A1 8.6 and A1 10.2 clones was less than for EJTF2 cells but became distinguishably greater than that of the vector control between the fifth and sixth day after seeding. All three A1 lines showed a trend approximately similar to the vector control on first 4 days of culture. It is worth noting that line A1 10.2 showed almost no change in proliferation rate when compared to the vector control and this was the line with the lowest level of exogenous construct expression of the three lines.

When two 1.1 stable cell lines were examined in terms of proliferation (Figure 4.15), it was revealed that clone 1.1-9 grew almost as fast as EJTF2 cells until day 4. Subsequently, proliferation decreased but still showed a greater rate than the vector control cells. By contrast, line 1.1-23 that expressed the 1.1 construct at a higher

level than line 1.1-9 revealed a trend of proliferation similar to vector transfected cells only until day 4 but subsequently the rate was almost as high as for EJTF2 cells.

Three clones expressing different levels of 2.1 construct were characterized by different proliferation rates as presented in Figure 4.16. Clone 2.1-15 that was shown to have the highest expression of exogenous plasmid, exhibited the highest growth, with a trend similar to the EJTF2 line. The proliferation of line 2.1-18 that showed a moderate expression of the 2.1 construct, was almost in agreement with the rate of the vector cells until day 4 but then increased on following days to levels similar to those observed for EJTF2 cells. Clone 2.1-1 exhibited proliferation comparable with vector control rates, compatible with the extremely low level of 2.1 construct expression.

These data indicate that forced expression of A1, 1.1 or 2.1 variants in NIH-3T3 fibroblasts altered the proliferation rate of the cells but only one line (2.1-15) reached a magnitude as great as the cells stably expressing the H-Ras^{G12V} oncogene.

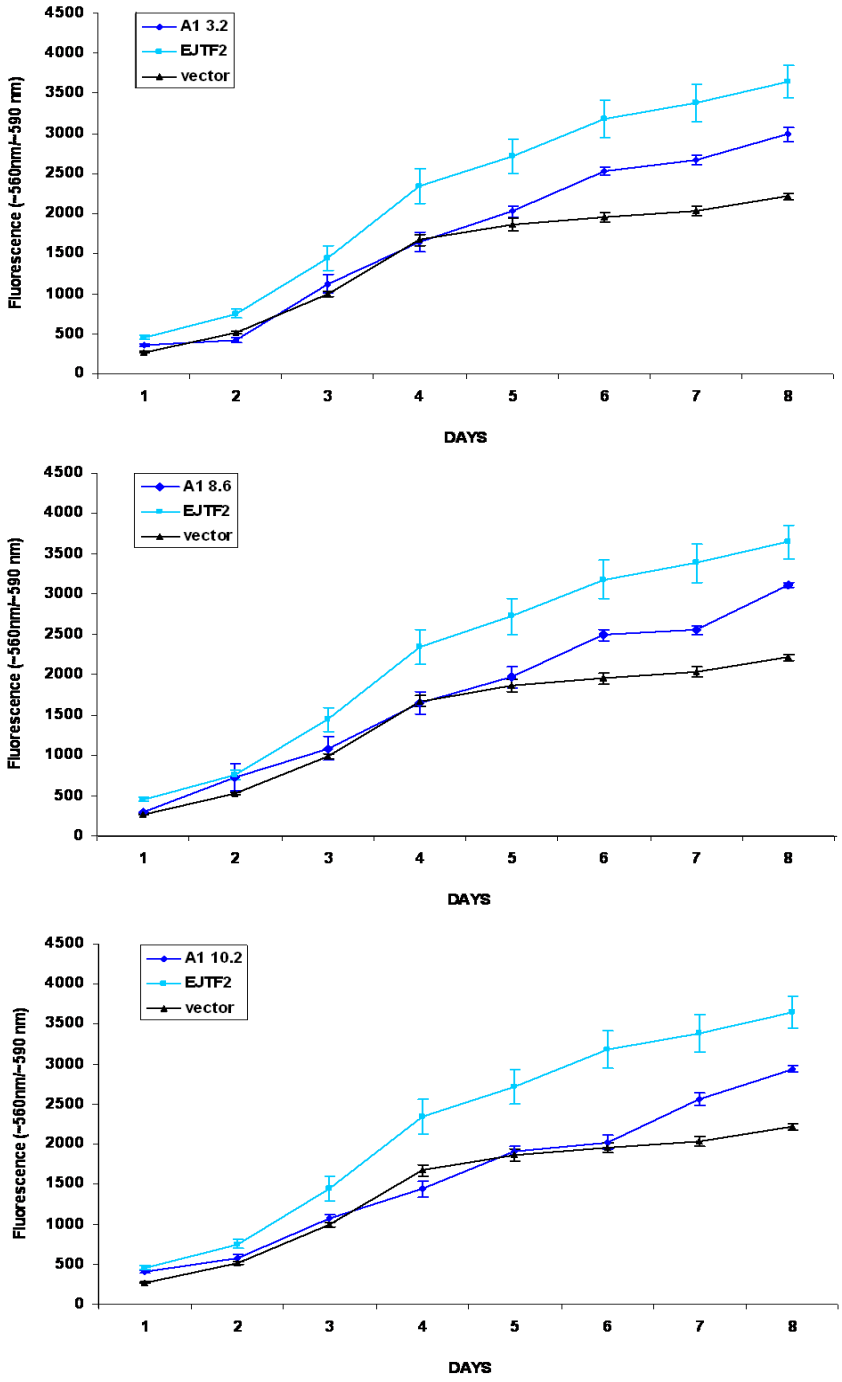

Figure 4.14 Proliferation rate of NIH-3T3 fibroblasts stably overexpressing A1. Three A1 stable cell lines **(A1 3.2, A1 8.6, A1 10.2)** along with control **EJTF2** cells or **empty-vector** lines were cultured in standard conditions up to 8 days during which they were subjected to the AlamarBlue® assay. Proliferation magnitude is expressed as the fluorescence intensity at indicated time points. Results are shown as ± SEM of three independent experiments, each performed five times.

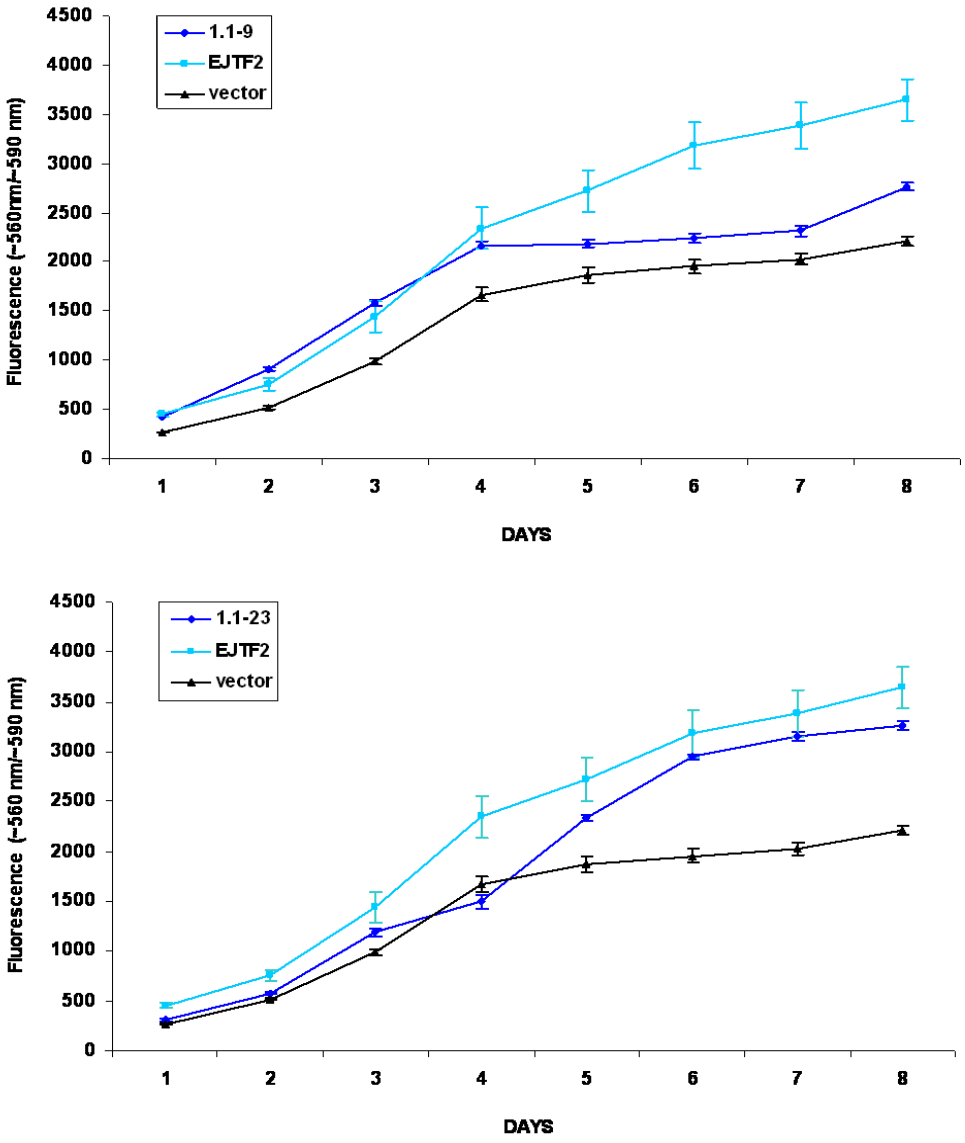

Figure 4.15 Proliferation rate of NIH-3T3 fibroblasts stably overexpressing 1.1. Two 1.1 stable cell lines **(1.1-9, 1.1-23)** along with control **EJTF2** cells or **empty-vector** lines were subjected to the AlamarBlue® assay. Proliferation magnitude is expressed as the fluorescence intensity at indicated time points. Results are shown as ± SEM of three independent experiments, each performed five times.

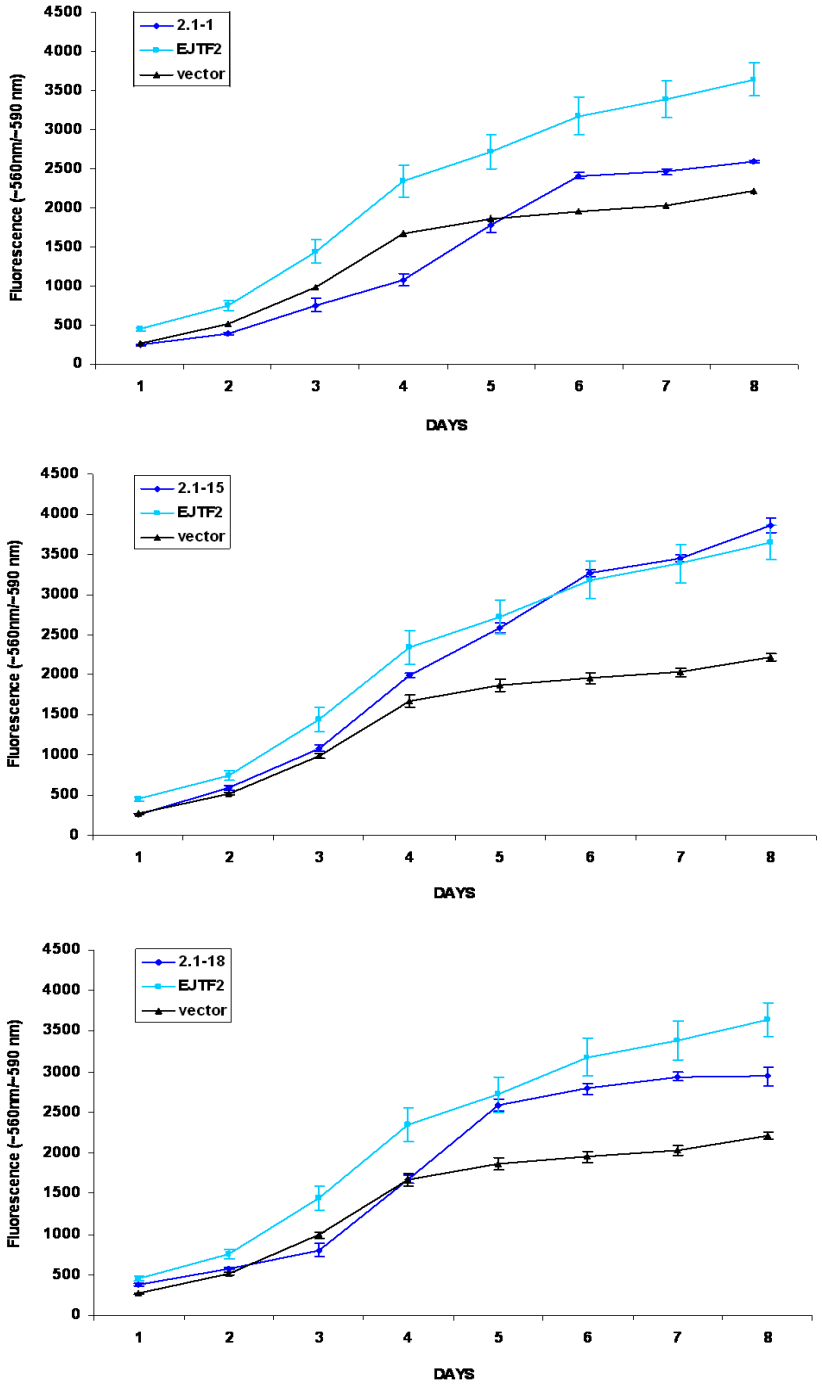

Figure 4.16 Proliferation rate of NIH-3T3 fibroblasts stably overexpressing 2.1. Three 2.1 stable cell lines **(2.1-1, 2.1-15, 2.1-18)** along with control **EJTF2** cells or **empty-vector** lines were cultured tested in the AlamarBlue® assay. Results are shown as ± SEM of three independent experiments, each performed five times.

4.2.2.2 Growth kinetics of eEF1A2 origin clones

The effects of A2 overexpression on proliferation rate were also assessed in three A2 stable cell lines and compared with controls as before. As shown in Figure 4.17, the proliferation rates of A2 7.2, A2 9.6 and A2 10.2 lines were considerably higher than that of both control cell lines.

Next, the growth of 2.2 stable cell lines was evaluated (Figure 4.18) and found to be noticeably enhanced for line 2.2-52, expressing the lowest levels of exogenous construct amongst the three clones. The proliferation rate for this cell line was considerably higher than for vector transfected or EJTF2 cells, however, an inexplicable decrease on day 5 and immediate increase on day 6 was observed. Transfectants of the line 2.2-1 proliferated at a faster rate than line 2.2-33 but with a trend similar to EJTF2 cells. Growth rates for clone 2.2-33 were less than control cells but greater than vector transfectants.

Cellular proliferation was also monitored in three representative 1.2 stable cell lines as presented in Figure 4.19. It was observed that all three clones showed enhanced cell growth, more than in the vector transfected line. It is noteworthy that clone 1.2-2 which expressed the highest levels of exogenous construct seemed to proliferate at the fastest rate. Line 1.2-39 expressing the lowest level of 1.2 grew at the slowest rate out of three tested lines and showed a similar effect as an empty vector control.

These findings suggest that overexpression of A2 construct markedly stimulated NIH-3T3 proliferation when compared to the effects observed in 2.2 and 1.2 variants. Forced expression of both, 2.2 and 1.2 variants affected the growth rate of mouse fibroblasts in comparison to vector transfectants but not to the same extent as EJTF2 cells, apart from clone 2.2-52.

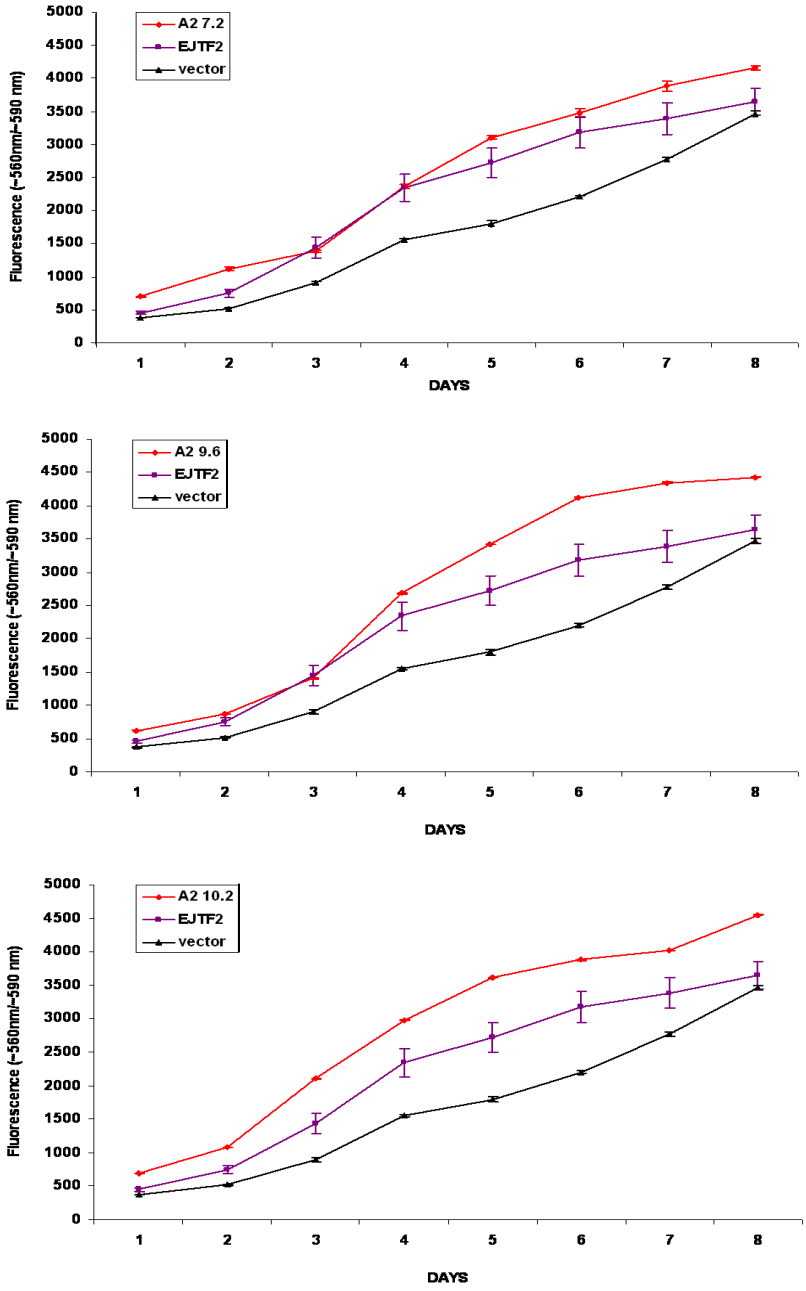

Figure 4.17 Effect of A2 overexpression on NIH-3T3 cells proliferation. Three stable A2 mouse fibroblast cell lines were subjected to determination of growth rate under standard culture conditions. Proliferation of A2 clones **(A2 7.2, A2 9.6, A2 10.2)** was compared to the stable lines of **empty-vector** or **EJTF2** cells. AlamarBlue® dye was applied to the culture media of the cells and fluorescence was measured up to 8 days after seeding. The results of growth magnitude are represented as the average fluorescence intensity at indicated time point (±SEM) calculated from three separate experiments (each performed five times).

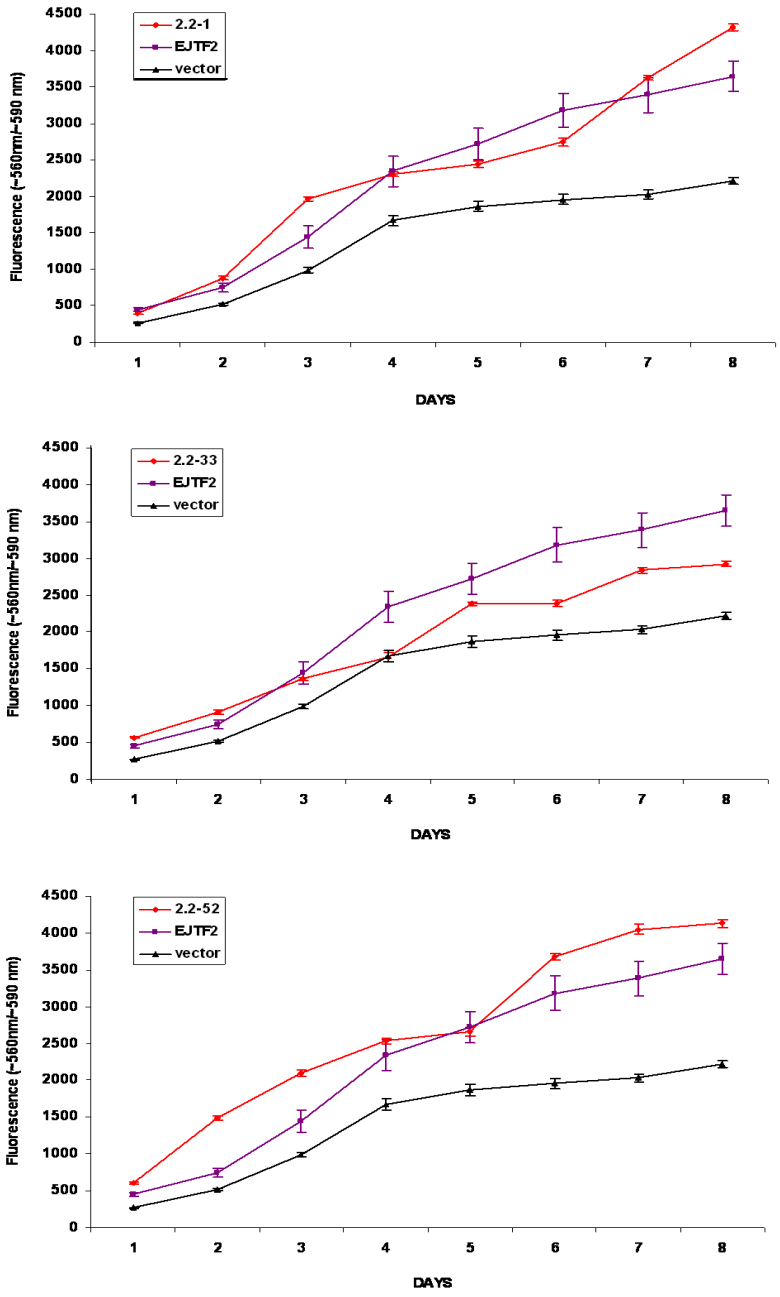

Figure 4.18 Effect of 2.2 overexpression on NIH-3T3 cells proliferation. Proliferation of 2.2 clones **(2.2-1, 2.2-33, 2.2-52)** was compared to the stable lines of **empty-vector** or **EJTF2** cells. The results of growth magnitude are represented as the average fluorescence intensity at indicated time point (±SEM) calculated from three separate experiments, each performed five times.

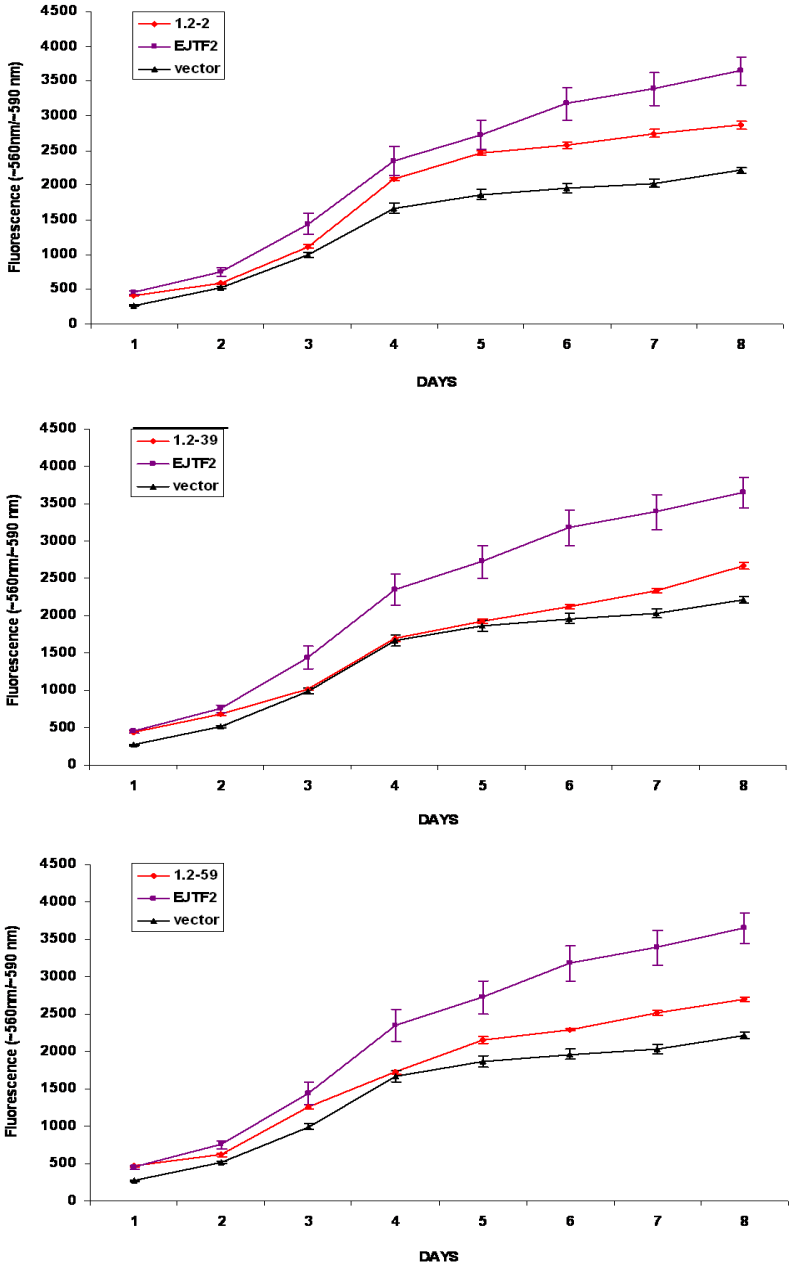

Figure 4.19 Effect of 1.2 overexpression on NIH-3T3 cells proliferation. Proliferation of A2 clones **(1.2-2, 1.2-39, 1.2-59)** was compared to the stable lines of **empty-vector** or **EJTF2** cells. The results of growth magnitude are represented as the average fluorescence intensity at indicated time point (±SEM) calculated from three separate experiments, each performed in five replicates.

4.2.3 Consequences of ectopic eEF1A variants overexpression on *in vitro* migration and invasion in different eEF1A origin stable cell lines

Cell migration is required for a variety of biological processes and alterations in regulation of migration lead to many diseases, including cancer. Increased cell motility and invasion are hallmarks of a metastatic phenotype (Yamaguchi et al., 2005, Sahai, 2005). In order to determine whether any of eEF1A variants plays a role in cell metastasis, selected stable cell lines (as reviewed in Table 3.2) were tested in established *in vitro* invasion and migration systems (Albini et al., 1987, Terranova et al., 1986). Both types of *in vitro* assays were performed as pilot studies and the experiment was carried out on 8 stable cell lines of eEF1A1 origin, on 9 stable cell lines of eEF1A2 origin and on control empty vector transfected lines. Highly motile HT-1080 cells were used as a positive control (Rasheed et al., 1974, Albini et al., 1987). Each cell line was tested in triplicate but cells for each repeat originated in individual culture dishes, each dish representing an individual aliquot from liquid nitrogen storage.

The motility of the cells was assessed in a transwell system where cells migrated through a porous membrane towards the lower chamber. In this instance, the chamber was filled with a serum-supplemented medium that acted as an attractant. As expected, the positive control of HT-1080 cells achieved a high level of motility values indicating a successful outcome.

Figure 4.20 illustrates the migration rate determined for NIH-3T3 stable cell lines of eEF1A1 origin. Quantification of the stable cell lines' motility showed that they were not migrating in a distinguishably different fashion from that of empty vector transfected cells; the percentages of motility in a relation to the negative control are summarized in Table 4.5. There was insufficient evidence to declare a difference in migration rates between A1 3.2 (P=0.165), A1 10.2 (P=0.061), 1.1-9 (P=0.840), 1.1-23 (P=0.124), 2.1-1 (P=0.206), 2.1-18 (P=0.377) cell lines and vector control group, however overexpression of exogenous plasmids had a significant effect on the migration of A1 8.6 (P=0.034) and 2.1-15 (P=0.036) in comparison to the vector transfected cells. These two clones expressed the highest levels of exogenous proteins within their groups.

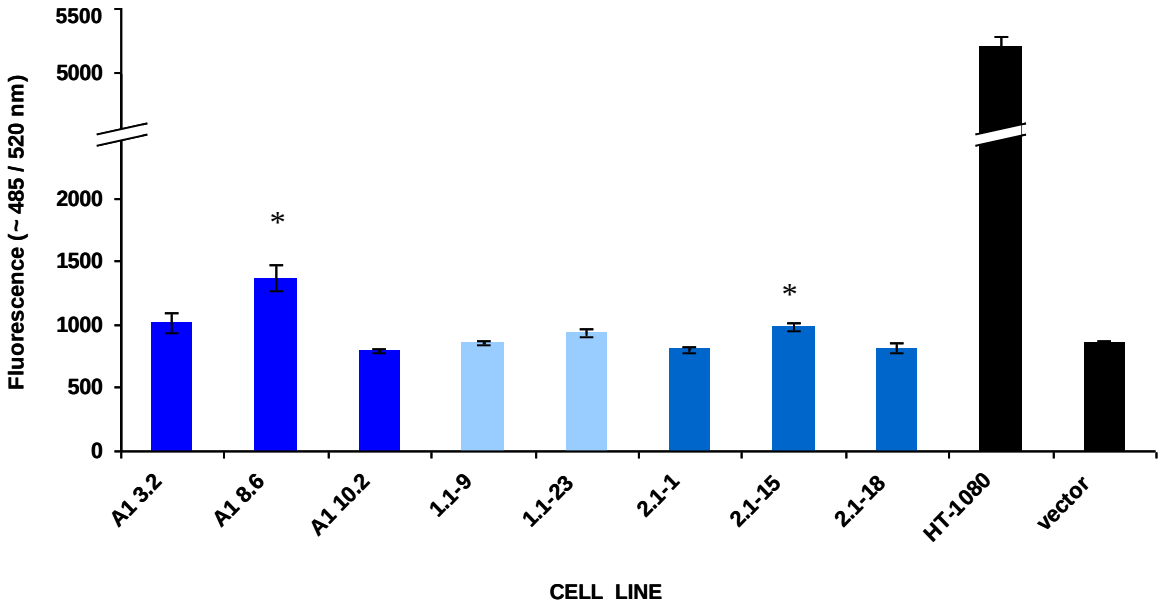

Figure 4.20 ***In vitro*** **studies of migration on selected NIH-3T3 stable cell lines of eEF1A1 origin.** Cell motility was determined in transwell chambers by plating equal numbers of the cells into the upper compartment and subsequent incubation for 24 hours with serum supplemented media in the lower compartment as an attractant element. Cells that migrated through the membrane were stained with fluorescent dye and the intensity of the fluorescence reflects motility. A1 8.6 and 2.1-15 lines showed a significant increase in cell motility compared with vector transfected control (*P<0.05, Student's t-test, two-tailed). The average fluorescence of three repeats within one experiment is given for each cell line (± SEM)

Table 4.5 *Summary of different eEF1A1 stable cell lines motility rate expressed as percentages in relation to the vector transfected cells control*

Cell line	% of the control
A1 3.2	119
A1 8.6	160
A1 10.2	93
1.1-9	99
1.1-23	109
2.1-1	94
2.1-15	115
2.1-18	95
vector	**100**

Additionally, the rates of the migration were evaluated for different stable cell lines of eEF1A2 origin as shown in Figure 4.21. The quantification of the migration rates for certain lines showed a small increase compared with the negative control as summarized in Table 4.6. There was no evidence of a difference in migration between A2 9.6 (P=0.519), A2 10.2 (P=0.581), 2.2-1 (P=0.737), 2.2-33 (P=0.789), 1.2-2 (P=0.318), 1.2-39 (P=0.482), 1.2-59 (P=0.459) lines and negative control cells, however there was an effect on migration of A2 7.2 (P=0.0499) and 2.2-52 (P=0.042) when compared to the vector transfected lines.

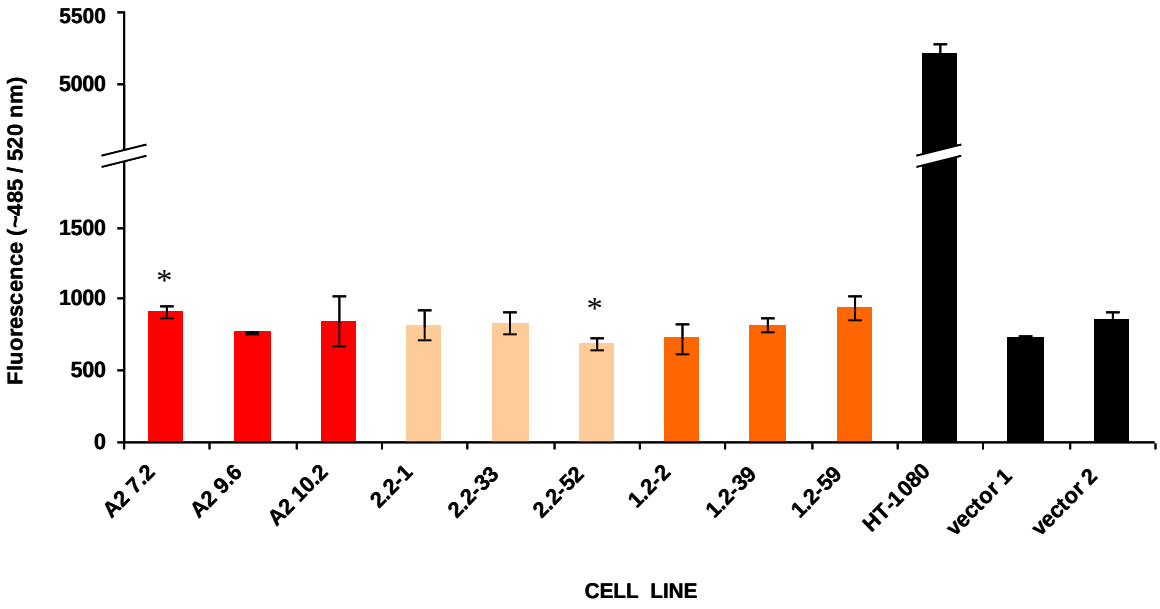

Figure 4.21 Quantification of *in vitro* motility within stable cell lines of different eEF1A2 origin. The cells that did not pass through the membrane were discarded whereas cells from the other side of the laminin membrane were fluorescently stained. The strength of the fluorescent signal reflected the magnitude of the cells migration capacities. The average fluorescence of three repeats within one experiment for each cell line is shown (± SEM, **P*<0.05, Student's *t*-test, two-tailed).

Table 4.6 *Evaluation of the migration rates for different eEF1A2 stable cell lines expressed as percentage values relative to empty vector transfected NIH-3T3 cells*

Cell line	% of the control
A2 7.2	126
A2 9.6	106
A2 10.2	116
2.2-1	95
2.2-33	97
2.2-52	80
1.2-2	84
1.2-39	95
1.2-59	109
vector 1	**100**
vector 2	**100**

To further investigate any possible association between increased cell motility and invasive potential of the cell lines, an ***in vitro*** **invasion** assay was performed. On this occasion, the capacity of the cells to migrate through a laminin coated layer towards serum supplemented medium (an attractant) was evaluated. The laminin coated layer served as a barrier to discriminate non-invasive from invasive cells. The HT-1080 cell line exhibited enhanced invasion capacity and was used as a positive control.

The invasiveness of different stable cell lines of eEF1A1 origin is shown in Figure 4.22. The lines were almost as invasive as the vector control cells. Statistical analysis showed no significant changes in invasion for A1 3.2 (P=0.601), A1 8.6 (P=0.153), A1 10.2 (P=0.052), 2.1-1 (P=0.384), 2.1-15 (P=0.375) and 2.1-18 (P=0.076) stable cell lines. There was a significant decrease in the invasive potential of 1.1-9 (P=0.037) and 1.1-23 (P=0.012) lines compared to the empty vector transfected control cells. The percentage difference in invasion ability between experimental and control cell lines is shown in Table 4.7.

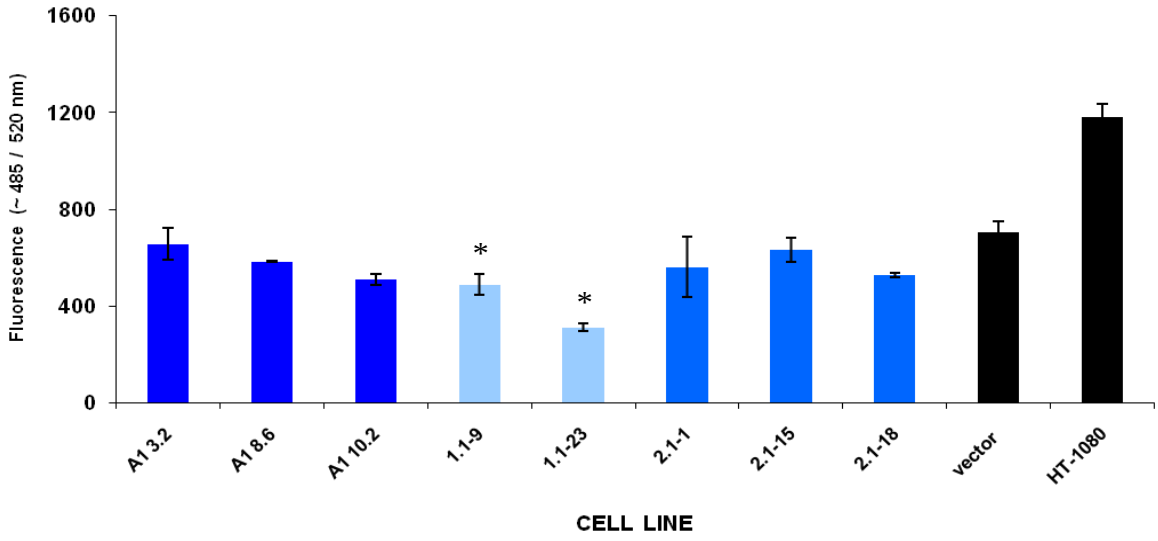

Figure 4.22 ***In vitro*** **invasiveness assay of different eEF1A1 expressing NIH-3T3 stable cell lines.** Cells were evaluated for their ability to invade laminin towards an attractant of serum supplemented DMEM in a Boyden chamber. The results are expressed as average invasion capacity (± SEM) calculated from three determinations for each cell line. * Significant difference between cell line and vector control (P<0.05, Student's t-test, two-tailed).

Table 4.7 *Quantification of the invasion capacity of different eEF1A1 stable cell lines expressed as the percentage values in comparison to empty vector transfected control*

Cell line	% of the control
A1 3.2	93
A1 8.6	83
A1 10.2	73
1.1-9	69
1.1-23	44
2.1-1	80
2.1-15	90
2.1-18	75
vector	**100**

Next, the invasive potential of different eEF1A2 expressing NIH-3T3 stable cell lines was determined as shown in Figure 4.23. Stable overexpression of A2, 2.2 or 1.2 constructs altered the invasion capacities of the cells when compared to the empty vector control. The ability of the cells to invade the laminin layer was significantly changed for A2 7.2 (P=0.0002), 2.2-52 (P=0.038) and 1.2-39 (P=0.017) lines but there was no significant change for A2 9.6 (P=0.407), A2 10.2 (P=0.099), 2.2-1 (P=0.894), 2.2-33 (P=0.433), 1.2-2 (P=0.459) and 1.2-59 (P=0.377) cell lines in comparison to the vector transfected control. The percentage difference in invasion between vector control and different eEF1A2 stable cell lines is shown in Table 4.8.

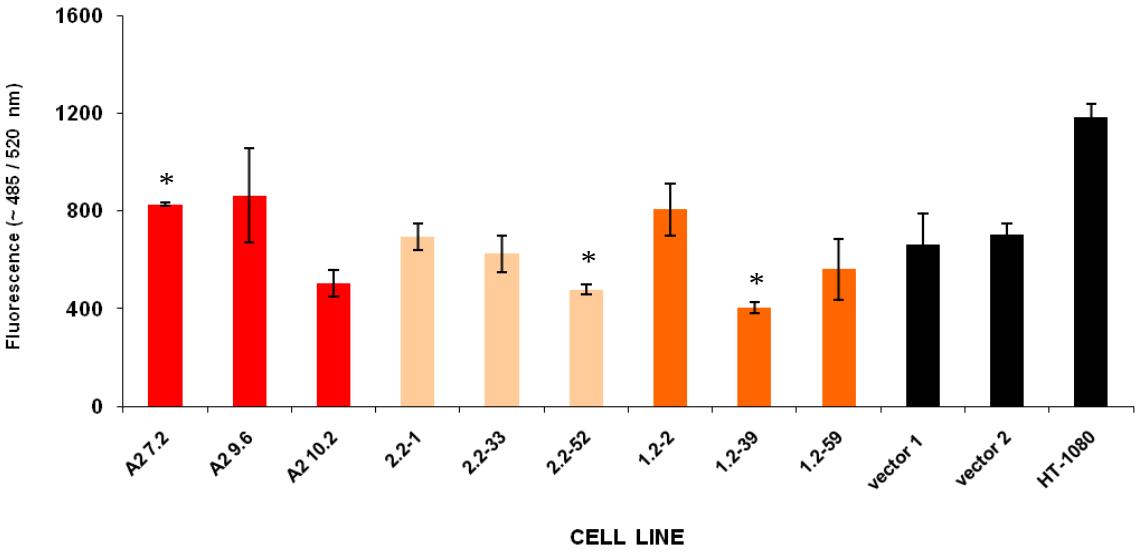

Figure 4.23 Invasive potential of different eEF1A2 origin stable cell lines across laminin-coated transwell chambers. Equal number of cells for each line were seeded on the top of the chamber's upper compartment and left for 24 hours to invade through the layer of laminin. The results are exhibited as the average ability to invade (± SEM) calculated from three determinations. * Significant difference compared to vector controls with $P<0.05$, Stuent's t-test, two-tailed

Table 4.8 *Evaluation of the in vitro invading capacities for different eEF1A2 stable cell lines exhibited as the percentage difference between the vector control and experimental samples*

Cell line	% of the control
A2 7.2	125
A2 9.6	130
A2 10.2	76
2.2-1	98
2.2-33	89
2.2-52	68
1.2-2	114
1.2-39	57
1.2-59	80
vector 1	**100**
vector 2	**100**

4.2.4 Investigation of the possible mechanism responsible for oncogenic potential of eEF1A forms

Anand and co-workers demonstrated the oncogenic potential of eEF1A2 showing that its ectopic expression in rodent fibroblasts resulted in anchorage independent growth, enhanced focus formation and gave rise to tumours when ES-2 ovarian cells expressing eEF1A2 were injected into nude mice (Anand *et al*., 2002). Intriguingly, is still unknown how eEF1A2 contributes to tumourigenesis. It was shown that gene amplification is not the only mechanism responsible for eEF1A2 overexpression and no activating mutations have been found. Moreover, there was also no correlation between methylation status and eEF1A2 expression as exhibited in a panel of ovarian tumours (Tomlinson *et al*., 2007). It is possible that the oncogenic properties of eEF1A2 might be associated with its conventional role in translation (i.e. increased protein synthesis rate) or perhaps with non-canonical functions that differ from those of the eEF1A1 form. On contrary, very little in this field is known about eEF1A1.

4.2.4.1 Influence of different eEF1A variants overexpression on the global protein synthesis

As both eEF1A variants act in the same way during translation elongation and they both are pivotal components of the translational machinery (Pan et al., 2004, Bischoff et al., 2000, Kahns et al., 1998), it was crucial to investigate whether any increase in global protein synthesis occurred while different eEF1A forms were overexpressed. Levels of total translation elongation factor 1A protein were elevated in 2.1 stable cell lines and all stable cell lines of eEF1A2 origin (as described in Sections 3.2.3.3 and 3.2.3.4 of Chapter 3).

In order to shed some light on this problem, determination of the protein synthesis rate of the cell lines was performed. This involved metabolic [^{35}S]

methionine/cysteine labelling of the cell lines stably expressing eEF1A1 or eEF1A2. Subsequently, incorporation of the radiolabelled amino acids into newly synthesized polypeptides was measured and the results of this assay are shown in Figure 4.24.

The rates of global protein synthesis for experimental samples were compared to controls (the lines transfected with empty vectors). High variation between cell lines was observed. The overall protein synthesis rates were not distinguishably higher than the levels seen in negative controls. Incorporation of radioactive amino acids was slightly increased for 2.1-1 (P=0.747), 2.1-18 (P=0.632) lines of eEF1A1 origin and for A2 7.2 (P=0.719), A2 10.2 (P=0.548), 2.2-52 (P=0.517), 1.2-2 (P=0.249), 1.2-59 (P=0.750) lines of eEF1A2 origin but these differences were not statistically significant from the vector controls. A minor decrease in global translation rate was seen for A1 3.2 (P=0.210), A1 8.6 (P=0.103), A1 10.2 (P=0.482), 1.1-9 (P=0.618), 2.1-15 (P=0.742), A2 9.6 (P=0.772), 2.2-1 (P=0.310) and 2.2-33 (P=0.162) stable cell lines but again this was not statistically significant.

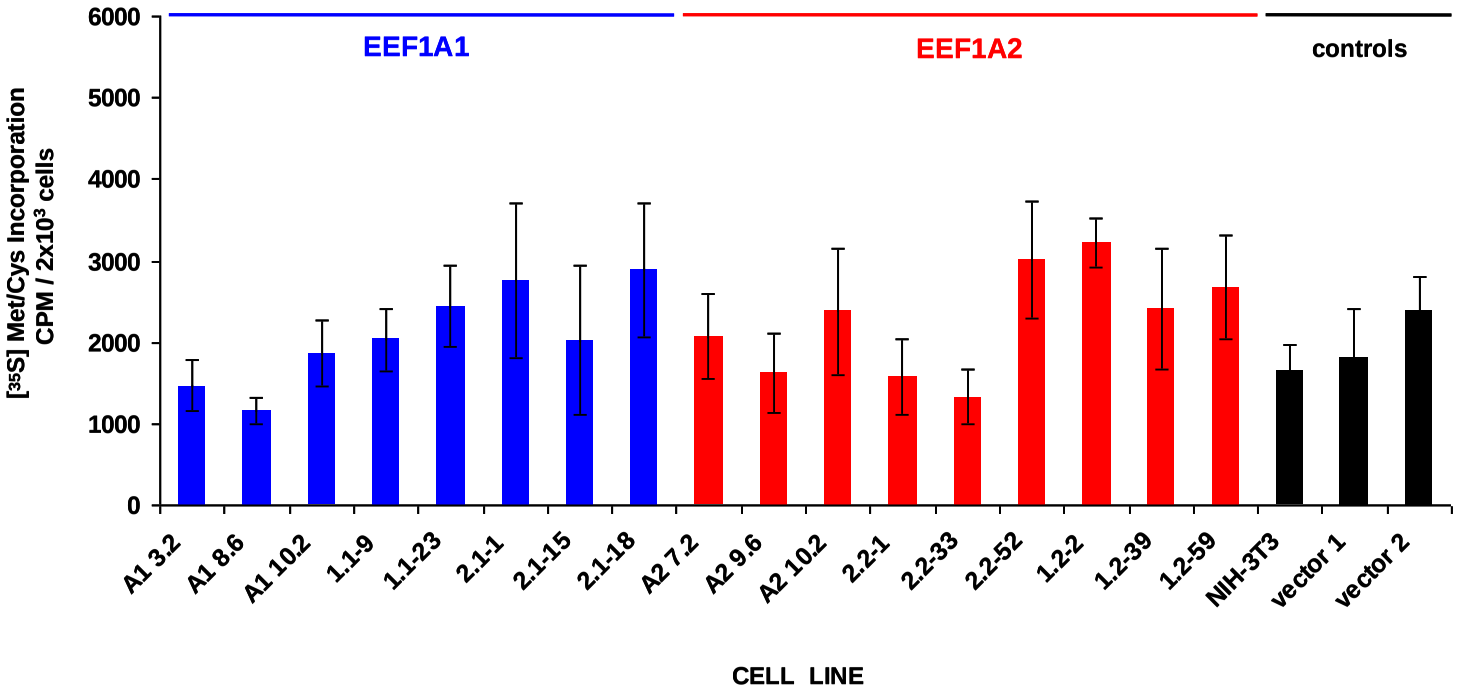

Figure 4.24 Effect of different eEF1A variants overexpression on the global synthesis rate of the NIH-3T3 stable cell lines. Values shown are representing average counts per minute readings for 2000 cells (± SEM), established from five independent determinations. The global synthesis rate was measured by [^{35}S] methionine/cysteine incorporation during 20-min labelling. Vector 1 stands for pcDNA3.1 and vector 2 means pDEST40. All A2 lines were compared with vector 1 but the rest of the cell lines was related to vector 2.

In order to investigate whether any relationship between global protein synthesis or overall eEF1A protein expression and transformed phenotype observations exists in the tested stable cell lines, Pearson's correlation coefficient (r) was computed. There was no association between translation rate and number of colonies (r = -0.247, n=19, P>0.05) or number of foci (r = 0.181, n=19, P>0.05) or *in vitro* invasion (r = -0.261, n=19, P>0.05) as summarized in scatter plots in Figure 4.25. A moderate negative association was seen between global protein synthesis rate and *in vitro* migration (r = -0.499, n=19, P<0.05). Cell lines with low levels of translation had a tendency to show increased migration, and conversely lines with a high protein synthesis rate had a tendency to show low levels of migration.

Interestingly, lines 2.1-1, 2.1-18, A2 7.2, A2 10.2, 2.2-52, 1.2-2 and 1.2-59 that had increased levels of total eEF1A, exhibited increase in overall protein synthesis rate. In contrast, lines 2.1-15, A2 9.6, 2.2-1, 2.2-33 and 1.2-39 which had increased eEF1A protein expression, were not characterized by elevated protein synthesis. Subsequently, a moderate positive association was confirmed between global protein translation and overall levels of the eEF1A protein (r= 0.454, n=19, P<0.05). Stable cell lines expressing high levels of overall eEF1A protein had a tendency to exhibit increased rate of global translation. However, there was no association between overall eEF1A protein expression and number of colonies (r = -0.200, n=19, P>0.05) or number of foci (r = 0.258, n=19, P>0.05) or *in vitro* migration (r = -0.371, n=19, P>0.05) or *in vitro* invasion (r = 0.169, n=19, P>0.05) as summarized in Figure 4.26.

Figure 4.25 Scatter plots of the relationships between protein synthesis rate and number of colonies (A), number of foci (B), rate of *in vitro* migration (C), *in vitro* invasion (D) or total eEF1A protein levels (E). Pearson product moment correlation coefficient (r) was calculated for each relationship and was shown in the corner of the corresponding box (P>0.05 for A, B, D whereas P<0.05 for C and E).

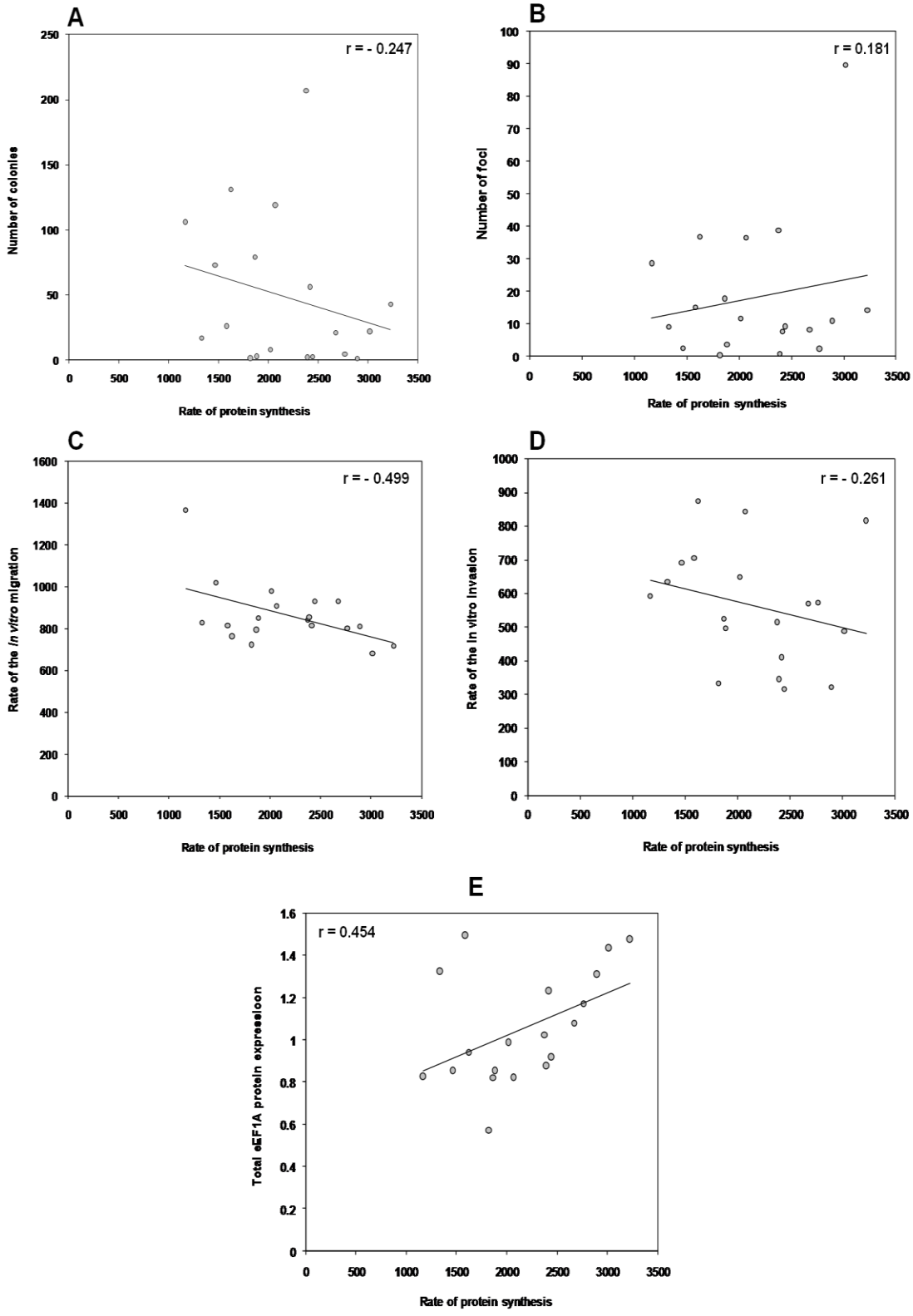
A
r = - 0.247
Number of colonies
Rate of protein synthesis
B
r = 0.181
Number of foci
Rate of protein synthesis
C
r = - 0.499
Rate of the in vitro migration
Rate of protein synthesis
D
r = - 0.261
Rate of the In vitro invasion
Rate of protein synthesis
E
r = 0.454
Total eEF1A protein expression
Rate of protein synthesis

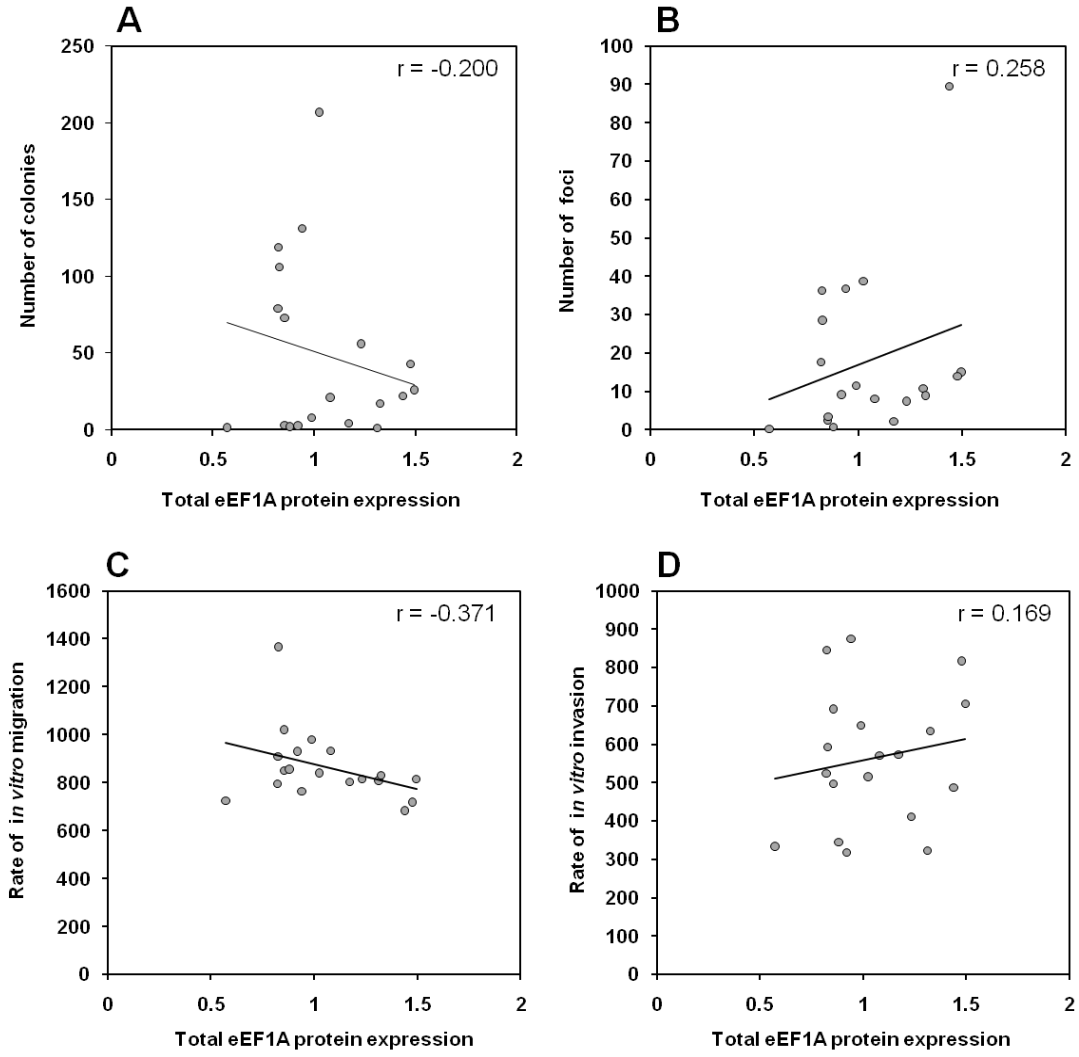

Figure 4.26 Scatter plots of the relationship between total eEF1A protein expression and number of colonies (A), number of foci (B), rate of *in vitro* migration (C) or *in vitro* invasion (D). Pearson product moment correlation coefficient (r) for each relationship is shown in the corner of the corresponding plot ($P>0.05$ for A, B, C and D).

4.3 Discussion

There is contradictory and incomplete evidence to link inappropriately regulated or expressed eEF1A1 with an involvement in tumourigenesis. For example, *EEF1A1* gene expression was significantly higher in primary glioblastomas (Scrideli et al., 2008) but it is noteworthy that eEF1A1 is predominantly expressed in glial cells (Pan et al., 2004, Newbery et al., 2007). Furthermore, eEF1A1 at the mRNA level stayed unchanged in cancers which overexpressed eEF1A2 (Anand et al., 2002, Cao et al., 2009). In contrast, eEF1A2 has been recognized as a potential oncogene in human malignancies of breast, lung, ovary, pancreas or liver (Tomlinson et al., 2005, Li et al., 2006, Anand et al., 2002, Cao et al., 2009, Schlaeger et al., 2008) and in mouse plasmacytomas (Li et al., 2010). Although the two eEF1A forms act in an equivalent manner at the elongation step of translation (Kahns et al., 1998), it has not yet been determined whether they exhibit any similarities for oncogenic capacity. Mechanisms used by eEF1A2 to transform cells have not been fully exploited and a major issue is whether oncogenicity is driven through changes in its conventional role in translation or rather by altered non-canonical functions.

Even though the effect of increased eEF1A2 expression has been studied in detail within various cell line systems, the consequences of eEF1A2 variants with chimeric 5'UTRs on cancer biology are unknown. Here, an attempt to simultaneously compare eEF1A1 and eEF1A2 in a panel of various *in vitro* transformation assays has been also shown for the first time and the possible meaning of the data obtained for the oncogenic potential of both eEF1A forms has been discussed. Overall trends among all of the stable cell lines clones that were observed in transformation assays are summarized in Table 4.9.

Table 4.9 *Characterization of different eEF1A origin stable cell lines with regard to their transformation capacities*

CELL LINE	V5-TAGGED PROTEIN	TOTAL eEF1A PROTEIN	PROTEIN SYNTHESIS	FOCI FORMATION	SOFT AGAR COLONY FORMATION	GROWTH RATE	INVASION	MIGRATION
A1 3.2	++	○	-	+	++	○	○	+
A1 8.6	+++	○	-	++	+++	○	-	+
A1 10.2	+	○	-	+	++	○	-	○
1.1-9	+	○	-	+	+	+	-	○
1.1-23	+	+	○	+	+	+	-	○
2.1-1	+	+	+	+	+	+	-	○
2.1-15	+++	++	-	+	+	++	○	+
2.1-18	+	+	+	+	+	+	-	○
A2 7.2	++++	+	+	++	+++	+++	+	+
A2 9.6	++++	+	-	++	+++	+++	+	○
A2 10.2	++++	+	+	++	+++	+++	-	○
2.2-1	+	++	-	+	+	++	○	○
2.2-33	++	+	-	+	+	+	-	○
2.2-52	+	++	+	+++	+	+++	-	○
1.2-2	++	++	+	+	+	+	+	○
1.2-39	+	+	○	+	++	○	-	○
1.2-59	++	○	+	+	+	+	-	+
MARKING SYSTEM	+ low ++ medium +++ /++++ high	○ not changed **+** increase	○ not changed **-** decrease **+** increase	+ <25 ++ 26-50 +++ >51	+ <50 ++ 51-150 +++ >151	○ not changed **+/++/+++** increase	○ not changed **-** decrease **+** increase	○ not changed **+** increase

The discovery that even low ectopic expression of eEF1A1 (as seen in the A1 clones) provoked transformed cell morphology, followed by foci and soft agar colonies formation was intriguing. However, some fragmentary knowledge exists, suggesting the possibility of eEF1A1 connection to cancer (Thornton et al., 2003). In addition, Tatsuka reported a mouse fibroblast cell line variant, constitutively expressing eEF1A1, that was highly susceptible to chemically or physically induced neoplastic transformation (Tatsuka et al., 1992). This can be explained by the fact that in the majority of studies with eEF1A1 performed in the past, antibodies or DNA probes that did not distinguish between the two eEF1A forms were used. The numbers of foci and colonies induced in soft agar by A1 lines were not as high as in A2 clones; however, expression of A2 construct was higher than A1 construct. Moreover, the stimulatory effect of eEF1A1 on the oncogenic potential of NIH-3T3 cells did not correlate with dramatically increased proliferation in comparison to the vector control lines. It is possible that eEF1A1 activation might be an early event during neoplastic transformation and that other mutagens are necessary to promote tumour (Thornton et al., 2003).

Incorporation of chimeric 5'UTRs in front of the eEF1A1 coding sequence resulted in a significant decrease of foci formation and almost complete abolition of the anchorage-independence in 1.1 and 2.1 stable cell lines. Although these cell lines have acquired a morphology characteristic of transformed cells, it was not reflected by malignant transformation. The proliferation rates of 1.1 and 2.1 lines were in excess over A1 clones and the increase in growth appeared to be proportional to the magnitude of the exogenous variant expression within particular clones. Clones with the 5'UTR from eEF1A2 (2.1) showed heightened proliferation compared with their counterpart clones with the 5'UTR from eEF1A1 (1.1). Importantly, only clone 2.1-15 showed a proliferation rate almost as high as positive control of NIH-3T3 cells stably expressing H-Ras^{G12V}. It cannot be excluded that different mechanisms confer proliferation and malignant transformation.

The finding showed herein, that plain eEF1A2 coding sequence overexpression was driving the transformed phenotype in NIH-3T3 cells was consistent with previous reports (Anand et al., 2002, Cao et al., 2009, Pinke et al., 2008). Cell lines of A2 7.2,

A2 9.6 and A2 10.2, characterised by constant overexpression of the eEF1A2 coding sequence, demonstrated not only loss of contact-inhibition capacity but also provoked foci formation and anchorage-independent growth. This sequence of events correlated with increased rates of proliferation within all three A2 clones.

Likewise, 2.2 and 1.2 lines displayed oncogenic phenotypes but the numbers of foci or colonies in soft agar were significantly lowered in comparison to the A2 clones, except clone 2.2-52. Moreover, 2.2 clones showed a similar trend of foci formation to that of 1.2 lines but the 1.2 clones acquired a higher clonogenicity in soft agar than 2.2 lines. Surprisingly, their proliferation rates were less pronounced than in clones with the 5'UTR from eEF1A2. Therefore, incorporation of any eEF1A 5'UTR led to a substantial but incomplete constraint of the *in vitro* oncogenic potential within the 2.2 and 1.2 stable cell lines. All three A2 clones proliferation exceeded the rates seen in EJTF2 cells whereas almost similar growth between 2.2 clones and this positive control was mostly observed, suggesting that the 5'UTR of eEF1A2 is necessary for regulatory purposes in growth stimulation, and substituting it for the 5'UTR of eEF1A1 led to a more efficient transforming phenotype.

The oncogenic potential of ectopic expression of different A1, 2.2 or 1.2 variants in NIH-3T3 cells could be explored further by *in vivo* studies in xenograft models in nude mice (Blair et al., 1983). Currently, it remains undetermined whether the expressed amounts of these variants are sufficient to induce more of the transformed phenotype. It is noteworthy that cells stably expressing eEF1A2 gave rise to tumours when injected into nude mice (Anand et al., 2002, Cao et al., 2009).

Next, the potential for *in vitro* migration and invasion was assessed for selected stable cell lines of different eEF1A origin. In this study, the intensity of fluorescence reflected the motility of the cells through a porous membrane and laminin layer, respectively.

Motility was significantly increased only for A1 8.6 and 2.1-15 clones (expressing the highest V5-tagged constructs levels) whereas the remaining eEF1A1 origin lines did not display any significant changes. Similarly, all the stable cell lines of eEF1A2 origin exhibited levels of migration comparable with empty vector clones,

even though A2 clones showed the highest proliferation rates. There was also no apparent elevation of *in vitro* invasion among different eEF1A variant stable cell lines, except line A2 7.2 (significant), A2 9.6 and 1.2-2 (not significant due to high variation between the samples). These observations were puzzling since Amiri and colleagues have shown that eEF1A2 overexpressed in BT-549 cells was an enhancer of migration and invasion in a PI3K/Akt dependent manner (Amiri et al., 2007). Moreover, the above results were also inconsistent with the increased *in vitro* cell motility and invasion reported for pancreatic adenocarcinoma SW1990 cell line, overexpressing eEF1A2, however there was no significance difference in adherence of these cells on laminin coated surfaces (Cao et al., 2009). It is possible that NIH-3T3 cells overexpressing different eEF1A variants show little affinity for laminin, hence the use of fibronectin or collagen layer as a crossing barrier could be more reliable. NIH-3T3 cells are not considered as invasive until transfected with activating oncogenes (Albini et al., 1987) but herein, even overexpression of eEF1A2 resulted in invasion efficiencies comparable to those of the negative control.

First, it should be kept in mind that invasion assays performed by Cao or Amiri were done on already transformed cell lines, hence a specific genetic background might be necessary to induce a high invasive potential of eEF1A2. Alternatively, mechanisms responsible for regulation of cellular proliferation and migration rates might be different from those that provoke invasive potential and transformed phenotype, depending on the cellular system used for experiments. To shed some light on this issue, the use of a 3D *in vitro* invasion model, for example by embedding cells between two collagen layers that resembles the tumour microenvironment situation *in vivo* more realistically, could be advantageous (Brekhman and Neufeld, 2009).

Currently, mechanisms considered for eEF1A2-driven oncogenesis propose that its upregulation causes either overall increase in protein synthesis or translation of a specific subset of proteins. Increased expression of the elements involved in assembling the translational machinery has been already well documented and linked to cancer (Ruggero and Pandolfi, 2003). When the intracellular stoichiometry for components of the protein synthesis apparatus is altered and more components are

available for immediate use, certain proteins that are normally poorly translated (for example due to their highly structured 5'UTR sequence) can increase their expression (Koromilas et al., 1992a). This exact mechanism activates many proto-oncogenes along with growth- or survival-related genes (Le Quesne et al., 2009, Ruggero and Pandolfi, 2003, Mamane et al., 2007).

For instance, elevated expression of $tRNA_i^{Met}$ or five subunits of the eukaryotic translation initiation factor 3 (eIF3a, eIF3b, eIF3c, eIF3h and eIF3i) stimulated global translation and subsequently led to oncogenic transformation of mouse embryonic fibroblasts. This stimulation of translational capacity caused an increase in synthesis of growth-regulating proteins like cyclin D1, c-Myc, ODC or FGF-2 (Marshall et al., 2008, Zhang et al., 2007).

One of assumption was that stable expression of any construct of eEF1A origin could lead to increase in overall level of eEF1A protein expression within the cells. Hence, a higher activity of combined eEF1A could provoke an increase in the global protein synthesis rate and perhaps more robust translation of mRNAs involved in growth and proliferation. In a few cell lines, for instance A2 7.2, A2 10.2 or 1.2-39, clearly high levels of eEF1A coincided with enhanced translation and fit perfectly with their ability to elevate cell growth and transformed phenotype. Therefore, it would be advantageous to determine the mRNA and protein levels of c-Myc or cyclin D1 in those stable cell lines in comparison to vector control lines. Moreover, it would be also interesting to know whether eEF1A is the only increased translational component or whether the translational apparatus is elevated in general.

Interestingly, on a few occasions or even within lines expressing the same construct, there was some inconsistency and clones A2 9.6, 2.2-1 or 2.2-33 expressed an increased level of overall eEF1A but did not show enhanced translation. However, these lines still presented oncogenic potential, suggesting that different mechanisms responsible for their higher proliferation rate and transformation could occur, despite the eEF1A status in the cells.

Results from assays performed on stable cell lines of eEF1A1 origin suggest that A1 clones almost exclusively provoked a transformed phenotype, regardless of the lack

of increase in eEF1A protein levels seen in the cells and a decreased translation rate. These results were in contrast with the A2 clones, suggesting that transformed phenotype is executed in a different manner. The oncogenic potential of overexpression of A1 constructs was diminished by incorporation of chimeric 5'UTRs. The most outstanding lines were 2.1-15 and 2.1-18 which had increased levels of total eEF1A protein, subtly enhanced global translation rates and higher proliferation, but did not necessarily display a transformed phenotype.

The notion that overexpression of different eEF1A variants could lead to general activation of cellular eEF1A, therefore promoting translational efficiency of certain oncogenic mRNAs seemed unlikely for some cell lines. They exhibited increased activity of eEF1A and a transformed phenotype but were not characterized by dramatically altered proliferation. Unfortunately, there was no significant association between rates of the protein synthesis and transformed phenotype among tested stable cell lines.

These inconsistencies among cell lines of the same type were puzzling but it might just underline that translation regulation of eEF1A is even more complex and multilayered; therefore perhaps each cell line's situation should be considered separately. All five determinations of the protein synthesis rates were done according to the same protocol, at the same time of the day and using stable cell lines in the logarithmic phase of growth. Perhaps change to a more reliable and non-radioactive method would give more consistent and explicable data. For example, a new method to monitor protein synthesis has been developed by Schmidt and co-workers as an advantageous alternative to the radioactive metabolic labelling (Schmidt et al., 2009). Surface sensing of translation (SUnSET) technique uses labelling of the cells with small and safe dosages of puromycin, a structural analogue of aminoacylated tRNAs, instead of conventional introduction of [^{35}S] methionine/cysteine to the cells. Puromycin incorporation into newly produced proteins is detected by monoclonal antibodies and allows monitoring and quantification of rates of global translation not only in individual cells (by ICC) but also in heterologous cell systems (by FACS).

Alternatively, even though all plasmids constitutively present in the stable cell lines were expressed from the same CMV promoter and clones for independent constructs were generated from the same nucleofection batch, it is likely that during transfection cDNA integrated into distinct sites within chromosomes. The problems of the clonal variation might be suppressed in future experiments by simultaneous usage of tetracycline or doxycycline inducible stable cell lines.

Although assessment of eEF1A1 oncogenic potential *in vitro* by transformation assays has not previously been shown, eEF1A2 was experimentally characterized as legitimate oncogene. NIH-3T3 and ES2 (ovarian clear cell carcinoma) cells generated to stably overexpress eEF1A2 gave rise to tumours when injected into nude mice (Anand *et al*., 2002). Constitutive overexpression of eEF1A2 in the SW1990 pancreatic adenocarcinoma cell line also resulted in colony formation in soft agar and increased proliferation rate (Cao et al., 2009). Ectopic expression of eEF1A2 in the SK-OV-3 clear cell carcinoma line provoked elevated proliferation (Pinke *et al.*, 2008), therefore the oncogenic effects of eEF1A2 is not restricted exclusively to the rodent fibroblasts cell system.

All three cell lines- ES2, SW1990 and SK-OV-3, are of cancerous origin where presence of eEF1A2 was either not confirmed at the mRNA level or its expression at the protein level was very poor. However, it is noteworthy that many cancer lines already carry activated oncogenes, and are predisposed to transformation (Perucho *et al.*, 1981). Therefore careful consideration should be taken with evaluation of eEF1A2 transformation abilities when taking advantage of cell lines established from human tumours. Nevertheless, if the transformed phenotype seen in these studies is due to the genetic background of NIH-3T3 cells, it would be reasonable to determine overexpression effects in other immortal cell line systems like Rat2 or Chinese hamster ovary cells (CHO-K1).

Results from A1, 1.1 and 2.1 stable cell lines provided a framework to conclude that the 5'UTR of eEF1A1 is sufficient to prevent neoplastic transformation. As the situation is less clear for eEF1A2, an alternative mechanism responsible for eEF1A2-driven oncogenesis should be considered, for example eEF1A2 might be

upregulated by phosphorylation. Interestingly, upregulation of eIF3a, eIF3b and eIF3c increased the overall level of eIF3, but upregulation of the eIF3h and eIF3i subunits did not cause such an increase, even though enhanced protein synthesis was still observed. It was revealed, that the oncogenic potential of eIF3h was stimulated by phosphorylation at Ser183 (Zhang et al., 2007, Zhang et al., 2008).

Certain other translation-involved factors, for instance eIF2α and eIF4E that have been recognized as oncogenes, are able to drive transformation as a result of alterations in their phosphorylation status. Either disruption in eIF2α phosphorylation by RNA-inducible kinase (PKR) or overexpression of eIF2α causing increase in levels of unphosphorylated initiation factor, promotes cellular proliferation and neoplastic transformation (Donze et al., 1995, Koromilas et al., 1992b, Tejada et al., 2009). By contrast, increased phospho-eIF4E levels promoted tumourigenesis (Lazaris-Karatzas et al., 1990, Wendel et al., 2007).

Both eEF1A1 and eEF1A2 appear to be capable of phosphorylation at a number of different residues (Soares et al., 2009), however it has not been yet elucidated whether there is any definite connection with transformation. Interestingly, amino acid sequence alignment of both eEF1A forms in a range of higher order eukaryotes showed three serine residues highly conserved in eEF1A2 (Ser 358, 393, 445) but not in eEF1A1. The last two amino acid sites achieved high probability scores of phosphorylation by PKC (protein kinase C) as determined by NetPhos prediction webtool (Soares et al., 2009). Additionally, Lamberti *et al*. showed Ser and Thr (Ser18, 157, 316, 383 and Thr 242, 432) as the most probable phosphorylation sites for C-Raf in their 3D model of human eEF1A, hypothesizing that it increases cell survival activity and cellular stability of the translation factor (Lamberti et al., 2007). Potential differences in phosphorylation status between eEF1A1 and eEF1A2 could shed some light whether this type of protein regulation might have some influence on transformed phenotype of eEF1A2.

Before proper identification of the phosphorylated residues in eEF1A forms by mass spectrometry could be carried out, a pilot assay needed to be performed. HeLa cells transiently transfected with A1 or A2 constructs could be chosen as an experimental system to detect other possible phosphorylation sites at yet unknown

serine residues. Attempts to investigate phosphorylation status of eEF1A2 were taken with anti-phosphoserine antibody as described by Lamberti (Lamberti et al., 2007), but without success (data not shown). Even though immunoprecipitation stage (IP) was efficient and the amounts of pulled down eEF1A proteins with antibodies directed against different epitope tags were satisfactory, this particular anti-phosphoserine antibody was not able to show any bands when IP reactions were subjected to immunoblotting. Although all precautions were taken to avoid unwanted dephosphorylation during preparation of cell lysates and phosphatase inhibitors were present in buffers for cell lysates production, these samples gave a range of nonspecific bands. Perhaps another antibody to detect proteins phosphorylated at serine residues would bring reliable results, but timing of the project did not allow for return to the assay.

Chapter 5: Immunohistochemical studies of the eEF1A variants expression on tumour microarrays

5.1 Introduction

Currently, the overexpression of eEF1A2 protein has been linked to a high proportion of tumours of several types, including breast, ovarian and pancreatic carcinomas (Tomlinson et al., 2005, Tomlinson et al., 2007, Pinke et al., 2007, Cao et al., 2009). However, to date, no extensive studies have been reported analysing the expression and distribution of eEF1A1 and eEF1A2 in colorectal cancer or hepatocellular and cutaneous malignancies. Initial immunohistochemical studies performed earlier in the laboratory suggested the possibility of eEF1A2 upregulation in a significant subset of primary colorectal carcinomas. In order to shed some light on this, immunohistochemistry was performed on commercially manufactured tumour microarrays (TMA) containing collections of liver, skin or colon cancers. Where possible, the relationship between eEF1A variants expression and clinical characteristics was also assessed.

5.2 Results

An array containing a panel of multiple normal human organ sections was used as a control for staining with the anti-eEF1A1 and anti-eEF1A2 antibodies and to assess expression of eEF1A forms in normal liver, colon and skin tissues. The expression of eEF1A1 and eEF1A2 was then examined independently by immunohistochemistry in different commercial tumour microarrays containing cores either from hepatocellular carcinoma, malignant melanoma or colorectal tumours. One of the arrays from the same batch was incubated with the anti-eEF1A1 antibody and the other one was stained with the anti-eEF1A2 antibody.

Staining was assessed in relation to tumour free cores indicated as 'normal' in the array description. The arrays were scored by two independent observers and if any discrepancy in the assessment of the cores occurred, they were reviewed to obtain an agreed score. Multiplying the staining intensity level (1-3) by the percentage of tumour cells present within that level was used to calculate a final histoscore. Histoscores of 0, 1-100, 101-200 and 201-300 were classified as negative, weak, moderate and strong, respectively. In addition, where clinical information was available for a commercial array, a Fisher's exact test was used to investigate any association between levels of eEF1A expression and clinicopathological characteristics. Representative microscope images of normal tissue controls are shown in Figure 5.1.

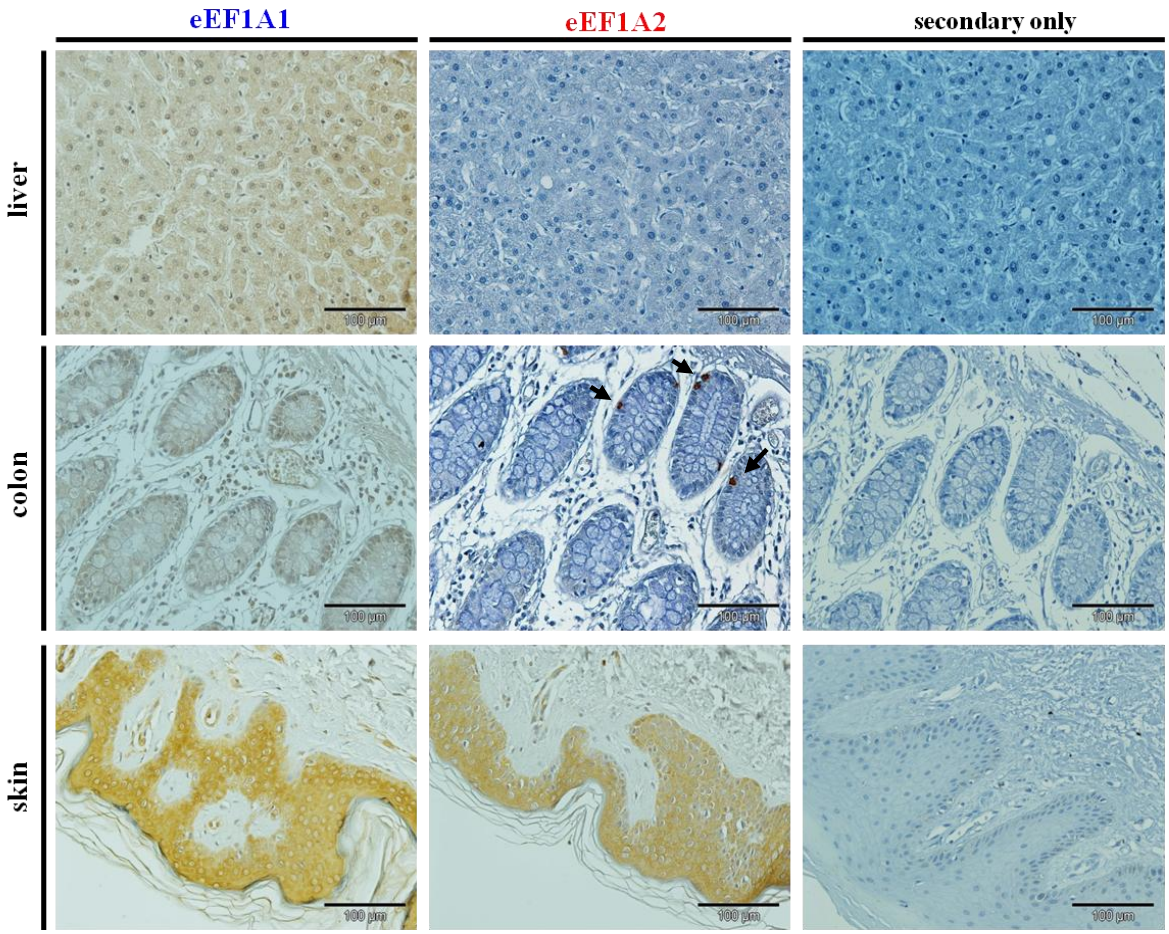

Figure 5.1 eEF1A1 and eEF1A2 immunostaining in normal human liver, colon and skin. Third column displays sections stained without primary antibodies (negative control). Liver shows no expression for eEF1A2 as expected. eEF1A2 was detected in the single cells of colonic crypts (marked with arrows). Similar pattern of eEF1A1 and eEF1A2 staining is present for cutaneous tissue. Magnification: 20x.

5.2.1 Immunohistochemistry of hepatocellular carcinoma TMA

The intensity of eEF1A1 and eEF1A2 expression was investigated in 41 hepatocellular carcinomas (HCC) on a commercial tumour microarray (Folio Biosciences). A large proportion of tumours showed no staining and so 30 of 41 tumours (73%) and 33 of 41 tumours (80%) were negative for eEF1A1 and eEF1A2, respectively. Twenty seven percent showed weak staining for eEF1A1 and 20% of HCC cores demonstrated weak immunoreactivity for eEF1A2 (Table 5.1).

On eleven of the eEF1A1 weak staining tumours, only 2 cores overlapped with the weak expression of eEF1A2.

Table 5.1 *Expression of eEF1A1 and eEF1A2 in primary hepatocellular carcinoma array*

	number analysed	negative	%	weak	%	moderate	%	strong	%
eEF1A1	41	30	**73**	11	**27**	0	**0**	0	**0**
eEF1A2	41	33	**80**	8	**20**	0	**0**	0	**0**

eEF1A1 was expressed uniformly across the sections and eEF1A2 was either seen in patches of cells or stained evenly across the core. Both eEF1A variants showed a diffuse cytoplasmic pattern within adenomous hepatocytes. Representative examples of staining are shown in Figure 5.2.

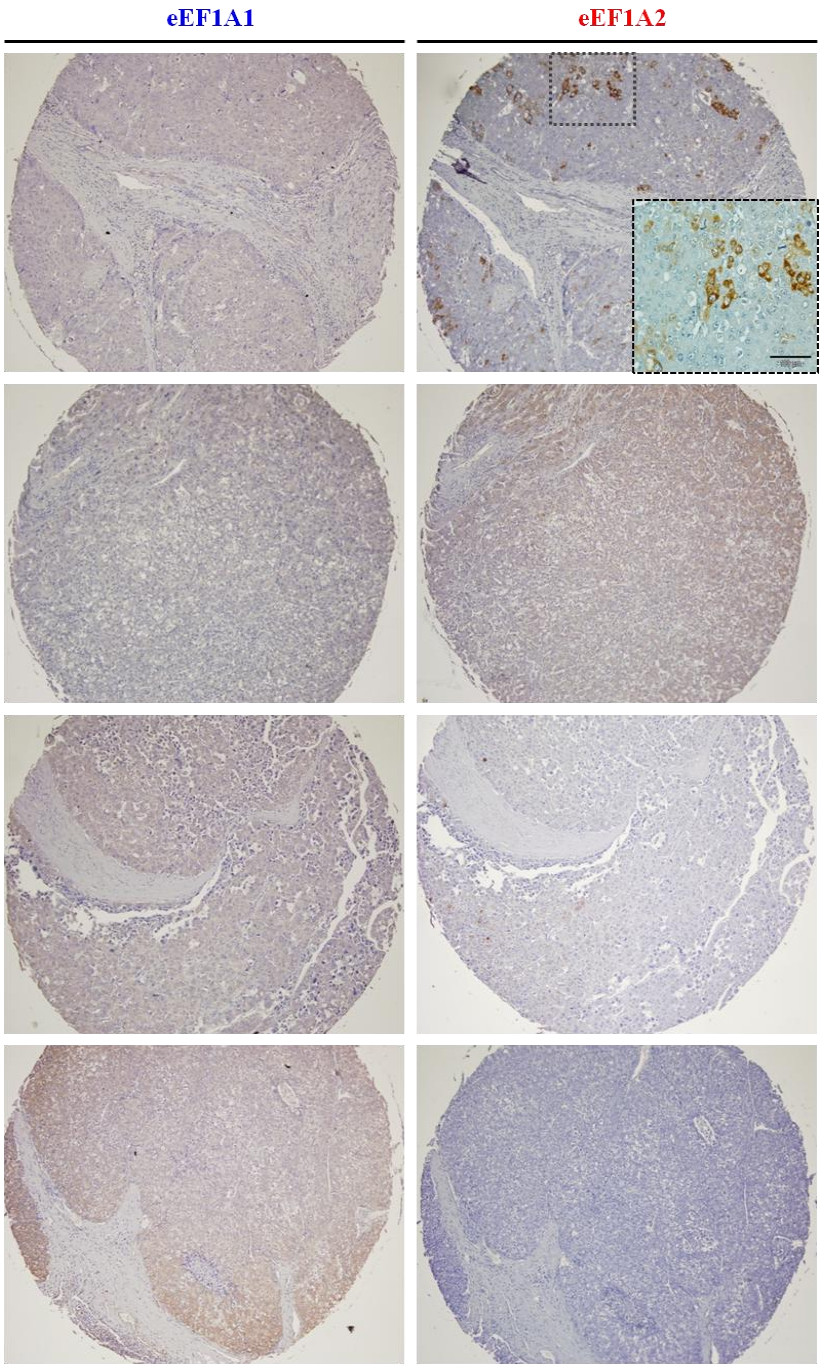

Figure 5.2 Expression of eEF1A1 and eEF1A2 in primary hepatocellular carcinoma. Staining of tumours with the eEF1A1 antibody was weak and uniform across the sections (left column). Expression of eEF1A2 in corresponding cores (right column) was negative or weak, or very rarely, in patches of neoplastic hepatocytes. Magnification: 4x (except square in top section with eEF1A2; 10x).

Only two clinicopathological characteristics were available with this tumour array: age and sex. Neither the age nor the gender of the donors was significantly associated with the expression levels of eEF1A1 or eEF1A2, as displayed in Table 5.2.

Table 5.2 *Relationship of eEF1A1 or eEF1A2 expression to clinical variables*

Characteristic		eEF1A1 Staining intensity				
		negative	weak	moderate	Strong	P^a
sex	F	4	0	0	0	0.559
	M	26	11	0	0	
age	0-40	8	0	0	0	0.052
	41-60	18	11	0	0	
	>60	4	0	0	0	

Characteristic		eEF1A2 Staining intensity				
		negative	weak	moderate	Strong	P^a
sex	F	5	0	0	0	0.563
	M	28	8	0	0	
age	0-40	8	0	0	0	0.182
	41-60	21	8	0	0	
	>60	4	0	0	0	

[a] Fisher's exact test

5.2.2 Immunohistochemistry on malignant melanoma TMA

Immunohistochemical staining of malignant melanoma with eEF1A1 and eEF1A2 antibodies was performed on two tumour microarrays manufactured by different companies (Biomax and Folio Biosciences). One tumour core on the Biomax array was non-scorable for both antibodies due to the high melanisation of the section.

It is noteworthy that eEF1A1 and eEF1A2 appeared to be expressed in the basal layer of epidermis-the layer where undifferentiated keratinocytes undergo a constant proliferation process (see Figure 5.1). Representative illustrations of eEF1A1 and eEF1A2 expression in malignant melanoma are displayed in Figures 5.3 and 5.4.

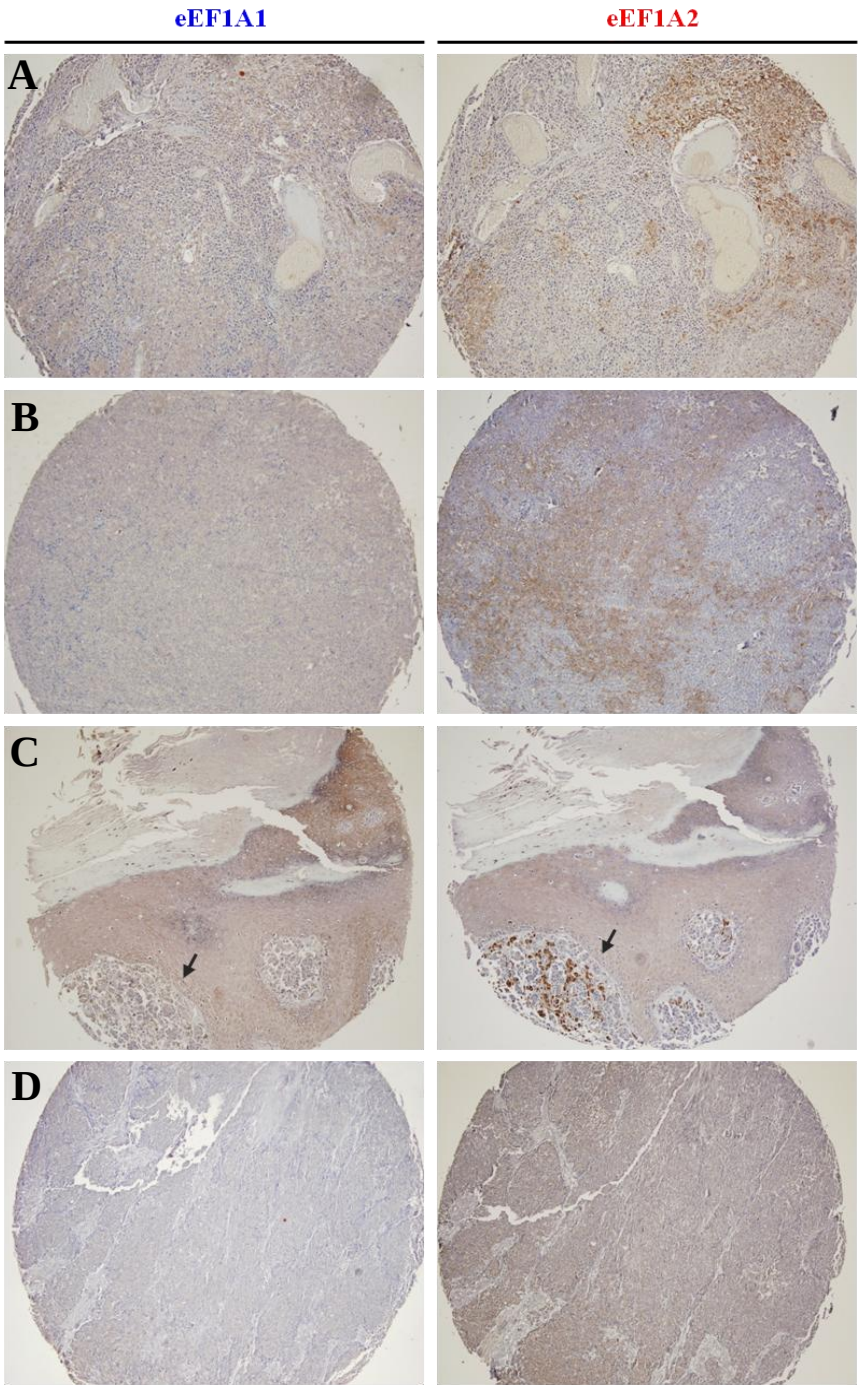

Figure 5.3 Representative examples of eEF1A1 and eEF1A2 immunostaining in malignant melanoma array. In majority of cases, weak uniform expression was observed for eEF1A1 whereas eEF1A2 was expressed in patches of cells or in the whole tumour section (A, B, D). No eEF1A1 staining other than in normal tissue was seen in neoplastic intraepidermal nests of melanocytes (C) whereas it was strong for eEF1A2, as indicated by arrows. Magnification: 10x.

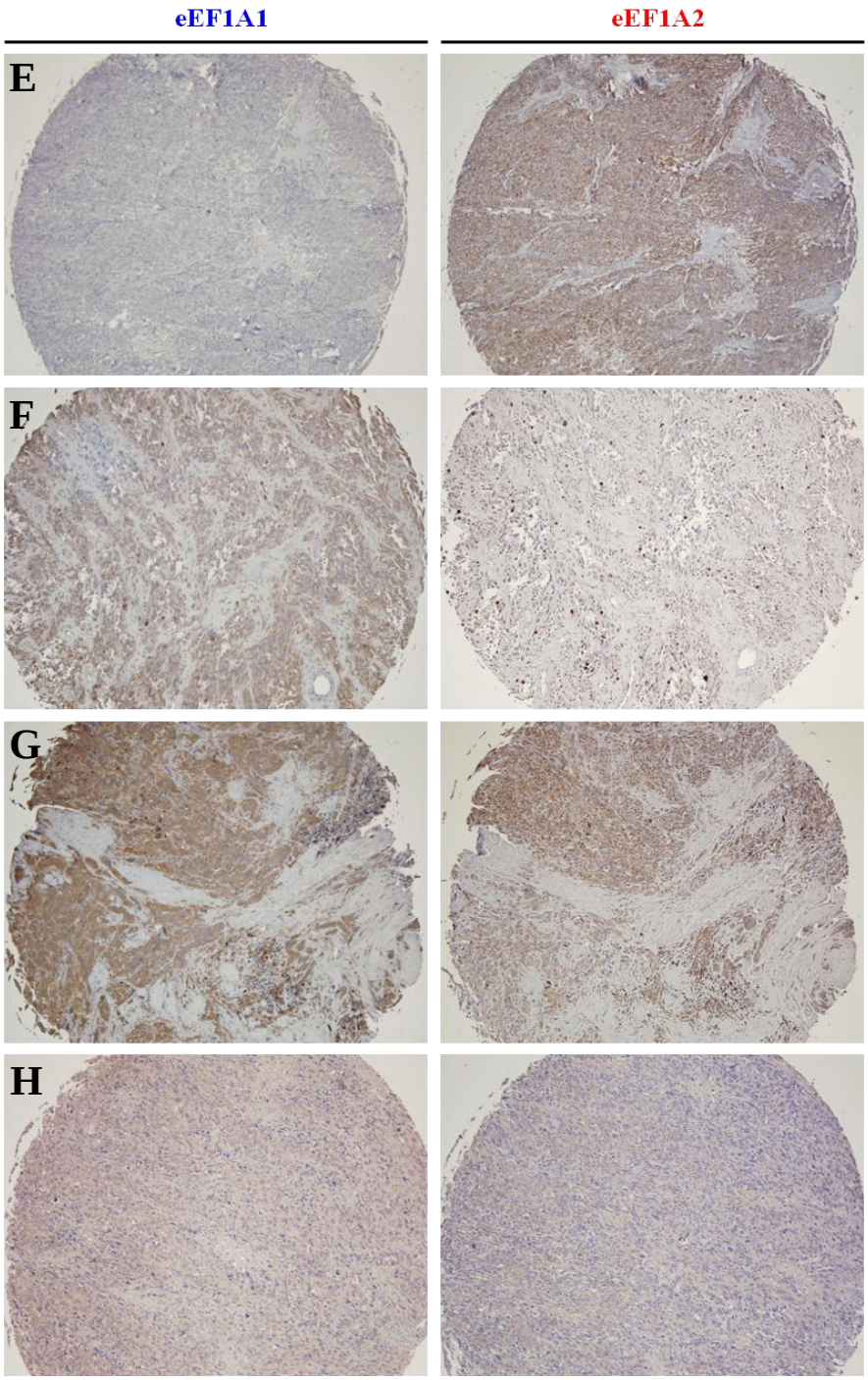

Figure 5.4 Expression of eEF1A1 and eEF1A2 in malignant melanoma was equally weak or equally moderate in a few tumour sections (G, H). In addition, several cores showed negative staining for eEF1A1 whereas eEF1A2 was moderately expressed (E). There were also sections negative for eEF1A2 staining (F) but modest expression of eEF1A1 protein was observed. Magnification: 10x.

On the Biomax array, weak **eEF1A1** staining was observed in 9 of 39 (23%) cases whereas negative tumours represented 30 of 39 (77%) cores as shown in Table 5.3. For the Folio Biosciences array, 2 of 31 tumours (6%) showed strong immunoreactivity, 5 of 31 tumours showed moderate staining (16%) and 24 of 31 cores (77%) showed weak staining, respectively (Table 5.5). Positive staining was uniform across the core and showed a diffuse cytoplasmic pattern. No stromal staining was observed.

For **eEF1A2** staining on the Biomax array (Table 5.3), one tumour demonstrated strong expression, 2 tumours moderate expression, 13 cores weak expression (33%) and 23 tumours displayed negative staining (59%), respectively. Six of thirty one (19%) tumours showed strong immunoreactivity, 8 of 31 (26%) displayed moderate staining, 13 of 31 (42%) weak staining and 4 tumours were negative (13%) on the Folio Biosciences array (Table 5.5). Immunohistochemistry with the eEF1A2 antibody showed a diffuse cytoplasmic subcellular localisation which was either uniform across the section or was seen in patches of cells. No stromal staining was observed.

Eleven tumours with weak eEF1A1 or eEF1A2 expression, 2 cores with moderate and one core with strong staining were overlapping between eEF1A1 and eEF1A2 positive tumour samples on Folio Biosciences array. Biomax array contained 21 cores negative and 5 cores with weak expression for eEF1A1 as well as for eEF1A2.

Tables 5.4 and 5.6 summarize the relationship between eEF1A variant expression and clinicopathological features; however, only age and sex were available for both commercial TMAs. There was no significant correlation between either eEF1A1 or eEF1A2 expression level and the gender or age of the donors.

Biomax TMA

Table 5.3 *Immunohistochemistry for eEF1A1 and eEF1A2 in malignant melanoma*

	number analysed	negative	%	weak	%	moderate	%	strong	%
eEF1A1	39	30	**77**	9	**23**	0	**0**	0	**0**
eEF1A2	39	23	**59**	13	**33**	2	**5**	1	**3**

Table 5.4 *Relationship between eEF1A1 or eEF1A2 expression and clinicopathological characteristics*

Characteristic		eEF1A1 Staining intensity				
		negative	weak	moderate	strong	*P*[a]
sex	F	14	3	0	0	0.704
	M	16	6	0	0	
age	0-40	6	2	0	0	0.886
	41-60	14	3	0	0	
	>61	10	4	0	0	

Characteristic		eEF1A2 Staining intensity				
		negative	weak	moderate	strong	*P*[a]
sex	F	9	7	1	0	0.797
	M	14	6	1	1	
age	0-40	3	5	0	0	0.102
	41-60	13	3	0	1	
	>61	7	5	2	0	

[a] Fisher's exact test.

Folio Biosciences TMA

Table 5.5 *Summary of eEF1A1 and eEF1A2 expression in malignant melanoma*

	number analysed	negative	%	weak	%	moderate	%	strong	%
eEF1A1	31	0	**0**	24	**77**	5	**16**	2	**7**
eEF1A2	31	4	**13**	13	**42**	8	**26**	6	**19**

Table 5.6 *Association between expression of eEF1A1 or eEF1A2 and clinicopathological features*

	Characteristic	eEF1A1 Staining intensity				
		negative	weak	moderate	strong	***P*[a]**
sex	F	0	10	3	1	0.812
	M	0	14	2	1	
age	0-40	0	4	1	0	0.999
	41-60	0	12	2	1	
	>61	0	8	2	1	
	Characteristic	**eEF1A2** Staining intensity				
		negative	weak	moderate	strong	***P*[a]**
sex	F	1	8	3	3	0.588
	M	3	5	5	3	
age	0-40	0	1	3	1	0.177
	41-60	2	6	5	2	
	>61	2	6	0	3	

[a] Fisher's exact test

5.2.3 Immunohistochemistry on colorectal carcinoma TMA

Tumour microarrays containing colorectal adenocarcinomas were obtained from Zymed and BioChain. Of the 26 tumour samples on the Zymed array (Table 5.7), one showed moderate expression of **eEF1A1** (4%), 11 showed weak expression (42%) and the remainder was negative. For **eEF1A2** immunostaining, 4 of 26 tumours (15%) displayed strong staining, 7 of 26 (27%) showed moderate staining, 9 of 26 (35%) showed weak staining and 6 tumours showed no eEF1A2 overexpression.

The same three tumour cores showed weak staining for eEF1A1 and for eEF1A2 and other 4 cores were negative for both eEF1A variants. Detailed clinical information was not available with this tumour array.

Zymed TMA

Table 5.7 *Expression of eEF1A1 and eEF1A2 in primary colorectal adenocarcinoma*

	number analysed	negative	%	weak	%	moderate	%	strong	%
eEF1A1	26	14	**54**	11	**42**	1	**4**	0	**0**
eEF1A2	26	6	**23**	9	**35**	7	**27**	4	**15**

For the BioChain array, 14 of 61 of tumours (23%) displayed strong eEF1A2 staining, 12 (20%) showed moderate staining, 20 (33%) showed weak staining and the remaining 15 tumours (24%) were negative (Table 5.8). Initially, there were 64 tumours on this array but due to loss or damage of three cores, these were considered as non-scorable and instead, 61 tumours were included for further analyses.

BioChain TMA

Table 5.8 *Expression of eEF1A2 in primary colorectal adenocarcinoma*

	number analysed	negative	%	weak	%	moderate	%	strong	%
eEF1A2	61	15	**24**	20	**33**	12	**20**	14	**23**

Unfortunately, it was impossible to perform immunohistochemical evaluation of the eEF1A1 expression on this array. The batch of the anti-eEF1A1 antibody which was generally available in the laboratory lost its specificity at the time when this particular array was delivered and concomitantly, the newly generated batch was still undergoing the optimisation process. To give a general overview of eEF1A1 expression in colorectal cancer, immunohistochemistry analysis obtained previously by Dr Julia Boyd (a former member of Professor Cathy Abbott group) is presented in Figure 5.5, alongside immunohistochemistry performed on the Zymed array as shown in Figure 5.6.

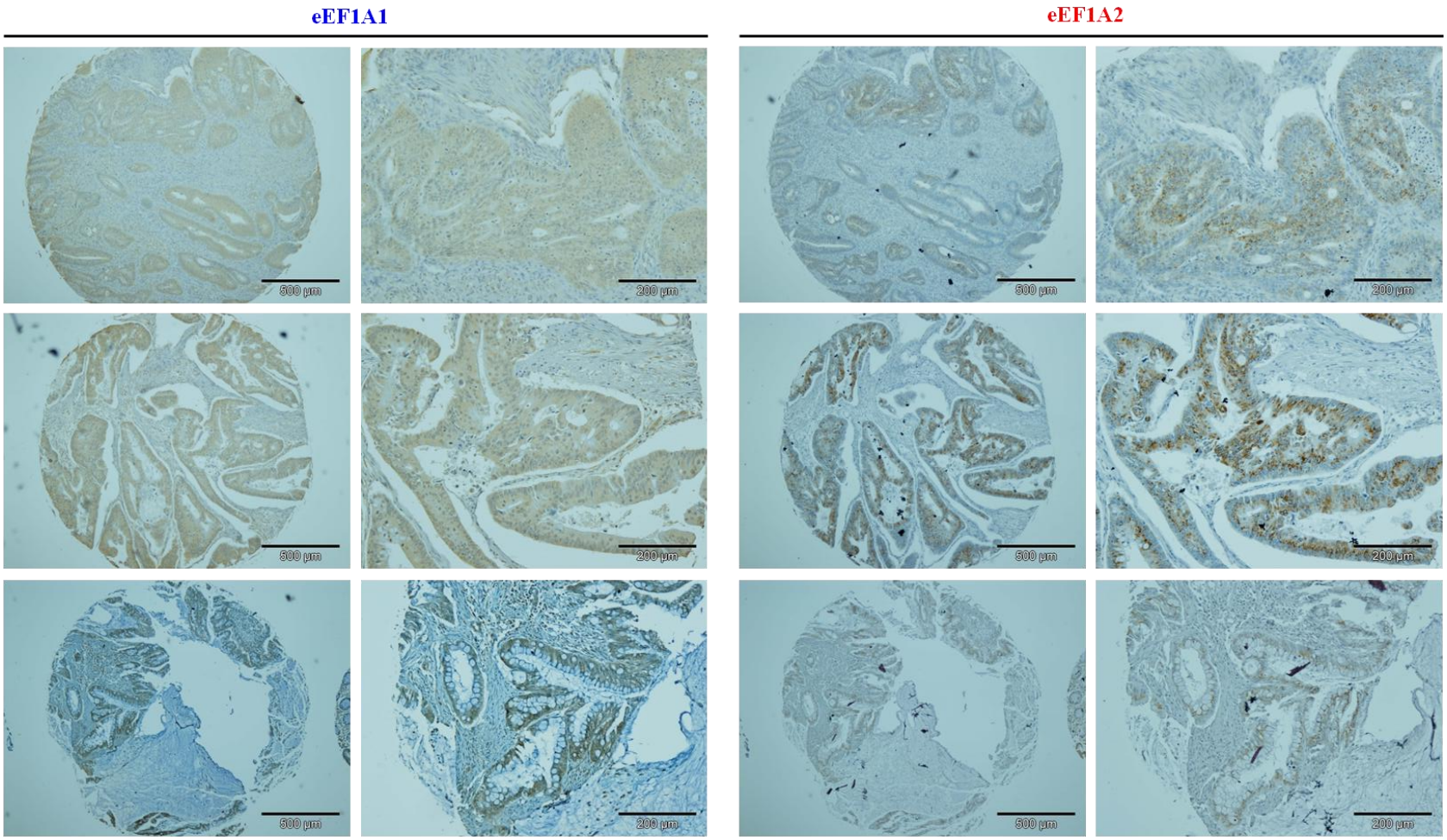

Figure 5.5 Immunohistochemical expression of eEF1A1 and eEF1A2 in primary colorectal carcinoma. Uniform moderate expression of eEF1A1 was observed in tumour sections whereas expression of eEF1A2 was more heterogonous. Array was subjected to immunohistochemistry by Dr Julia Boyd. Magnification: 4x (whole cores), 10x (selected fragments).

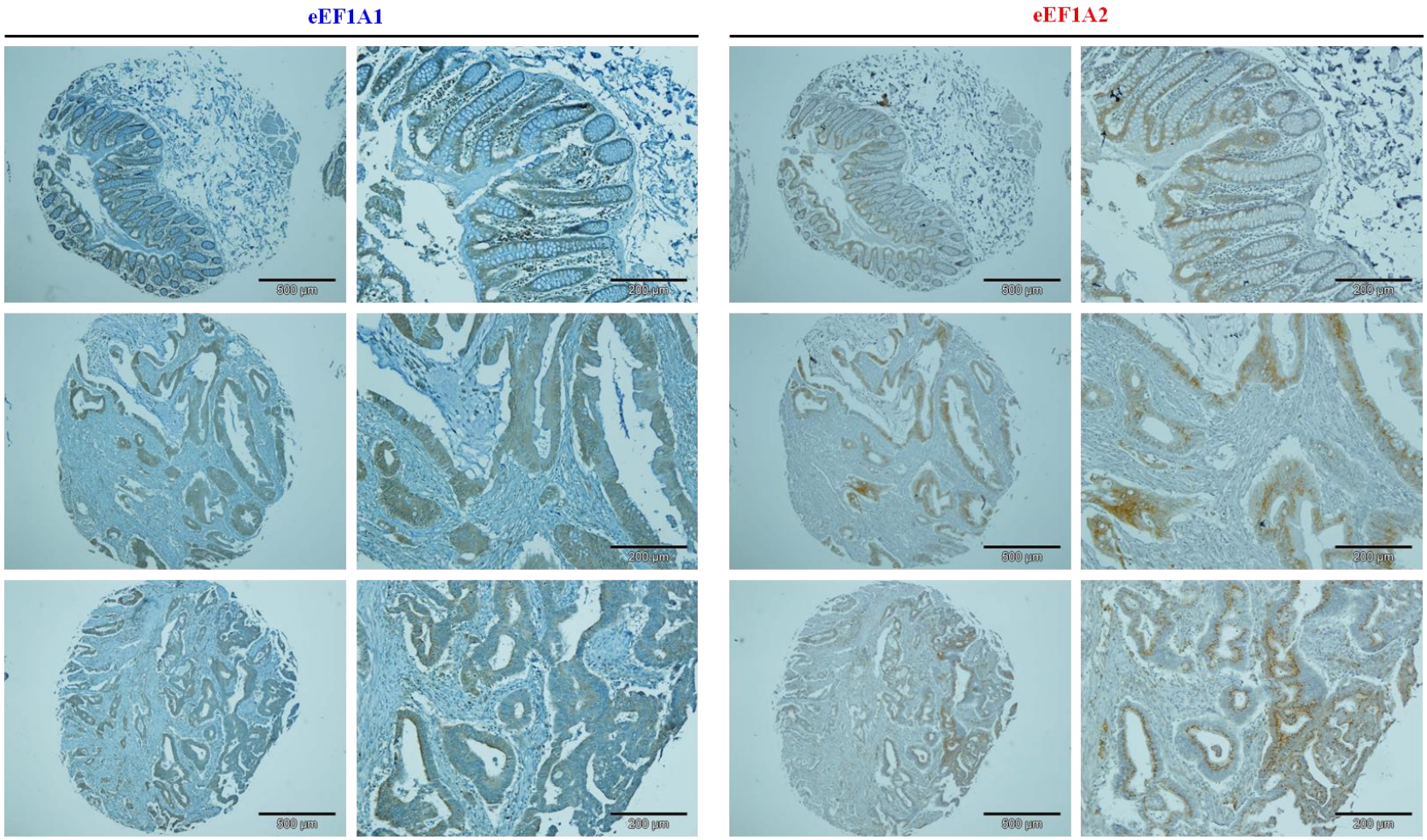

Figure 5.6 Immunohistochemical analysis of eEF1A1 and eEF1A2 expression in colorectal adenocarcinomas on Zymed array. Low (4x) and high (10x) magnification of the corresponding core images are shown.

The expression of eEF1A1 in normal colon was widespread; however staining was not very strong. Within a given section of normal colon, up to two cells per crypt showed moderate eEF1A2 expression and these cells were localised toward the base of the crypt (see Figure 5.1). This was in agreement with previous observations in the laboratory and the similar pattern that is also seen in mice (Newbery et al., 2007); these cells are almost certainly enteroendocrine cells.

In the tumour sections, no stromal staining was seen for either eEF1A variant. Tumour staining with the eEF1A1 antibody was uniform across the whole section. Positive staining of eEF1A2 in tumours was observed in cells of epithelial origin; however, the pattern of staining differed between tumours. The most common pattern was characterised by ubiquitous cytoplasmic expression of eEF1A2 in a large area of the core. In a smaller proportion of tumours, clear perinuclear staining in single entrapped cells, an accumulation of granular species on the one side of the nucleus in all neighbouring cells and distinct cytoplasmic staining in patches of cells were additionally observed. The perinuclear accumulation of eEF1A2 appears to reflect the staining pattern seen in neuroendocrine cells and as such may be a surrogate phenotype for cancer rather than any biological function of eEF1A2 (personal communication with Professor David Harrison, pathologist). Representative images of eEF1A2 expression patterns in colorectal tumours are shown in Figures 5.7 and 5.8.

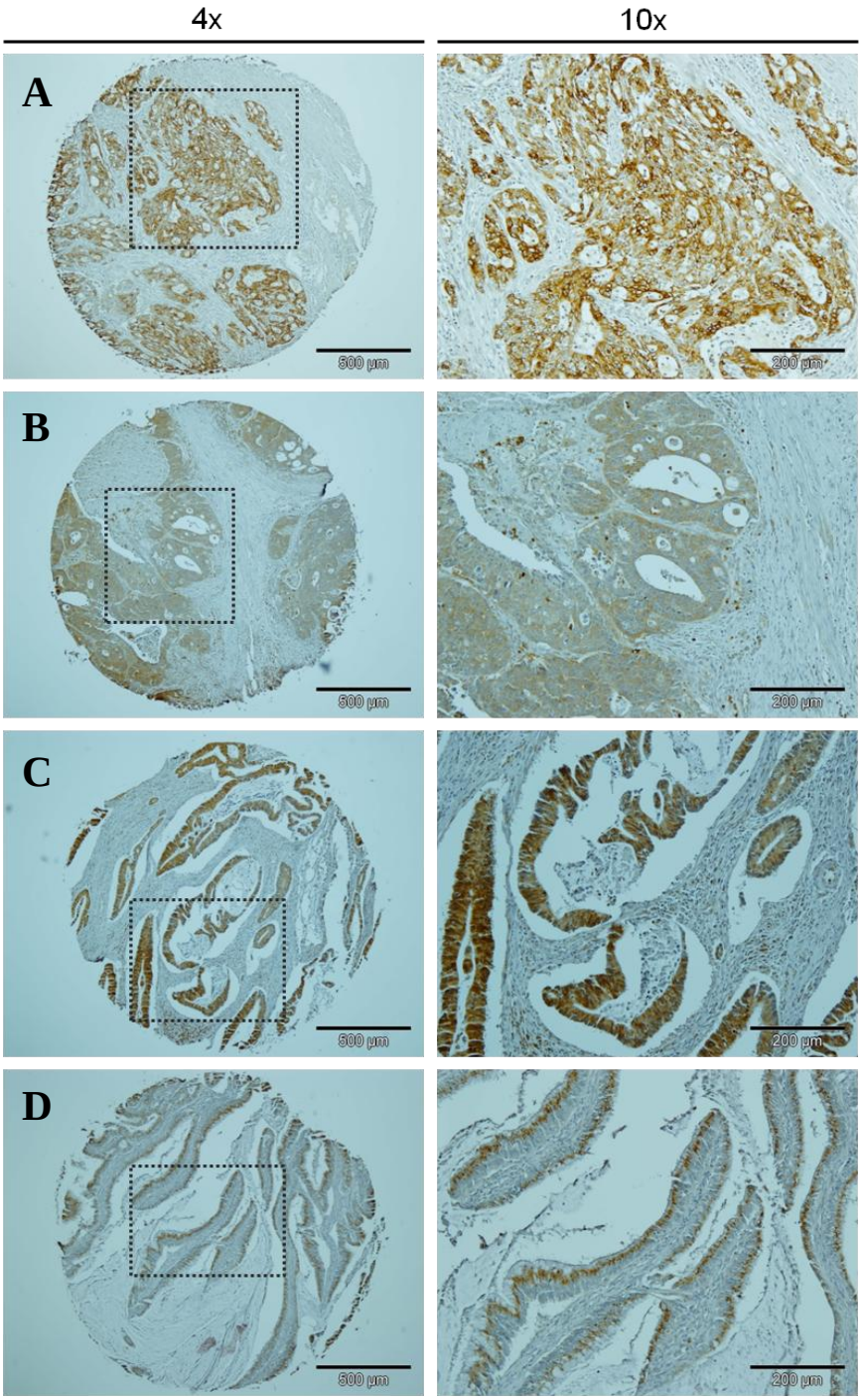

Figure 5.7 Representative illustrations of different patterns for eEF1A2 expression in colorectal tumours. (A, B, C) Diffuse cytoplasmic staining of the tumour cells in a large proportion of the cancer section. **(D)** Granular staining within neoplastic epithelial cells. The right column (10x) represents selected fragments of the cores from the left column (4x).

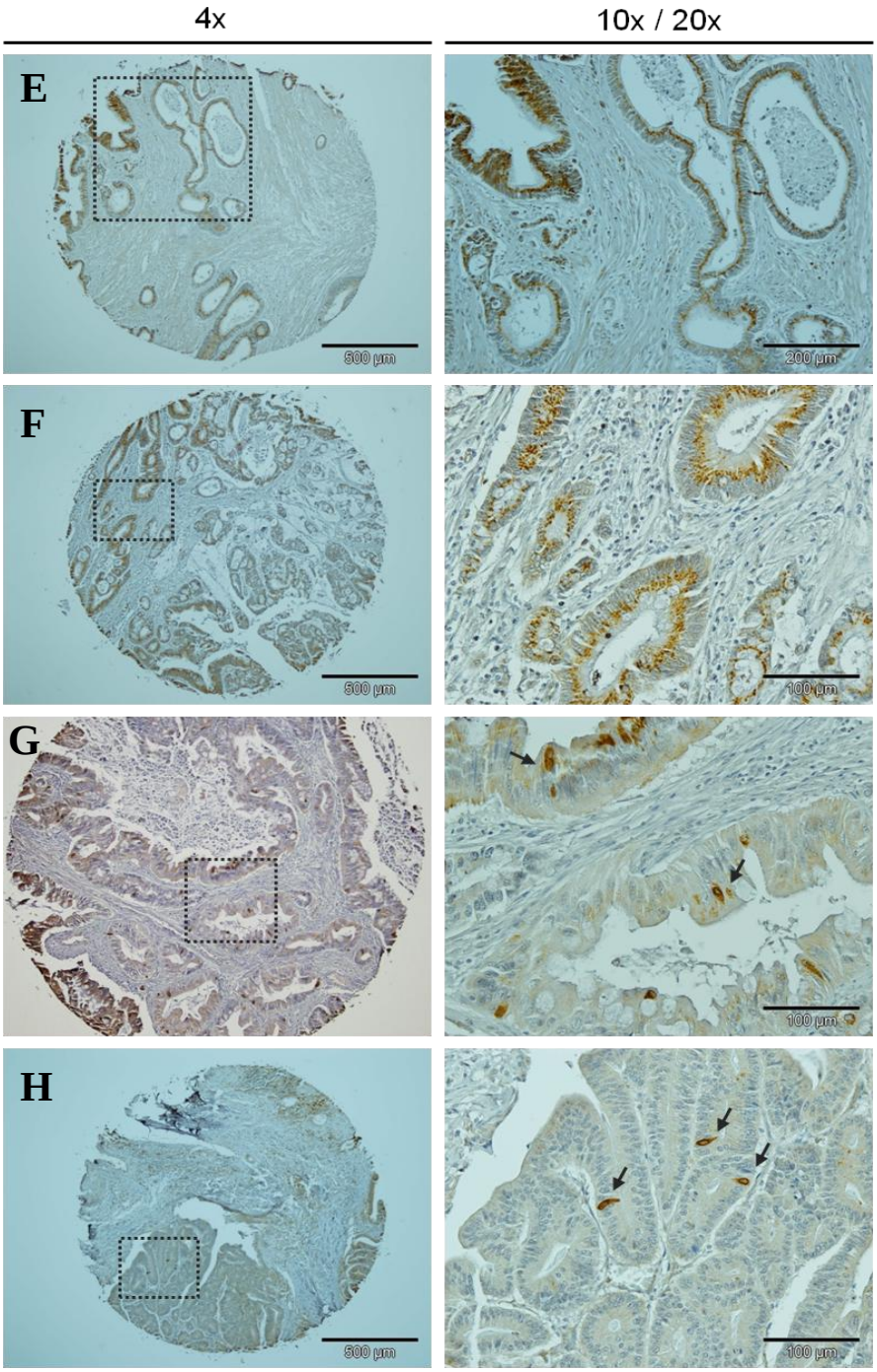

Figure 5.8 Examples of the heterogonous expression of the eEF1A2 protein in a panel of colorectal tumours. (E, F) Granular staining of the eEF1A2 is located on one side of the nuclei of the neighbouring cells. **(G, H)** Neoplastic cells show a moderate cytoplasmic staining but strong perinuclear staining in neuroendocrine cells as indicated by arrows. Illustrations on the right are a higher magnification (10x, 20x) of the left column images (4x).

Clinical diagnostic data, including patient age, sex, primary tumour assessment, tumour differentiation, lymph node status and metastasis were available for the samples on the BioChain TMA; therefore, a relationship between eEF1A2 expression and these clinical variables could be determined as shown in Table 5.9. There was no significant correlation between these clinical features and eEF1A2 level, except that there appeared to be an association between eEF1A2 expression and a small number of positive lymph nodes (P = 0.024, Fisher's exact test). This suggests that overexpression of eEF1A2 could be an early event in colorectal cancer.

Table 5.9 *Relationship between expression of eEF1A2 and clinicopathological variables in colorectal tumour array*

Characteristic		eEF1A2 Staining intensity				
		negative	weak	moderate	strong	*P*[a]
sex	F	5	9	6	6	0.863
	M	10	11	6	8	
age	0-40	1	2	2	0	0.462
	41-60	4	6	5	8	
	>61	10	12	5	6	
T	Tx	1	1	0	0	0.248
(primary tumour classification)	T1	0	0	0	0	
	T2	7	12	4	8	
	T3	6	4	8	6	
	T4	1	3	0	0	
N	N0	13	12	6	10	**0.024**
	N1	0	0	4	0	
(regional lymph nodes)	N2	1	6	1	3	
	N3	1	2	0	1	
	N4	0	0	1	0	
M	M0	14	17	10	11	0.726
(distant metastasis)	M1	1	3	2	3	
tumour differentiation	poorly	2	1	1	1	0.412
	moderately	5	9	4	6	
	well	8	10	5	4	
	other	0	0	2	3	

[a] Fisher's exact test.

5.3 Discussion

This study describes the immunohistochemical analysis of eEF1A1 and eEF1A2 expression in liver, skin and colorectal tumour microarrays, as in the literature, there is very little information about possible engagement or expression pattern of eEF1A forms in these cancer types. A combination of multiple tumours in one array provides a simple and comprehensive tool to assess the expression pattern of a candidate biomarker between different stages of a specific cancer or allows expression of one biomarker to be compared to that of another candidate in the same experimental setting (Nocito et al., 2001).

Analysis of eEF1A1expression in a panel of **hepatocellular carcinomas** showed that about 27% of tested cores displayed weak staining and the remainder appeared to have no more staining than normal liver. Thus, it is tempting to speculate that aberrations in eEF1A1 expression are not commonly seen in hepatocellular carcinoma. Interestingly, weak staining was found in an equally small percentage of cases for eEF1A2 expression and only two cores showing weak expression of eEF1A1 exhibited weak staining of eEF1A2. Investigation of eEF1A variant-specific expression at the protein level has not been previously reported. However, some information is available about the levels of eEF1A variant expression at the RNA level in HCC. Based on LongSAGE analyses of gene specific tag hits, 104 genes were found to be significantly upregulated in HCC when compared to their expression profile in normal liver, including *EEF1A1* with an approximate fold change of 26 (Dong et al., 2009) but it is not known how many hepatocellular carcinoma samples were used in this experiment. In addition, the *EEF1A2* gene was amplified in HCC according to the array-based CGH performed on 67 hepatocellular carcinoma cases and also found to be overexpressed by real time-PCR in 20 HCC cell line samples (Schlaeger et al., 2008). Would these alterations in gene expression be reflected at the protein level? What are the levels of *EEF1A1* or *EEF1A2* expression in tumours which showed in study herein only low increase in corresponding protein expression (in comparison to normal liver)?

Is there any functional significance of eEF1A1 or eEF1A2 expression at low levels in HCC? It is all not that clear but eEF1A1 was identified as an interacting partner for DLC1 (deleted in liver cancer 1) by protein precipitation and mass spectrometry (Zhong et al., 2009). The SAM (sterile alpha motif) domain of DLC1 was implicated in the suppression of cell migration by the recruitment of eEF1A1 to the cell membrane periphery and ruffles. SAM mutants failed to recruit eEF1A1 and did not affect cell migration. DLC1 is a Rho-GTPase-activating protein and a candidate tumour suppressor which is commonly deleted in liver or breast tumours (Zhong et al., 2009). Since only two HCC cores with positive expression for eEF1A1 and eEF1A2 overlapped in my IHC study, it is tempting to speculate that eEF1A variants could have different biological meaning (if any) in liver cancer. Based on a real-time PCR approach, *EEF1A2* overexpression was reported in two hepatocellular carcinoma cases which harboured mutations in *PIK3CA* (PI3K, catalytic alpha polypeptide) along with activation of the Akt pathway (Boyault et al., 2007). As eEF1A2 has been associated with the mediation of cell motility in a PI3K/Akt dependent manner (Amiri et al., 2007), it is possible that upregulation of eEF1A2 might foster Akt signalling which is activated in a large proportion of human HCC (Schlaeger et al., 2008), but this requires further analysis.

Using immunohistochemistry on two **malignant melanoma** arrays, this study showed that overall, eEF1A1 was significantly overexpressed only in 10% of tumours (7/71) whereas eEF1A2 was highly abundant in about 24% (17/71) cases. There are no other reports about expression of eEF1A1 and eEF1A2 at the protein level. As for the gene analyses, abundance of *EEF1A2* transcript was reported for two highly metastatic malignant melanoma cell lines but not for the poorly metastatic 1F6 line (Joseph et al., 2004, de Wit et al., 2002). On the other hand, a gradual increase in mRNA expression of eEF1A2 was seen in patients' lesions representing chronological stages of melanocytic tumour progression (de Wit et al., 2002). The engagement of eEF1A in malignant melanoma remains unclear; however, it would be interesting to test expression of eEF1A2 at the protein level at different stages of melanoma progression, including dysplastic naevi, radial and vertical growth phases to see whether eEF1A2

expression correlates with any tumour stage. There were more cases with moderate and strong staining for both eEF1A forms on the array obtained from Folio Biosciences than on the array from Biomax. Even though clinicopathological features other than age and sex were not provided, it is very likely that the cores on each array represent different proportions of tumour staging, which might explain discrepancies between arrays, if indeed expression of eEF1A2 is dependent on tumour progression. As these arrays were manufactured by different companies, it is also possible that any discrepancies in tissue fixation or storage could have an influence on the overall outcome of the eEF1A staining.

The most obvious differences between expression of eEF1A variants were observed in the immunostaining of **colorectal cancer** arrays. Overall, only 4% of colorectal tumours showed significant overexpression of eEF1A1; however, only 26 cancers were tested for eEF1A1 immunopositivity in the studies herein. In contrast, upregulated eEF1A2 was seen in a high proportion (43%; 37/87) of primary colorectal tumours. The majority of tumours presented with a lack of regional lymph node metastasis, which was significantly associated with eEF1A2 expression (negative and weak). As the number of tumour-positive lymph nodes increased, there were as many tumours exhibiting negative or weak eEF1A2 staining as cores displaying moderate and strong eEF1A2 expression. A similar association was noticed between the lack of distant metastasis and eEF1A2 immunostaining; however, this relationship was not statistically significant. Even though this needs to be confirmed with a larger number of samples, along with clinical information, these preliminary data suggest that eEF1A2 expression status might be associated with early events in colorectal carcinogenesis.

How eEF1A2 could contribute to colorectal cancer remains unclear but these immunohistochemical studies support the observations obtained earlier in the laboratory, as in these studies too, eEF1A2 was found to be upregulated in a high proportion of primary colorectal carcinoma cases. In addition, analyses of *EEF1A2* copy number and methylation status by real-time PCR and bisulfite-PCR in a few CRC cell lines indicated that neither gene amplification nor hypomethylation appears to be solely sufficient to

drive eEF1A2 overexpression (Jan Bergmann, unpublished data). Another possible explanation is that upregulation of eEF1A2 is triggered by changes in the specific microRNA expression pattern. More recently, using a combination of sequence-based matches and hybridization energy, Lee and colleagues identified a new class of microRNAs called miBridge which have the ability to interact simultaneously with specific sites in the 5' and 3' UTR of target mRNAs. Among the predicted mRNAs, eEF1A2 was a potential target of miBridge candidate miR-663 (Lee et al., 2009a). Interestingly, miR-663 belongs to the colorectal microRNAome and was implicated as a tumour suppressor since it was downregulated in 5 human gastric cancer cell lines when compared to normal gastric cells profile (Cummins et al., 2006b, Pan et al., 2010). When miR-663 was re-introduced into BGC823 and SNU5 gastric cancer cell lines, decreased proliferation *in vitro*, chromosomal aberrations alongside mitotic catastrophe, and reduced tumour growth *in vivo* in xenografted mice were reported (Pan et al., 2010). Since the *in situ* predicted interaction sites for miR-663 are within both untranslated regions of eEF1A2 (Lee et al., 2009a), it suggests this microRNA might be a critical regulator of eEF1A2 abundance in the cell. This is highly intriguing, especially that resveratrol treatment of SW480 colon adenocarcinoma cells resulted in upregulation of miR-663 (Tili et al., 2010). Resveratrol (trans-3,4',5-trihydroxystilbene) is an antioxidant derived from grapes and other plants which has shown cardiovascular and cancer preventive properties and is used in the human cancer prevention preclinical studies. It induces apoptosis through upregulation of proapoptotic genes and concurrently reduces expression of anti-apoptotic genes (Tili et al., 2010). Furthermore, NIH-3T3 cells stably transfected with eEF1A2 exhibited reduced anchorage independent growth after treatment with resveratrol and resveratrol downregulated eEF1A2 in insulin- or serum- stimulated PA-1 ovarian cancer cells (Lee et al, 2009b). It would be interesting to assess experimentally whether eEF1A2 is a true target for miR-663 and if there are any correlations in expression between them in normal colon, colorectal tumours and colorectal cancer cell lines.

On the other hand, if upregulated eEF1A2 is indeed engaged in the early events of CRC, it might contribute to malignancy by interacting with proteins involved in

cytoskeletal rearrangements. Such changes in the cytoskeleton contribute to an increase in carcinoma cell motility and a more aggressive tumour phenotype. In a yeast two-hybrid approach of a mouse brain cDNA library, eEF1A2 was used as bait and fascin was reported as an interacting partner alongside other cytoskeleton proteins, for example ABP280 (filamin) and RanBPM (Ran-binding protein in the microtubule-organizing center) (Chang and Wang, 2006). Fascin is an actin-bundling protein which is absent from normal colorectal epithelial cells but shows significant cytoplasmic subcellular distribution when these become neoplastic. Since it is upregulated in benign adenomas and promotes motility in adenoma cells *in vitro*, fascin is implicated as an early biomarker for more aggressive colorectal adenocarcinomas (Hashimoto et al., 2006, Qualtrough et al., 2009). It would be interesting to establish whether these two proteins cooperate in colorectal tumours and whether there is any functional significance in this interaction for tumour invasion and metastasis.

In summary, eEF1A2 was expressed in a large proportion of colorectal tumours (43%) at a moderate to high level but no obvious upregulation of this elongation factor was observed among cutaneous and hepatocellular malignancies. In contrast, eEF1A1 expression remained near constant in colorectal, skin and liver cancers when compared with normal tissue counterparts.

Chapter 6: General discussion

6.1 Summary of results

Protein synthesis is crucial for the proper functioning of cells and alterations in the activity and control of translational machinery have been implicated in multiple diseases, including cancer (Le Quesne at al., 2009). Eukaryotic translation elongation factor 1A is responsible for the delivery of the aa-tRNA to the A-site of the ribosome upon guanine nucleotide exchange but apart from its obvious role in protein synthesis, it has been linked to other cellular processes. During the last decade, eEF1A2 has been implicated as an oncogene (Anand et al., 2002). Despite numerous studies on the role and expression status of eEF1A2 in tumourigenesis, the precise mechanism responsible for oncogenicity remains unknown. Furthermore, there is currently no detailed information about any contribution of eEF1A1 to cancer progression. The main objectives of this project were to compare the significance of both eEF1A forms in oncogenesis, and to establish their distribution in cancer types in which eEF1A expression has not previously been investigated in detail.

In order to look at eEF1A1 and eEF1A2 properties in cells, constructs carrying each variant coding sequence with or without its own 5'UTR, and each variant with the 5'UTR from the other eEF1A form, were introduced to NIH-3T3 fibroblasts either transiently or constitutively. The data from transient experiments revealed that incorporation of human eEF1A1 and eEF1A2 led to a decrease in endogenous eEF1A1 expression at the mRNA and protein level. A more substantial decline was seen when any of the 5'UTR was present. Dynamic interplay between eEF1A forms was identified within the first 24 hours after transfection but once the expression of the exogenous variants started to decrease, endogenous eEF1A1 returned to the same level as that seen in controls. In almost all stable cell lines, the levels of endogenous eEF1A1 remained roughly the same, at both the mRNA and protein level, as in control clones. Overall, cellular levels of eEF1A1 appear to be subjected to tight regulation.

Stable cell lines which were generated in this thesis were subjected to various *in vitro* tumourigenicity assays. NIH-3T3 cells developed neoplastic transformation upon ectopic expression of eEF1A1 by producing foci and gaining anchorage-independent growth in soft agar. They did not, however, show any substantial increase in proliferation. The incorporation of chimeric 5'UTRs into the eEF1A1 construct almost completely abolished clonogenicity in soft agar and reduced foci formation, even though these lines displayed increased proliferation rates. On the other hand, forced expression of eEF1A2 into mouse fibroblasts resulted in the most aggressive phenotype and heightened proliferation. Significantly lowered transforming capacity was seen in eEF1A2 clones with the addition of any of the 5'UTRs, but it did not result in the full annulment of the neoplastic phenotype. The 5'UTR from eEF1A2 appeared to influence cellular proliferation and clones with its addition were characterised by a higher growth rate than clones carrying constructs with the 5'UTR derived from eEF1A1. With the exception of a few clones, there was no apparent increase in migration and invasion of the cell lines stably expressing eEF1A. Increased levels of overall eEF1A protein in different stable cell lines appeared to correlate only partially with elevated protein synthesis rate but not with transformed phenotype. Therefore, another mechanism than eEF1A-mediated increase in protein synthesis might be responsible for driving oncogenesis. Alterations in phosphorylation of either eEF1A1 or eEF1A2 are an attractive possibility linking eEF1A and tumourigenesis (Soares et al., 2009, Lin at al., 2010).

In this study, moderate to high expression of eEF1A2 protein was observed in 43% of colorectal cancers analysed. In one of the colorectal tumour arrays, the level of eEF1A2 expression appeared to be inversely correlated ($P = 0.024$) with metastasis in lymph nodes. Furthermore, no substantial upregulation of eEF1A2 at the protein level was seen in hepatocellular carcinoma and malignant melanoma arrays. In contrast, eEF1A1 protein expression was mostly weak or absent in these malignancies.

6.2 Future work

6.2.1 The role of eEF1A in oncogenesis

More extensive analyses are necessary to shed light on mechanisms by which eEF1A1 and eEF1A2 could act as oncogenes. As the data from studies on translation rates in stable cell lines were variable, it is necessary to repeat these experiments. In addition, HCT116 colorectal cancer cell lines (which express both eEF1A forms) with constitutive knockdowns of eEF1A1 and eEF1A2 are available in the laboratory. They could be used to determine whether lowered expression of any eEF1A variant is sufficient to abolish the transformed phenotype and whether there is any effect on overall protein synthesis rate. Methods described within this thesis could be performed to verify the above issues.

Moreover, the A2 stable cell lines described herein were subjected to analysis using mouse whole-genome expression microarrays by fellow PhD student Mariam Fida. She investigated changes in gene expression which occur when eEF1A2 is constantly upregulated and searched for candidates correlating with human tumourigenesis. Several plausible candidates were indentified, including *Srpx2* (Sushi repeat containing protein, X-linked 2) and *Tpd52* (tumour protein D52) genes which were upregulated by more than 2-fold, whereas *Rhox5* (reproductive homeobox on the X chromosome 5) was lowered almost 5-fold. *SRPX2* is overexpressed in human gastric cancer cells and is associated with enhanced cellular motility and adhesion (Tanaka et al., 2009). *TPD52* is upregulated in many cancers and when it is ectopically overexpressed in mouse fibroblasts, a neoplastic phenotype and progression to metastasis were observed (Lewis at al., 2007). *RHOX5* was reported to be upregulated by therapeutic epigenetic drugs in breast and colon cancer cells (Li et al., 2009). It would be of interest to look whether changes at the mRNA level reflect alterations at the protein levels, for example using stable isotope labelling by amino acids in cell culture (SILAC) approach (Ong et al., 2002). It could be also verified at the RNA and protein level whether similar changes in expression of the above

candidates are seen in eEF1A2-transiently transfected cells. Some of these experiments are currently in progress (Mariam Fida). If alterations in plausible candidates expression are not observed in transient experiments but indeed, only in A2 stable cell lines, then perhaps eEF1A2 upregulation has more long-term impact on these candidates and inappropriately expressed eEF1A2 is a prerequisite for the sequence of events which lead to tumour development. If so, then it is interesting to test whether these proteins could interact directly or indirectly with eEF1A2 *in vitro* and *in vivo* using yeast two-hybrid and co-localisation approaches. In case where interaction with eEF1A2 is confirmed, it would be essential to look if transformed phenotype is affected. The experiments would involve searching for cell lines with high and low levels of candidates and eEF1A2 in order to create stable double knockdowns and double overexpressions. Stable cell lines would be then tested for response to apoptosis, rates of proliferation, alterations in neoplastic phenotype along with migration and invasion.

6.2.2 The mechanism responsible for eEF1A2 oncogenicity

The precise mechanism by which eEF1A2 becomes upregulated in different tumours remains unclear but perhaps looking into any differences in the phosphorylation status between tumour and normal tissues would give some clues. Two serine residues (Ser358 and Ser393) appear to be attractive candidates for such modification, especially as they are strictly conserved in other species that express eEF1A2 and because these are equally well conserved as alanine and phenylalanine in eEF1A1 (Soares et al., 2009). Phosphorylation of these sites could be confirmed by mass spectrometry and specific phospho-antibodies could also be raised to investigate any possible association with tumourigenesis. If there is any difference in phosphorylation pattern at these residues between normal and cancer cells, phosphorylation mimics could be created through mutagenesis of serines to aspartic acid, glutamic acid and also to the non-phosphorylatable equivalent residues of eEF1A1. Such generated cell lines could be subsequently tested in a repertoire of transformation assays as described herein. It would

be also informative to determine whether eEF1A2 was phosphorylated at these candidate residues in the neoplastic stable cell lines described in this thesis.

Potentially, any differences in the phosphorylation pattern between eEF1A forms might shed some light into their oncogenic capacity. Threonines at positions 217 and 227 are eEF1A1-specific candidate residues for phosphorylation (Soares et al, 2009). In order to address these questions, similar experiments could be executed as described above for the eEF1A2 variant. In addition, to gain more knowledge about the phosphorylation status of eEF1A1, it would be interesting to check the phosphorylation of serine at residue 300 in transformed eEF1A1 stable cell lines and different tumours or cancer cell lines. Lin *et al.* observed that TβR-I (transforming growth factor β type I receptor)-mediated phosphorylation of eEF1A1 at Ser300 is associated with inhibition of protein synthesis and proliferation. Phosphorylation of Ser300 was also decreased in human breast tumours (Lin et al., 2010). It is noteworthy that this serine position and the surrounding amino acids are exactly the same in both eEF1A1 and eEF1A2 sequence. Hence, it should be determined whether a similar functional significance is true for eEF1A2, but as the amino acid context is identical, it becomes more difficult to track the biological meaning for eEF1A variants independently. Cell lines with mimicked versions of candidate phosphorylation sites in eEF1A1 and eEF1A2 need to be tested for possible alterations in protein synthesis rates.

Currently many studies of the development of different tumours show alterations in the microRNA expression pattern between normal and cancer tissues. Therefore, significant upregulation of eEF1A2 in cancer could be mediated by the inappropriate expression of specific microRNAs, and candidates discussed in Chapters 1 and 5 would be the obvious choices to investigate. This would initially involve looking into the correlation between expression levels of eEF1A2 and let-7f or miR-663 in normal and tumour cell lines of different origins using real-time PCR. Plausible candidates could be then either overexpressed or downregulated using precursor molecules or inhibitors to see if they trigger any differences in eEF1A2 expression at the mRNA and protein level. It cannot be ruled out that a microRNA-mediated effect on eEF1A2 abundance is driven indirectly, therefore using

co-transfections of precursors or inhibitors with expression vectors containing a reporter linked to the 3'UTR (and 5'UTR for experiments with miR-663) from eEF1A2 could shed some light on this.

Ultimately, if there is no correlation between eEF1A2 upregulation and these candidates, microRNA microarrays could be applied to cell lines with eEF1A2 knock down and overexpression to search for new candidates for eEF1A2 control.

6.2.3 Expression of eEF1A in colon, liver and skin cancer

Immunohistochemical analysis of eEF1A2 expression in colorectal tumours suggests it could be a useful biomarker in this malignancy. Expanding these studies to a larger number of tumour samples and to the relationships between levels of protein expression and histopathological variables would give more insight into the role of eEF1A2 in colon cancer. Professor David Harrison has established a library of several hundred clinical samples of colorectal carcinoma cases, supported with clinical features and follow up history. eEF1A2 expression could be therefore monitored on a large scale at the protein and mRNA levels and survival prognosis could be established. As studies in the normal colon show that eEF1A2 is present in single cells of colonic crypts, it is intriguing how this expression pattern changes and expands in colorectal tumours. Hence, it is necessary to test the expression status of eEF1A2 at different stages of this cancer development to establish the exact point at which eEF1A2 becomes inappropriately expressed. Moreover, this study showed that there was no significant upregulation of eEF1A2 in hepatocellular carcinoma and melanoma cases. Consequently, it would be interesting to test what exactly happens with eEF1A2 in liver and skin cancers that makes it of less importance in these particular malignancies. It would require to screen for any changes in eEF1A2 expression at the mRNA level and to look into gene amplification status, methylation status or any mutations of eEF1A2 in tumour samples and corresponding tumour cell lines. Are there any direct inhibitors of eEF1A2 upregulation in these malignancies? Is there only one dominant mechanism or is it rather a multilayered deregulation that drives the oncogenicity of eEF1A2 in

different tumours? Are these mechanisms cancer type specific and do they depend on genetic background? These questions remain open for further investigation.

These studies have to be simultaneously expanded to eEF1A1 expression in more cases of colon, skin and liver tumours in order to determine whether eEF1A1 remains truly unchanged at the mRNA and protein level. If so, it is necessary to investigate what mechanism could be responsible for such an effect. Using real-time PCR and Western blotting would help to establish whether this level is quantitatively comparable to that seen in the corresponding normal tissues as, for example, liver is an organ with a very high abundance of eEF1A1. On the other hand, what is the biological significance of eEF1A1 if it is only slightly upregulated as shown in several tumour cases within this study? As eEF1A1 is implicated in pro-apoptotic functioning, is this some sort of a defence mechanism that is induced to protect this organ from cancer? Answers to these questions remain unknown.

6.3 Concluding remarks

This study provides further insight into how eEF1A1 and eEF1A2 function in transformation, looks into the relationship between eEF1A and translation and cancer, elucidates the expression status of eEF1A proteins in certain tumours, and for the first time, shows that eEF1A1 can act as an oncogene under certain circumstances. Undoubtedly, further investigation is necessary to determine the specific mechanism by which eEF1A2 is upregulated and linked to development of various neoplasms. More work is also required to establish to what extent a vast repertoire of non-canonical functions is shared between eEF1A variants and whether these functions have any significance in oncogenesis.

References

ABRAMOFF, M. D., MAGELHAES, P. J. & RAM, S. J. 2004. Image Processing with ImageJ. *Biophotonics International,* 11**,** 36-42.

ALBINI, A., IWAMOTO, Y., KLEINMAN, H. K., MARTIN, G. R., AARONSON, S. A., KOZLOWSKI, J. M. & MCEWAN, R. N. 1987. A rapid in vitro assay for quantitating the invasive potential of tumor cells. *Cancer Res,* 47**,** 3239-45.

ALON, U., BARKAI, N., NOTTERMAN, D. A., GISH, K., YBARRA, S., MACK, D. & LEVINE, A. J. 1999. Broad patterns of gene expression revealed by clustering analysis of tumor and normal colon tissues probed by oligonucleotide arrays. *Proc Natl Acad Sci U S A,* 96**,** 6745-50.

AMERICAN CANCER SOCIETY. Cancer facts and figures 2010. Atlanta: American Cancer Society 2010.

AMIRI, A., NOEI, F., JEGANATHAN, S., KULKARNI, G., PINKE, D. E. & LEE, J. M. 2006. eEF1A2 activates Akt and stimulates Akt-dependent actin remodeling, invasion and migration. *Oncogene,* 26**,** 3027-40.

ANAND, N., MURTHY, S., AMANN, G., WERNICK, M., PORTER, L. A., CUKIER, I. H., COLLINS, C., GRAY, J. W., DIEBOLD, J., DEMETRICK, D. J. & LEE, J. M. 2002. Gene encoding protein elongation factor EEF1A2 is a putative oncogene in ovarian cancer. *Nature Genetics,* 31**,** 301-305.

ANDERSEN, G. R., PEDERSEN, L., VALENTE, L., CHATTERJEE, I., KINZY, T. G., KJELDGAARD, M. & NYBORG, J. 2000. Structural basis for nucleotide exchange and competition with tRNA in the yeast elongation factor complex eEF1A:eEF1Balpha. *Mol Cell,* 6**,** 1261-6.

ANDERSEN, G. R., VALENTE, L., PEDERSEN, L., KINZY, T. G. & NYBORG, J. 2001. Crystal structures of nucleotide exchange intermediates in the eEF1A-eEF1Balpha complex. *Nat Struct Biol,* 8**,** 531-4.

ANDERSEN, K. M., MADSEN, L., PRAG, S., JOHNSEN, A. H., SEMPLE, C. A., HENDIL, K. B. & HARTMANN-PETERSEN, R. 2009. Thioredoxin Txnl1/TRP32 is a redox-active cofactor of the 26 S proteasome. *J Biol Chem,* 284**,** 15246-54.

ANN, D. K., LIN, H. H., LEE, S., TU, Z. J. & WANG, E. 1992. Characterization of the statin-like S1 and rat elongation factor 1 alpha as two distinctly expressed messages in rat. *J Biol Chem,* 267**,** 699-702.

ANN, D. K., MOUTSATSOS, I. K., NAKAMURA, T., LIN, H. H., MAO, P. L., LEE, M. J., CHIN, S., LIEM, R. K. & WANG, E. 1991. Isolation and characterization of the rat chromosomal gene for a polypeptide (pS1) antigenically related to statin. *J Biol Chem,* 266**,** 10429-37.

ARAVALLI, R. N., STEER, C. J. & CRESSMAN, E. N. 2008. Molecular mechanisms of hepatocellular carcinoma. *Hepatology,* 48**,** 2047-63.

AUST, D. E., MUDERS, M., KOHLER, A., SCHMIDT, M., DIEBOLD, J., MULLER, C., LOHRS, U., WALDMAN, F. M. & BARETTON, G. B. 2004. Prognostic relevance of 20q13 gains in sporadic colorectal cancers: a FISH analysis. *Scand J Gastroenterol,* 39**,** 766-72.

AVNI, D., BIBERMAN, Y. & MEYUHAS, O. 1997. The 5' terminal oligopyrimidine tract confers translational control on TOP mRNAs in a cell type- and sequence context-dependent manner. *Nucleic Acids Res,* 25**,** 995-1001.

AVNI, D., SHAMA, S., LORENI, F. & MEYUHAS, O. 1994. Vertebrate mRNAs with a 5'-terminal pyrimidine tract are candidates for translational repression in quiescent cells: characterization of the translational cis-regulatory element. *Mol Cell Biol,* 14**,** 3822-33.

BAG, J. 2001. Feedback inhibition of poly(A)-binding protein mRNA translation. A possible mechanism of translation arrest by stalled 40 S ribosomal subunits. *J Biol Chem,* 276**,** 47352-60.

BALMANA, J., CASTELLS, A. & CERVANTES, A. 2010. Familial colorectal cancer risk: ESMO Clinical Practice Guidelines. *Ann Oncol,* 21 Suppl 5**,** v78-81.

BASSELL, G. J., POWERS, C. M., TANEJA, K. L. & SINGER, R. H. 1994. Single mRNAs visualized by ultrastructural in situ hybridization are principally localized at actin filament intersections in fibroblasts. *J Cell Biol,* 126**,** 863-76.

BATULAN, Z., SHINDER, G. A., MINOTTI, S., HE, B. P., DOROUDCHI, M. M., NALBANTOGLU, J., STRONG, M. J. & DURHAM, H. D. 2003. High threshold for induction of the stress response in motor neurons is associated with failure to activate HSF1. *J Neurosci,* 23**,** 5789-98.

BISCHOFF, C., KAHNS, S., LUND, A., JORGENSEN, H. F., PRAESTEGAARD, M., CLARK, B. F. & LEFFERS, H. 2000. The human elongation factor 1 A-2 gene (EEF1A2): complete sequence and characterization of gene structure and promoter activity. *Genomics,* 68**,** 63-70.

BLAIR, D. G., COOPER, C. S., OSKARSSON, M. K., EADER, L. A. & VANDE WOUDE, G. F. 1983. Tumorigenesis by transected cells in nude mice: a new method for detecting cellular transforming genes. *Prog Clin Biol Res,* 119**,** 79-90.

BOARDMAN, P. E., SANZ-EZQUERRO, J., OVERTON, I. M., BURT, D. W., BOSCH, E., FONG, W. T., TICKLE, C., BROWN, W. R., WILSON, S. A. & HUBBARD, S. J. 2002. A comprehensive collection of chicken cDNAs. *Curr Biol,* 12**,** 1965-9.

BOHNSACK, M. T., REGENER, K., SCHWAPPACH, B., SAFFRICH, R., PARASKEVA, E., HARTMANN, E. & GORLICH, D. 2002. Exp5 exports eEF1A via tRNA from nuclei and synergizes with other transport pathways to confine translation to the cytoplasm. *EMBO J,* 21**,** 6205-15.

BOLAND, C. R. & GOEL, A. 2010. Microsatellite instability in colorectal cancer. *Gastroenterology,* 138**,** 2073-2087 e3.

BOYAULT, S.,RICKMAN, D.S., de REYNIES, A., BALABAUD, C., REBOUISSOU, S., JEANNOT, E., HERAULT, A., SARIC, J., BELGHITI, J., FRANCO, D., BIOULAC-SAGE, P., LAURENT-PUIG, P., ZUCMAN-ROSSI, J. 2007. Transcriptome classification of HCC is related to gene alterations and to new therapeutic targets. *Hepatology*, 45, 42-52.

BRAAKHUIS, B. J., TABOR, M. P., KUMMER, J. A., LEEMANS, C. R. & BRAKENHOFF, R. H. 2003. A genetic explanation of Slaughter's concept of field cancerization: evidence and clinical implications. *Cancer Res,* 63**,** 1727-30.

BREKHMAN, V. & NEUFELD, G. 2009. A novel asymmetric 3D in-vitro assay for the study of tumor cell invasion. *BMC Cancer,* 9**,** 415.

BUNNEY, T. D. & KATAN, M. 2010. Phosphoinositide signalling in cancer: beyond PI3K and PTEN. *Nat Rev Cancer,* 10**,** 342-52.

CALADO, A., TREICHEL, N., MULLER, E. C., OTTO, A. & KUTAY, U. 2002. Exportin-5-mediated nuclear export of eukaryotic elongation factor 1A and tRNA. *EMBO J,* 21**,** 6216-24.

CALDAROLA, S., AMALDI, F., PROUD, C. G. & LORENI, F. 2004. Translational regulation of terminal oligopyrimidine mRNAs induced by serum and amino acids involves distinct signaling events. *J Biol Chem,* 279**,** 13522-31.

CALDERWOOD, S. K., KHALEQUE, M. A., SAWYER, D. B. & CIOCCA, D. R. 2006. Heat shock proteins in cancer: chaperones of tumorigenesis. *Trends Biochem Sci,* 31**,** 164-72.

CANS, C., PASSER, B. J., SHALAK, V., NANCY-PORTEBOIS, V., CRIBLE, V., AMZALLAG, N., ALLANIC, D., TUFINO, R., ARGENTINI, M., MORAS, D., FIUCCI, G., GOUD, B., MIRANDE, M., AMSON, R. & TELERMAN, A. 2003. Translationally controlled tumor protein acts as a guanine nucleotide dissociation inhibitor on the translation elongation factor eEF1A. *Proc Natl Acad Sci U S A,* 100**,** 13892-7.

CAO, H., ZHU, Q., HUANG, J., LI, B., ZHANG, S., YAO, W. & ZHANG, Y. 2009. Regulation and functional role of eEF1A2 in pancreatic carcinoma. *Biochem Biophys Res Commun,* 380**,** 11-6.

CARNEIRO, N. P., HUGHES, P. A. & LARKINS, B. A. 1999. The eEFIA gene family is differentially expressed in maize endosperm. *Plant Mol Biol,* 41**,** 801-13.

CARR-SCHMID, A., VALENTE, L., LOIK, V. I., WILLIAMS, T., STARITA, L. M. & KINZY, T. G. 1999. Mutations in elongation factor 1beta, a guanine nucleotide exchange factor, enhance translational fidelity. *Mol Cell Biol,* 19**,** 5257-66.

CHAMBERS, D. M., PETERS, J. & ABBOTT, C. M. 1998. The lethal mutation of the mouse wasted (wst) is a deletion that abolishes expression of a tissue-specific isoform of translation elongation factor 1alpha, encoded by the Eef1a2 gene. *Proc Natl Acad Sci U S A,* 95**,** 4463-8.

CHANG, R. & WANG, E. 2007. Mouse translation elongation factor eEF1A-2 interacts with Prdx-I to protect cells against apoptotic death induced by oxidative stress. *J Cell Biochem,* 100**,** 267-78.

CHEKULAEVA, M. & FILIPOWICZ, W. 2009. Mechanisms of miRNA-mediated post-transcriptional regulation in animal cells. *Curr Opin Cell Biol,* 21**,** 452-60.

CHEN, E., PROESTOU, G., BOURBEAU, D. & WANG, E. 2000. Rapid up-regulation of peptide elongation factor EF-1alpha protein levels is an immediate early event during oxidative stress-induced apoptosis. *Exp Cell Res,* 259**,** 140-8.

CHODNIEWICZ, D. & KLEMKE, R. L. 2004. Guiding cell migration through directed extension and stabilization of pseudopodia. *Exp Cell Res,* 301**,** 31-7.

CHUANG, S. M., CHEN, L., LAMBERTSON, D., ANAND, M., KINZY, T. G. & MADURA, K. 2005. Proteasome-mediated degradation of cotranslationally damaged proteins involves translation elongation factor 1A. *Mol Cell Biol,* 25**,** 403-13.

CIOCCA, D. R. & CALDERWOOD, S. K. 2005. Heat shock proteins in cancer: diagnostic, prognostic, predictive, and treatment implications. *Cell Stress Chaperones,* 10**,** 86-103.

CONDEELIS, J. 1995. Elongation factor 1 alpha, translation and the cytoskeleton. *Trends Biochem Sci,* 20**,** 169-70.

CREW, J. P., FUGGLE, S., BICKNELL, R., CRANSTON, D. W., DE BENEDETTI, A. & HARRIS, A. L. 2000. Eukaryotic initiation factor-4E in superficial and muscle invasive bladder cancer and its correlation with vascular endothelial growth factor expression and tumour progression. *Br J Cancer,* 82**,** 161-6.

CRICK, F. 1970. Central dogma of molecular biology. *Nature,* 227**,** 561-3.

CUMMINS, D. L., CUMMINS, J. M., PANTLE, H., SILVERMAN, M. A., LEONARD, A. L. & CHANMUGAM, A. 2006a. Cutaneous malignant melanoma. *Mayo Clin Proc,* 81**,** 500-7.

CUMMINS, J. M., HE, Y., LEARY, R. J., PAGLIARINI, R., DIAZ, L. A., SJOBLOM, T., BARAD, O., BENTWICH, Z., SZAFRANSKA, A. E., LABOURIER, E., RAYMOND, C. K., ROBERTS, B. S., JUHL, H., KINZLER, K. W., VOGELSTEIN, B. & VELCULESCU, V. E. 2006b. The colorectal microRNAome. *Proc Natl Acad Sci U S A,* 103, 3687-92.

DAHIYA, N., SHERMAN-BAUST, C. A., WANG, T. L., DAVIDSON, B., SHIH IE, M., ZHANG, Y., WOOD, W., 3RD, BECKER, K. G. & MORIN, P. J. 2008. MicroRNA expression and identification of putative miRNA targets in ovarian cancer. *PLoS One,* 3**,** e2436.

DAKUBO, G. D., JAKUPCIAK, J. P., BIRCH-MACHIN, M. A. & PARR, R. L. 2007. Clinical implications and utility of field cancerization. *Cancer Cell Int,* 7**,** 2.

DE MOOR, C. H., MEIJER, H. & LISSENDEN, S. 2005. Mechanisms of translational control by the 3' UTR in development and differentiation. *Semin Cell Dev Biol,* 16**,** 49-58.

DE WIT, N. J., BURTSCHER, H. J., WEIDLE, U. H., RUITER, D. J. & VAN MUIJEN, G. N. 2002. Differentially expressed genes identified in human melanoma cell lines with different metastatic behaviour using high density oligonucleotide arrays. *Melanoma Res,* 12**,** 57-69.

DEMMA, M., WARREN, V., HOCK, R., DHARMAWARDHANE, S. & CONDEELIS, J. 1990. Isolation of an abundant 50,000-dalton actin filament bundling protein from Dictyostelium amoebae. *J Biol Chem,* 265**,** 2286-91.

DEVER, T. E., COSTELLO, C. E., OWENS, C. L., ROSENBERRY, T. L. & MERRICK, W. C. 1989. Location of seven post-translational modifications in rabbit elongation factor 1 alpha including dimethyllysine, trimethyllysine, and glycerylphosphorylethanolamine. *J Biol Chem,* 264**,** 20518-25.

DEVER, T. E., GLYNIAS, M. J. & MERRICK, W. C. 1987. GTP-binding domain: three consensus sequence elements with distinct spacing. *Proc Natl Acad Sci U S A,* 84**,** 1814-8.
DHARMAWARDHANE, S., DEMMA, M., YANG, F. & CONDEELIS, J. 1991. Compartmentalization and actin binding properties of ABP-50: the elongation factor-1 alpha of Dictyostelium. *Cell Motil Cytoskeleton,* 20**,** 279-88.

DJE, M. K., MAZABRAUD, A., VIEL, A., LE MAIRE, M., DENIS, H., CRAWFORD, E. & BROWN, D. D. 1990. Three genes under different developmental control encode elongation factor 1-alpha in Xenopus laevis. *Nucleic Acids Res,* 18**,** 3489-93.

DONG, H., GE, X., SHEN, Y., CHEN, L., KONG, Y., ZHANG, H., MAN, X., TANG, L., YUAN, H., WANG, H., ZHAO, G. & JIN, W. 2009. Gene expression profile analysis of human hepatocellular carcinoma using SAGE and LongSAGE. *BMC Med Genomics,* 2**,** 5.

DONG, X. Y., RODRIGUEZ, C., GUO, P., SUN, X., TALBOT, J. T., ZHOU, W., PETROS, J., LI, Q., VESSELLA, R. L., KIBEL, A. S., STEVENS, V. L., CALLE, E. E. & DONG, J. T. 2008. SnoRNA U50 is a candidate tumor-suppressor gene at 6q14.3 with a mutation associated with clinically significant prostate cancer. *Hum Mol Genet,* 17**,** 1031-42.

DONZE, O., JAGUS, R., KOROMILAS, A. E., HERSHEY, J. W. & SONENBERG, N. 1995. Abrogation of translation initiation factor eIF-2 phosphorylation causes malignant transformation of NIH 3T3 cells. *Embo J,* 14**,** 3828-34.

DURSO, N. A. & CYR, R. J. 1994. A calmodulin-sensitive interaction between microtubules and a higher plant homolog of elongation factor-1 alpha. *Plant Cell,* 6**,** 893-905.

DUTTAROY, A., BOURBEAU, D., WANG, X. L. & WANG, E. 1998. Apoptosis rate can be accelerated or decelerated by overexpression or reduction of the level of elongation factor-1 alpha. *Exp Cell Res,* 238**,** 168-76.

ECKHARDT, K., TROGER, J., REISSMANN, J., KATSCHINSKI, D. M., WAGNER, K. F., STENGEL, P., PAASCH, U., HUNZIKER, P., BORTER, E., BARTH, S., SCHLAFLI, P., SPIELMANN, P., STIEHL, D. P., CAMENISCH, G. & WENGER, R. H. 2007. Male germ cell expression of the PAS domain kinase PASKIN and its novel target eukaryotic translation elongation factor eEF1A1. *Cell Physiol Biochem,* 20**,** 227-40.

EDMONDS, B. T., MURRAY, J. & CONDEELIS, J. 1995. pH regulation of the F-actin binding properties of Dictyostelium elongation factor 1 alpha. *J Biol Chem,* 270**,** 15222-30.

EDMONDS, B. T., WYCKOFF, J., YEUNG, Y. G., WANG, Y., STANLEY, E. R., JONES, J., SEGALL, J. & CONDEELIS, J. 1996. Elongation factor-1 alpha is an overexpressed actin binding protein in metastatic rat mammary adenocarcinoma. *J Cell Sci,* 109 (Pt 11)**,** 2705-14.

EJIRI, S.-I. 2002. Moonlighting functions of polypeptide elongation factor 1: from actin bundling to zinc finger protein R1- associated nuclear localization. *Biosci. Biotechnol. Biochem.,* 66**,** 1-21.

ESQUELA-KERSCHER, A. & SLACK, F. J. 2006. Oncomirs - microRNAs with a role in cancer. *Nat Rev Cancer,* 6**,** 259-69.

FARAZI, P. A. & DEPINHO, R. A. 2006. Hepatocellular carcinoma pathogenesis: from genes to environment. *Nat Rev Cancer,* 6**,** 674-87.

FECHER, L. A., CUMMINGS, S. D., KEEFE, M. J. & ALANI, R. M. 2007. Toward a molecular classification of melanoma. *J Clin Oncol,* 25**,** 1606-20.

FERLAY, J., PARKIN, D. M. & STELIAROVA-FOUCHER, E. 2010a. Estimates of cancer incidence and mortality in Europe in 2008. *Eur J Cancer,* 46**,** 765-81.

FERLAY, J., SHIN, H. R., BRAY, F., FORMAN, D., MATHERS, C. & PARKIN, D. M. 2010b. Estimates of worldwide burden of cancer in 2008: GLOBOCAN 2008. *Int J Cancer* (ahead of print).

FRAZIER, M. L., INAMDAR, N., ALVULA, S., WU, E. & KIM, Y. H. 1998. Few point mutations in elongation factor-1gamma gene in gastrointestinal carcinoma. *Mol Carcinog,* 22**,** 9-15.

GOLDSTEIN, B. G. & GOLDSTEIN, A. O. 2001. Diagnosis and management of malignant melanoma. *Am Fam Physician,* 63**,** 1359-68, 1374.

GONEN, H., SMITH, C. E., SIEGEL, N. R., KAHANA, C., MERRICK, W. C., CHAKRABURTTY, K., SCHWARTZ, A. L. & CIECHANOVER, A. 1994. Protein synthesis elongation factor EF-1 alpha is essential for ubiquitin-dependent degradation of certain N alpha-acetylated proteins and may be substituted for by the bacterial elongation factor EF-Tu. *Proc Natl Acad Sci U S A,* 91**,** 7648-52.

GRANT, A. G., FLOMEN, R. M., TIZARD, M. L. & GRANT, D. A. 1992. Differential screening of a human pancreatic adenocarcinoma lambda gt11 expression library has identified increased transcription of elongation factor EF-1 alpha in tumour cells. *Int J Cancer,* 50**,** 740-5.

GRASSI, G., SCAGGIANTE, B., FARRA, R., DAPAS, B., AGOSTINI, F., BAIZ, D., ROSSO, N. & TIRIBELLI, C. 2007. The expression levels of the translational factors eEF1A 1/2 correlate with cell growth but not apoptosis in hepatocellular carcinoma cell lines with different differentiation grade. *Biochimie,* 89**,** 1544-52.

GROSS, S. R. & KINZY, T. G. 2005. Translation elongation factor 1A is essential for regulation of the actin cytoskeleton and cell morphology. *Nat Struct Mol Biol,* 12**,** 772-8.

GROSS, S. R. & KINZY, T. G. 2007. Improper organization of the actin cytoskeleton affects protein synthesis at initiation. *Mol Cell Biol,* 27**,** 1974-89.

GROSSHANS, H., HURT, E. & SIMOS, G. 2000. An aminoacylation-dependent nuclear tRNA export pathway in yeast. *Genes Dev,* 14**,** 830-40.

HARRIS, M. N., OZPOLAT, B., ABDI, F., GU, S., LEGLER, A., MAWUENYEGA, K. G., TIRADO-GOMEZ, M., LOPEZ-BERESTEIN, G. & CHEN, X. 2004. Comparative proteomic analysis of all-trans-retinoic acid treatment reveals systematic posttranscriptional control mechanisms in acute promyelocytic leukemia. *Blood,* 104**,** 1314-23.

HASHIMOTO, Y., SKACEL, M., LAVERY, I. C., MUKHERJEE, A. L., CASEY, G. & ADAMS, J. C. 2006. Prognostic significance of fascin expression in advanced colorectal cancer: an immunohistochemical study of colorectal adenomas and adenocarcinomas. *BMC Cancer*. 6, 241-51.

HERSHEY, J. W. 1991. Translational control in mammalian cells. *Annu Rev Biochem,* 60**,** 717-55.

HORNSTEIN, E., GIT, A., BRAUNSTEIN, I., AVNI, D. & MEYUHAS, O. 1999. The expression of poly(A)-binding protein gene is translationally regulated in a growth-dependent fashion through a 5'-terminal oligopyrimidine tract motif. *J Biol Chem,* 274**,** 1708-14.

HORNSTEIN, E., TANG, H. & MEYUHAS, O. 2001. Mitogenic and nutritional signals are transduced into translational efficiency of TOP mRNAs. *Cold Spring Harb Symp Quant Biol,* 66**,** 477-84.

HOUGHTON, A. N. & POLSKY, D. 2002. Focus on melanoma. *Cancer Cell,* 2**,** 275-8.

HOVEMANN, B., RICHTER, S., WALLDORF, U. & CZIEPLUCH, C. 1988. Two genes encode related cytoplasmic elongation factors 1 alpha (EF-1 alpha) in Drosophila melanogaster with continuous and stage specific expression. *Nucleic Acids Res,* 16**,** 3175-94.

IADEVAIA, V., CALDAROLA, S., TINO, E., AMALDI, F. & LORENI, F. 2008. All translation elongation factors and the e, f, and h subunits of translation initiation factor 3 are encoded by 5'-terminal oligopyrimidine (TOP) mRNAs. *Rna,* 14**,** 1730-6.

INFANTE, C., ASENSIO, E., CANAVATE, J. P. & MANCHADO, M. 2008. Molecular characterization and expression analysis of five different elongation factor 1 alpha genes in the flatfish Senegalese sole (Solea senegalensis Kaup): differential gene expression and thyroid hormones dependence during metamorphosis. *BMC Mol Biol,* 9**,** 19.

ISOLA, J. J., KALLIONIEMI, O. P., CHU, L. W., FUQUA, S. A., HILSENBECK, S. G., OSBORNE, C. K. & WALDMAN, F. M. 1995. Genetic aberrations detected by comparative genomic hybridization predict outcome in node-negative breast cancer. *Am J Pathol,* 147**,** 905-11.

JACKSON, R. J., HELLEN, C. U. & PESTOVA, T. V. 2010. The mechanism of eukaryotic translation initiation and principles of its regulation. *Nat Rev Mol Cell Biol,* 11**,** 113-27.

JASKUNAS, S. R., LINDAHL, L. & NOMURA, M. 1975. Identification of two copies of the gene for the elongation factor EF-Tu in E. coli. *Nature,* 257**,** 458-62.

JEFFERIES, H. B., THOMAS, G. & THOMAS, G. 1994. Elongation factor-1 alpha mRNA is selectively translated following mitogenic stimulation. *J Biol Chem,* 269**,** 4367-72.

JEGANATHAN, S. & LEE, J. M. 2007. Binding of elongation factor eEF1A2 to phosphatidylinositol 4-kinase beta stimulates lipid kinase activity and phosphatidylinositol 4-phosphate generation. *J Biol Chem,* 282**,** 372-80.

JEGANATHAN, S., MORROW, A., AMIRI, A. & LEE, J. M. 2008. Eukaryotic elongation factor 1A2 cooperates with phosphatidylinositol-4 kinase III beta to stimulate production of filopodia through increased phosphatidylinositol-4,5 bisphosphate generation. *Mol Cell Biol,* 28**,** 4549-61.

JOHNSSON, A., ZEELENBERG, I., MIN, Y., HILINSKI, J., BERRY, C., HOWELL, S. B. & LOS, G. 2000. Identification of genes differentially expressed in association with acquired cisplatin resistance. *Br J Cancer,* 83**,** 1047-54.

JOSEPH, P., O'KERNICK, C. M., OTHUMPANGAT, S., LEI, Y. X., YUAN, B. Z. & ONG, T. M. 2004. Expression profile of eukaryotic translation factors in human cancer tissues and cell lines. *Mol Carcinog,* 40**,** 171-9.

KAHNS, S., LUND, A., KRISTENSEN, P., KNUDSEN, C. R., CLARK, B. F., CAVALLIUS, J. & MERRICK, W. C. 1998. The elongation factor 1 A-2 isoform from rabbit: cloning of the cDNA and characterization of the protein. *Nucleic Acids Res,* 26**,** 1884-90.

KALLIONIEMI, A., KALLIONIEMI, O. P., PIPER, J., TANNER, M., STOKKE, T., CHEN, L., SMITH, H. S., PINKEL, D., GRAY, J. W. & WALDMAN, F. M. 1994. Detection and mapping of amplified DNA sequences in breast cancer by comparative genomic hybridization. *Proc Natl Acad Sci U S A,* 91**,** 2156-60.

KANDA, A., KAWAI, H., SUTO, S., KITAJIMA, S., SATO, S., TAKATA, T. & TATSUKA, M. 2005. Aurora-B/AIM-1 kinase activity is involved in Ras-mediated cell transformation. *Oncogene,* 24**,** 7266-72.

KATO, M. V., SATO, H., NAGAYOSHI, M. & IKAWA, Y. 1997. Upregulation of the elongation factor-1alpha gene by p53 in association with death of an erythroleukemic cell line. *Blood,* 90**,** 1373-8.

KHACHO, M., MEKHAIL, K., PILON-LAROSE, K., PAUSE, A., COTE, J. & LEE, S. 2008. eEF1A is a novel component of the mammalian nuclear protein export machinery. *Mol Biol Cell,* 19**,** 5296-308.

KHALYFA, A., BOURBEAU, D., CHEN, E., PETROULAKIS, E., PAN, J., XU, S. & WANG, E. 2001. Characterization of elongation factor-1A (eEF1A-1) and eEF1A-2/S1 protein expression in normal and wasted mice. *J Biol Chem,* 276**,** 22915-22.

KIDO, T. & LAU, Y. F. 2008. The human Y-encoded testis-specific protein interacts functionally with eukaryotic translation elongation factor eEF1A, a putative oncoprotein. *Int J Cancer,* 123**,** 1573-85.

KIM, S. & COULOMBE, P. A. 2010. Emerging role for the cytoskeleton as an organizer and regulator of translation. *Nat Rev Mol Cell Biol,* 11**,** 75-81.

KINZLER, K. W. & VOGELSTEIN, B. 1996. Lessons from hereditary colorectal cancer. *Cell,* 87**,** 159-70.

KNUDSEN, S. M., FRYDENBERG, J., CLARK, B. F. & LEFFERS, H. 1993. Tissue-dependent variation in the expression of elongation factor-1 alpha isoforms: isolation and characterisation of a cDNA encoding a novel variant of human elongation-factor 1 alpha. *Eur J Biochem,* 215**,** 549-54.

KOBAYASHI, M., ISHIDA, H., SHINDO, T., NIWA, S., KINO, M., KAWAMURA, K., KAMIYA, N., IMAMOTO, T., SUZUKI, H., HIROKAWA, Y., SHIRAISHI, T., TANIZAWA, T., NAKATANI, Y. & ICHIKAWA, T. 2008. Molecular analysis of multifocal prostate cancer by comparative genomic hybridization. *Prostate,* 68**,** 1715-24.

KOBAYASHI, Y. & YONEHARA, S. 2008. Novel cell death by downregulation of eEF1A1 expression in tetraploids. *Cell Death Differ,* 16**,** 139-150.

KOROMILAS, A. E., LAZARIS-KARATZAS, A. & SONENBERG, N. 1992a. mRNAs containing extensive secondary structure in their 5' non-coding region translate efficiently in cells overexpressing initiation factor eIF-4E. *Embo J,* 11**,** 4153-8.

KOROMILAS, A. E., ROY, S., BARBER, G. N., KATZE, M. G. & SONENBERG, N. 1992b. Malignant transformation by a mutant of the IFN-inducible dsRNA-dependent protein kinase. *Science,* 257**,** 1685-9.

KULKARNI, G., TURBIN, D. A., AMIRI, A., JEGANATHAN, S., ANDRADE-NAVARRO, M. A., WU, T. D., HUNTSMAN, D. G. & LEE, J. M. 2007. Expression of protein elongation factor eEF1A2 predicts favorable outcome in breast cancer. *Breast Cancer Res Treat,* 102**,** 31-41.

KURIYAMA, R., SAVEREIDE, P., LEFEBVRE, P. & DASGUPTA, S. 1990. The predicted amino acid sequence of a centrosphere protein in dividing sea urchin eggs is similar to elongation factor (EF-1 alpha). *J Cell Sci,* 95 (Pt 2)**,** 231-6.

LAM, D. C., GIRARD, L., SUEN, W. S., CHUNG, L. P., TIN, V. P., LAM, W. K., MINNA, J. D. & WONG, M. P. 2006. Establishment and expression profiling of new lung cancer cell lines from Chinese smokers and lifetime never-smokers. *J Thorac Oncol,* 1**,** 932-42.

LAMBERTI, A., LONGO, O., MARRA, M., TAGLIAFERRI, P., BISMUTO, E., FIENGO, A., VISCOMI, C., BUDILLON, A., RAPP, U. R., WANG, E., VENUTA, S., ABBRUZZESE, A., ARCARI, P. & CARAGLIA, M. 2007. C-Raf antagonizes apoptosis induced by IFN-alpha in human lung cancer cells by phosphorylation and increase of the intracellular content of elongation factor 1A. *Cell Death Differ,* 14**,** 952-62.

LAU, J., CASTELLI, L. A., LIN, E. C. & MACAULAY, S. L. 2006. Identification of elongation factor 1alpha as a potential associated binding partner for Akt2. *Mol Cell Biochem,* 286**,** 17-22.

LAZARIS-KARATZAS, A., MONTINE, K. S. & SONENBERG, N. 1990. Malignant transformation by a eukaryotic initiation factor subunit that binds to mRNA 5' cap. *Nature,* 345**,** 544-7.

LE QUESNE, J. P., SPRIGGS, K. A., BUSHELL, M. & WILLIS, A. E. 2009. Dysregulation of protein synthesis and disease. *J Pathol,* 220**,** 140-51.

LEE, I., AJAY, S. S., YOOK, J. I., KIM, H. S., HONG, S. H., KIM, N. H., DHANASEKARAN, S. M., CHINNAIYAN, A. M. & ATHEY, B. D. 2009a. New class of microRNA targets containing simultaneous 5'-UTR and 3'-UTR interaction sites. *Genome Res*, 19, 1175-83.

LEE, J. M. 2003. The role of protein elongation factor eEF1A2 in ovarian cancer. *Reprod Biol Endocrinol,* 1**,** 69.

LEE, M. H., CHOI, B. Y., KUNDU, J. K., SHIN, Y. K., NA, H. K. & SURH, Y. J. 2009b. Resveratrol suppresses growth of human ovarian cancer cells in culture and in a murine xenograft model: eukaryotic elongation factor 1A2 as a potential target. *Cancer Res,* 69**,** 7449-58.

LEE, M. H. & SURH, Y. J. 2009. eEF1A2 as a putative oncogene. *Ann N Y Acad Sci,* 1171**,** 87-93.

LEE, S., ANN, D. K. & WANG, E. 1994. Cloning of human and mouse brain cDNAs coding for S1, the second member of the mammalian elongation factor-1 alpha gene family: analysis of a possible evolutionary pathway. *Biochem Biophys Res Commun,* 203**,** 1371-7.

LEE, S., FRANCOEUR, A. M., LIU, S. & WANG, E. 1992. Tissue-specific expression in mammalian brain, heart, and muscle of S1, a member of the elongation factor-1 alpha gene family. *J Biol Chem,* 267**,** 24064-8.

LEE, S., LEBLANC, A., DUTTAROY, A. & WANG, E. 1995. Terminal differentiation-dependent alteration in the expression of translation elongation factor-1 alpha and its sister gene, S1, in neurons. *Exp Cell Res,* 219**,** 589-97.

LEE, S., STOLLAR, E. & WANG, E. 1993a. Localization of S1 and elongation factor-1 alpha mRNA in rat brain and liver by non-radioactive in situ hybridization. *J Histochem Cytochem,* 41**,** 1093-8.

LEE, S., WOLFRAIM, L. A. & WANG, E. 1993b. Differential expression of S1 and elongation factor-1 alpha during rat development. *J Biol Chem,* 268**,** 24453-9.

LEFEVER, S., VANDESOMPELE, J., SPELEMAN, F. & PATTYN, F. 2009. RTPrimerDB: the portal for real-time PCR primers and probes. *Nucleic Acids Res,* 37**,** D942-5.

LEI, Y. X., CHEN, J. K. & WU, Z. L. 2002. Blocking the translation elongation factor-1 delta with its antisense mRNA results in a significant reversal of its oncogenic potential. *Teratog Carcinog Mutagen,* 22**,** 377-83.

LEVY, S., AVNI, D., HARIHARAN, N., PERRY, R. P. & MEYUHAS, O. 1991. Oligopyrimidine tract at the 5' end of mammalian ribosomal protein mRNAs is required for their translational control. *Proc Natl Acad Sci U S A,* 88**,** 3319-23.

LEWIS, J. D., PAYTON, L. A., WHITFORD, J. G., BYRNE, J. A., SMITH, D. I., YANG, L. & BRIGHT, R. K. 2007. Induction of tumorigenesis and metastasis by the murine orthologue of tumor protein D52. *Mol Cancer Res*, 5, 133-44.

LI, B. D., LIU, L., DAWSON, M. & DE BENEDETTI, A. 1997. Overexpression of eukaryotic initiation factor 4E (eIF4E) in breast carcinoma. *Cancer,* 79**,** 2385-90.

LI, Q., BARTLETT, D. L., GORRY, M. C., O'MALLEY, M. E. & GUO, Z. S. 2009. Three epigenetic drugs up-regulate homeobox gene Rhox5 in cancer cells through overlapping and distinct molecular mechanisms. *Mol Pharmacol*, 76, 1072-81.

LI, R., WANG, H., BEKELE, B. N., YIN, Z., CARAWAY, N. P., KATZ, R. L., STASS, S. A. & JIANG, F. 2006. Identification of putative oncogenes in lung adenocarcinoma by a comprehensive functional genomic approach. *Oncogene,* 25**,** 2628-35.

LI, Z., QI, C. F., SHIN, D. M., ZINGONE, A., NEWBERY, H. J., KOVALCHUK, A. L., ABBOTT, C. M. & MORSE, H. C., 3RD 2010. Eef1a2 promotes cell growth, inhibits apoptosis and activates JAK/STAT and AKT signaling in mouse plasmacytomas. *PLoS One,* 5**,** e10755.

LIN, K. W., YAKYMOVYCH, I., JIA, M., YAKYMOVYCH, M. & SOUCHELNYTSKYI, S. 2010. Phosphorylation of eEF1A1 at Ser300 by TβR-I results in inhibition of mRNA translation. *Curr Biol*, 20, 1615-25.

LIU, G., GRANT, W. M., PERSKY, D., LATHAM, V. M., JR., SINGER, R. H. & CONDEELIS, J. 2002. Interactions of elongation factor 1alpha with F-actin and beta-actin mRNA: implications for anchoring mRNA in cell protrusions. *Mol Biol Cell,* 13**,** 579-92.

LIU, G., TANG, J., EDMONDS, B. T., MURRAY, J., LEVIN, S. & CONDEELIS, J. 1996. F-actin sequesters elongation factor 1alpha from interaction with aminoacyl-tRNA in a pH-dependent reaction. *J Cell Biol,* 135**,** 953-63.

LIU, Y. & WU, F. 2010. Global burden of aflatoxin-induced hepatocellular carcinoma: a risk assessment. *Environ Health Perspect,* 118**,** 818-24.

LIVINGSTONE, M., ATAS, E., MELLER, A. & SONENBERG, N. 2010. Mechanisms governing the control of mRNA translation. *Phys Biol,* 7**,** 021001.

LUND, A., KNUDSEN, S. M., VISSING, H., CLARK, B. & TOMMERUP, N. 1996. Assignment of human elongation factor 1alpha genes: EEF1A maps to chromosome 6q14 and EEF1A2 to 20q13.3. *Genomics,* 36**,** 359-61.

LUND, E., GUTTINGER, S., CALADO, A., DAHLBERG, J. E. & KUTAY, U. 2004. Nuclear export of microRNA precursors. *Science,* 303**,** 95-8.

LUTSEP, H. L. & RODRIGUEZ, M. 1989. Ultrastructural, morphometric, and immunocytochemical study of anterior horn cells in mice with "wasted" mutation. *J Neuropathol Exp Neurol,* 48**,** 519-33.

MADSEN, H. O., POULSEN, K., DAHL, O., CLARK, B. F. & HJORTH, J. P. 1990. Retropseudogenes constitute the major part of the human elongation factor 1 alpha gene family. *Nucleic Acids Res,* 18**,** 1513-6.

MAMANE, Y., PETROULAKIS, E., MARTINEAU, Y., SATO, T. A., LARSSON, O., RAJASEKHAR, V. K. & SONENBERG, N. 2007. Epigenetic activation of a subset of mRNAs by eIF4E explains its effects on cell proliferation. *PLoS One,* 2**,** e242

MANSILLA, F., FRIIS, I., JADIDI, M., NIELSEN, K. M., CLARK, B. F. & KNUDSEN, C. R. 2002. Mapping the human translation elongation factor eEF1H complex using the yeast two-hybrid system. *Biochem J,* 365**,** 669-76.

MARKOWITZ, S. D., DAWSON, D. M., WILLIS, J. & WILLSON, J. K. 2002. Focus on colon cancer. *Cancer Cell,* 1**,** 233-6.

MARSHALL, L., KENNETH, N. S. & WHITE, R. J. 2008. Elevated tRNA(iMet) synthesis can drive cell proliferation and oncogenic transformation. *Cell,* 133**,** 78-89.

MARTELLI, A. M., FAENZA, I., BILLI, A. M., MANZOLI, L., EVANGELISTI, C., FALA, F. & COCCO, L. 2006. Intranuclear 3'-phosphoinositide metabolism and Akt signaling: new mechanisms for tumorigenesis and protection against apoptosis? *Cell Signal,* 18**,** 1101-7.

MATEYAK, M. K. & KINZY, T. G. 2010. eEF1A: thinking outside the ribosome. *J Biol Chem,* 285**,** 21209-13.

MATHUR, S., CLEARY, K. R., INAMDAR, N., KIM, Y. H., STECK, P. & FRAZIER, M. L. 1998. Overexpression of elongation factor-1gamma protein in colorectal carcinoma. *Cancer,* 82**,** 816-21.

MAZUMDER, B., SESHADRI, V. & FOX, P. L. 2003. Translational control by the 3'-UTR: the ends specify the means. *Trends Biochem Sci,* 28**,** 91-8.

MEHTA, A., TROTTA, C. R. & PELTZ, S. W. 2006. Derepression of the Her-2 uORF is mediated by a novel post-transcriptional control mechanism in cancer cells. *Genes Dev,* 20**,** 939-53.

MEYLE, K. D. & GULDBERG, P. 2009. Genetic risk factors for melanoma. *Hum Genet,* 126**,** 499-510.

MEYUHAS, O. 2000. Synthesis of the translational apparatus is regulated at the translational level. *Eur J Biochem,* 267**,** 6321-30.

MICHIELSEN, P. P., FRANCQUE, S. M. & VAN DONGEN, J. L. 2005. Viral hepatitis and hepatocellular carcinoma. *World J Surg Oncol,* 3**,** 27.

MIMORI, K., MORI, M., TANAKA, S., AKIYOSHI, T. & SUGIMACHI, K. 1995. The overexpression of elongation factor 1 gamma mRNA in gastric carcinoma. *Cancer,* 75**,** 1446-9.

MITA, K., MORIMYO, M., ITO, K., SUGAYA, K., EBIHARA, K., HONGO, E., HIGASHI, T., HIRAYAMA, Y. & NAKAMURA, Y. 1997. Comprehensive cloning of Schizosaccharomyces pombe genes encoding translation elongation factors. *Gene,* 187**,** 259-66.

MIYAGI, Y., SUGIYAMA, A., ASAI, A., OKAZAKI, T., KUCHINO, Y. & KERR, S. J. 1995. Elevated levels of eukaryotic translation initiation factor eIF-4E, mRNA in a broad spectrum of transformed cell lines. *Cancer Lett,* 91**,** 247-52.

MOHLER, J. L., MORRIS, T. L., FORD, O. H., 3RD, ALVEY, R. F., SAKAMOTO, C. & GREGORY, C. W. 2002. Identification of differentially expressed genes associated with androgen-independent growth of prostate cancer. *Prostate,* 51**,** 247-55.

MOLINA, H., HORN, D. M., TANG, N., MATHIVANAN, S. & PANDEY, A. 2007. Global proteomic profiling of phosphopeptides using electron transfer dissociation tandem mass spectrometry. *Proc Natl Acad Sci U S A,* 104**,** 2199-204.

MOORE, R. C. & CYR, R. J. 2000. Association between elongation factor-1alpha and microtubules in vivo is domain dependent and conditional. *Cell Motil Cytoskeleton,* 45**,** 279-92.

MOORE, R. C., DURSO, N. A. & CYR, R. J. 1998. Elongation factor-1alpha stabilizes microtubules in a calcium/calmodulin-dependent manner. *Cell Motil Cytoskeleton,* 41**,** 168-80.

MUNSHI, R., KANDL, K. A., CARR-SCHMID, A., WHITACRE, J. L., ADAMS, A. E. & KINZY, T. G. 2001. Overexpression of translation elongation factor 1A affects the organization and function of the actin cytoskeleton in yeast. *Genetics,* 157**,** 1425-36.

MURTHI, A., SHAHEEN, H. H., HUANG, H. Y., PRESTON, M. A., LAI, T. P., PHIZICKY, E. M. & HOPPER, A. K. 2010. Regulation of tRNA bidirectional nuclear-cytoplasmic trafficking in Saccharomyces cerevisiae. *Mol Biol Cell,* 21**,** 639-49.

NATHAN, C. O., FRANKLIN, S., ABREO, F. W., NASSAR, R., DE BENEDETTI, A., WILLIAMS, J. & STUCKER, F. J. 1999. Expression of eIF4E during head and neck tumorigenesis: possible role in angiogenesis. *Laryngoscope,* 109**,** 1253-8.

NEWBERY, H. J., GILLINGWATER, T. H., DHARMASAROJA, P., PETERS, J., WHARTON, S. B., THOMSON, D., RIBCHESTER, R. R. & ABBOTT, C. M. 2005. Progressive loss of motor neuron function in wasted mice: effects of a spontaneous null mutation in the gene for the eEF1 A2 translation factor. *J Neuropathol Exp Neurol,* 64**,** 295-303.

NEWBERY, H. J., LOH, D. H., O'DONOGHUE, J. E., TOMLINSON, V. A., CHAU, Y. Y., BOYD, J. A., BERGMANN, J. H., BROWNSTEIN, D. & ABBOTT, C. M. 2007. Translation elongation factor eEF1A2 is essential for post-weaning survival in mice. *J Biol Chem,* 282**,** 28951-9.

NOCITO, A., KONONEN, J., KALLIONIEMI, O. P. & SAUTER, G. 2001. Tissue microarrays (TMAS) for high-throughput molecular pathology research. *Int J Cancer*, 94, 1-5.

OHTA, K., TORIYAMA, M., MIYAZAKI, M., MUROFUSHI, H., HOSODA, S., ENDO, S. & SAKAI, H. 1990. The mitotic apparatus-associated 51-kDa protein from sea urchin eggs is a GTP-binding protein and is immunologically related to yeast polypeptide elongation factor 1 alpha. *J Biol Chem,* 265**,** 3240-7.

ONG, S. E., BLAGOEV, B., KRATCHMAROVA, I., KRISTENSEN, D. B., STEEN, H., PANDEY, A. & MANN, M. 2002. Stable isotope labeling by amino acids in cell culture, SILAC, as a simple and accurate approach to expression proteomics. *Mol Cell Proteomics*, 1, 376-86.

OWEN, C. H., DEROSIER, D. J. & CONDEELIS, J. 1992. Actin crosslinking protein EF-1a of Dictyostelium discoideum has a unique bonding rule that allows square-packed bundles. *J Struct Biol,* 109**,** 248-54.

ØROM, U. A., NIELSEN, F. C. & LUND, A. H. 2008. MicroRNA-10a binds the 5'UTR of ribosomal protein mRNAs and enhances their translation. *Mol Cell,* 30**,** 460-71.

PALMIERI, G., CAPONE, M., ASCIERTO, M. L., GENTILCORE, G., STRONCEK, D. F., CASULA, M., SINI, M. C., PALLA, M., MOZZILLO, N. & ASCIERTO, P. A. 2009. Main roads to melanoma. *J Transl Med,* 7**,** 86.

PAN, J., HU, H., ZHOU, Z., SUN, L., PENG, L., YU, L., SUN, L., LIU, J., YANG, Z. & RAN, Y. 2010. Tumor-suppressive *mir-663* gene induces mitotic catastrophe growth arrest in human gastric cancer cells. *Oncol Rep*, 24, 105-12.

PAN, J., RUEST, L. B., XU, S. & WANG, E. 2004. Immuno-characterization of the switch of peptide elongation factors eEF1A-1/EF-1alpha and eEF1A-2/S1 in the central nervous system during mouse development. *Brain Res Dev Brain Res,* 149**,** 1-8.

PANASYUK, G., NEMAZANYY, I., FILONENKO, V., NEGRUTSKII, B. & EL'SKAYA, A. V. 2008. A2 isoform of mammalian translation factor eEF1A displays increased tyrosine phosphorylation and ability to interact with different signalling molecules. *Int J Biochem Cell Biol,* 40**,** 63-71.

PARKIN, D. M., BRAY, F., FERLAY, J. & PISANI, P. 2005. Global cancer statistics, 2002. *CA Cancer J Clin,* 55**,** 74-108.

PASTAN, I. & WILLINGHAM, M. 1978. Cellular transformation and the 'morphologic phenotype' of transformed cells. *Nature,* 274**,** 645-50.

PECORARI, L., MARIN, O., SILVESTRI, C., CANDINI, O., ROSSI, E., GUERZONI, C., CATTELANI, S., MARIANI, S. A., CORRADINI, F., FERRARI-AMOROTTI, G., CORTESI, L., BUSSOLARI, R., RASCHELLA, G., FEDERICO, M. R. & CALABRETTA, B. 2009. Elongation Factor 1 alpha interacts with phospho-Akt in breast cancer cells and regulates their proliferation, survival and motility. *Mol Cancer,* 8**,** 58.

PENDARIES, C., TRONCHERE, H., PLANTAVID, M. & PAYRASTRE, B. 2003. Phosphoinositide signaling disorders in human diseases. *FEBS Lett,* 546**,** 25-31.

PERUCHO, M., GOLDFARB, M., SHIMIZU, K., LAMA, C., FOGH, J. & WIGLER, M. 1981. Human-tumor-derived cell lines contain common and different transforming genes. *Cell,* 27**,** 467-76.

PICKERING, B. M. & WILLIS, A. E. 2005. The implications of structured 5' untranslated regions on translation and disease. *Semin Cell Dev Biol,* 16**,** 39-47.

PINKE, D. E., KALLOGER, S. E., FRANCETIC, T., HUNTSMAN, D. G. & LEE, J. M. 2008. The prognostic significance of elongation factor eEF1A2 in ovarian cancer. *Gynecol Oncol,* 108**,** 561-8.

PINO, M. S. & CHUNG, D. C. 2010. The chromosomal instability pathway in colon cancer. *Gastroenterology,* 138**,** 2059-72.

QUALTROUGH, D., SINGH, K., BANU, N., PARASKEVA, C. & PIGNATELLI, M. 2009. The actin-bundling protein fascin is overexpressed in colorectal adenomas and promotes motility in adenoma cells *in vitro*. *Br J Cancer,* 101, 1124-9.

RASHEED, S., NELSON-REES, W. A., TOTH, E. M., ARNSTEIN, P. & GARDNER, M. B. 1974. Characterization of a newly derived human sarcoma cell line (HT-1080). *Cancer,* 33**,** 1027-33.

REHMSMEIER, M., STEFFEN, P., HOCHSMANN, M. & GIEGERICH, R. 2004. Fast and effective prediction of microRNA/target duplexes. *Rna,* 10**,** 1507-17.

RODNINA, M. V. & WINTERMEYER, W. 2009. Recent mechanistic insights into eukaryotic ribosomes. *Curr Opin Cell Biol*, 21, 435-43.

ROSENBERRY, T. L., KRALL, J. A., DEVER, T. E., HAAS, R., LOUVARD, D. & MERRICK, W. C. 1989. Biosynthetic incorporation of [3H]ethanolamine into protein synthesis elongation factor 1 alpha reveals a new post-translational protein modification. *J Biol Chem,* 264**,** 7096-9.

ROSENWALD, I. B., CHEN, J. J., WANG, S., SAVAS, L., LONDON, I. M. & PULLMAN, J. 1999. Upregulation of protein synthesis initiation factor eIF-4E is an early event during colon carcinogenesis. *Oncogene,* 18**,** 2507-17.

ROSENWALD, I. B., HUTZLER, M. J., WANG, S., SAVAS, L. & FRAIRE, A. E. 2001. Expression of eukaryotic translation initiation factors 4E and 2alpha is increased frequently in bronchioloalveolar but not in squamous cell carcinomas of the lung. *Cancer,* 92**,** 2164-71.

ROZEN, S. & SKALETSKY, H. 2000. Primer3 on the WWW for general users and for biologist programmers. *Methods Mol Biol,* 132**,** 365-86.

RUEST, L. B., MARCOTTE, R. & WANG, E. 2002. Peptide elongation factor eEF1A-2/S1 expression in cultured differentiated myotubes and its protective effect against caspase-3-mediated apoptosis. *J Biol Chem,* 277**,** 5418-25.

RUGGERO, D. & PANDOLFI, P. P. 2003. Does the ribosome translate cancer? *Nat Rev Cancer,* 3**,** 179-92.

SAHAI, E. 2005. Mechanisms of cancer cell invasion. *Curr Opin Genet Dev,* 15**,** 87-96.

SCHIRMAIER, F. & PHILIPPSEN, P. 1984. Identification of two genes coding for the translation elongation factor EF-1 alpha of S. cerevisiae. *EMBO J,* 3**,** 3311-5.

SCHLAEGER, C., LONGERICH, T., SCHILLER, C., BEWERUNGE, P., MEHRABI, A., TOEDT, G., KLEEFF, J., EHEMANN, V., EILS, R., LICHTER, P., SCHIRMACHER, P. & RADLWIMMER, B. 2008. Etiology-dependent molecular mechanisms in human hepatocarcinogenesis. *Hepatology,* 47**,** 511-20.

SCHMIDT, E. K., CLAVARINO, G., CEPPI, M. & PIERRE, P. 2009. SUnSET, a nonradioactive method to monitor protein synthesis. *Nat Methods,* 6**,** 275-7.

SCHWARTZ, D. R., KARDIA, S. L., SHEDDEN, K. A., KUICK, R., MICHAILIDIS, G., TAYLOR, J. M., MISEK, D. E., WU, R., ZHAI, Y., DARRAH, D. M., REED, H., ELLENSON, L. H., GIORDANO, T. J., FEARON, E. R., HANASH, S. M. & CHO, K. R. 2002. Gene expression in

ovarian cancer reflects both morphology and biological behavior, distinguishing clear cell from other poor-prognosis ovarian carcinomas. *Cancer Res,* 62**,** 4722-9.

SCRIDELI, C. A., CARLOTTI, C. G., JR., OKAMOTO, O. K., ANDRADE, V. S., CORTEZ, M. A., MOTTA, F. J., LUCIO-ETEROVIC, A. K., NEDER, L., ROSEMBERG, S., OBA-SHINJO, S. M., MARIE, S. K. & TONE, L. G. 2008. Gene expression profile analysis of primary glioblastomas and non-neoplastic brain tissue: identification of potential target genes by oligonucleotide microarray and real-time quantitative PCR. *J Neurooncol,* 88**,** 281-91.

SELGA, E., OLEAGA, C., RAMIREZ, S., DE ALMAGRO, M. C., NOE, V. & CIUDAD, C. J. 2009. Networking of differentially expressed genes in human cancer cells resistant to methotrexate. *Genome Med,* 1**,** 83.

SHAMOVSKY, I., IVANNIKOV, M., KANDEL, E. S., GERSHON, D. & NUDLER, E. 2006. RNA-mediated response to heat shock in mammalian cells. *Nature,* 440**,** 556-60.

SHAMOVSKY, I. & NUDLER, E. 2008. New insights into the mechanism of heat shock response activation. *Cell Mol Life Sci,* 65**,** 855-61.

SHIBUI-NIHEI, A., OHMORI, Y., YOSHIDA, K., IMAI, J., OOSUGA, I., IIDAKA, M., SUZUKI, Y., MIZUSHIMA-SUGANO, J., YOSHITOMO-NAKAGAWA, K. & SUGANO, S. 2003. The 5' terminal oligopyrimidine tract of human elongation factor 1A-1 gene functions as a transcriptional initiator and produces a variable number of Us at the transcriptional level. *Gene,* 311**,** 137-45.

SHIINA, N., GOTOH, Y., KUBOMURA, N., IWAMATSU, A. & NISHIDA, E. 1994. Microtubule severing by elongation factor 1 alpha. *Science,* 266**,** 282-5.

SHIN, S. I., FREEDMAN, V. H., RISSER, R. & POLLACK, R. 1975. Tumorigenicity of virus-transformed cells in nude mice is correlated specifically with anchorage independent growth in vitro. *Proc Natl Acad Sci U S A,* 72**,** 4435-9.

SHLOMIT, R., AYALA, A. G., MICHAL, D., NINETT, A., FRIDA, S., BOLESLAW, G., GAD, B., GIDEON, R. & SHLOMI, C. 2000. Gains and losses of DNA sequences in childhood brain tumors analyzed by comparative genomic hybridization. *Cancer Genet Cytogenet,* 121**,** 67-72.

SHULTZ, L. D., SWEET, H. O., DAVISSON, M. T. & COMAN, D. R. 1982. 'Wasted', a new mutant of the mouse with abnormalities characteristic to ataxia telangiectasia. *Nature,* 297**,** 402-4.

SILVERA, D., FORMENTI, S. C. & SCHNEIDER, R. J. 2010. Translational control in cancer. *Nat Rev Cancer,* 10**,** 254-66.

SLAUGHTER, D. P., SOUTHWICK, H. W. & SMEJKAL, W. 1953. Field cancerization in oral stratified squamous epithelium; clinical implications of multicentric origin. *Cancer,* 6**,** 963-8.

SLOBIN, L. I. 1980. The role of eucaryotic factor Tu in protein synthesis. The measurement of the elongation factor Tu content of rabbit reticulocytes and other mammalian cells by a sensitive radioimmunoassay. *Eur J Biochem,* 110**,** 555-63.

SLOBIN, L. I. & RAO, M. N. 1993. Translational repression of EF-1 alpha mRNA in vitro. *Eur J Biochem,* 213**,** 919-26.

SOARES, D. C., BARLOW, P. N., NEWBERY, H. J., PORTEOUS, D. J. & ABBOTT, C. M. 2009. Structural models of human eEF1A1 and eEF1A2 reveal two distinct surface clusters of sequence variation and potential differences in phosphorylation. *PLoS One,* 4**,** e6315.

SONG, J. M., PICOLOGLOU, S., GRANT, C. M., FIROOZAN, M., TUITE, M. F. & LIEBMAN, S. 1989. Elongation factor EF-1 alpha gene dosage alters translational fidelity in Saccharomyces cerevisiae. *Mol Cell Biol,* 9**,** 4571-5.

STAPULIONIS, R., KOLLI, S. & DEUTSCHER, M. P. 1997. Efficient mammalian protein synthesis requires an intact F-actin system. *J Biol Chem,* 272**,** 24980-6.

SUDA, M., FUKUI, M., SOGABE, Y., SATO, K., MORIMATSU, A., ARAI, R., MOTEGI, F., MIYAKAWA, T., MABUCHI, I. & HIRATA, D. 1999. Overproduction of elongation factor 1alpha, an essential translational component, causes aberrant cell morphology by affecting the control of growth polarity in fission yeast. *Genes Cells,* 4**,** 517-27.

SUEHIRO, Y., SAKAMOTO, M., UMAYAHARA, K., IWABUCHI, H., SAKAMOTO, H., TANAKA, N., TAKESHIMA, N., YAMAUCHI, K., HASUMI, K., AKIYA, T., SAKUNAGA, H., MUROYA, T., NUMA, F., KATO, H., TENJIN, Y. & SUGISHITA, T. 2000. Genetic aberrations detected by comparative genomic hybridization in ovarian clear cell adenocarcinomas. *Oncology,* 59**,** 50-6.

SUNDSTROM, P., SMITH, D. & SYPHERD, P. S. 1990. Sequence analysis and expression of the two genes for elongation factor 1 alpha from the dimorphic yeast Candida albicans. *J Bacteriol,* 172**,** 2036-45.

TANAKA, K., ARAO, T., MAEGAWA, M., MATSUMOTO, K., KANEDA, H., KUDO, K., FUJITA, Y., YOKOTE, H., YANAGIHARA, K., YAMADA, Y., OKAMOTO, I., NAKAGAWA, K. & NISHIO, K. 2009. SRPX2 is overexpressed in gastric cancer and promotes cellular migration and adhesion. *Int J Cancer*, 124, 1072-80.

TANNER, M. M., GRENMAN, S., KOUL, A., JOHANNSSON, O., MELTZER, P., PEJOVIC, T., BORG, A. & ISOLA, J. J. 2000. Frequent amplification of chromosomal region 20q12-q13 in ovarian cancer. *Clin Cancer Res,* 6**,** 1833-9.

TANNER, M. M., TIRKKONEN, M., KALLIONIEMI, A., COLLINS, C., STOKKE, T., KARHU, R., KOWBEL, D., SHADRAVAN, F., HINTZ, M., KUO, W. L. & ET AL. 1994. Increased copy number at 20q13 in breast cancer: defining the critical region and exclusion of candidate genes. *Cancer Res,* 54**,** 4257-60.

TATSUKA, M., MITSUI, H., WADA, M., NAGATA, A., NOJIMA, H. & OKAYAMA, H. 1992. Elongation factor-1 alpha gene determines susceptibility to transformation. *Nature,* 359**,** 333-6.

TEJADA, S., LOBO, M. V., GARCIA-VILLANUEVA, M., SACRISTAN, S., PEREZ-MORGADO, M. I., SALINAS, M. & MARTIN, M. E. 2009. Eukaryotic initiation factors (eIF) 2alpha and 4E expression, localization, and phosphorylation in brain tumors. *J Histochem Cytochem,* 57**,** 503-12.

TERRANOVA, V. P., HUJANEN, E. S., LOEB, D. M., MARTIN, G. R., THORNBURG, L. & GLUSHKO, V. 1986. Use of a reconstituted basement membrane to measure cell invasiveness and select for highly invasive tumor cells. *Proc Natl Acad Sci U S A,* 83**,** 465-9.

THOMAS, G. & THOMAS, G. 1986. Translational control of mRNA expression during the early mitogenic response in Swiss mouse 3T3 cells: identification of specific proteins. *J Cell Biol,* 103**,** 2137-44.

THOMPSON, J. D., HIGGINS, D. G. & GIBSON, T. J. 1994. CLUSTAL W: improving the sensitivity of progressive multiple sequence alignment through sequence weighting, position-specific gap penalties and weight matrix choice. *Nucleic Acids Res*, 22, 4673-80.

THORGEIRSSON, S. S. & GRISHAM, J. W. 2002. Molecular pathogenesis of human hepatocellular carcinoma. *Nat Genet,* 31**,** 339-46.

THORNTON, S., ANAND, N., PURCELL, D. & LEE, J. 2003. Not just for housekeeping: protein initiation and elongation factors in cell growth and tumorigenesis. *J Mol Med,* 81**,** 536-48.

TILI, E., MICHAILLE, J. J., ALDER, H., VOLINIA, S., DELMAS, D., LATRUFFE, N. & CROCE, C. M. 2010. Resveratrol modulates the levels of microRNAs targeting genes encoding tumor-suppressors and effectors of TGFβ signalling pathway in SW480 cells. Biochem Pharmacol, Epub ahead of print.

TOMLINSON, V. A., NEWBERY, H. J., BERGMANN, J. H., BOYD, J., SCOTT, D., WRAY, N. R., SELLAR, G. C., GABRA, H., GRAHAM, A., WILLIAMS, A. R. & ABBOTT, C. M. 2007. Expression of eEF1A2 is associated with clear cell histology in ovarian carcinomas: overexpression of the gene is not dependent on modifications at the EEF1A2 locus. *Br J Cancer,* 96**,** 1613-20.

TOMLINSON, V. A., NEWBERY, H. J., WRAY, N. R., JACKSON, J., LARIONOV, A., MILLER, W. R., DIXON, J. M. & ABBOTT, C. M. 2005. Translation elongation factor eEF1A2 is a potential oncoprotein that is overexpressed in two-thirds of breast tumours. *BMC Cancer,* 5**,** 113.

TSAI, W. L. & CHUNG, R. T. 2010. Viral hepatocarcinogenesis. *Oncogene,* 29**,** 2309-24.

UETSUKI, T., NAITO, A., NAGATA, S. & KAZIRO, Y. 1989. Isolation and characterization of the human chromosomal gene for polypeptide chain elongation factor-1 alpha. *J Biol Chem,* 264**,** 5791-8.

UONG, A. & ZON, L. I. 2010. Melanocytes in development and cancer. *J Cell Physiol,* 222**,** 38-41.

VAN ROOIJ, E., LIU, N. & OLSON, E. N. 2008. MicroRNAs flex their muscles. *Trends Genet*, 24, 159-66.

VERHAGEN, P. C., HERMANS, K. G., BROK, M. O., VAN WEERDEN, W. M., TILANUS, M. G., DE WEGER, R. A., BOON, T. A. & TRAPMAN, J. 2002. Deletion of chromosomal region 6q14-16 in prostate cancer. *Int J Cancer,* 102**,** 142-7.

VIVANCO, I. & SAWYERS, C. L. 2002. The phosphatidylinositol 3-Kinase AKT pathway in human cancer. *Nat Rev Cancer,* 2**,** 489-501.

VOORMA, H. O., THOMAS, A. A. & VAN HEUGTEN, H. A. 1994. Initiation of protein synthesis in eukaryotes. *Mol Biol Rep,* 19**,** 139-45.

VOYTIK-HARBIN, S. L., BRIGHTMAN, A. O., WAISNER, B., LAMAR, C. H. & BADYLAK, S. F. 1998. Application and evaluation of the alamarBlue assay for cell growth and survival of fibroblasts. *In Vitro Cell Dev Biol Anim,* 34**,** 239-46.

WELSH, G. I. & PROUD, C. G. 1992. Regulation of protein synthesis in Swiss 3T3 fibroblasts. Rapid activation of the guanine-nucleotide-exchange factor by insulin and growth factors. *Biochem J,* 284 (Pt 1)**,** 19-23.

WENDEL, H. G., SILVA, R. L., MALINA, A., MILLS, J. R., ZHU, H., UEDA, T., WATANABE-FUKUNAGA, R., FUKUNAGA, R., TERUYA-FELDSTEIN, J., PELLETIER, J. & LOWE, S. W. 2007. Dissecting eIF4E action in tumorigenesis. *Genes Dev,* 21**,** 3232-7.

WHITTAKER, S., MARAIS, R. & ZHU, A. X. 2010. The role of signaling pathways in the development and treatment of hepatocellular carcinoma. *Oncogene,* 29**,** 4989-5005.

WILKIE, G. S., DICKSON, K. S. & GRAY, N. K. 2003. Regulation of mRNA translation by 5'- and 3'-UTR-binding factors. *Trends Biochem Sci,* 28**,** 182-8.

WONG, C. M. & NG, I. O. 2008. Molecular pathogenesis of hepatocellular carcinoma. *Liver Int,* 28**,** 160-74.

WU, J. & BAG, J. 1998. Negative control of the poly(A)-binding protein mRNA translation is mediated by the adenine-rich region of its 5'-untranslated region. *J Biol Chem,* 273**,** 34535-42.

XU, W. L., WANG, X. L., WANG, H. & LI, X. B. 2007. Molecular characterization and expression analysis of nine cotton GhEF1A genes encoding translation elongation factor 1A. *Gene,* 389**,** 27-35.

YAMAGUCHI, H., WYCKOFF, J. & CONDEELIS, J. 2005. Cell migration in tumors. *Curr Opin Cell Biol,* 17**,** 559-64.

YANG, F., DEMMA, M., WARREN, V., DHARMAWARDHANE, S. & CONDEELIS, J. 1990. Identification of an actin-binding protein from Dictyostelium as elongation factor 1a. *Nature,* 347**,** 494-6.

YANG, W. & BOSS, W. F. 1994. Regulation of phosphatidylinositol 4-kinase by the protein activator PIK-A49. Activation requires phosphorylation of PIK-A49. *J Biol Chem,* 269**,** 3852-7.

YANG, W., BURKHART, W., CAVALLIUS, J., MERRICK, W. C. & BOSS, W. F. 1993. Purification and characterization of a phosphatidylinositol 4-kinase activator in carrot cells. *J Biol Chem,* 268**,** 392-8.

YOSHIHAMA, M., UECHI, T., ASAKAWA, S., KAWASAKI, K., KATO, S., HIGA, S., MAEDA, N., MINOSHIMA, S., TANAKA, T., SHIMIZU, N. & KENMOCHI, N. 2002. The human ribosomal protein genes: sequencing and comparative analysis of 73 genes. *Genome Res,* 12**,** 379-90.

ZABIEROWSKI, S. E. & HERLYN, M. 2010. Embryonic stem cells as a model for studying melanocyte development. *Methods Mol Biol,* 584**,** 301-16.

ZENDER, L., VILLANUEVA, A., TOVAR, V., SIA, D., CHIANG, D. Y. & LLOVET, J. M. 2010. Cancer gene discovery in hepatocellular carcinoma. *J Hepatol,* 52**,** 921-9.

ZHANG, J., GUO, H., MI, Z., GAO, C., BHATTACHARYA, S., LI, J. & KUO, P. C. 2009. EF1A1-actin interactions alter mRNA stability to determine differential osteopontin expression in HepG2 and Hep3B cells. *Exp Cell Res,* 315**,** 304-12.

ZHANG, L., PAN, X. & HERSHEY, J. W. 2007. Individual overexpression of five subunits of human translation initiation factor eIF3 promotes malignant transformation of immortal fibroblast cells. *J Biol Chem,* 282**,** 5790-800.

ZHANG, L., SMIT-MCBRIDE, Z., PAN, X., RHEINHARDT, J. & HERSHEY, J. W. 2008. An oncogenic role for the phosphorylated h-subunit of human translation initiation factor eIF3. *J Biol Chem,* 283**,** 24047-60.

ZHONG, D., ZHANG, J., YANG, S., SOH, U. J., BUSCHDORF, J. P., ZHOU, Y. T., YANG, D. & LOW, B. C. 2009. The SAM domain of the RhoGAP DLC1 binds EF1A1 to regulate cell migration. *J Cell Sci,* 122**,** 414-24.

ZHOU, X., TEMAM, S., OH, M., PUNGPRAVAT, N., HUANG, B. L., MAO, L. & WONG, D. T. 2006. Global expression-based classification of lymph node metastasis and extracapsular spread of oral tongue squamous cell carcinoma. *Neoplasia,* 8**,** 925-32.

ZHU, H., LAM, D. C., HAN, K. C., TIN, V. P., SUEN, W. S., WANG, E., LAM, W. K., CAI, W. W., CHUNG, L. P. & WONG, M. P. 2007. High resolution analysis of genomic aberrations by metaphase and array comparative genomic hybridization identifies candidate tumour genes in lung cancer cell lines. *Cancer Lett,* 245**,** 303-14.

ZHU, J., SPENCER, E. D. & KASPAR, R. L. 2003. Differential translation of TOP mRNAs in rapamycin-treated human B lymphocytes. *Biochim Biophys Acta,* 1628**,** 50-5.